

AD-A264 968



NASA
Contractor Report 191117

Army Research Laboratory
Contractor Report ARL-CR-11

(2)

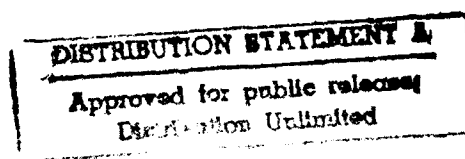
Global Dynamic Modeling of a Transmission System

F.K. Choy and W. Qian
University of Akron
Akron, Ohio

DTIC
SPL
MAY 21 1993

April 1993

Prepared for
Lewis Research Center and U.S. Army Research Laboratory
Under Grant NAG3-900



NASA
National Aeronautics and
Space Administration



93-11317



93 5 20 02 6

OUTLINE

1. Introduction
 - 1.1 Introduction
 - 1.2 Review of Previous Work
 - 1.3 Scope and Objectives
2. Formulation of Generalized Equations of Motion
 - 2.1 Dynamics of Rotor-Bearing-Gear System
 - 2.2 Dynamics of Gear Box Structure
 - 2.3 Coupled System Dynamics
 - *3-D Lateral-Axial Coupled Bearing Supports
 - *Gear Mesh Normal and Frictional Forces
 - *Effects of Foundation Motion
3. Formulation of Modal Synthesis Procedure
 - 3.1 Modal Characteristics of Rotor-Bearing-Gear Systems
 - 3.2 Modal Characteristics of Gear Box Structure
 - 3.3 Orthogonality of Modal Shapes
 - 3.4 Modal Transformation of Equations of Motion
4. Numerical solution Procedure:
5. Experimental Studies
 - 5.1 Evaluation of Experimental Modal Characteristics
 - 5.2 Experimental Investigations of System Dynamics
 - 5.3 Experimental Investigations of Gear Box Noise
6. Correlation and Benchmarking of System Dynamics by Numerical Procedures with Experimental Results
 - 6.1 Gear Box System Modal Characteristics
 - 6.2 Rotor-Bearing-Gear Transient Vibrations
 - 6.3 Gear Box Transient Dynamics

7. Correlation of Noise and Vibrations

- 7.1 Correlation of Experimental Noise and Vibration Data**
- 7.2 Predictions of Noise by Numerical Simulations and Correlation with Experimental Results**

8. Conclusions and Summary

9. References

Appendix A Derivation of Transfer Matrix Equation

Appendix B Program Data Input Instruction

Appendix C Listing of Program

Appendix D Sample Input File

NOMENCLATURE

- A = rotor modal displacement of (X, θ_x)
 A_c = casing modal displacement of ($X_c, X_{c\theta}$)
 B = rotor modal displacement of (Y, θ_y)
 B_c = rotor modal displacement of ($Y_c, Y_{c\theta}$)
 $[C_b]$ = bearing damping matrix
 $[C_c]$ = casing structure damping matrix
 $[\bar{C}_b]$ = $[\Phi]^T [C_b] [\Phi]$
 $[\bar{C}_c]$ = $[\Phi_c]^T [C_c] [\Phi_c]$
 $[\bar{C}_s]$ = $[\Phi_s] [C_s] [\Phi_s]$
 D = rotor modal displacement of Z
 D_t = rotor modal displacement of θ_t
 D_c = casing modal displacement of ($Z_c, Z_{c\theta}$)
 $\{F(t)\}$ = external and mass-imbalance excitations
 $\{F_G(t)\}$ = gear force
 $\{F_c(t)\}$ = force acting on casing structure
 $\{F_s(t)\}$ = shaft bow force = $[K_s] \{W_s\}$
 $[G_A]$ = rotor angular acceleration
 $[G_v]$ = gyroscopic
 $[\bar{G}_A]$ = $[\Phi]^T [G_A] [\Phi]$
 $[\bar{G}_v]$ = $[\Phi]^T [G_v] [\Phi]$
 $[K_b]$ = bearing stiffness

Accession For	
NTIS Serial	<input checked="" type="checkbox"/>
DTIC Type	<input type="checkbox"/>
Uncontrolled	<input type="checkbox"/>
J. Classification	
By _____	
Distribution/	
Availability Codes	
Dist	Civil and/or Special
A-1	

NOMENCLATURE (cont'd)

$[K_c]$	=	casing structure stiffness
$[K_s]$	=	shaft bow stiffness
$[K_A]$	=	$\frac{1}{2} \{ [K_{bx}] + [K_{by}] \}$
$[\bar{K}_b]$	=	$[\Phi]^T [K_b] [\Phi]$
$[\bar{K}_A]$	=	$[\Phi]^T [K_A] [\Phi]$
$[\bar{K}_c]$	=	$[\Phi_c]^T [K_c] [\Phi_c]$
$[M]$	=	mass matrix of rotor
$[M_c]$	=	mass matrix of casing structure
$[W]$	=	generalized displacement vector of rotor
$[W_c]$	=	generalized displacement vector of casing
μ	=	friction coefficient between the gear teeth surface
α	=	angle of orientation
ω	=	critical speed of rotor
ω_c	=	critical speed of casing

GLOBAL DYNAMIC MODELING OF A TRANSMISSION SYSTEM

F.K. Choy and W. Qian

University of Akron

Department of Mechanical Engineering

Akron, Ohio 44325-3903

ABSTRACT

This report outlines the work performed on global dynamic simulation and noise correlation of gear transmission systems at The University of Akron. The objective of this work is to develop a comprehensive procedure to simulate the dynamics of the gear transmission system coupled with the effects of gear box vibrations. The developed numerical model is benchmarked with results from experimental tests at NASA Lewis Research Center.

The modal synthesis approach is used to develop the global transient vibration analysis procedure used in the model. Modal dynamic characteristics of the rotor-gear-bearing system are calculated by the matrix transfer method while those of the gear box are evaluated by the finite element method (NASTRAN). A three-dimensional, axial-lateral coupled bearing model is used to couple the rotor vibrations with the gear box motion. The vibrations between the individual rotor systems are coupled through the non-linear gear mesh interactions. The global equations of motion are solved in modal coordinates and the transient vibration of the system is evaluated by a variable time-stepping integration scheme.

The relationship between housing vibration and resulting noise of the gear transmission system is generated by linear transfer functions using experimental data. A nonlinear relationship of the noise components to the fundamental mesh frequency is developed using the hypercoherence function. The numerically simulated vibrations and

predicted noise of the gear transmission system are compared with the experimental results from the gear noise test rig at NASA Lewis Research Center. Results of the comparison indicate that the global dynamic model developed can accurately simulate the dynamics of a gear transmission system.

1. INTRODUCTION

1.1 Introduction

Recently there has been an increase in the use of gear transmissions in both defense and commercial applications. The ever increasing speed and torque requirements of newer transmission systems often result in excessive noise and vibration at both the gear mesh and the gear box structure. Large vibrations in gear transmission systems result in excessive gear tooth wear and possible tooth root crack formation which, in turn, will lead to premature gear failure. In addition, excessive noise produced by a gear transmission in an aircraft, results in strained communications between crew and ground stations, and possible hearing loss for crew and passengers. Thus, in order to assure a quiet, smooth and safe operation of a gear transmission system it is necessary to understand the dynamics of the system under various operating conditions as well as the noise produced under these conditions.

To understand the global dynamics of the system during operation, the vibrational characteristics of the following major components need to be examined:

- i) The dynamics of the rotor bearing system - The dynamics of each rotor system are excited by its rotational torque, gear mesh dynamics, and imbalance effects. The dynamics of each individual rotor are coupled with other rotors through the gear mesh forces. Each rotor is also coupled with the gear box structure through the bearing support system.
- ii) The dynamics of the gear mesh system - The forces produced by the meshing of the gear teeth can be evaluated through the relative motion and the torque transfer between the two rotor systems.

- iii) The dynamics of the gear box system - The vibration of the gear box and its coupling effects with each rotor system is evaluated. In addition, the coupling effects of the gear box vibrations with the foundation motion through the ground support system is also examined.
- iv) The global system vibration - The determination of the global vibration of the system during various operating conditions is necessary.
- v) The relationships between noise and vibration - To understand the source of excessive noise, the relationships between noise and vibration of the system is required.

To further understand the present state of the art and the necessary effort to accomplish the above requirements, a brief description of previous work performed and the scope of this study are presented in the next two sections.

1.2 Review of Previous Work

In the past two decades, significant progress has been achieved in analytical/numerical simulations as well as experimental investigations of gear transmission systems. For both analytical and experimental studies, two major trends of investigations were developed, namely, i) the study of localized dynamics, stress and deformation, and thermal interactions between the two meshing gear teeth, and ii) the global dynamics and noise of the system due to the effects of the gear teeth interactions. An outline of the previous work in these areas is presented in the following paragraphs.

A large amount of work is reported in the literature on analyzing the localized effects of gear tooth interactions. In the area of experimental investigations, a significant amount of work was performed at NASA Lewis Research Center over the last ten years. These studies include the measurement of tooth stress [Oswald 1987, Krantz 1992], gear tooth lubricant and thermal effects [Akin 1989, Lewicki 1992, Townsend 1991a 1991b, El-

Bayoumy 1989], gear tooth friction [Rebbecki 1991], and gear tooth material and fatigue [Townsend 1979, 1988]. Some analytical studies include gear surfaces stresses, lubricant cooling effect [El-Bayoumy 1989], gear tooth surface profile investigations [Kittur 1989, Lin 1988, Litvin 1991a, 1991b] and the dynamics of bevel gears [Handschuh 1991a, 1991b, Mark 1987]. The above outline represents only a small portion of the literature on the state of the art in gear tooth analysis.

In comparison, there is much less available in the literature on the study of the global dynamics of a transmission system. There have been some studies on the vibration analysis of a single gear stage [August 1982, Choy 1988, Cornell 1981, Lin and Houser 1987, Mark 1982, Pike 1987]. Some work has been reported on multistage gear dynamic analysis [Choy 1990, David 1987, Ozguven and Houser 1988]. However, only limited work is reported in the area of experimental analysis of the global dynamics of a transmission system [Mitchell 1986, Oswald 1992]. Similarly, there is limited work on the comparison of experimental results with analytical studies [Choy 1987, 1991, Singh 1990]. Reported research is even more limited in the areas of noise analysis and noise prediction in gear transmission systems. Some work on predicting and verifying the noise field of a gear transmission system has only recently been reported (Seybert 1991, Oswald 1992).

1.3 Scope and Objectives

As illustrated above, with the limited amount of literature available on modeling gear transmission systems, a comprehensive analytical and experimental procedure is necessary for the complete understanding of the dynamics and resulting noise of a transmission system. In this project, a numerical model is developed to simulate the vibrations of a multistage gear

system. The ultimate goal in this project is to develop a methodology to predict the noise and vibration of a gear transmission system.

During the early stages of this work several main objectives were established in an effort to guide the development of the global model in the direction of achieving the project goal. These main objectives are:

- 1) The gear/rotor part of the model should be capable of simulating multistage gear systems, variable rotor geometries, shaft residual bow, mass imbalances, and nonlinear stiffness and friction of the gear tooth.
- 2) The bearing support part of the model must be capable of coupling the dynamics of the gear/rotor system with the housing dynamics in both the in-plane and out-of-plane directions.
- 3) The finite element model of the housing must accurately predict the major vibration modes of the actual housing. Experimental results will be used to verify and improve the model.
- 4) A relationship needs to be established between the housing vibrations and resulting noise production to complete the gear initiated vibration/noise transmission path.

The key to achieving the ultimate goal of developing a global dynamic model that accurately predicts the noise and vibration of a transmission system was to successfully meet each of the main objectives presented above. Meeting these objectives required comparing and validating each part of the model, and the total model, with experimental data during each stage of development of the global dynamic model.

The remaining sections of this report document the details of developing the global model and verifying/refining the model with experimental data from the gear noise test rig at NASA Lewis Research Center.

2. FORMULATION OF GENERALIZED EQUATIONS OF MOTION

2.1 Dynamics of Rotor-Bearing-Gear System

The equations of motion for each individual gear-shaft system can be written in matrix form [Choy 1991] as:

$$[M]\{\ddot{W}\} + [G_v]\{\dot{W}\} + [G_A]\{W\} + [C_b]\{\dot{W} - \dot{W}_c\} + [K_b]\{W - W_c\} + [K_s]\{W - W_r\} = \{F(t)\} + \{F_G(t)\} \quad (2.1)$$

where the generalized displacement vector $\{W\}$ consists of the three displacement vectors, X, Y, Z, with the corresponding lateral θ_x , θ_y , and torsional θ_z rotational vectors as

$$\{W\} = \begin{Bmatrix} (X) \\ (\theta_x) \\ (Y) \\ (\theta_y) \\ (Z) \\ (\theta_z) \end{Bmatrix} \quad (2.2)$$

The equations of motion shown in Eq. (2.1) includes the effects of a) inertia, [M], b) gyroscopic forces $[G_v]$, c) rotor angular acceleration, $[G_A]$, d) bearing direct and cross-coupling damping, $[C_b]$, e) bearing axial and lateral cross-coupling stiffness, $[K_b]$, [LIM 1990], f) casing vibration, $\{W - W_c\}$, g) shaft residual bow, $\{W - W_r\}$, h) external and mass-imbalance excitations, $\{F(t)\}$, and i) nonlinear gear forces through gear mesh coupling

$\{F_G(t)\}$. For a multiple gear-shaft system, the equations of motion presented in Eq. (2.1) will be repeated for each individual shaft. The motions of the individual shafts are coupled to each other through the gear mesh forces, and the shaft motions are coupled to the casing through the bearing stiffness $[K_b]$ and damping $[C_b]$.

2.2 Dynamics of Gear Box Structure

The equations of motion for the casing can be written as:

$$[M_c]\{\ddot{W}_c\} + [C_b]\{\dot{W}_c - \dot{W}\} + [K_b]\{W_c - W\} + [C_c]\{\dot{W}_c\} + [K_c]\{W_c\} = \{F_c(t)\} \quad (2.3)$$

where $\{W_c\}$ represents the generalized displacement vector of the casing structure,

$$\{W_c\} = \begin{Bmatrix} (X_c) \\ (X_{c\theta}) \\ (Y_c) \\ (Y_{c\theta}) \\ (Z_c) \\ (Z_{c\theta}) \end{Bmatrix} \quad (2.4)$$

The equations of motion of the casing structure, given in Eq. (2.3), include the effects of concentrated mass $[M_c]$, structure members damping $[C_c]$, stiffness of the structural members $[K_c]$, and casing-to-rotor bearing stiffness $[K_b]$ and damping $[C_b]$. The effects of foundation motion are incorporated into the system through the forcing function $F_c(t)$.

2.3 Coupled System Dynamics

The dynamics between each individual rotor system and the casing structure are coupled through the bearing support and the gear mesh systems. Three models are used to couple the dynamics of the system, namely; i) the 3-D lateral-axial bearing, ii) the normal and frictional gear mesh forces, and iii) the casing-ground support system.

3-D Lateral-Axial Bearing Model

This model is used to develop two types of coupling in the system dynamics. a) The relative motion between the rotor and the casing structure at the bearing locations will be used to generate the coupling forces. b) The dynamics between the lateral and axial motion at the bearing supports will be coupled due to the effects of the bearing configuration.

In this simulation, a previously developed bearing model [Singh and Lim 1990] is used. A six degrees of freedom ball bearing stiffness matrix $[K_{bi}]$ is used for each bearing support location, where

$$[K]_{bi} = \begin{bmatrix} k_{xx}, k_{x\theta}, k_{xy}, k_{x\theta}, k_{xz} & 0 \\ k_{\theta,x}, k_{\theta,y}, k_{\theta,\theta}, k_{\theta,z} & 0 \\ k_{yy}, k_{y\theta}, k_{yz} & 0 \\ \text{symmetric } k_{\theta,\theta}, k_{\theta,z} & 0 \\ k_{zz} & 0 \\ 0 & 0 \end{bmatrix}_{bi} \quad (2.5)$$

Note that the bearing stiffness matrix generated not only couples the displacement in all three directions, it also provides coupling between the moments generated due to the bending of the rotor. In this analysis, the bearing stiffness matrix generated for each bearing is incorporated into the global bearing stiffness matrix $[K_b]$ in equations 2.1 and 2.3.

Gear Mesh Normal and Frictional Forces

The gear mesh forces are evaluated using a previously developed methodology [Boyd and Pike 1985]. The procedure evaluates the nonlinear gear mesh stiffness $[K_g]$ for a variety of multi-mesh epicyclic gear systems with internal, buttress, or helical tooth forms. The major assumptions used in this procedure are as follows:

1. The flexible ring gear rim and carrier flexibility option is assumed to be only along the line-of-action of each respective gear mesh.
2. The static output torque is assumed to be divided evenly among either the planet carrier segments or the ring gear rim segments, depending on the type of planetary system.
3. Any radial component of motion is assumed to be secondary to the tooth-pair motion along the line-of-action.
4. The damping of carrier and ring rim segments is assumed to be insignificant relative to the tooth-pair mesh damping.

The nonlinear gear mesh forces for the Kth individual gear-shaft system, Fig. 2.1, using nonlinear gear stiffness [Boyd 1989] and gear tooth friction [Rebbechi 1991], are given as:

x-force

$$F_{Gxk} = \sum_{i=1, i \neq k}^n K_{ki} [-R_{ci} \Theta_{ci} - R_{ck} \Theta_{ck} + (X_{ci} - X_{ck}) \cos \alpha_{ki} + (Y_{ci} - Y_{ck}) \sin \alpha_{ki}] [\cos \alpha_{ki} + (sign)(\mu)(\sin \alpha_{ki})] \quad (2.6)$$

y-force

$$F_{Gyk} = \sum_{i=1, i \neq k}^n K_{ki} [-R_{ci} \Theta_{ci} - R_{ck} \Theta_{ck} + (X_{ci} - X_{ck}) \cos \alpha_{ki} + (Y_{ci} - Y_{ck}) \sin \alpha_{ki}] [\sin \alpha_{ki} + (sign)(\mu)(\cos \alpha_{ki})] \quad (2.6)$$

and torsional

$$F_{Gik} = \sum_{i=1, i \neq k}^n R_{ck} \{K_{ki} [(-R_{ci} \Theta_{ci} - R_{ck} \Theta_{ck}) + (X_{ci} - X_{ck}) \cos \alpha_{ki} + (Y_{ci} - Y_{ck}) \sin \alpha_{ki}]\} \quad (2.8)$$

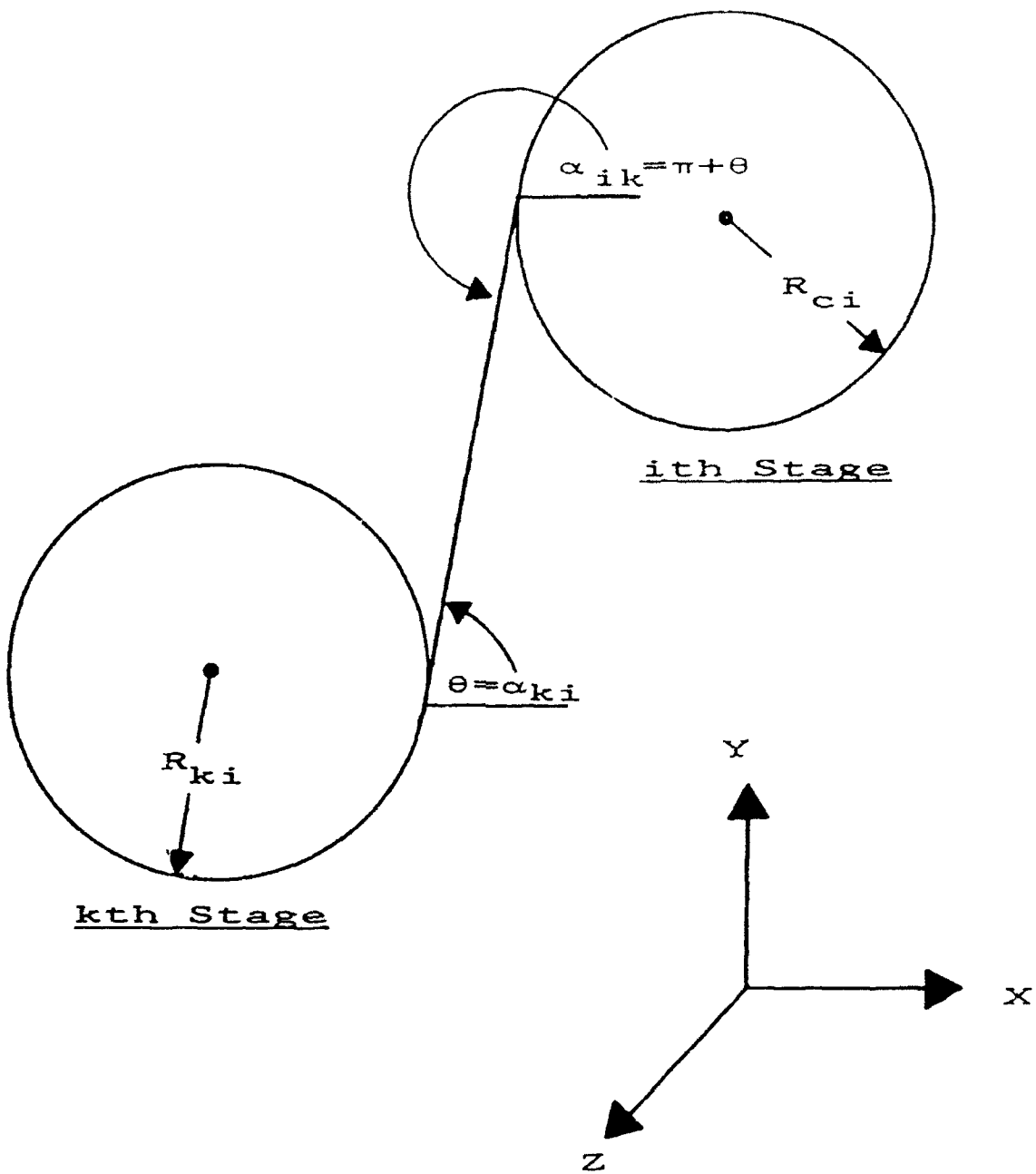


Figure 2.1 Gear Mesh Geometry for Force Calculation

where μ is the coefficient of friction between the gear tooth surface and "SIGN" is the unity sign function to provide the sign change when the mating teeth pass the pitch point [Rebbechi 1991].

Effects of Foundation Motion

The effects of foundation motion are incorporated as part of the forcing function input $F_c(t)$ in the casing equation (Eq. 2.3). The forcing function due to foundation motion can be calculated as the product of the support stiffness $[K_p]$ and the relative motion between the casing and ground at the support locations as

$$\{F_c(t)\} = [K_p] \{W_c - W_g\} \quad (2.9)$$

where W_g is the vector for ground displacement as a function of time.

3. FORMULATION OF MODAL SYNTHESIS PROCEDURE

The generalized equations of motion developed in the previous chapter are solved through the modal synthesis procedure. Using the undamped modes for both the rotor-bearing-gear system and the gear box structure, the generalized equations of motion for the system are transformed into the corresponding modal coordinates. This procedure will significantly reduce the degrees of freedom of the system, and also provide an estimate of the modal excitations at the various modes. A detailed description of the procedure is outlined in the following sections.

3.1 Modal Characteristics of Rotor-Bearing-Gear Systems

For each rotor-bearing-gear system, the modal characteristics are evaluated using the matrix-transfer method [Choy 1988, 1989, 1991]. In this analysis, the rotor system is modelled by sections of massless shafts and concentrated masses. For simplicity in computation, the following assumptions are used in this procedure.

- i) The complexity in the rotor geometry is modelled by sections of massless shafts with concentrated mass attached at both ends.
- ii) Only the direct stiffness of the bearing is incorporated in the calculation of the undamped natural frequencies and mode shapes. The cross-coupling stiffness and damping terms are cast into the right-hand-side of the equation as a forcing function.
- iii) An averaged stiffness for both x and y direction is used and assures a circular symmetric system.

- iv) Gyroscopic moments are not considered in the modal calculations and will be incorporated as forcing functions in the transient calculations. However, rotational inertia effects are included in this procedure.

A detailed description of the equations used in this matrix transfer procedure is given in Appendix A. The natural frequencies and corresponding mode shapes calculated for each rotor system, are incorporated into the modal equation described in the later sections. The undamped modal characteristics evaluation procedure is installed as part of the main computer code, with the undamped modal characteristics generated automatically during each run.

3.2 Modal Characteristics of Gear Box Structure

In evaluating the modal characteristics of the gear box structure, a finite element model is used. The NASTRAN FE code is used with the following options:

- i) Rectangular plate and beam elements are used to model the basic structure of the gear box.
- ii) Boundary elements are used to model the ground supports of the gear box with corresponding boundary support conditions.
- iii) Natural frequencies and 3-dimensional orthonormal mode shapes are evaluated and used as input for the modal synthesis program.
- iv) A description of the input/output with the NASTRAN code is given in Appendix B.

3.3 Orthogonality of Modal Shapes

For each individual rotor system, the equation of motion for the undamped system is:

$$[M]\{\ddot{W}\} + [[K_s] + [K_A]]\{W\} = 0 \quad (3.1)$$

with the average bearing support stiffness from the x-y direction [Choy 1991] given as:

$$[K_A] = \frac{1}{2} \{[K_{bx}] + [K_{by}]\} \quad (3.2)$$

The orthogonality condition for the orthonormal modes $[\Phi]$ are

$$[\Phi]^T [M] [\Phi] = [I] \quad (3.3)$$

and

$$[\Phi]^T [K_s + K_A] [\Phi] = [\omega^2] \quad (3.4)$$

Similarly, a set of orthogonality conditions can be derived for the casing equation of

$$[M_c]\{\ddot{W}_c\} + [C_c]\{\dot{W}_c\} + [K_c]\{W_c\} = 0 \quad (3.5)$$

with the orthonormal mode $[\Phi_c]$ such that

$$[\Phi_c]^T [M_c] [\Phi_c] = [I] \quad (3.6)$$

$$[\Phi_c]^T [C_c] [\Phi_c] = [\bar{C}_c] \quad (3.7)$$

$$[\Phi_c]^T [K_c] [\Phi_c] = [\omega_c^2] \quad (3.8)$$

These orthogonal conditions are used in the modal transformation presented in the next section.

3.4 Modal Transformation of Equations of Motion

The modal transformation procedure can be developed by assuming that the generalized displacements can be represented by a linear combination of the modal characteristics, such that for the rotor system

$$\{W\} = \begin{Bmatrix} [\Phi_x] \{A\} \\ [\Phi_{x\theta}] \{A\} \\ [\Phi_y] \{B\} \\ [\Phi_{y\theta}] \{B\} \\ [\Phi_z] \{D\} \\ [\Phi_{z\theta}] \{D\} \end{Bmatrix} \quad (3.9)$$

where A, B, D, and D_c are the time dependent modal excitation functions, and [Φ_x], [Φ_{xθ}]
[Φ_y], [Φ_{yθ}], [Φ_z], [Φ_{zθ}] are the matrix containing the orthonormal modes of the corresponding
rotor system. Similarly, for the casing structure,

$$\{W_c\} = \begin{Bmatrix} [\Phi_{cx}] \{A_c\} \\ [\Phi_{cx\theta}] \{A_c\} \\ [\Phi_{cy}] \{B_c\} \\ [\Phi_{cy\theta}] \{B_c\} \\ [\Phi_{cz}] \{D_c\} \\ [\Phi_{cz\theta}] \{D_c\} \end{Bmatrix} \quad (3.10)$$

Pre-multiplying the generalized equation of motion by the orthonormal modes, and using the orthogonality condition developed in the previous section, the equation for the rotor system (2.1) can be transformed into the modal coordinates as:

$$[\bar{I}] \{\ddot{Z}\} + [\bar{G}_v] \{\dot{Z}\} + [\bar{G}_A] \{Z\} + [\bar{C}_b] \{\dot{Z}\} - [\bar{K}_b - \bar{K}_A] \{Z\} + [\Phi]^T [C_b] [\Phi_c] \{\dot{Z}_c\} + [\omega^2] \{Z\} - [\Phi]^T [K_b] [\Phi_c] \{Z_c\} = [\Phi]^T \{F(t) + F_G(t) + F_c(t)\} \quad (3.11)$$

and for the casing (Eq. 2.3) as

$$[\bar{I}] \{\ddot{Z}_c\} + [\bar{C}_c] \{\dot{Z}_c\} + [\omega_c^2] \{Z_c\} + [\bar{K}_b] \{Z_c\} + [\bar{C}_b] \{\dot{Z}_c\} - [\Phi_c]^T [K_b] [\Phi] \{Z\} - [\Phi_c]^T [C_b] [\Phi] \{\dot{Z}\} = [\Phi_c]^T \{F_c(t)\} \quad (3.12)$$

where

$$\{Z\} = \begin{Bmatrix} \{A\} \\ \{B\} \\ \{D\} \\ \{D_c\} \end{Bmatrix} \quad \{Z_c\} = \begin{Bmatrix} \{A_c\} \\ \{B_c\} \\ \{D_c\} \end{Bmatrix} \quad (3.13)$$

Note that in equations (3.11 and 3.12) the modal acceleration terms \ddot{Z} and \ddot{Z}_c for the rotor and the casing are uncoupled and can be evaluated by solving the set of simultaneous matrix equations.

4. NUMERICAL SOLUTION PROCEDURES

To evaluate the transient dynamics of the rotor-casing system, the modal equations (3.11 and 3.12) are rewritten as:

$$[I]\{\ddot{Z}\} = [\bar{G}_v]\{\dot{Z}\} - [\bar{G}_A]\{Z\} - [\bar{C}_b]\{\dot{Z}\} + [\bar{K}_b - \bar{K}_A]\{Z\} - [\Phi]^T[C_b][\Phi_c]\{\dot{Z}_c\} - [\omega^2]\{Z\} + [\Phi]^T[K_b][\Phi_c]\{Z_c\} + [\Phi]^T\{F(t) + F_G(t) + F_s(t)\} \quad (4.1)$$

and for the casing

$$[I]\{\ddot{Z}_c\} = [\bar{C}_c]\{\dot{Z}_c\} - [\omega_c^2]\{Z_c\} - [\bar{K}_b]\{Z_c\} - [\bar{C}_b]\{\dot{Z}_c\} + [\Phi_c]^T[K_b][\Phi]\{Z\} + [\Phi_c]^T[C_b][\Phi]\{\dot{Z}\} + [\Phi_c]^T\{F_c(t)\} \quad (4.2)$$

Using the appropriate initial conditions for the modal velocity $\{\dot{Z}\}$ and displacement $\{Z\}$, the modal accelerations $\{\ddot{Z}\}$ can be solved. The solution procedure for the algorithm is given as follows.

1. Input Initial Conditions to Calculate Modal Accelerations
2. Use Variable Time-stepping Integration Scheme to Evaluate Modal Velocity and Displacement at next time step.
3. Calculate Velocity and Displacement in Generalized Coordinates.

4. Calculate Nonlinear Gear Mesh Forces due to Relative Motion Between the Two Gears.
5. Calculate Bearing Forces due to Relative Motion Between the Rotor and the Casing.
6. Calculate Modal Bearing and Gear Forces.
7. Repeat from Step No. 2.

5. EXPERIMENTAL STUDIES

Test results from the gear noise test rig, Fig. 5.1, at NASA Lewis Research Center were used in this study to refine and validate the global dynamic model developed. Three phases of experimental studies were performed, namely; i) the determination of static modal characteristics using the impulse-response technique; ii) the transient vibration of both rotor and the gear box structure during operation; and iii) the noise production at the gear box surfaces. An outline of the experimental studies are presented below:

5.1 Evaluation of Experimental Modal Characteristics

The gear transmission system used in this test is shown in Fig. 5.2. The gear system consists of a pair of identical parallel axis gears supported by rolling element bearings. The surface of the gear box structure is segmented into 116 nodal points. The impulse-response technique was used to determine the transfer functions of the system. An impact hammer was applied at various nodes on the surface of the gearbox. Three accelerometers, one on a surface in the x-direction, another in the y-direction, and the last in the z-direction, were used to obtain the resulting responses from the impacts. Natural frequencies and their corresponding mode shapes excited during the experiment were evaluated using a two channel dynamic signal analyzer with a PC-based modal software. The modal characteristics

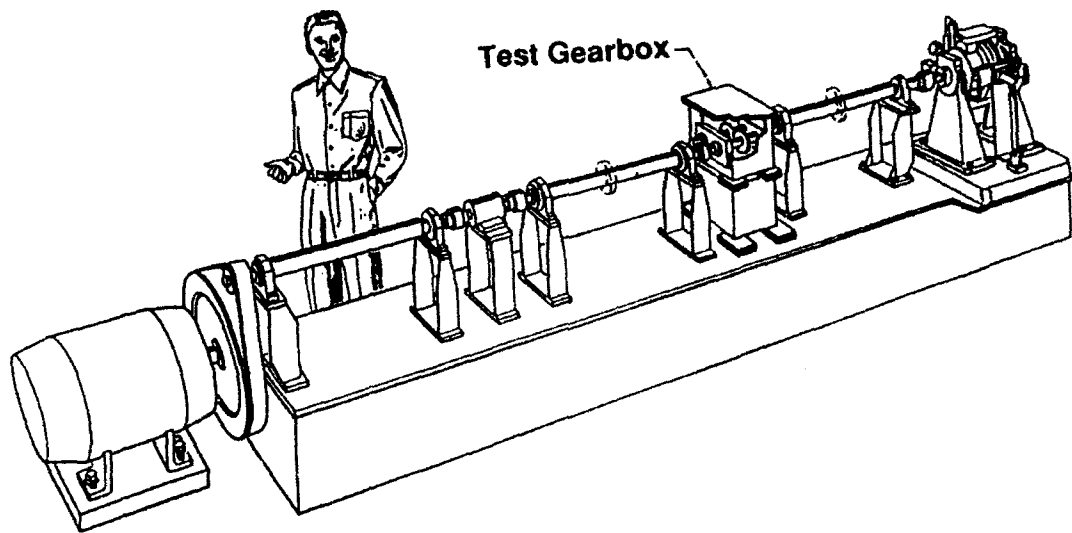


Figure 5.1 Schematic of NASA Gear Noise Rig

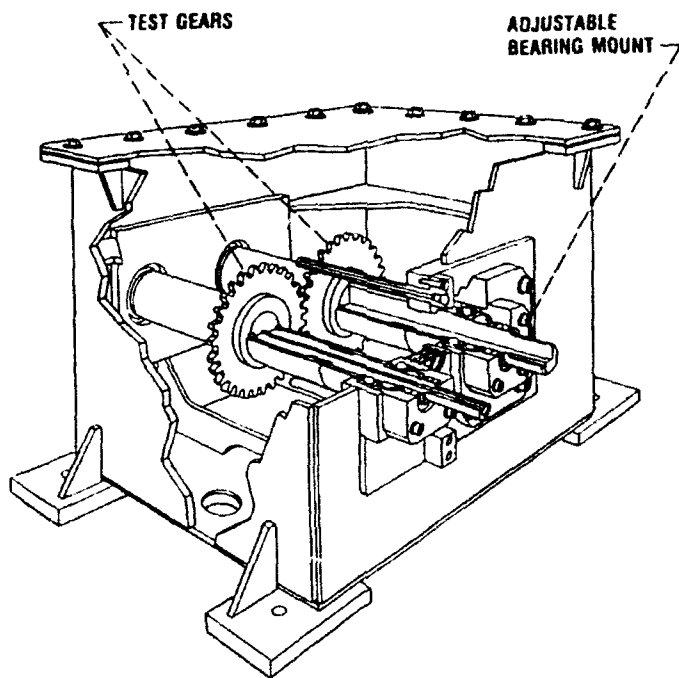


Figure 5.2 Drawing of NASA Test Gearbox

found during the experiment were compared to those generated by the numerical model for verification purposes, as well as for the selection of numerically modelled mode shapes.

5.2 Experimental Investigations of System Dynamics

To study the dynamics of the system during operation, a 150kW(200 Hp) variable speed electric motor is used to power the rig at one end. An eddy-current dynamometer is used for power absorbing at the opposite end. The parameters of the test gears are given in Table 5.1. During this test, several accelerometers were placed on the x, y, and z surfaces of the gear box to monitor the vibrations of the gear box structure. In addition, two sets of non-contacting proximitors were placed inside the gear box at locations next to the gear mesh to monitor the vibrations of the two rotor systems. The vibration signals of the gear box surface and the rotors were recorded over a range of operating speeds from 1500 to 6000 rpm. A two channel dynamic signal analyzer was used to compute the frequency spectra (waterfall diagram) of the vibrations of the gear box in x, y, and z directions. The frequency spectra for the lateral vibrations of the rotor at the gear locations were also computed. The results of this phase of the experimental work was compared to those from the numerical model for verification of the numerical procedure and improvement of the numerical modelling of the gear transmission components (bearing model, gear mesh model, rotor model, gear box model, etc.).

5.3 Experimental Investigations of Gear Box Noise

To investigate the relationship between the gear box vibration and the noise, a special noise test program was introduced. A special set of identical parallel axis gears (25 tooth) were used in this test. While the vibration measurement set-up is very similar to those mentioned in the previous section (5.2), two additional acoustic microphones were used in

this experiment. Both microphones were placed over the top cover of the gear box with one in the vertical direction and the other at a 45 degree angle from the vertical. Rotor vibration, gear box vibration, and the resulting noise was obtained while operating at various running speeds. A correlation between the gear box vibrations and the noise level was performed in the frequency domain using linear transfer and cross-correlation functions. The Nonlinear Hypercoherence function [Jong 1986] developed at NASA Marshall Space Flight Center was also used to generate a relationship between the noise and the vibration data in order to develop a noise prediction algorithm for the global dynamic model.

TABLE 5.1 - TEST GEAR PARAMETERS

Gear Type	Standard involute, full-depth tooth
Number teeth	28
Module, mm (diametral pitch in. ⁻¹)	3.174 (8)
Face width, mm (in.)	6.35 (0.25)
Pressure angle, deg	20
Theoretical contact ratio	1.64
Driver modification amount, mm (in.)	0.023 (0.0009)
Driven modification amount, mm (in.)	0.025 (0.0010)
Driver modification start, deg	24
Driven modification start, deg	24
Tooth-root radius, mm (in.)	1.35 (0.053)
Gear quality	AGMA class 13
Nominal (100 percent) torque, N-min(in.-lb)	71.77 (635.25)

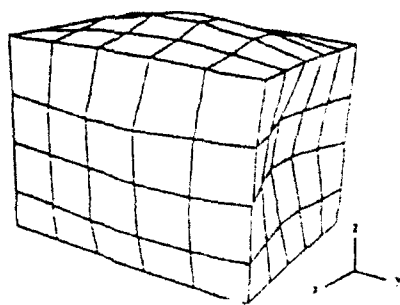
6. CORRELATION AND BENCHMARKING OF SYSTEM DYNAMICS BY NUMERICAL PROCEDURES WITH EXPERIMENTAL RESULTS

This chapter presents the correlation between the numerical simulations of the dynamics of the gear transmission system with the experimental results. Three major phases of the system dynamics were examined, namely; i) the gear box modal characteristics, ii) the dynamics of the rotor-gear systems, and iii) the vibration of the gear box structure. A detailed comparison and benchmarking of the results are given in the following sections.

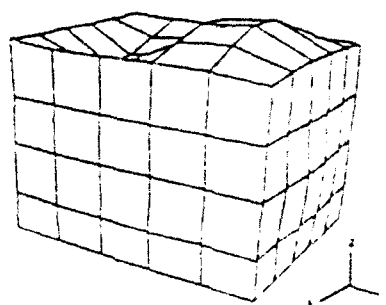
6.1 Gear Box System modal Characteristics

To experimentally determine the modal characteristics of the gear box structure, the impact testing technique described in the previous chapter was applied to obtain the natural frequencies and mode shapes of the system. During this test, a total of 8 major vibratory modes were excited between a frequency range of 0 to 3000 Hz. The excited natural frequencies and their corresponding mode shapes are shown in Fig. 6.1.

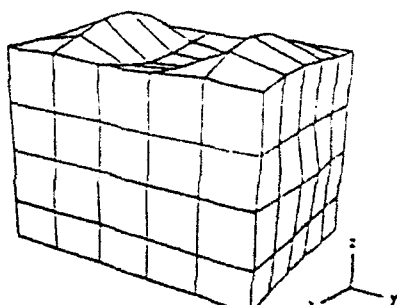
The experimentally obtained modes, shown in Fig. 6.1, represent the major vibration modes of the gear noise rig in the 0 to 3 kHz region. Although these modal frequencies are only a small part of the total modes of the system, they represent a major part of the total global vibration of the system. In order to produce an accurate analytical simulation of the test gearbox, a similar set of modes were generated using a finite element model (NASTRAN) of the gear box structure. Out of a total of 25 modes existing in the analytical model in the 0 to 3 kHz frequency region, the eight dominant modes were used to represent the gear box dynamic characteristics. These analytically simulated modes are shown in Fig. 6.2. As shown in Table 6.1, the natural frequencies of the simulated modes are within 5 percent of the measured modes. The three-dimensional analytical mode shapes are very



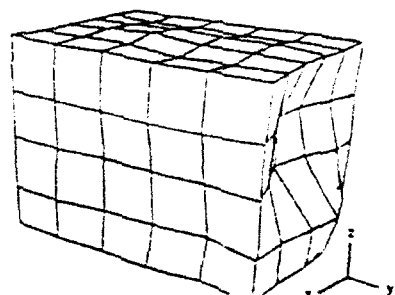
Mode 1 (658.37 Hz)



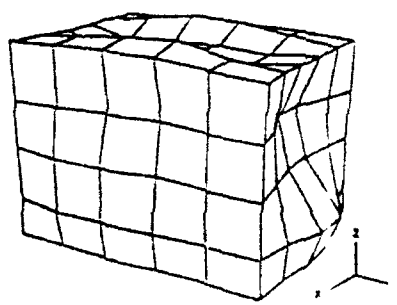
Mode 2 (1048.56 Hz)



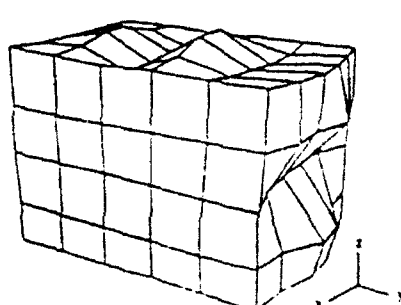
Mode 3 (1709.77 Hz)



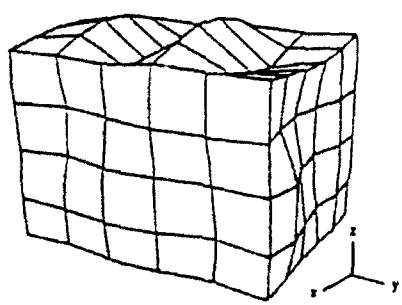
Mode 4 (1999.95 Hz)



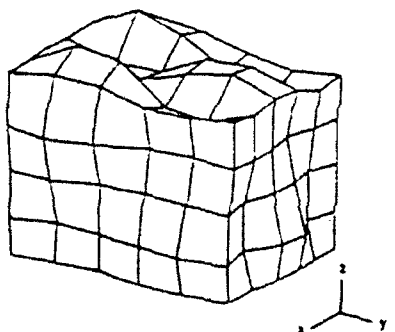
Mode 5 (2275.69 Hz)



Mode 6 (2535.77 Hz)



Mode 7 (2722.16 Hz)



Mode 8 (2961.71 Hz)

Figure 6.1 Experimentally Determined Mode Shapes of the Gear Box (0 to 3000 Hz)

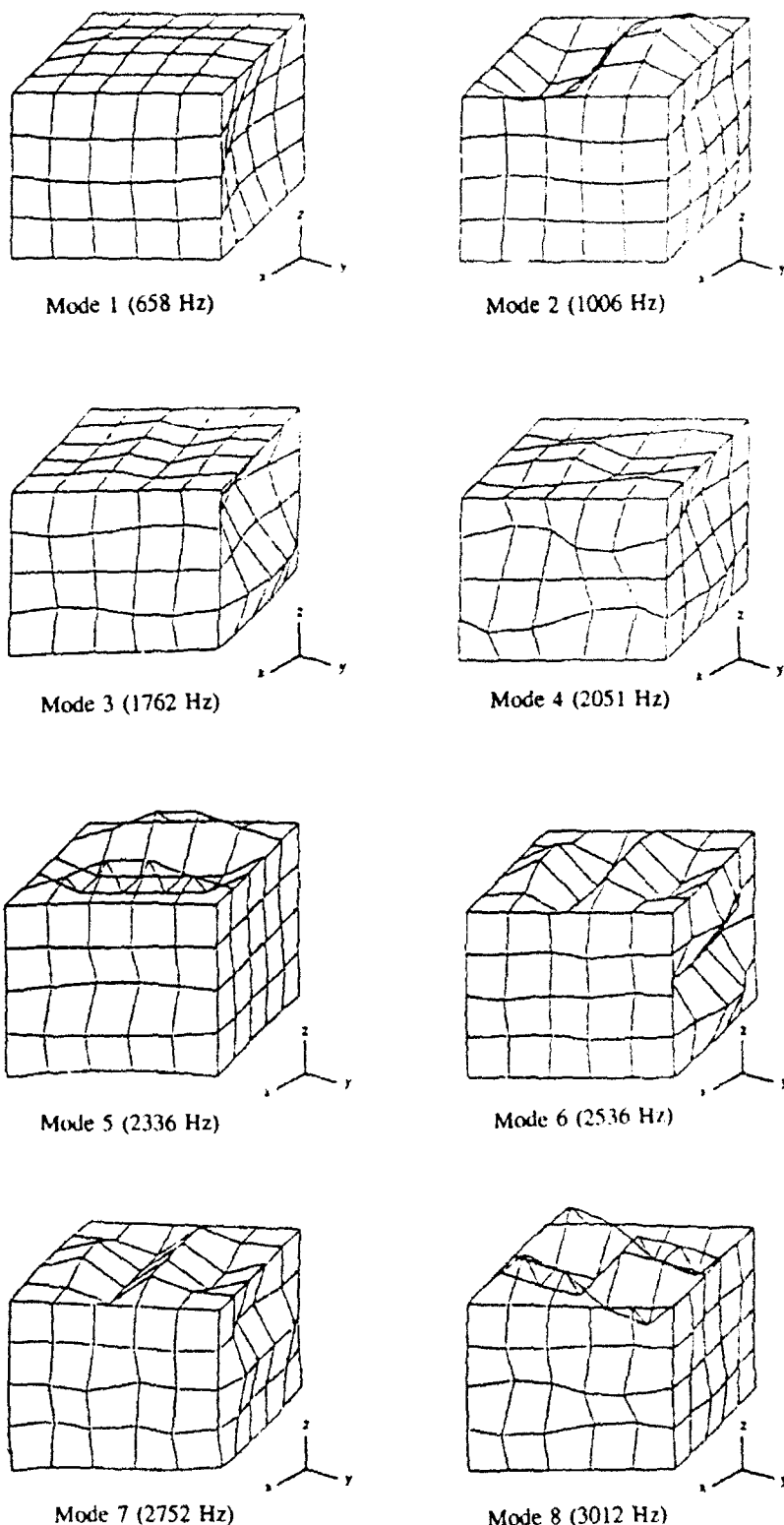


Figure 6.2 Analytically Determined Mode Shapes of the Gear Box
(0 to 3000 Hz)

similar to the experimental modes shapes (Fig. 6.1). The correlation of the results between the analytical model and the experimental measurements confirms the accuracy of the dynamic representation of the test gear box using only a limited amount of modes. In addition, this correlation of the experimental modal characteristics with the numerical model also helps to reduce the number of modes being used in the numerical simulation to achieve an accurate result.

6.2 Rotor-Bearing-Gear Transient Vibrations

For the dynamic study of the rotor-bearing system, it was found that, during a slow roll (low speed run) of the rotor-gear assembly, a substantial residual bow exists in the rotor system as shown by its large orbital motion given in Fig. 6.3. Figure 6.3A represents the orbit of the driver rotor at the gear location and Fig. 6.3B represents those of the driven rotor. Note that the circular orbit existed in the driver rotor at slow roll represents the residual bow deformation of the rotor. The elliptical orbit in the driven rotor is due to a combination of the residual bow effects and the vertical gear force from the torque of the driving rotor. In order to analytically simulate the influence of this effect, a residual bow of 2 mils (0.05 mm) is incorporated into the numerical model.

To numerically simulate the dynamics of the rotor-bearing-gear system, the model shown in Fig. 6.4 was used. Figures 6.5 - 6.14 show the comparison of the rotor orbital motion between the numerical simulations and experimental studies for a range of operating speeds from 1500 - 6000 rpm, with a 500 rpm increment. In these figures (6.5 - 6.14), stage 1 represents the motion of the driving rotor near the gear mesh and stage 2 represents the driven rotor

**TABLE 6.1 - COMPARISON OF EXPERIMENTAL
MEASURED AND ANALYTICAL MODELED NATURAL FREQUENCIES**

Experimental, Hz	Analytical, Hz	Difference, percent
658	658	0
1049	1006	-4.1
1710	1762	3.0
2000	2051	2.6
2276	2336	2.6
2536	1536	0
2722	2752	1.1
2962	3012	1.7

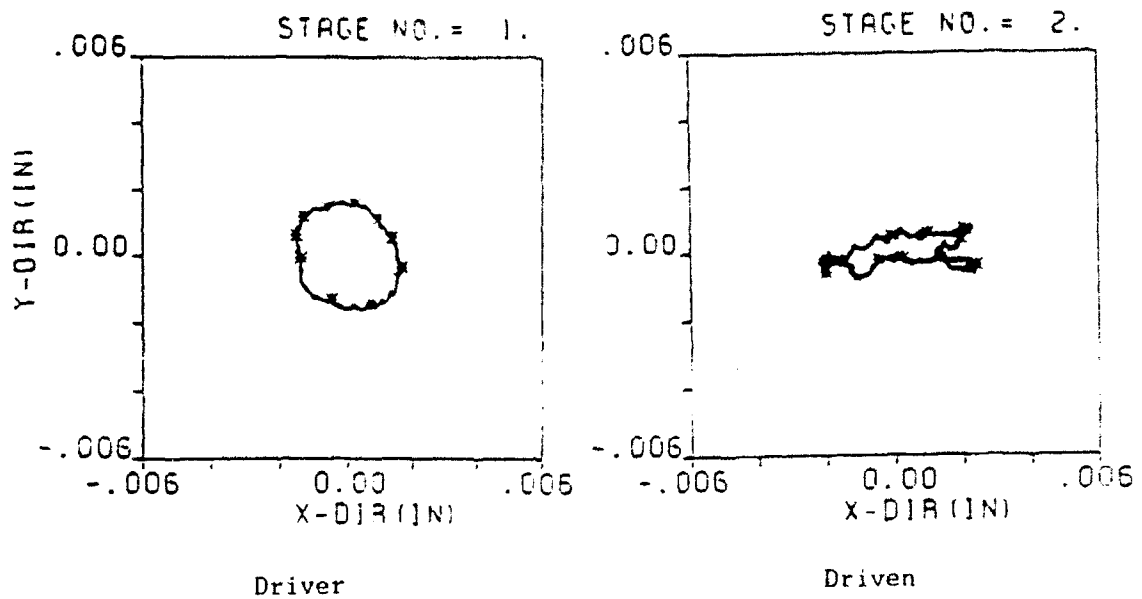


Figure 6.3 Orbital Motion of the Driver and the Driven Rotors During Slow Roll from Experimental Study

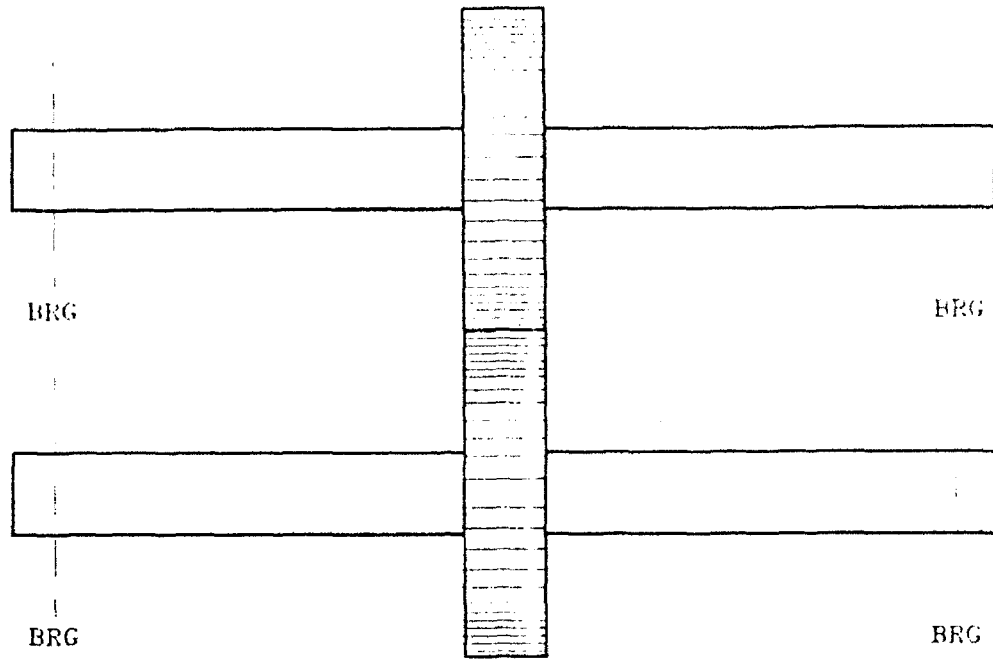


Figure 6.4 Schematic of Rotor-Gear-Bearing Model

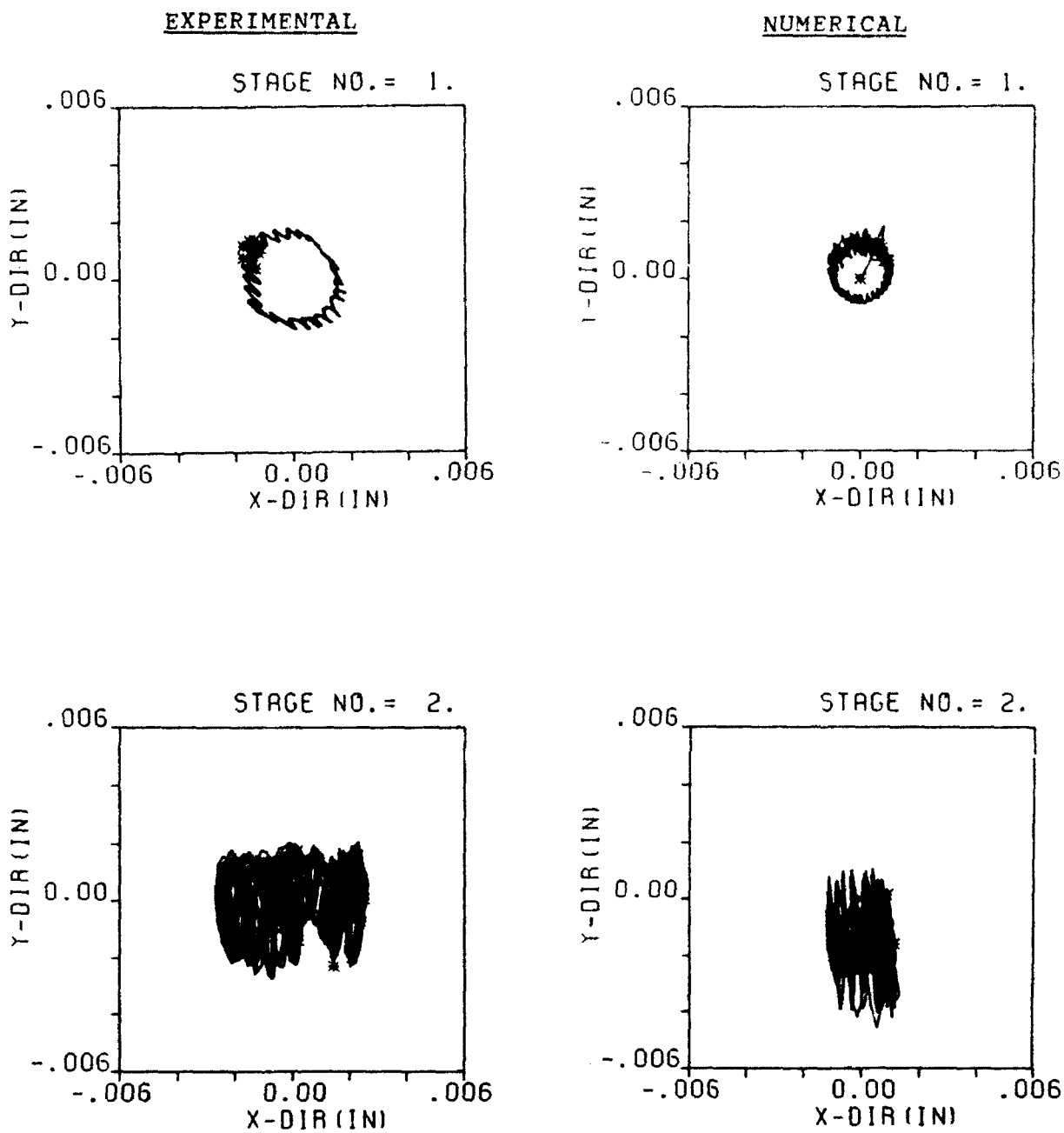


Figure 6.5 Orbital Motion of the Driver and the Driven Rotors from Experimental Study and Numerical Simulation at 1500 rpm

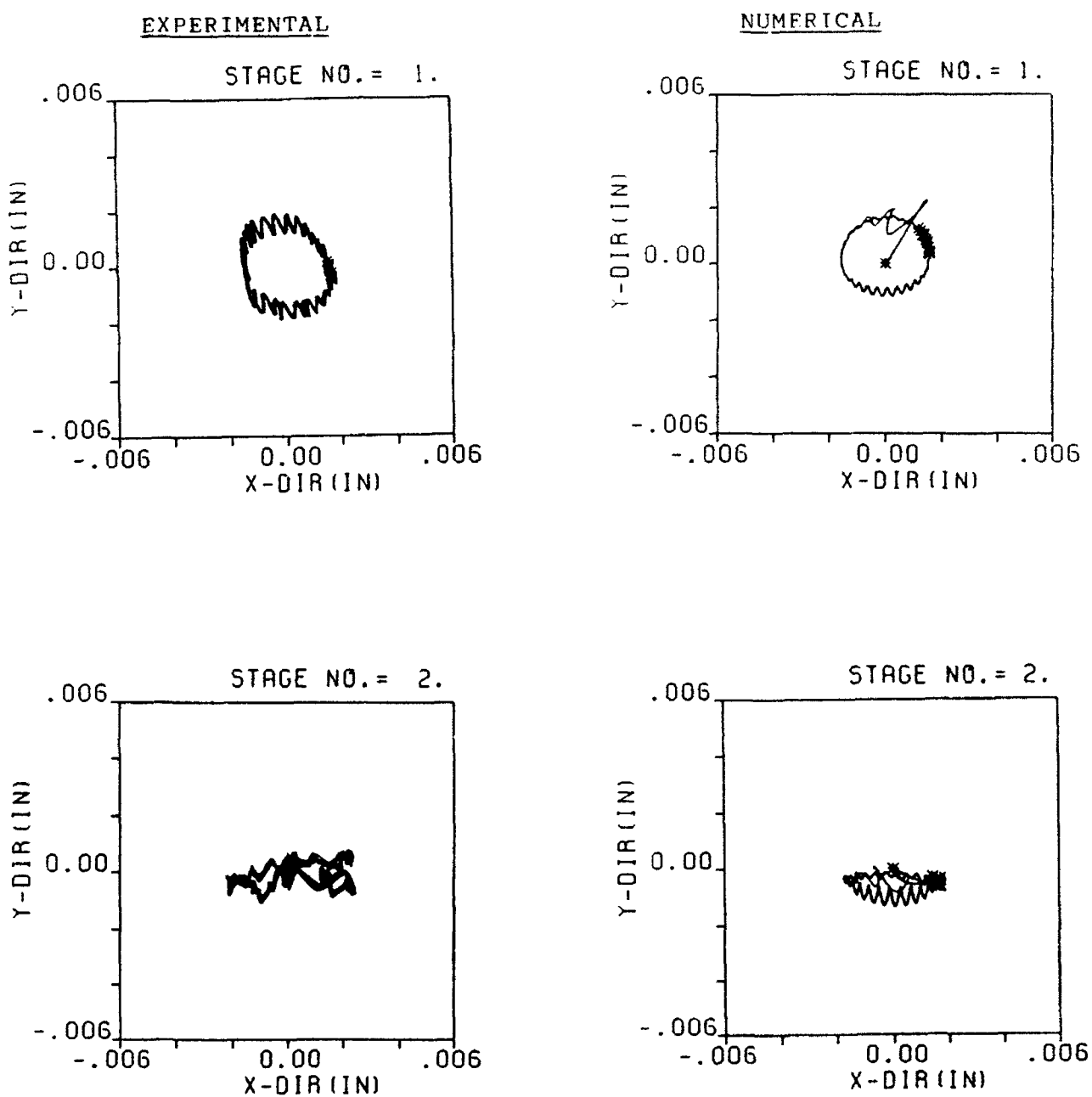
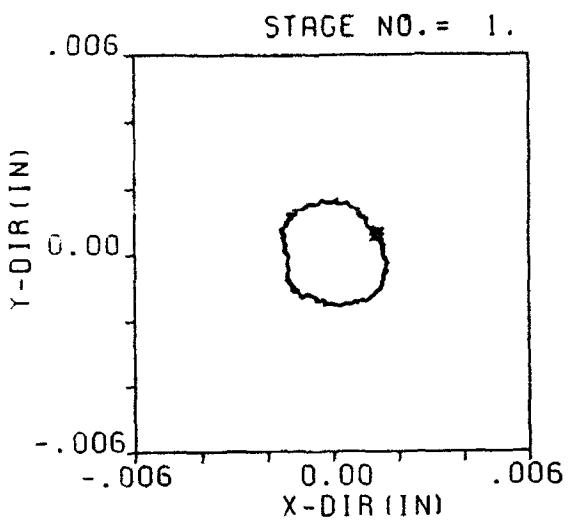
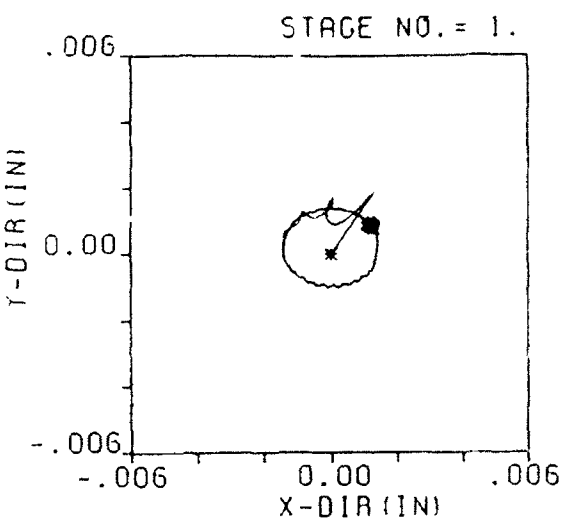


Figure 6.6 Orbital Motion of the Driver and the Driven Rotors from Experimental Study and Numerical Simulations at 2000 rpm

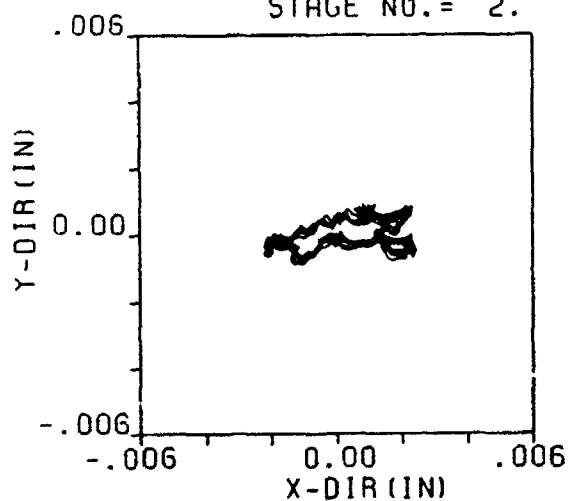
EXPERIMENTAL



NUMERICAL



STAGE NO. = 2.



STAGE NO. = 2.

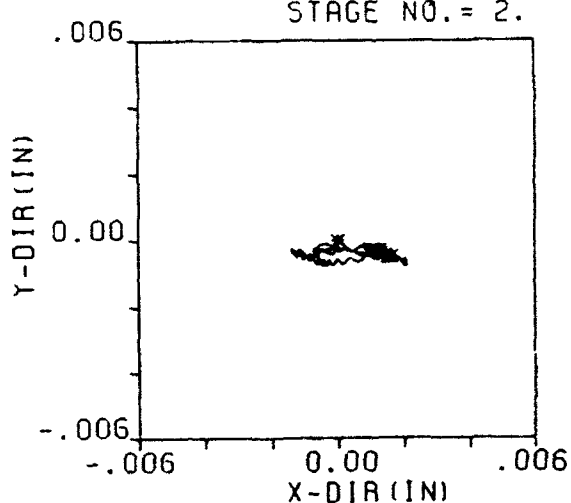
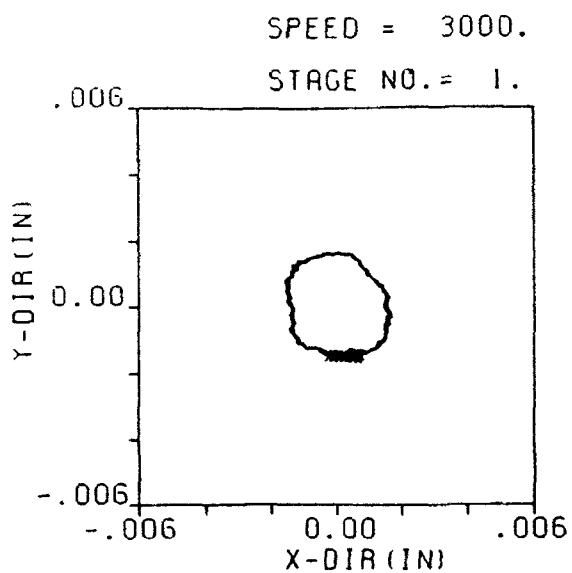
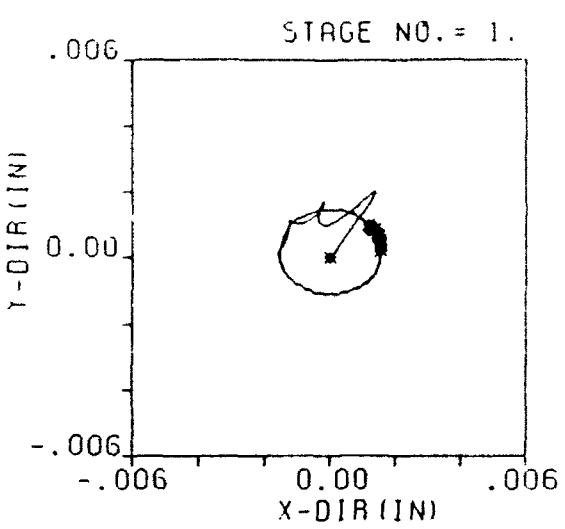


Figure 6.7 Orbital Motion of the Driver and the Driven Rotors from Experimental Study and Numerical Simulation at 2500 rpm

EXPERIMENTAL

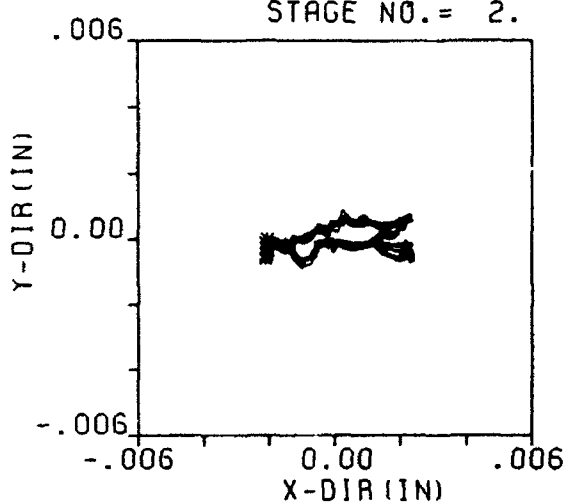


NUMERICAL



SPEED = 3000.

STAGE NO. = 2.



STAGE NO. = 2.

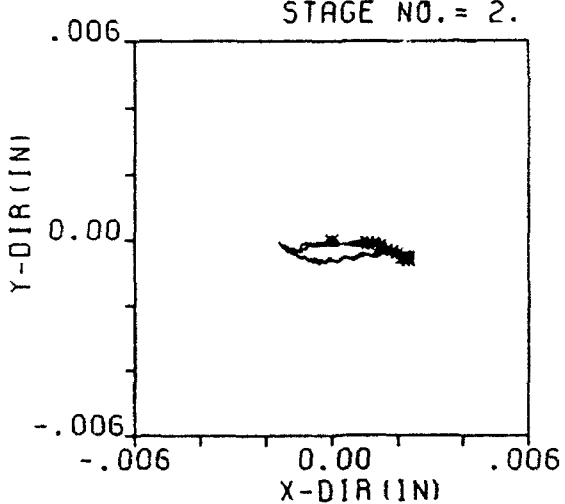
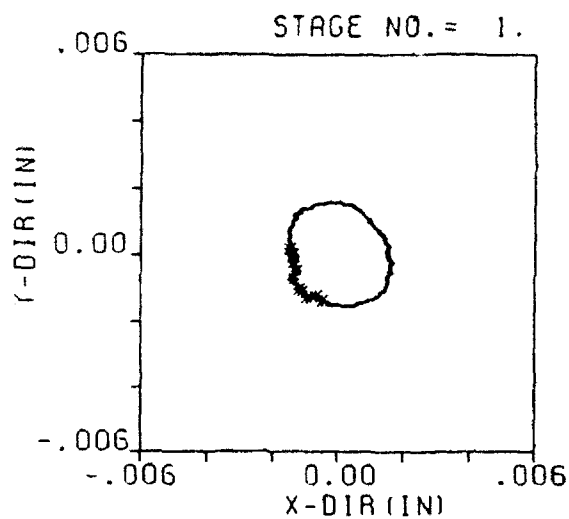
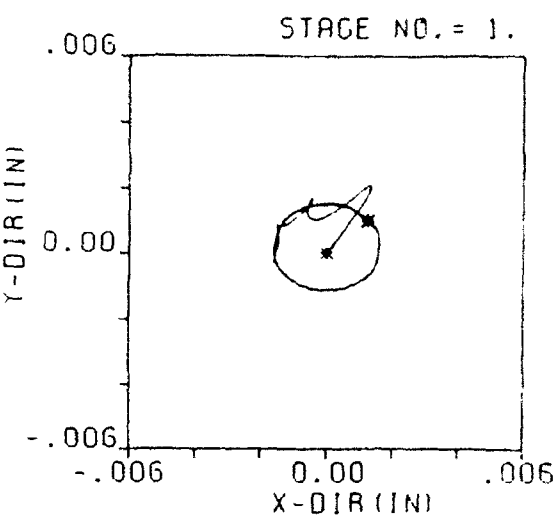


Figure 6.8 Orbital Motion of the Driver and the Driven Rotors from Experimental Study and Numerical Simulation at 3000 rpm

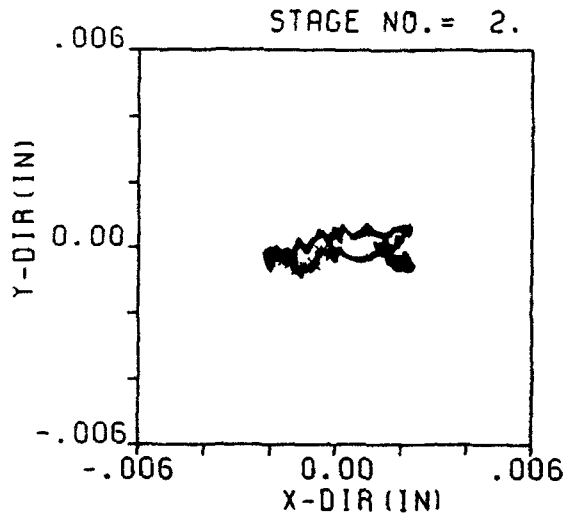
EXPERIMENTAL



NUMERICAL



STAGE NO. = 2.



STAGE NO. = 2.

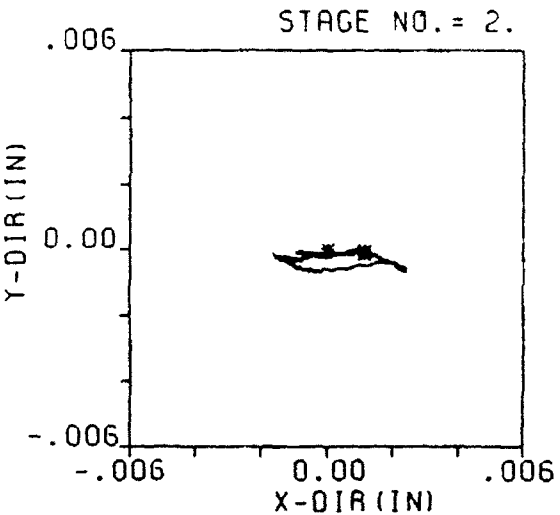
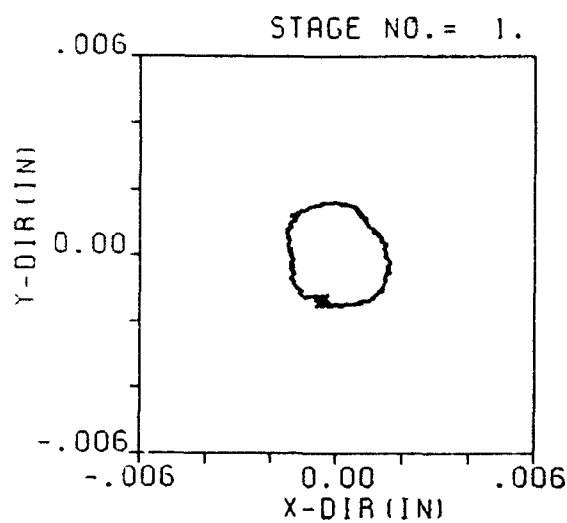
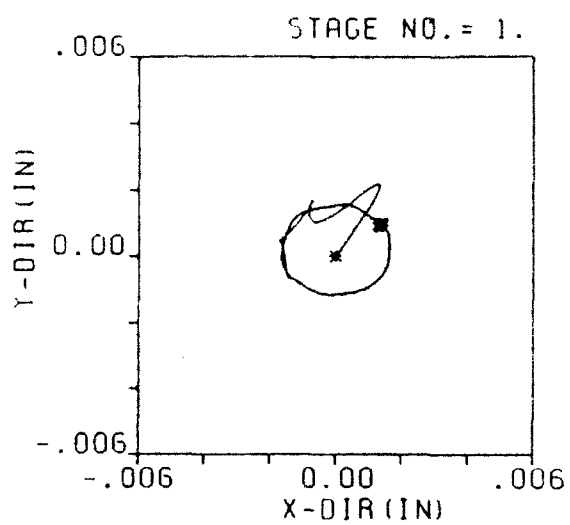


Figure 6.9 Orbital Motion of the Driver and the Driven Rotors from Experimental Study and Numerical Simulations at 3500 rpm

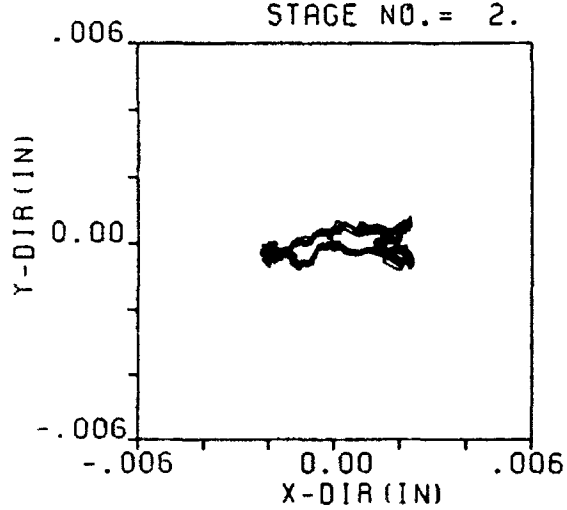
EXPERIMENTAL



NUMERICAL



STAGE NO. = 2.



STAGE NO. = 2.

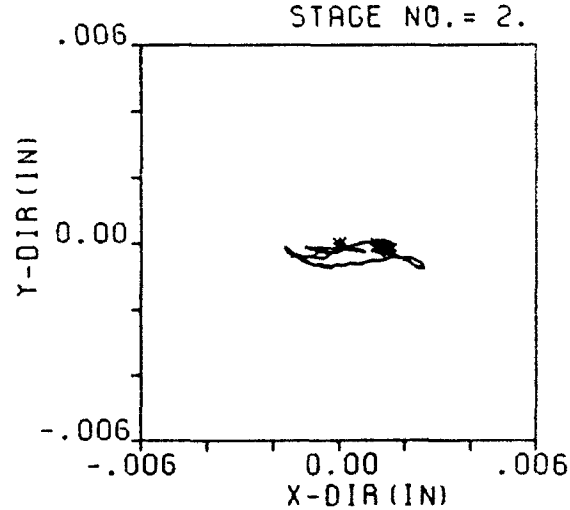
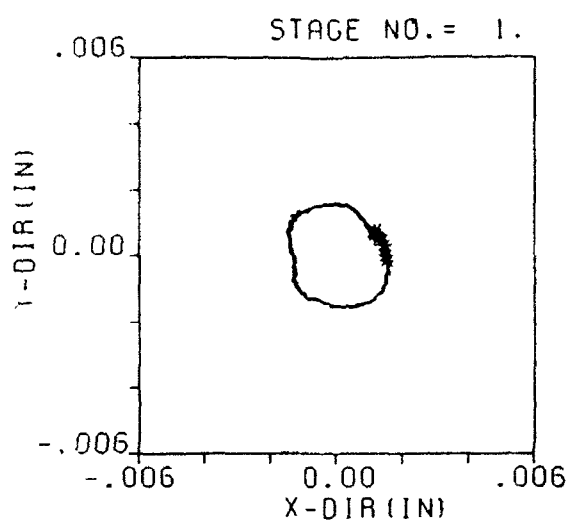
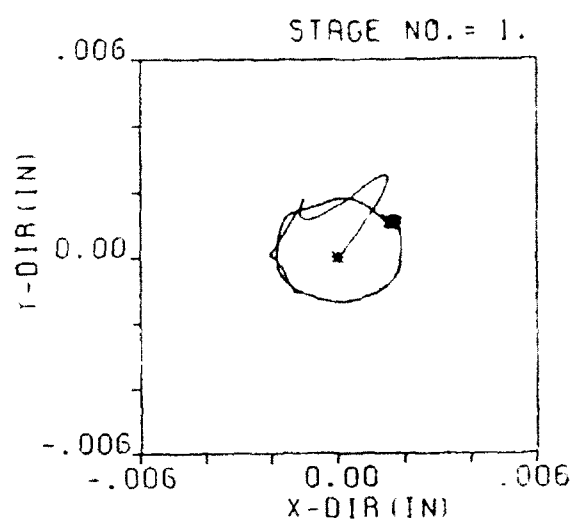


Figure 6.10 Orbital Motion of the Driver and the Driven Rotors from Experimental Study and Numerical Simulations at 4000 rpm

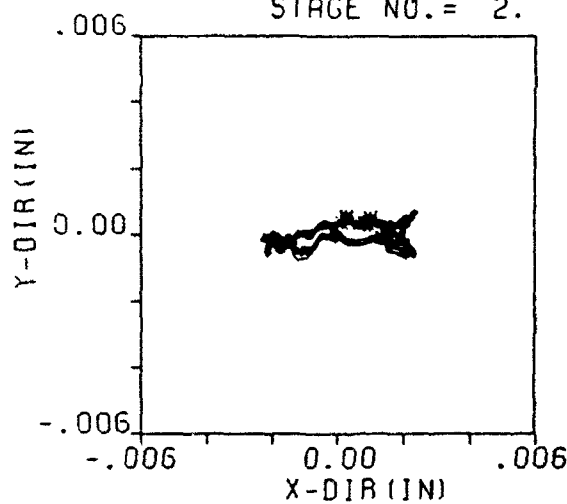
EXPERIMENTAL



NUMERICAL



STAGE NO. = 2.



STAGE NO. = 2.

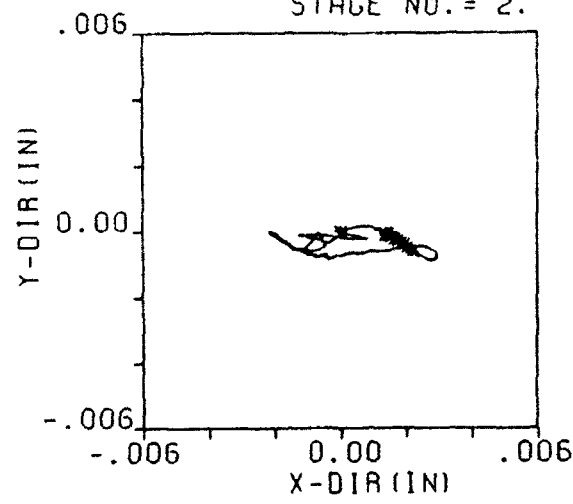
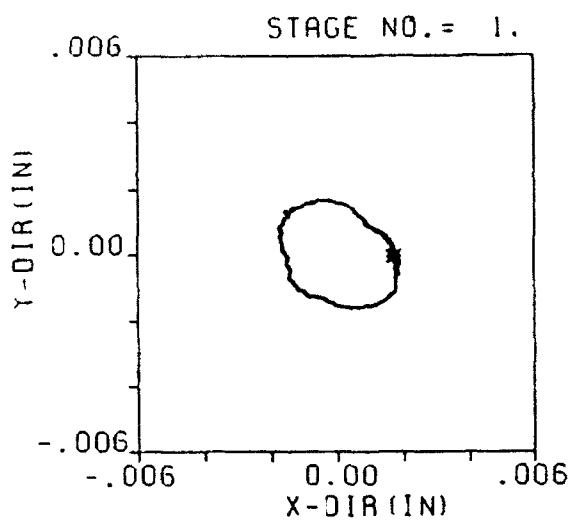
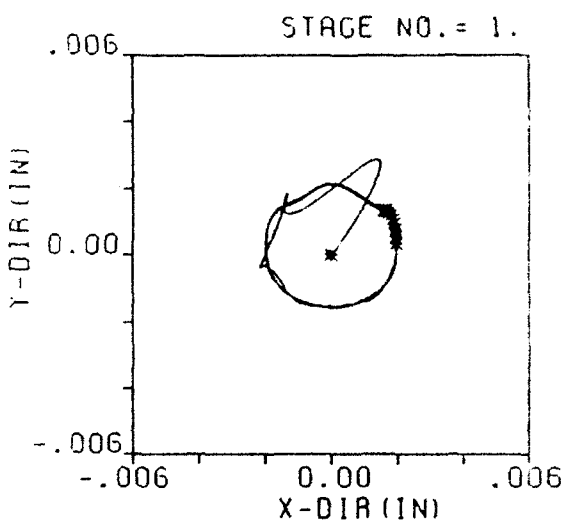


Figure 6.11 Orbital Motion of the Driver and the Driven Rotors from Experimental Study and Numerical Simulations at 4500 rpm

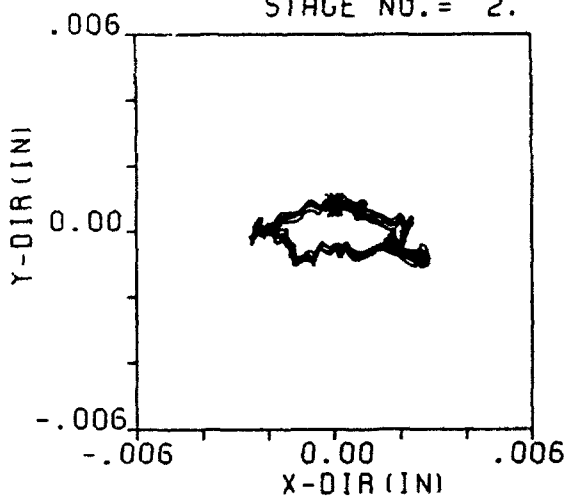
EXPERIMENTAL



NUMERICAL



STAGE NO. = 2.



STAGE NO. = 2.

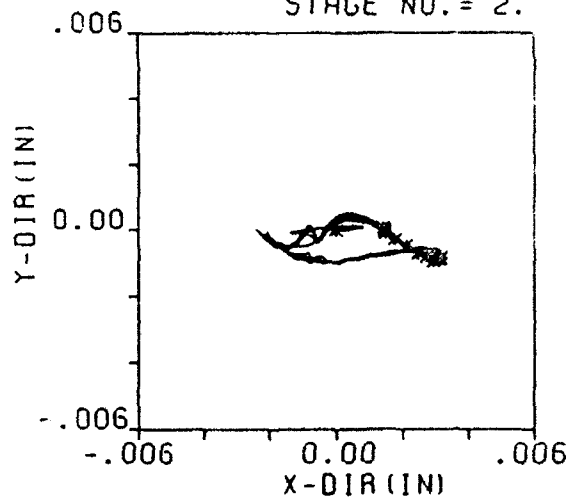
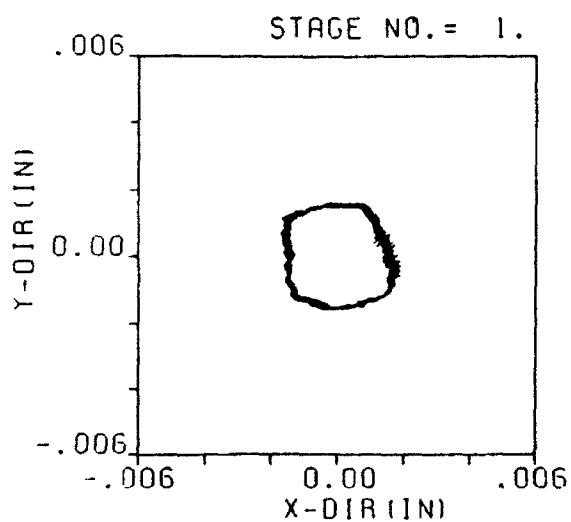
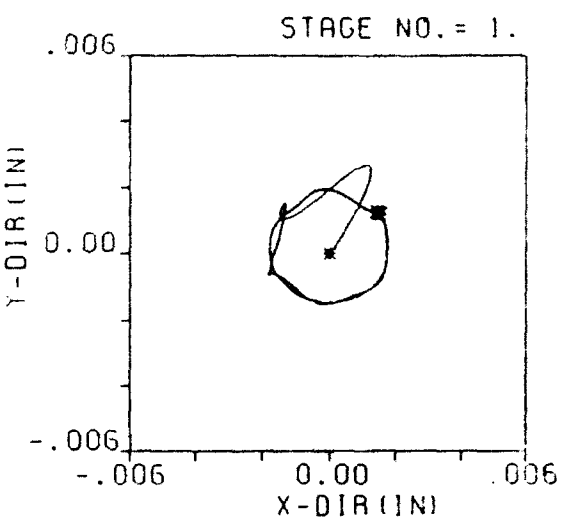


Figure 6.12 Orbital Motion of the Driver and the Driven Rotors from Experimental Study and Numerical Simulations at 5000 rpm

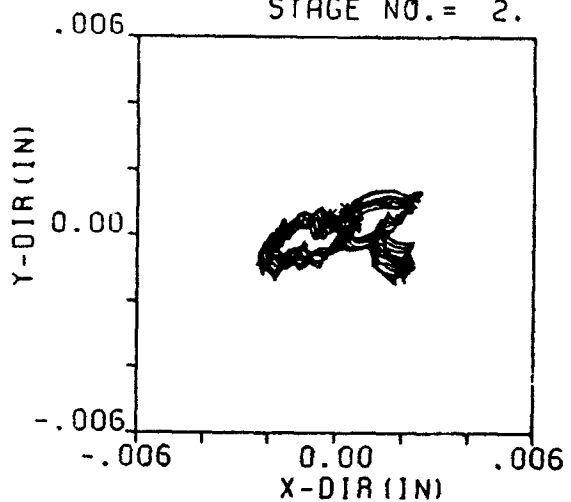
EXPERIMENTAL



NUMERICAL



STAGE NO. = 2.



STAGE NO. = 2.

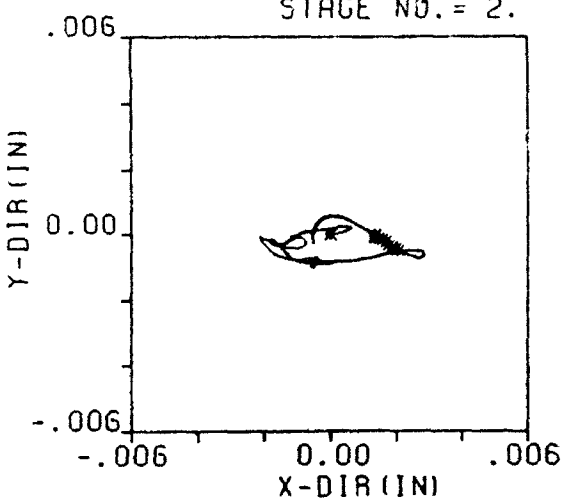
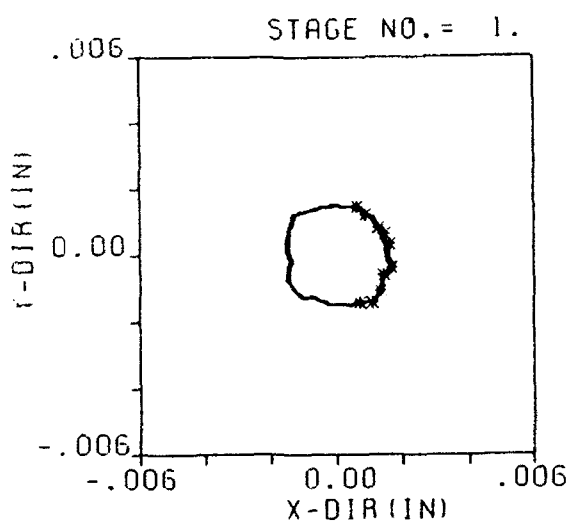
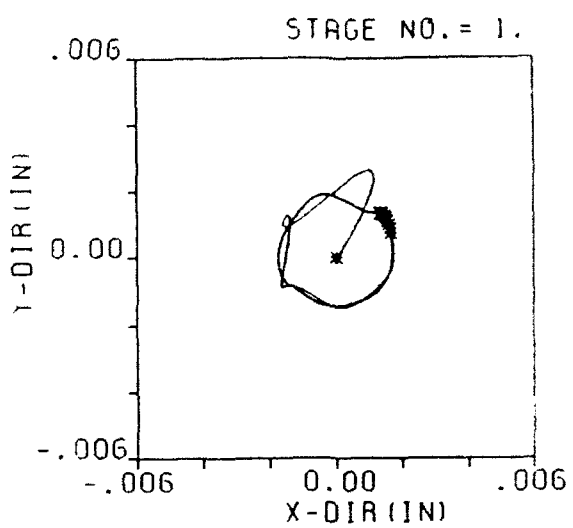


Figure 6.13 Orbital Motion of the Driver and the Driven Rotors from Experimental Study and Numerical Simulations at 5500 rpm

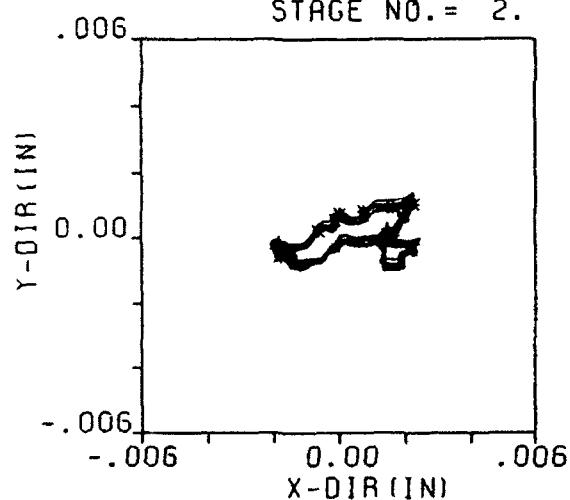
EXPERIMENTAL



NUMERICAL



STAGE NO. = 2.



STAGE NO. = 2.

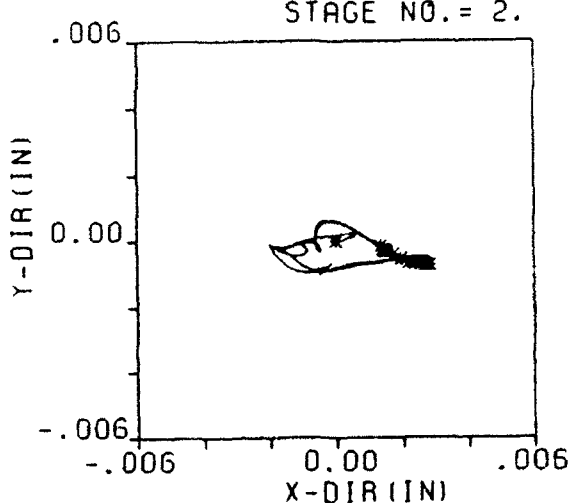


Figure 6.14 Orbital Motion of the Driver and the Driven Rotors from Experimental Study and Numerical Simulations at 6000 rpm

near the gear mesh. Note that a substantial magnitude of the circular orbit in the driver rotor represents the residual bow deformation of the rotor. The elliptical orbit in the driven rotor is attributed to a combination of the residual bow effects and the normal gear force from the torque of the driving rotor. The slightly large amplitudes of orbital motion existing at running speeds of 1500 rpm and 5000 rpm are due to the excitation frequencies being closed to one of the natural frequencies of the rotor system. Very similar trends in orbital shapes and magnitudes were observed in both the experimental and numerical studies, which verifies the validity of the numerical procedures as well as the modelling accuracy. Figure 6.15 and 6.16 represent frequency spectra of the vibration generated from both the experimental and the numerical procedures. The excellent agreement in both results further verifies the validity of the numerical study.

6.3 Gear Box Transient Dynamics

In order to predict the noise of the transmission system during operation, the vibration of the gear box must be accurately modelled. In this section, the comparison between experimental and predicted gear box vibrations is presented.

Figure 6.17, 6.18, and 6.19 present the vibration frequency spectra of the gear box surface from both experimental and numerical studies, in the x, y, and z directions, respectively.

Note in Fig. 6.17A, the experimental results of the casing vibration in the x-direction shows a major vibration component at 28 times the shaft frequency. This is due to the excitation of the gear tooth pass frequency (28 tooth gear) at the various shaft speeds. A closer examination of this excited frequency component shows that two major vibration peaks

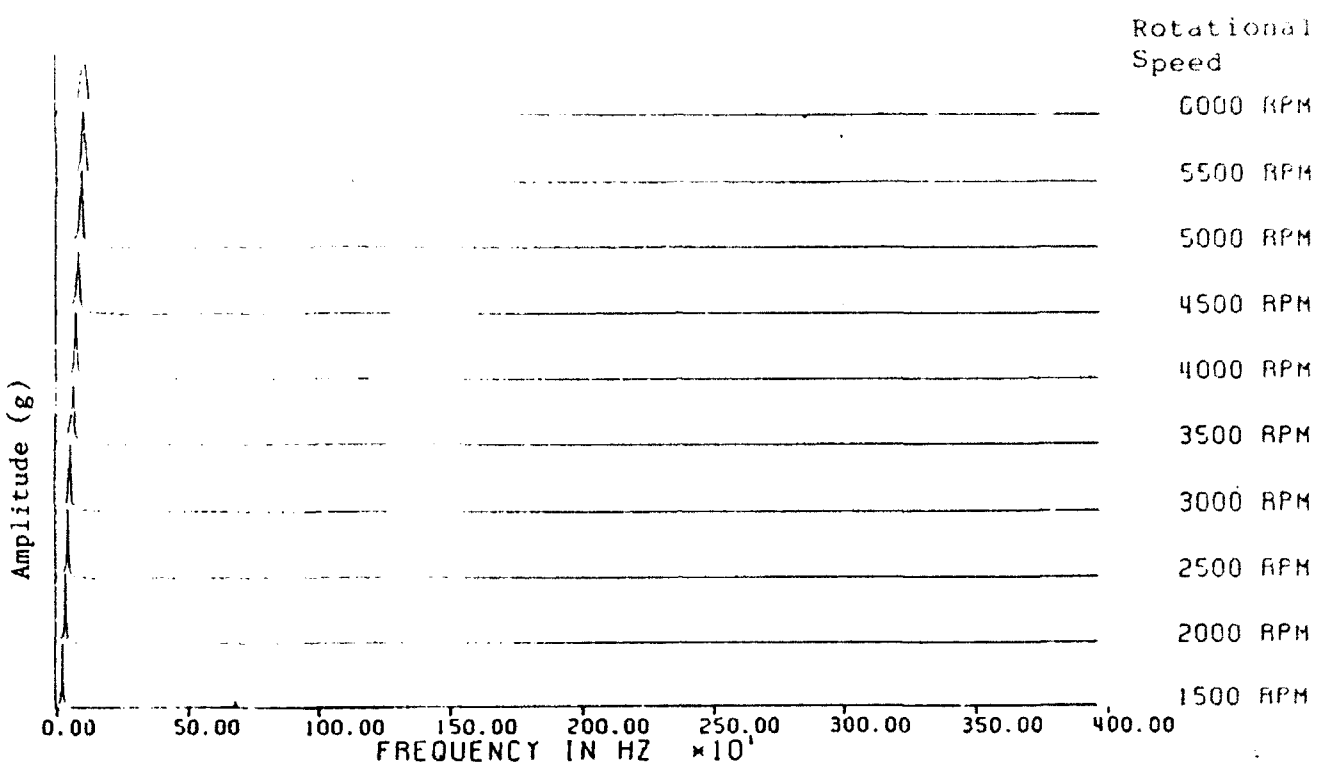


Figure 6.15A Frequency Spectra of the X-direction Vibration of the 1st Rotor from Experimental Study

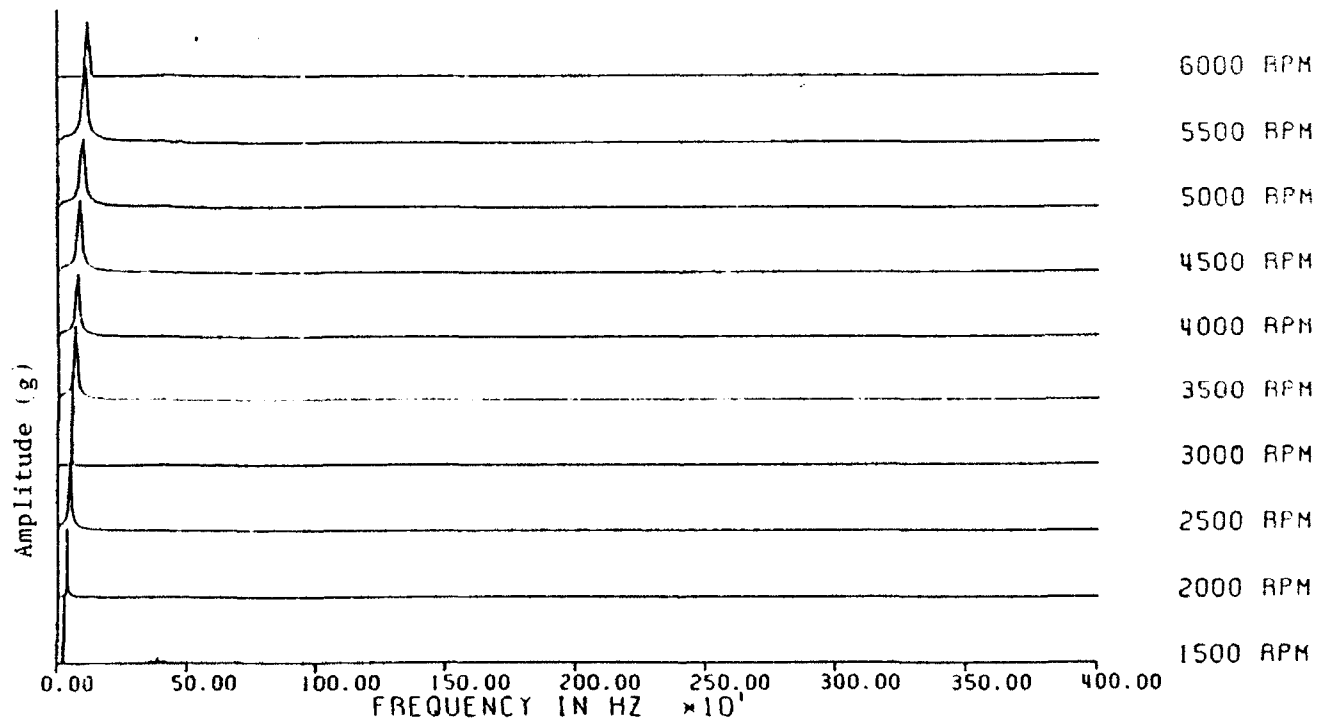


Figure 6.15B Frequency Spectra of the X-direction Vibration of the 1st Rotor from Numerical Simulation

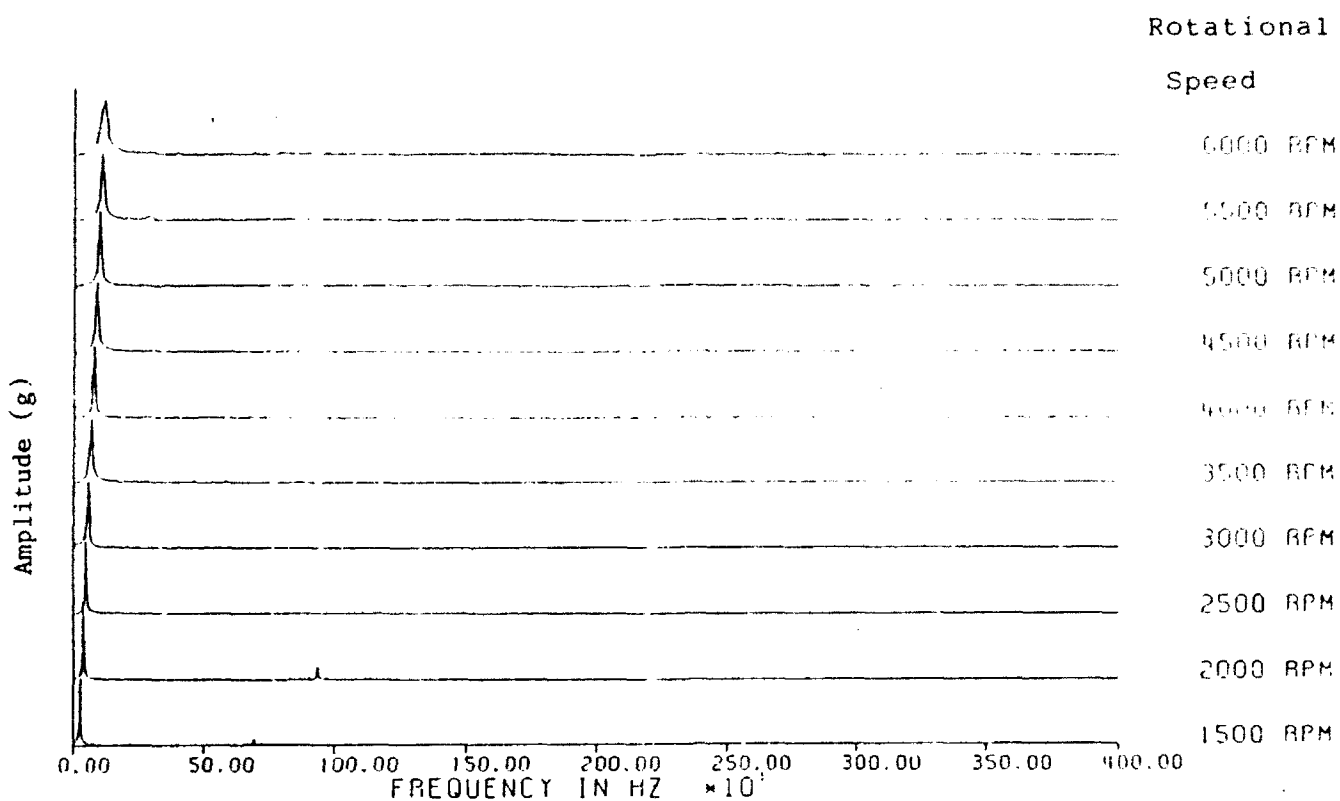


Figure 6.15C Frequency Spectra of the Y-direction Vibration of the 1st Rotor from Experimental Study

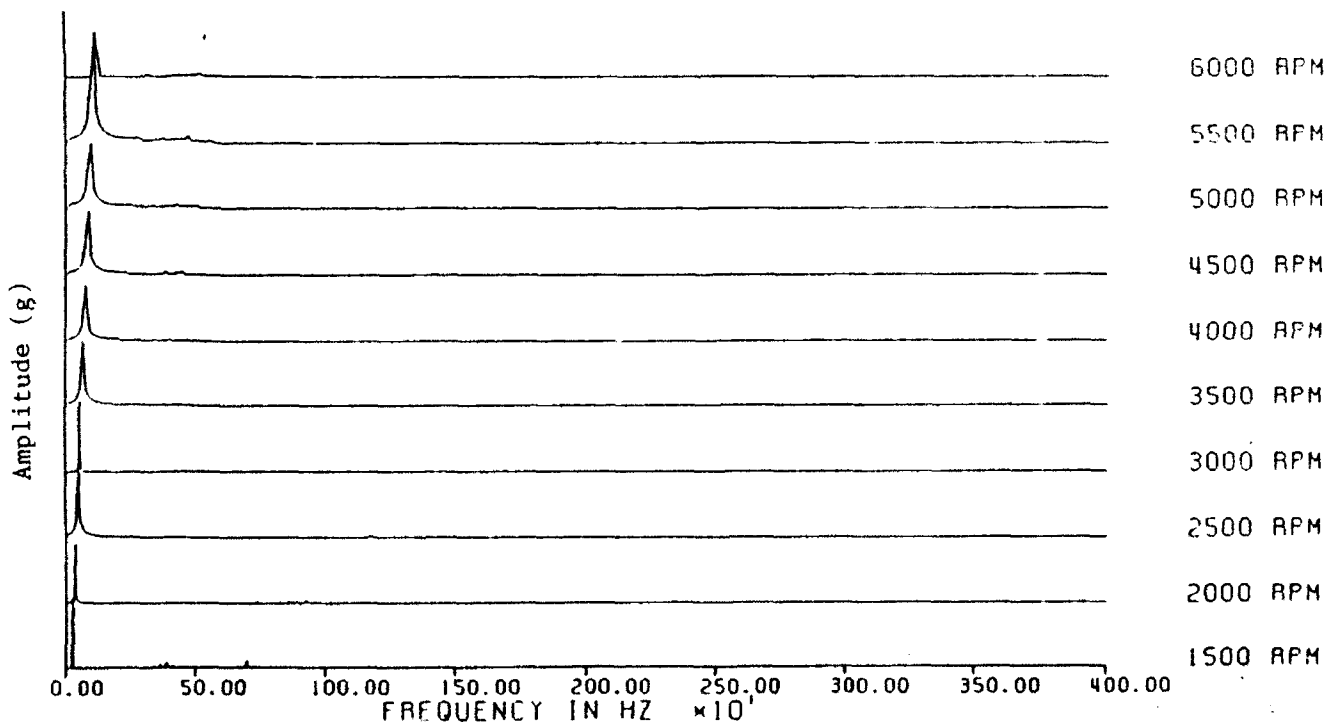


Figure 6.15D Frequency Spectra of the Y-direction Vibration of the 1st Rotor from Numerical Simulation

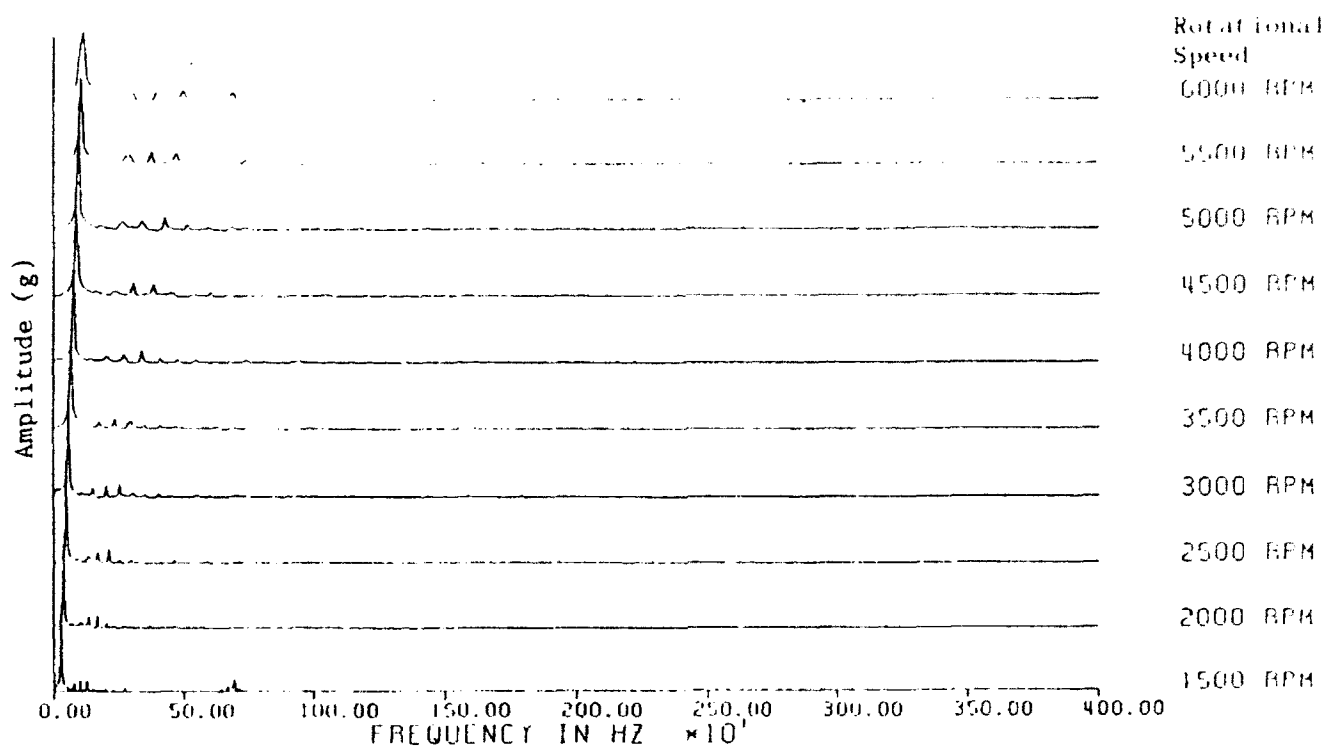


Figure 6.16A Frequency Spectra of the X-direction Vibration of the 2nd Rotor from Experimental Study

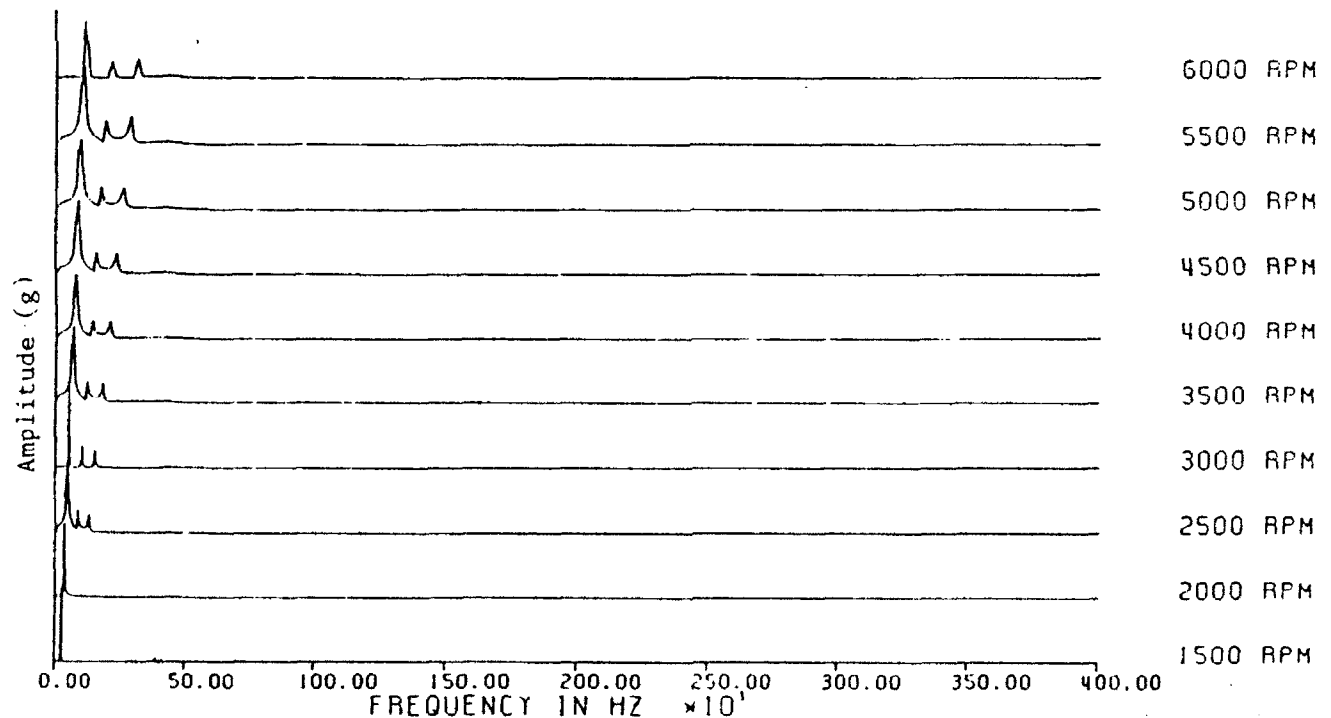


Figure 6.16B Frequency Spectra of the X-direction Vibration of the 2nd Rotor from Numerical Simulation

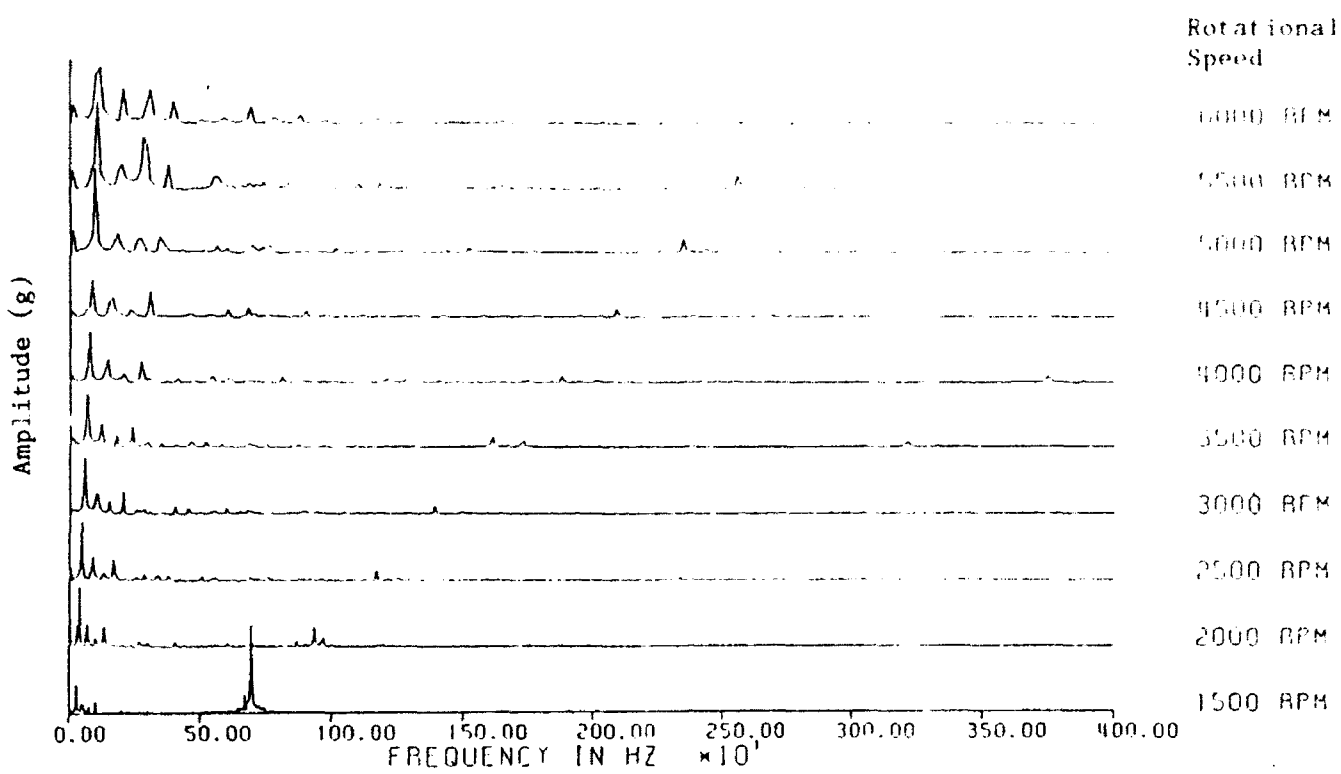


Figure 6.16C Frequency Spectra of the Y-direction Vibration of the 2nd Rotor from Experimental Study

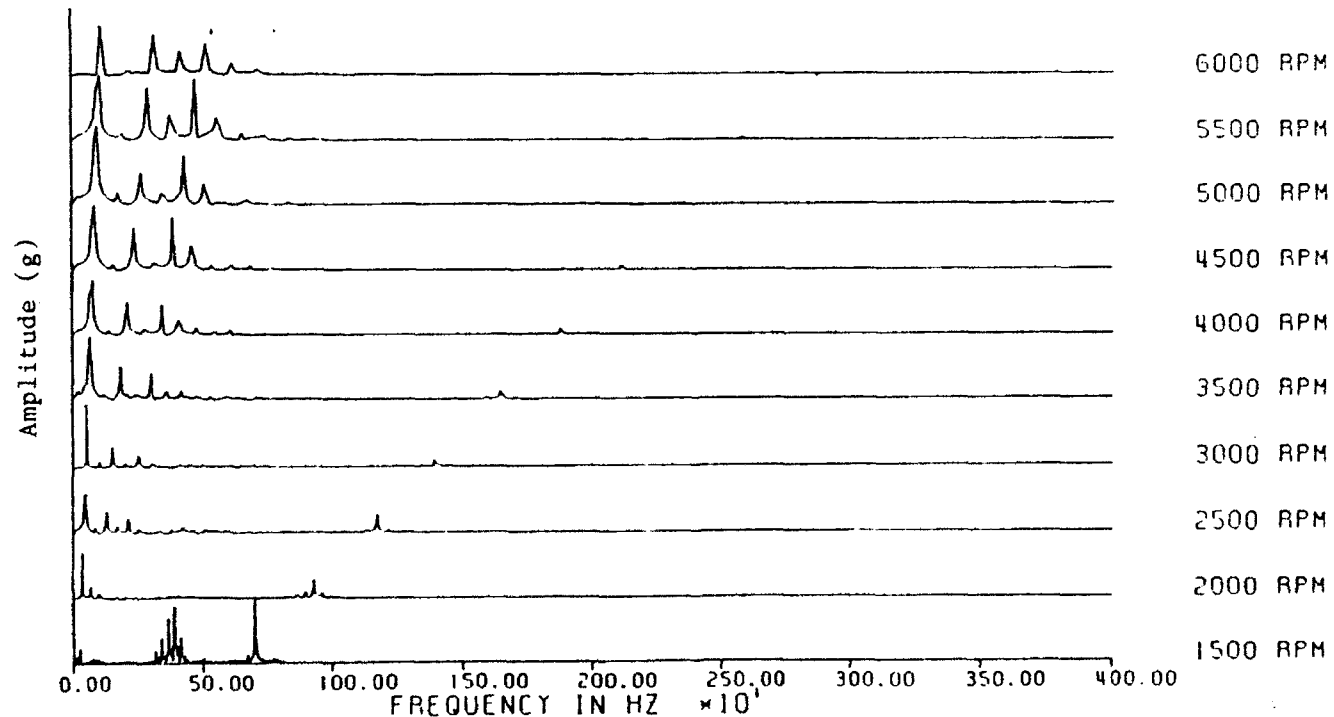


Figure 6.16D Frequency Spectra of the Y-direction Vibration of the 2nd Rotor from Numerical Simulation

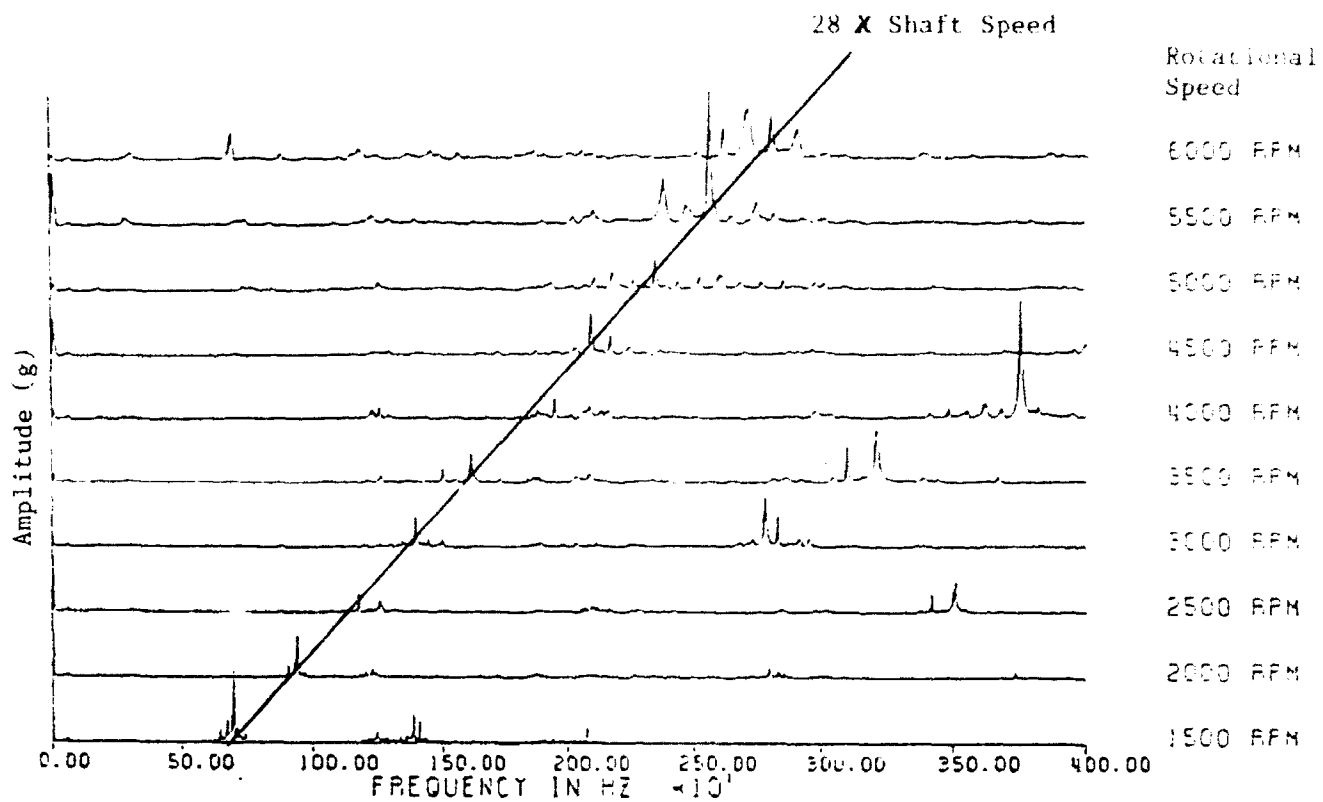


Figure 6.17A Frequency Spectra of the X-direction Vibration of the Gear Box from Experimental Study

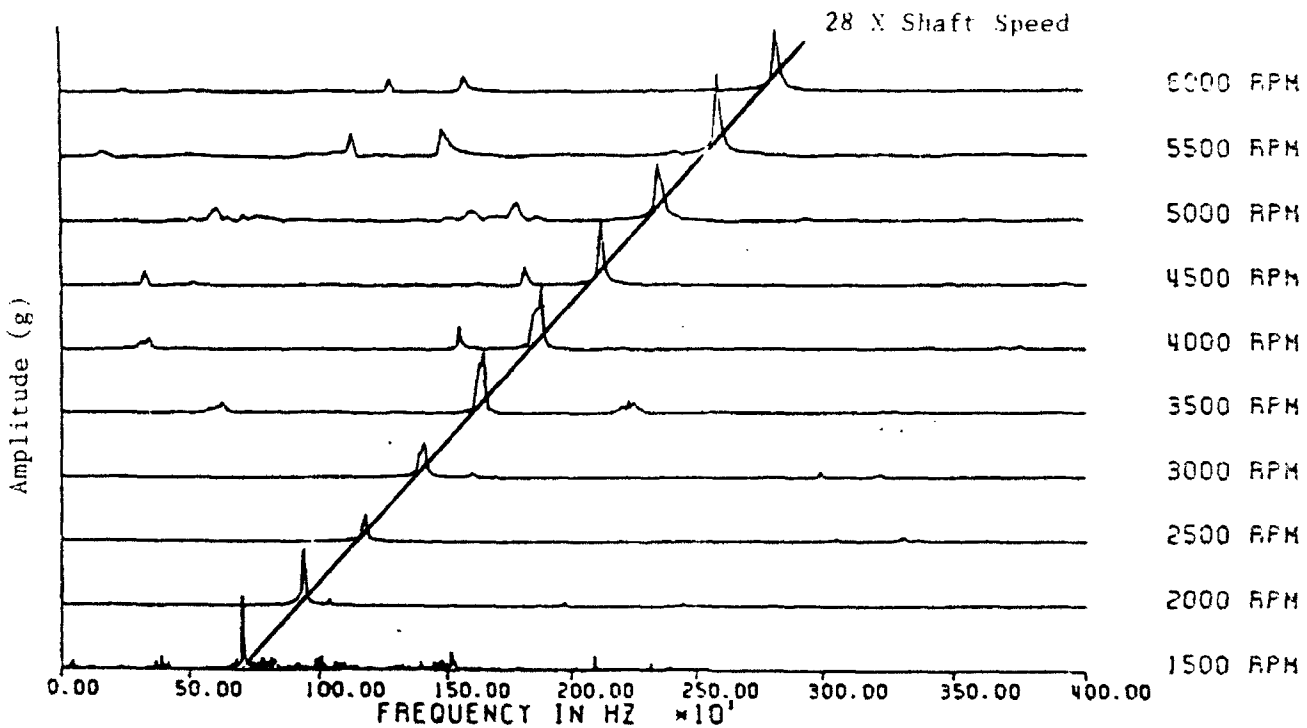


Figure 6.17B Frequency Spectra of the X-direction Vibration of the Gear Box from Numerical Simulations

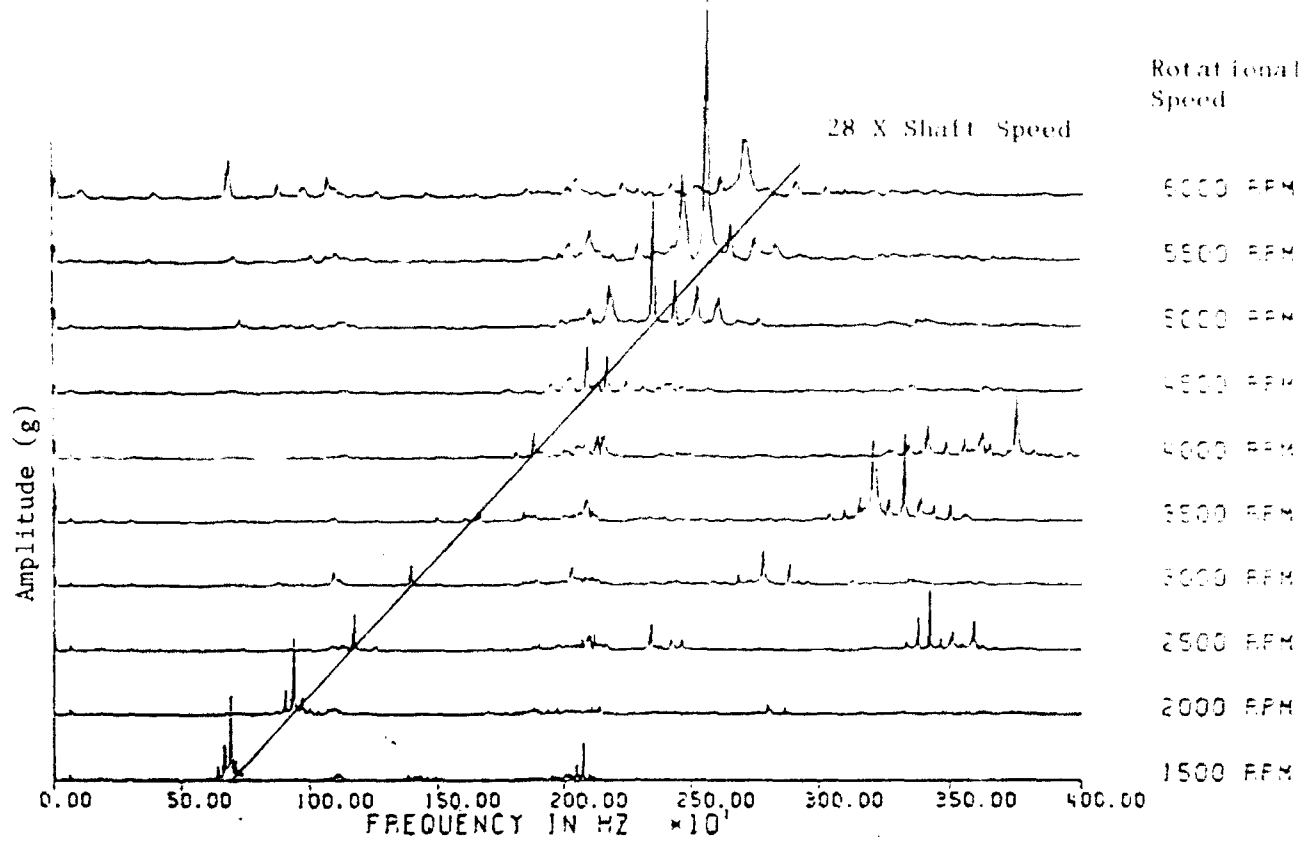


Figure 6.18A Frequency Spectra of the Y-direction Vibration of the Gear Box from Experimental Study

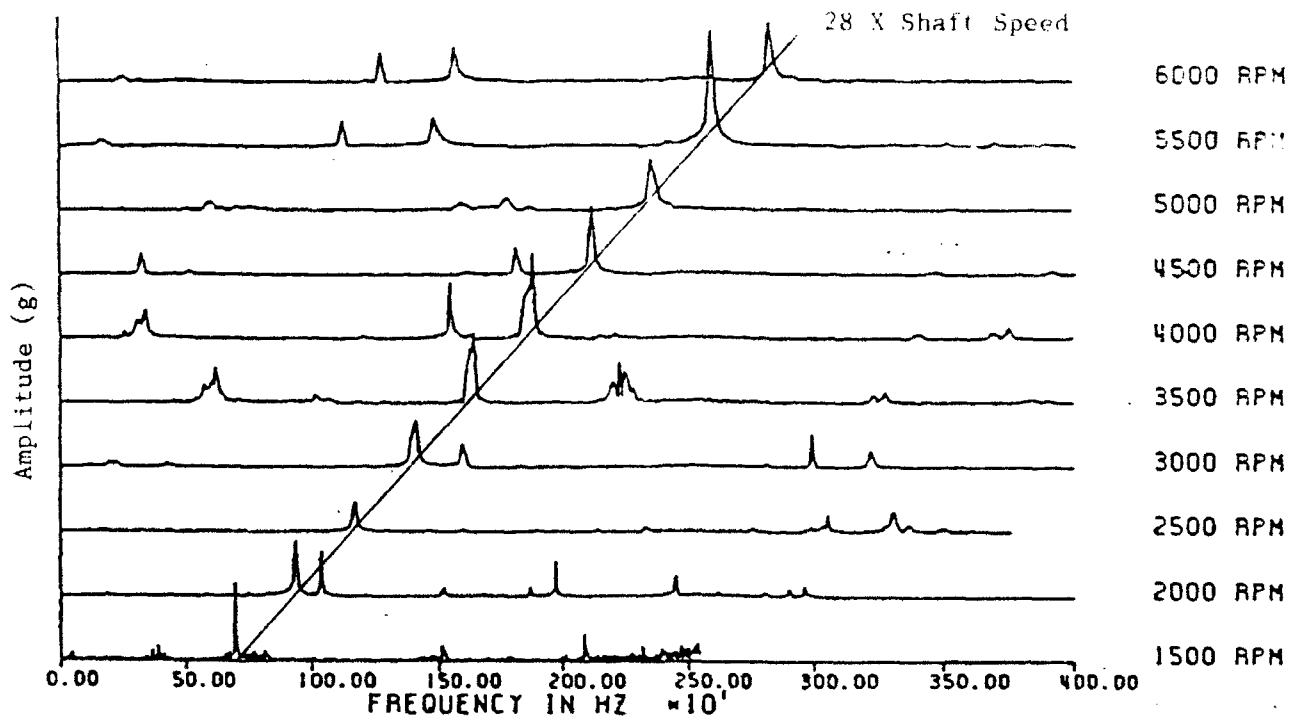


Figure 6.18B Frequency Spectra of the Y-direction Vibration of the Gear Box from Numerical Simulations

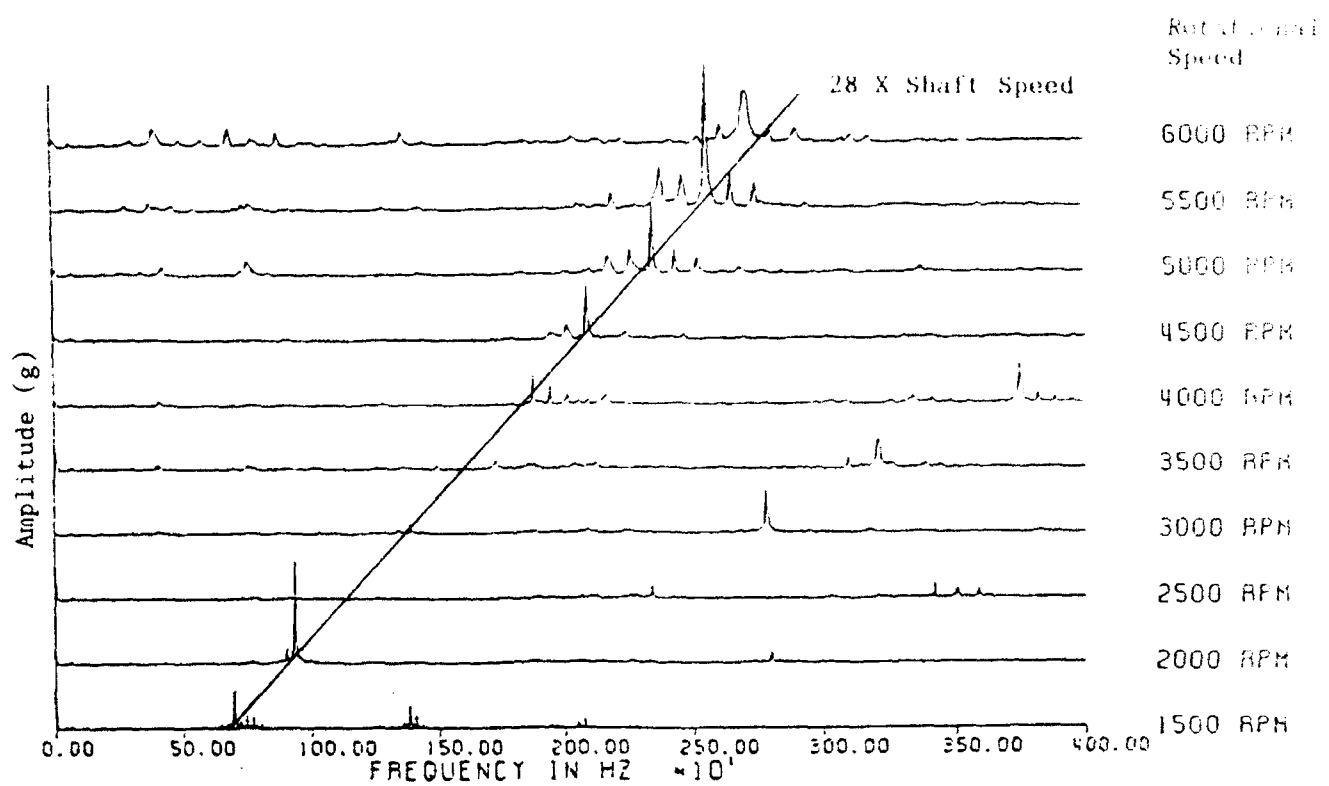


Figure 6.19A Frequency Spectra of the Z-direction Vibration of the Gear Box from Experimental Study

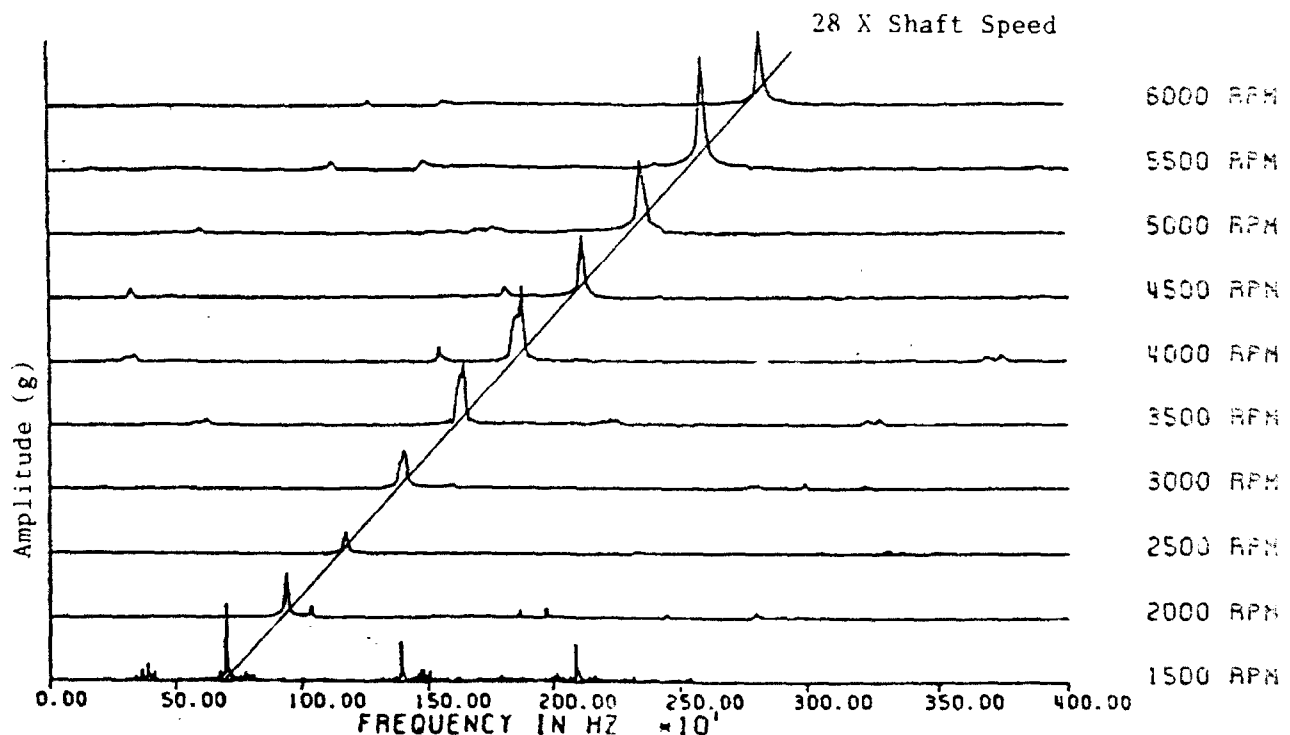


Figure 6.19B Frequency Spectra of the Z-direction Vibration of the Gear Box from Numerical Simulations

occur at the running speeds of 1500 rpm, at the tooth pass frequency of 700 Hz, and at 5500 rpm, at the tooth pass frequency of 2560 Hz. These peaks are a result of the tooth pass frequency exciting two of the major natural frequencies of the housing, namely the 658 Hz and 2536 Hz modes. The presence of other modes can be seen, however, the 658 and 2536 Hz modes, when excited by the gear mesh frequency, dominate the spectra.

When comparing the predicted vibration spectra with the measured spectra, it was found that although the actual amplitude values did not always agree, the general trends of the spectra were very similar. The predicted vibration spectra of the housing in the x-direction is given in Figure 6.17B. In comparing Figures 6.17A and 6.17B, the predicted amplitude at the gear mesh frequency at 1500 rpm is only 3% above the measured value. The comparison at 5500 rpm is not that close, where the predicted amplitude is 38% below the measured value. In comparing trends, the predicted spectra show the same gear mesh frequency induced excitation of the 658 Hz and 2536 Hz modes, as found in the measured spectra, at the running speeds of 1500 and 5500 rpm, respectively.

Figures 6.18A and 6.18B, and Figures 6.19A and 6.19B present the comparison of predicted and measured housing vibration spectra in the y and z directions, respectively. The results of the comparison are the same as those presented for the housing vibration in the x-direction (Figure 6.17A and 6.17B). Actual values of the components in the spectra were not always in good agreement, however, the general trends between the predicted and measured housing vibration spectra were very similar. Also, as seen in Figure 6.19B, at the 1500 rpm speed, the model predicts the second and third harmonic of the gear mesh frequency. As shown in Figure 6.19A, the measured vibration confirms the presence of these two harmonics at the 1500 rpm running speed.

7. CORRELATION OF NOISE AND VIBRATION

In order to predict the noise generated in a gear transmission system, a two-phase procedure was developed to correlate the noise and vibration data obtained during experimental studies; namely, i) linear correlation through transfer functions, and ii) nonlinear correlation through hypercoherence functions. The relationships derived in this study are used to predict gear box noise from the numerical simulations of the gear box vibrations. A detailed description of the procedures used are presented in the following sections.

7.1 Correlation of Experimental Noise and Vibration Data

In this experiment, a new set of gears consisting of two identical 25-tooth gears were installed in the gear box shown in Fig. 5.2. While the vibration of the gear box surfaces was monitored by accelerometers, as described in section 6.2, the noise data was obtained by microphones, as described in section 6.3. The vibration data for the top surface of the gear box for operating speeds of 3000, 4000, and 5000 rpm are shown in Fig. 7.1, with the corresponding noise data given in Fig. 7.2.A and 7.2.B. Figure 7.3 presents the frequency and power spectra of both the vibration and noise signals at 3000 rpm running speed. Note that in the vibration spectrum, a small frequency component exists at the mesh frequency of 1250 Hz with two very large components at 3-times the mesh frequency (3750 Hz), and 4-times mesh frequency (5000 Hz). In the noise spectrum, while frequency components of considerable magnitudes are observed at the mesh frequency of 1250 Hz, and at 2 and 3-times mesh frequency (2500 and 3750 Hz), a large amplitude frequency component is also noticed at 400 Hz. This 400 Hz frequency component does not coincide with any of the major vibration frequencies at the top surface of the gear box. A closer examination of the

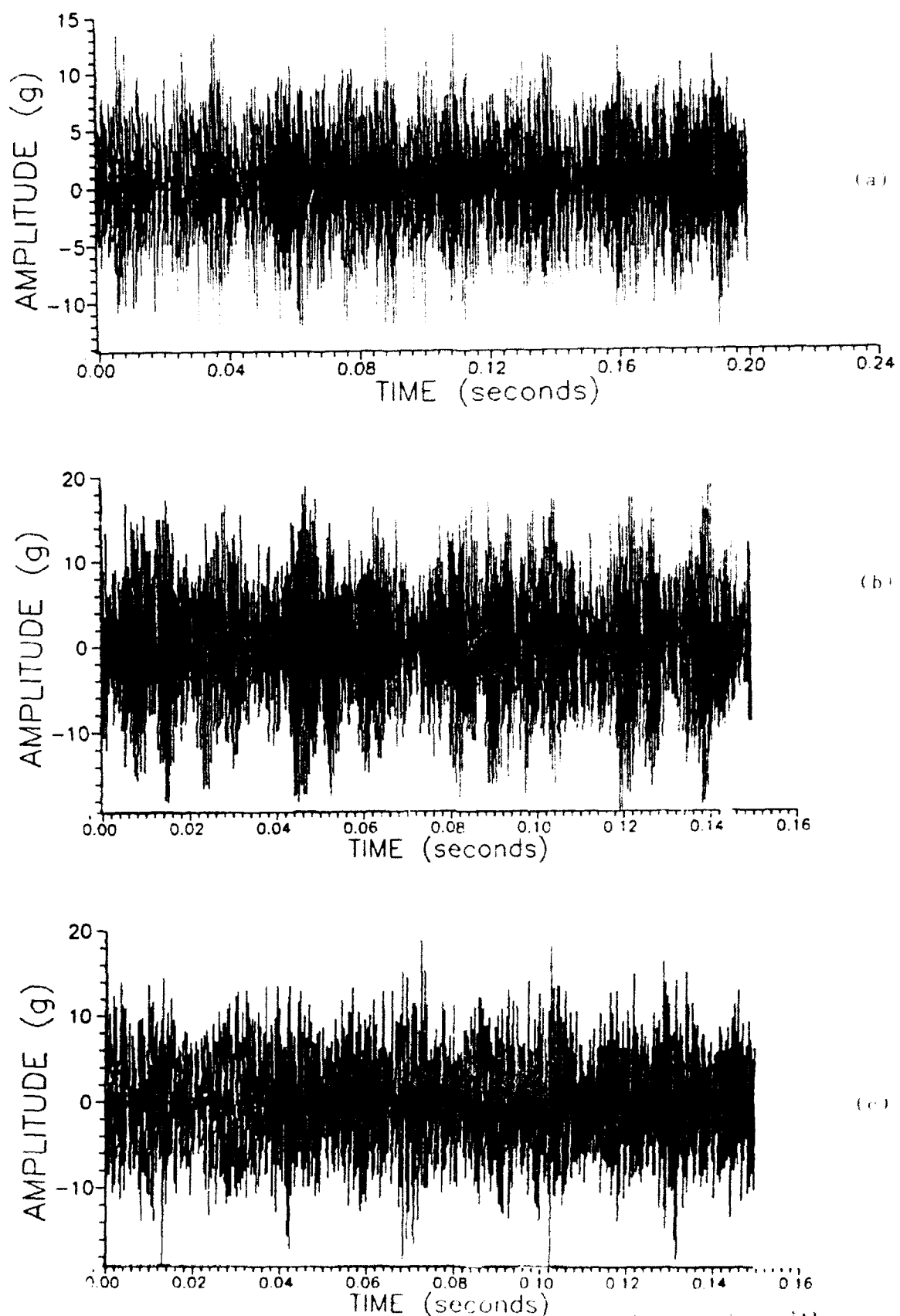


Figure 7.1 Time vibration signal at top cover of the gear box with rotor operating speed
 (a) at 3,000 rpm, (b) at 4,000 rpm, and (c) 5,000 rpm

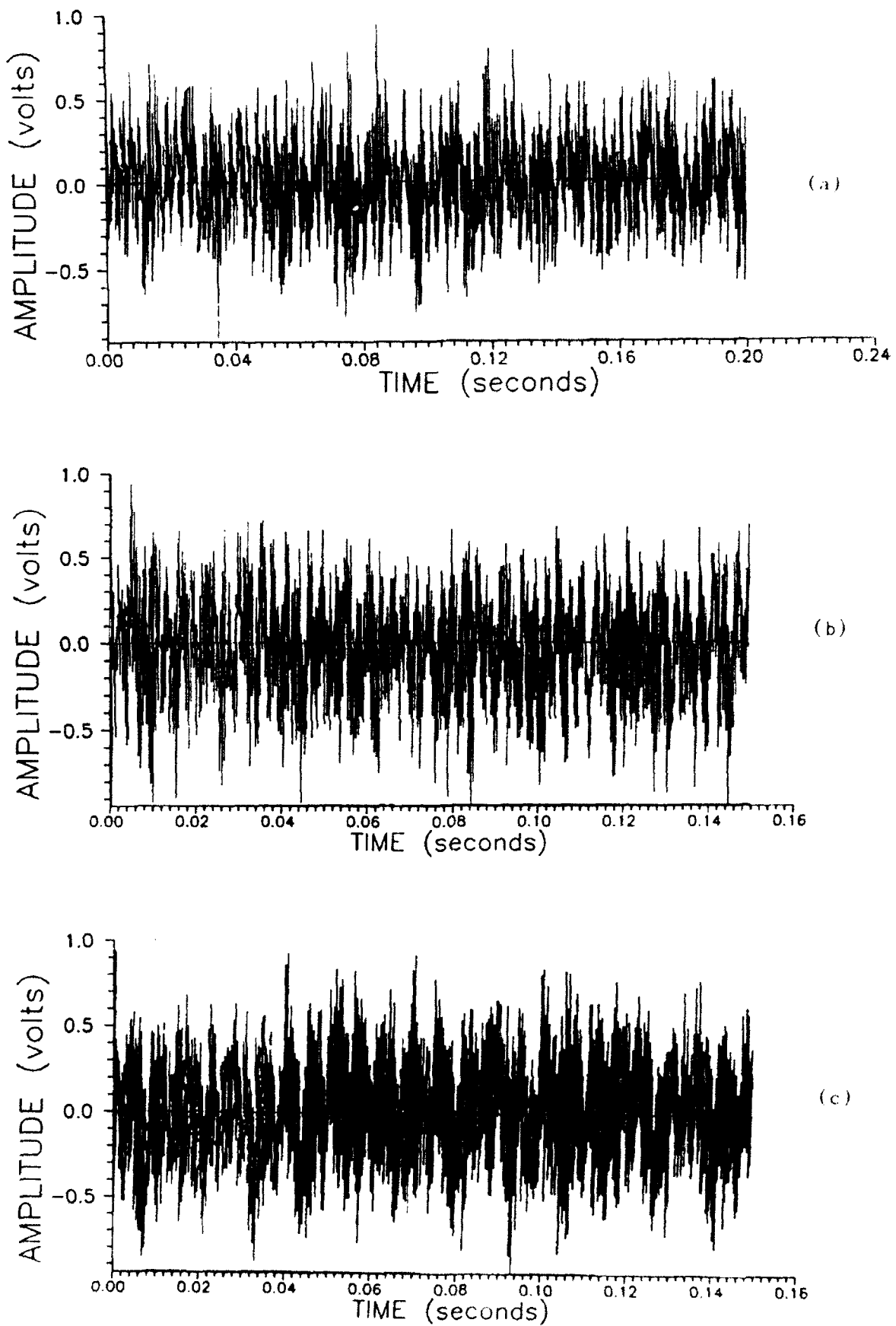


Figure 7.2 A Time noise signal from microphone no. 1 located vertically at top cover of the gear box with rotor operating speed (a) at 3,000 rpm, (b) at 4,000 rpm, and (c) at 5,000 rpm

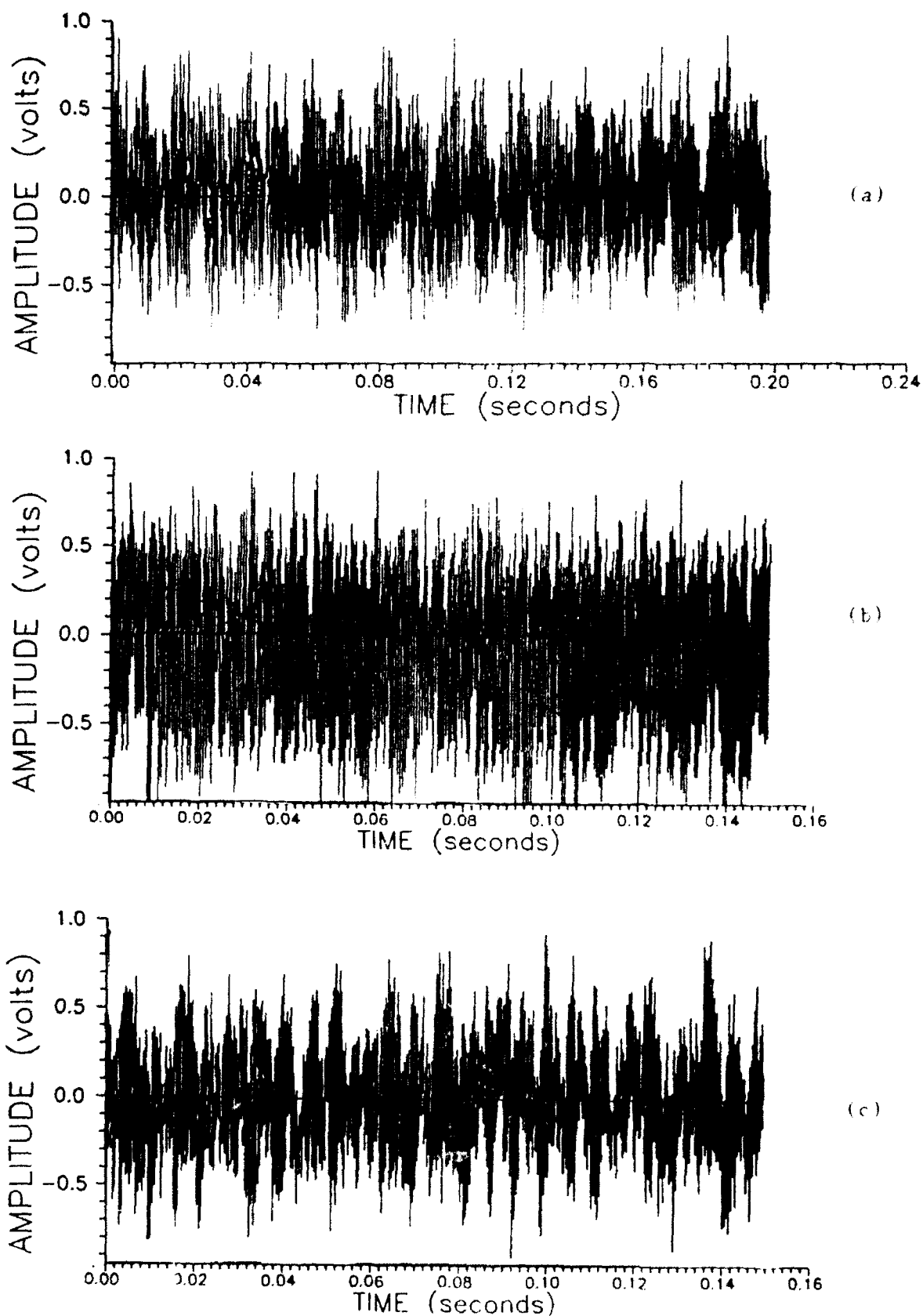


Figure 7.2B Time noise signal from microphone no. 2 located 45-degrees
at top cover of the gear box with rotor operating speed
(a) at 3,000 rpm, (b) at 4,000 rpm, (c) at 5,000 rpm

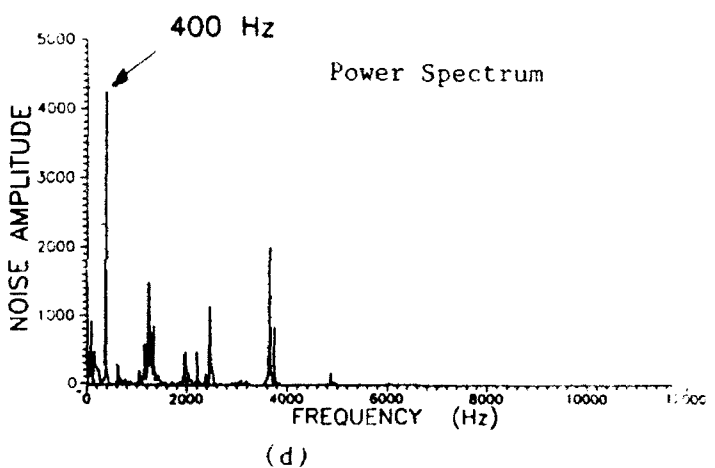
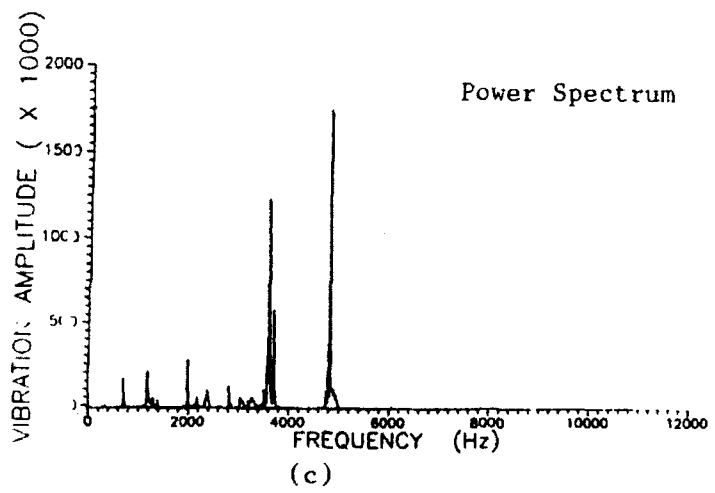
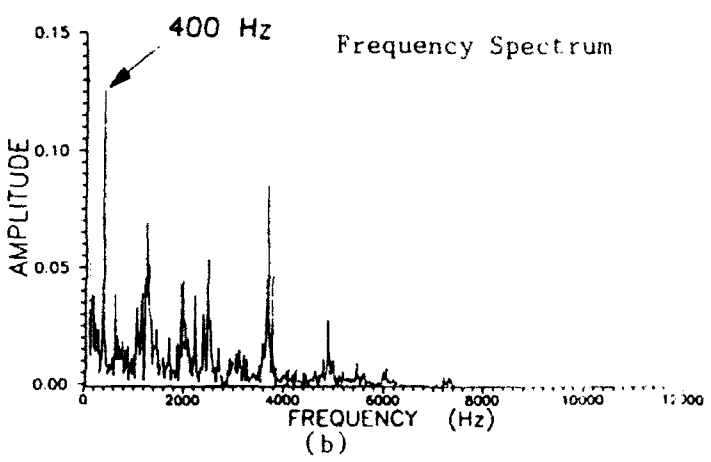
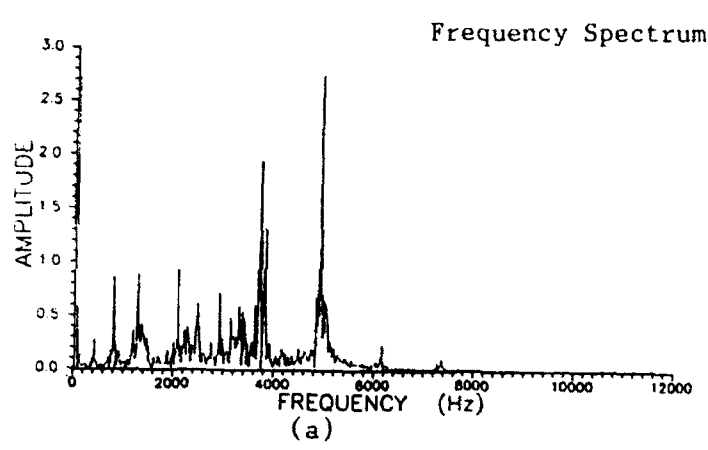


Figure 7.3 Frequency spectrum for (a) vibration, (b) noise from microphone no. 1, and power spectrum for (c) vibration, (d) noise from microphone no. 1, at the operating speed of 3,000 rpm.

system dynamic characteristics reveals that the 400 Hz frequency is an excitation of one of the natural frequencies of the rotor system, which has a very small amplitude in the gear box vibration spectrum. A logical explanation is that noise is being produced at the rotor-gear system at 400 Hz and is not being transferred to the vibration of the gear box surface. This phenomenon is further verified by the very large amplitude of the vibration-to-noise transfer function at 400 Hz as given in Fig. 7.4A. A linear coherence function between the noise and vibration signals is also given in Fig. 7.4B.

Figure 7.5 shows the comparison of the frequency and power spectra between the results of the gear box vibrations with the noise signal from microphone No. 2 (45 degrees from vertical). Note that in this case, the two signals are much better correlated. In Fig. 7.5B, the noise spectrum shows the largest component at 3-times mesh frequency (3750 Hz) and two other major components at mesh frequency (1250 Hz) and 4-times mesh frequency (5000 Hz). Although a sizable component still exists at 400 Hz, it is relatively small compared with those of the multiples of the mesh frequency. Again, the logical explanation for this phenomenon is due to the fact that the 400 Hz frequency component produced by the rotor will not radiate through the gear box surface and cannot be picked up by the 45 degree microphone. The vibration-to-noise transfer and coherence functions for the second microphone are given in Fig. 7.6.

Figures 7.7 and 7.8 present respectively the frequency and power spectra, and the transfer and coherence functions of the gear box system at the rotor running speed of 4000 rpm. The frequency spectra in Fig. 7.7 shows a significant frequency component at the 3-times mesh frequency (5000 Hz) while major noise components are noted at the rotor natural frequency of 400 Hz and the primary mesh frequency (1667 Hz). The results are attributed

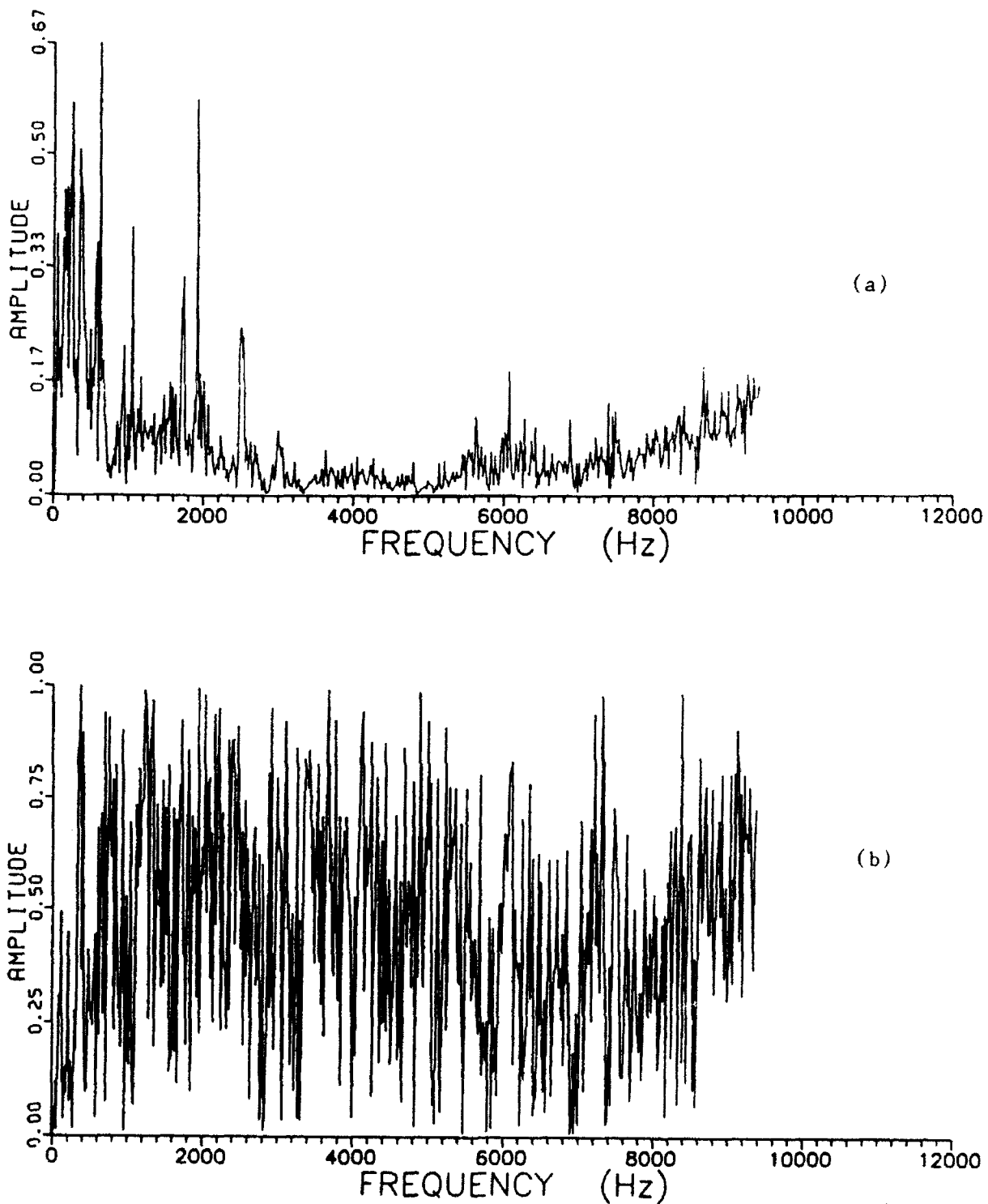


Figure 7.4 (a) Transfer function and (b) coherence function, between noise (microphone no. 1) and vibration at the operating speed of 3,000 rpm

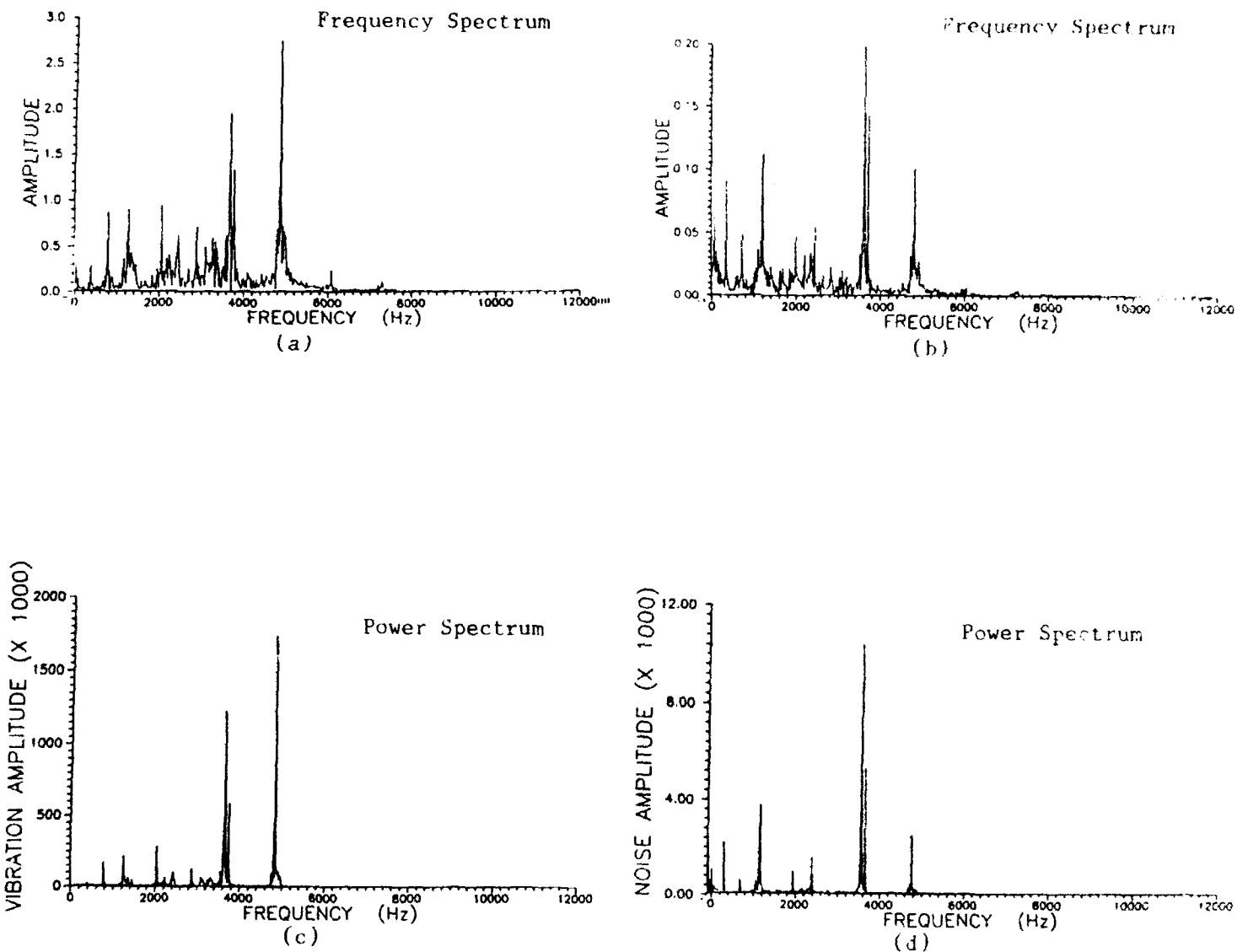


Figure 7.5 Frequency spectrum for (a) vibration, (b) noise from microphone no. 2, and power spectrum for (c) vibration, (d) noise from microphone no. 2, at the operating speed of 3,000 rpm.

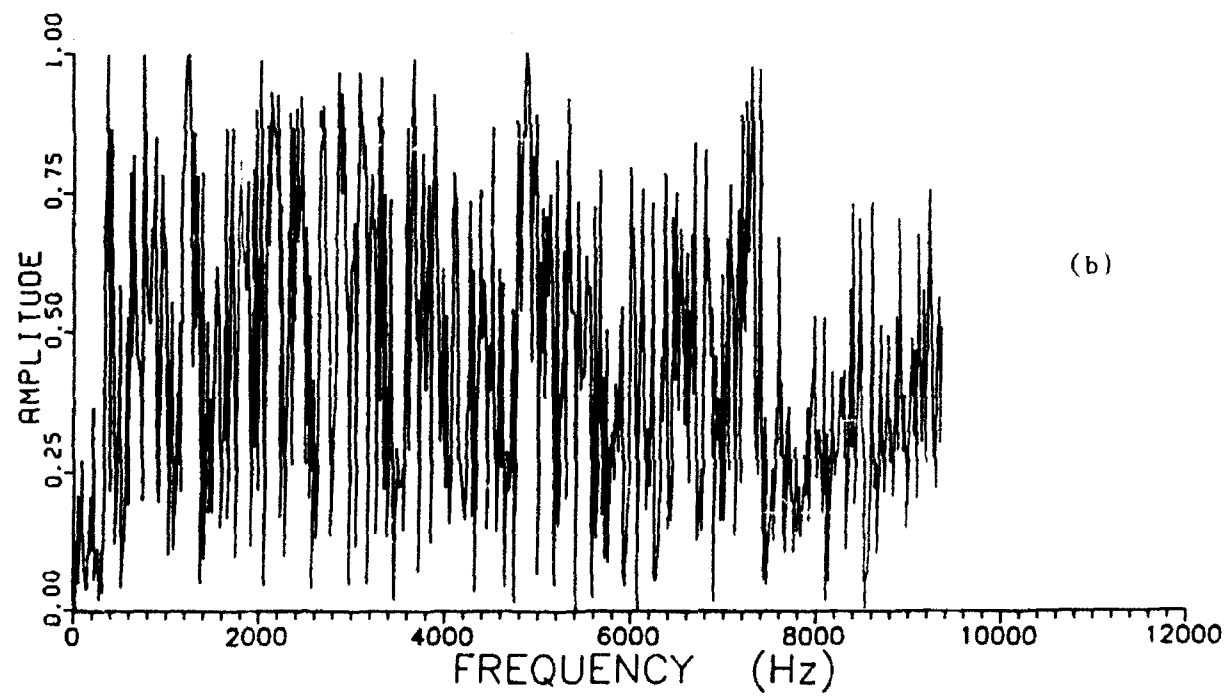
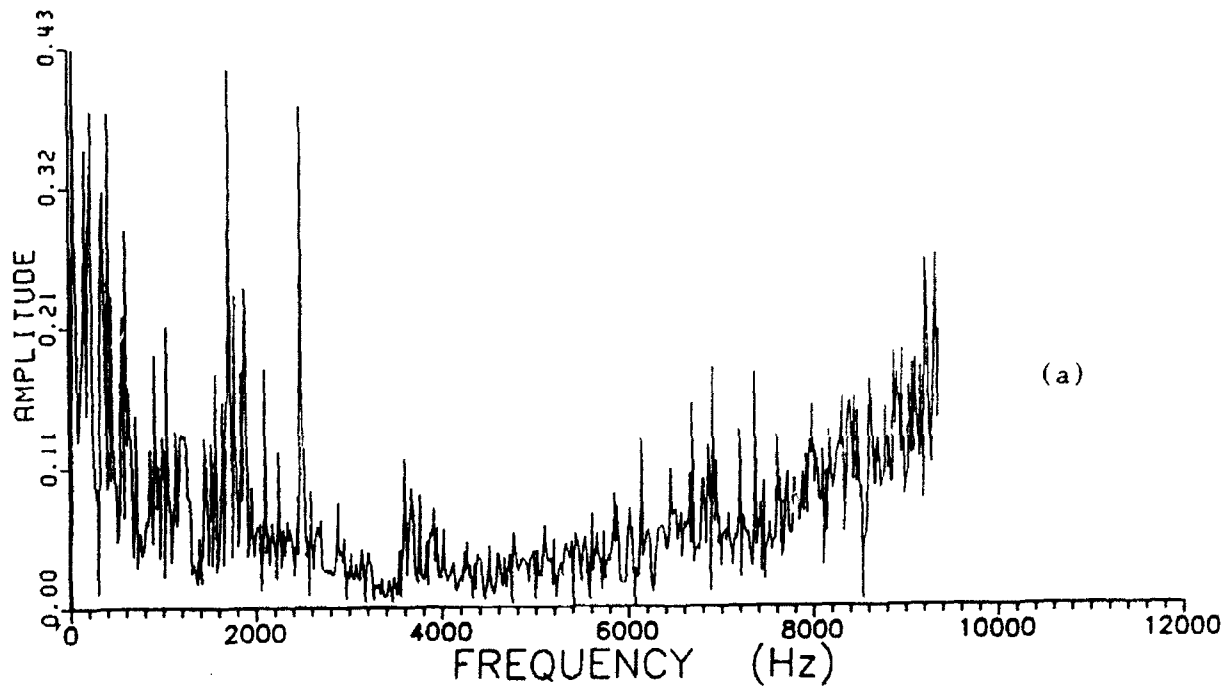


Figure 7.6 (a) Transfer function and (b) coherence function, between noise (microphone no. 2) and vibration at the operating speed of 3,000 rpm

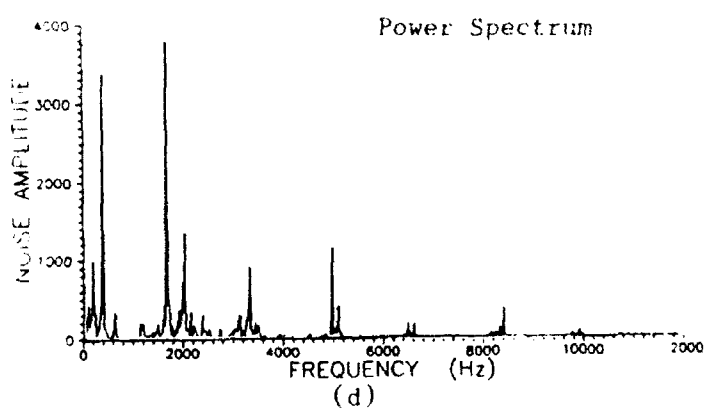
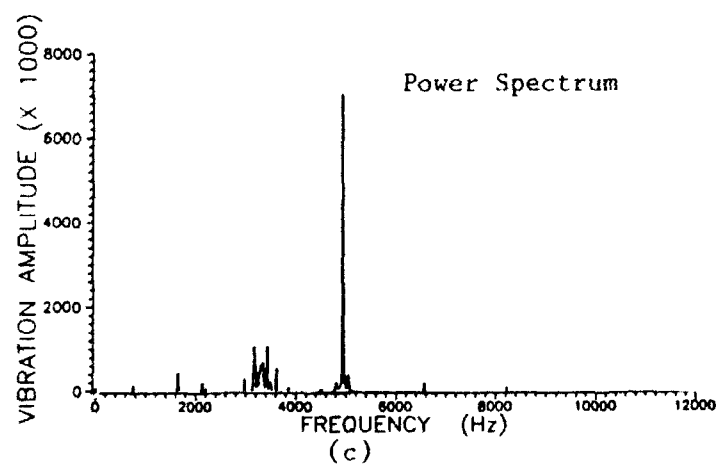
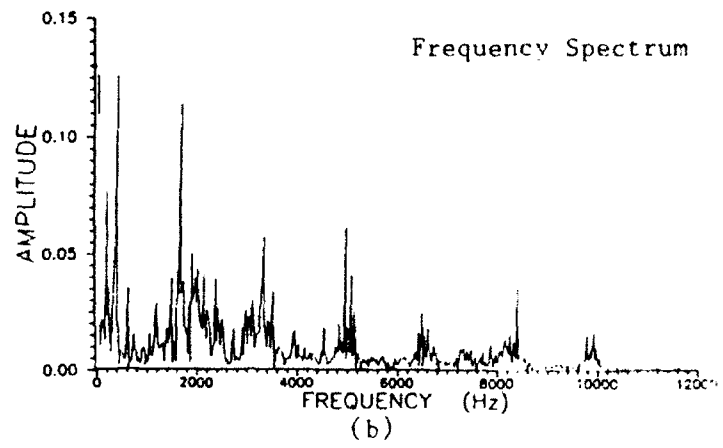
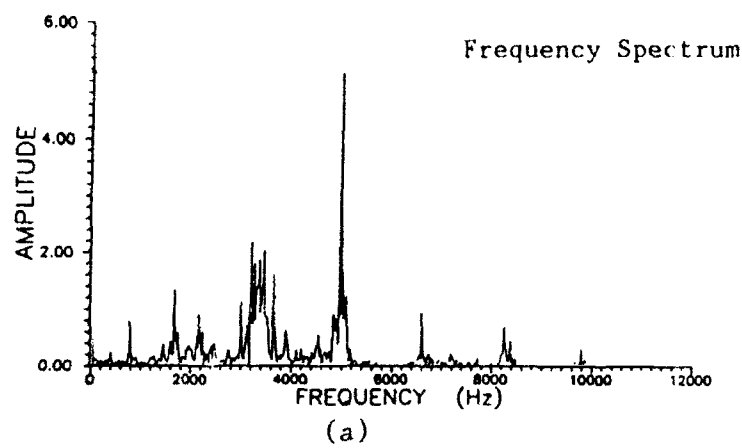


Figure 7.7 Frequency spectrum for (a) vibration, (b) noise from microphone no. 1, and power spectrum for (c) vibration, (d) noise from microphone no. 2, at the operating speed of 4,000 rpm.

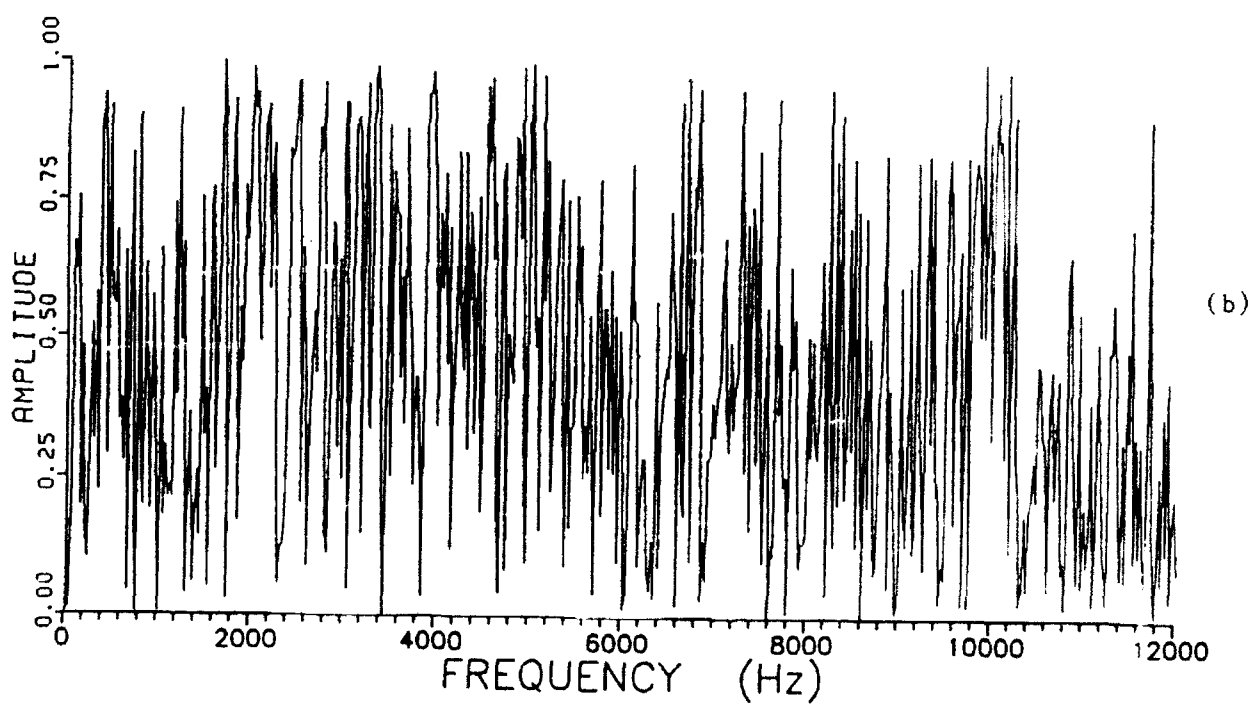
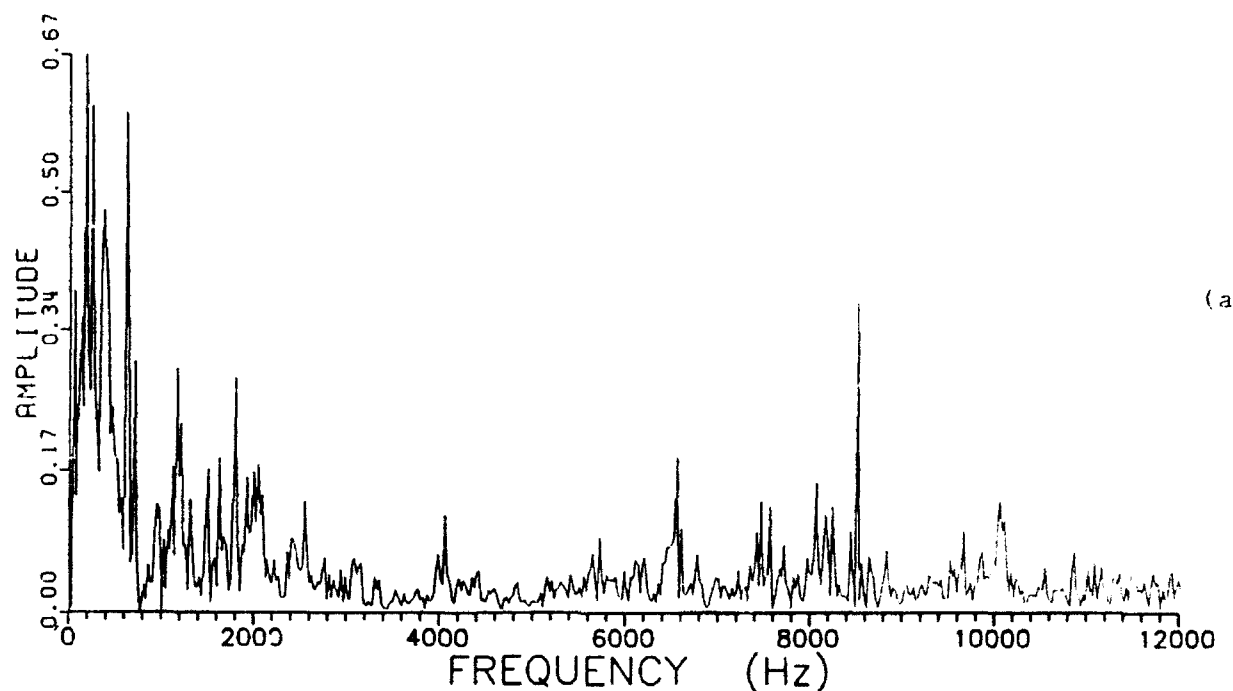


Figure 7.8 (a) Transfer function and (b) coherence function, between noise (microphone no. 1) and vibration at the operating speed of 4,000 rpm

to the fact that the noise due to the natural frequencies of the rotor system do not effectively contribute to the vibration of the gear box. The significant amplitudes in the vibration spectrum, other than the original mesh frequency, is due to the excitation of the natural frequencies of the gear box at the multiples of the mesh frequency. In the case of the 3000 rpm running speed, natural frequencies of 3750 rpm (3-times mesh frequency) and 5000 rpm (4-times) are excited. Figure 7.9 shows the comparison of the frequency spectra of the second microphone. Note again, that the 400 Hz component diminishes while the noise frequency components of the basic mesh frequency and its multiples are the major contributors. The transfer and coherence functions for this case is given in Fig. 7.10.

For the case of a rotor running speed of 5000 rpm, the frequency and power spectra of the gear box vibration and noise are given in Fig. 7.11. Note that the major vibration frequencies excited are the basic mesh frequency at 2083 Hz, 2-times at 4166 Hz, and 3-times at 6250 Hz. The magnitudes of these components are relatively lower than those at the 4000 rpm running speed. This is due to the fact that these frequencies are not close to any of the major vibration modes of the gear box. Even though at this running speed the noise frequency spectrum shows a more consistent trend with the vibration spectrum, a strong frequency component still exists at 400 Hz, which is not detected in the vibration spectrum. The transfer and coherence spectra for this case is given in fig. 7.12. For the second microphone, the noise signal spectrum, Fig. 7.13, shows a similar trend as those of microphone No. 1, with a considerably smaller 400 Hz component. The transfer and coherence function for this case is given in Fig. 7.14.

From the above discussion, it can be concluded that in the frequency domain, most of the noise components, other than the 400 Hz contributions, exist at multiples of the mesh

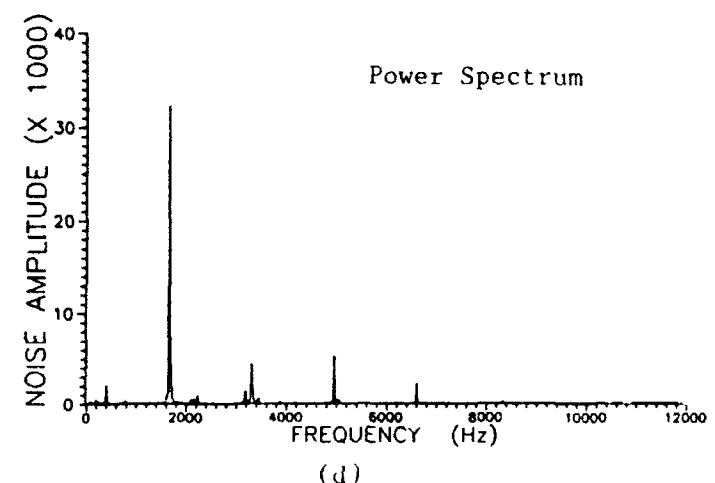
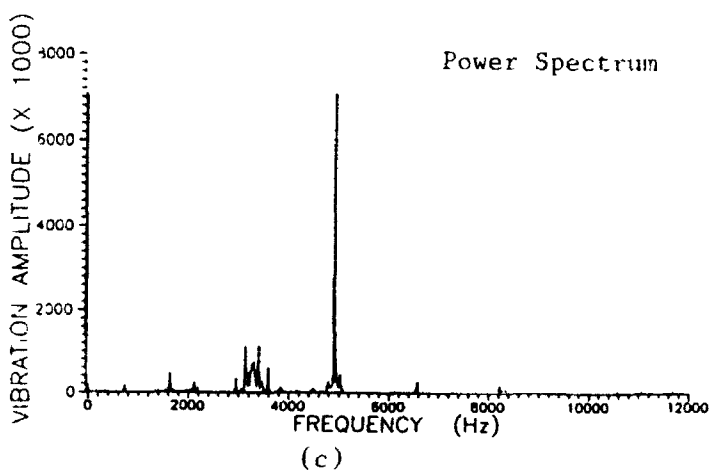
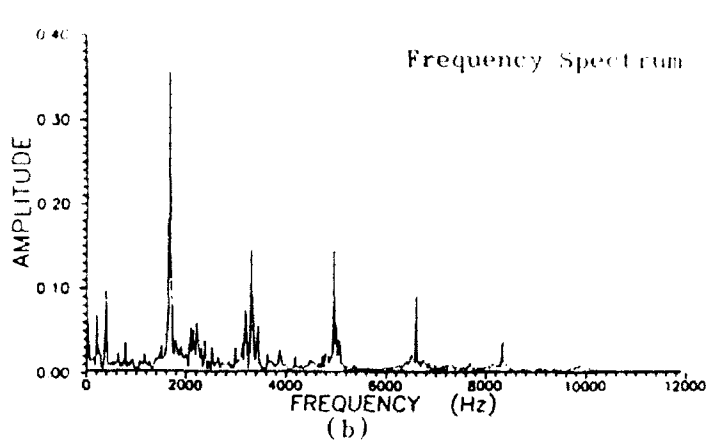
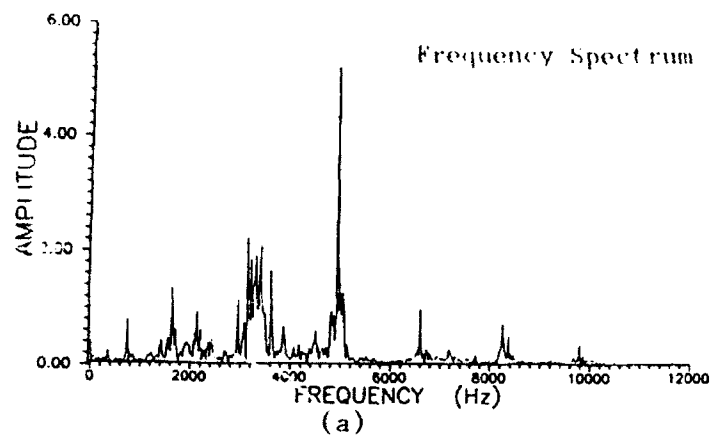


Figure 7.9 Frequency spectrum for (a) vibration, (b) noise from microphone no. 2, and power spectrum for (c) vibration, (d) noise from microphone no. 2, at the operating speed of 4,000 rpm.

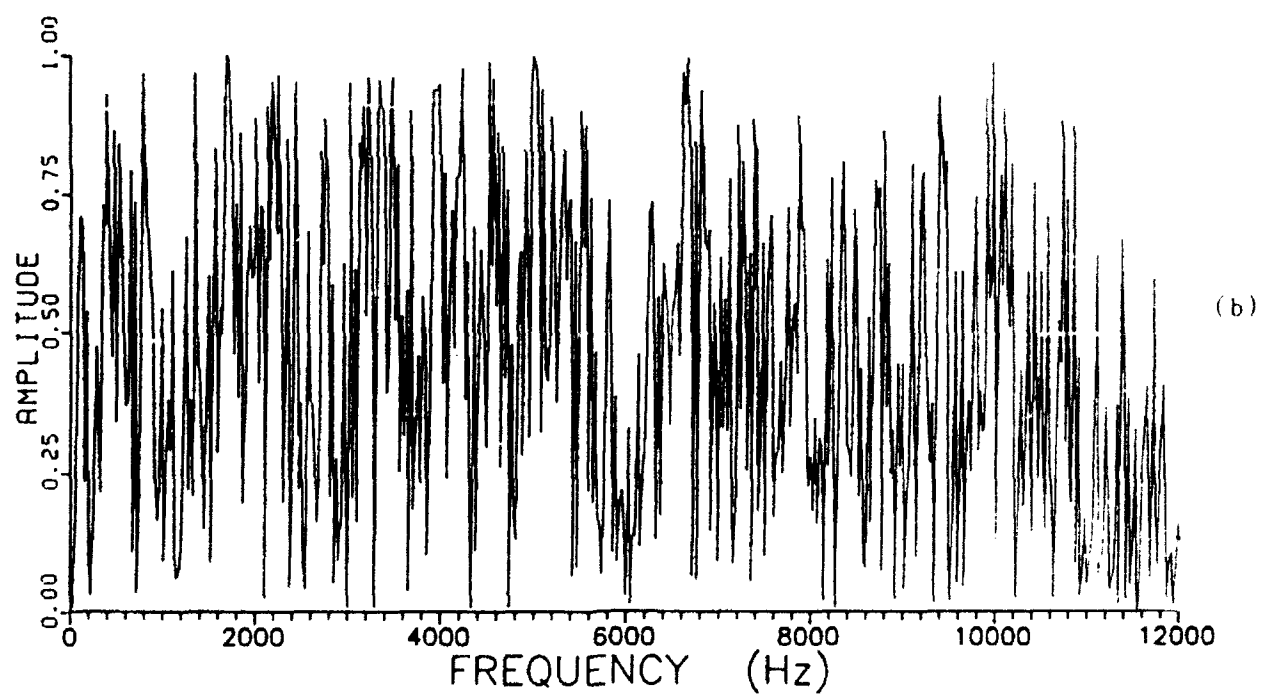
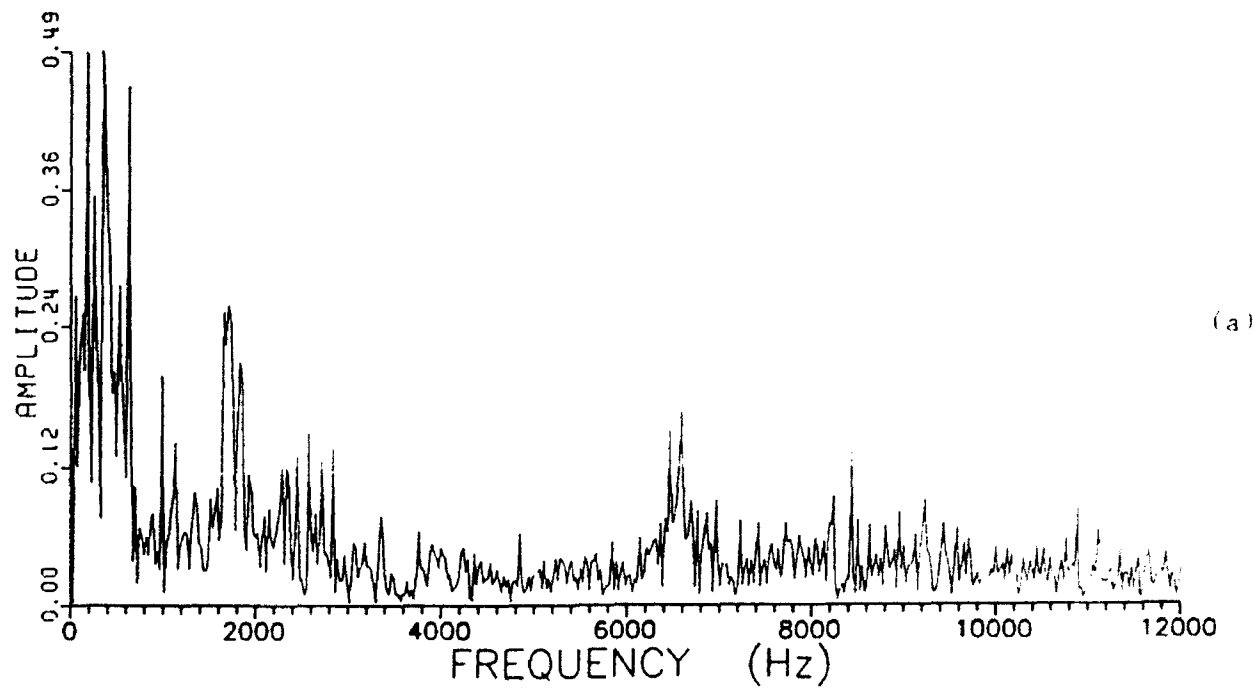


Figure 7.10 (a) Transfer function and (b) coherence function, between noise (microphone no. 2) and vibration at the operating speed of 4,000 rpm

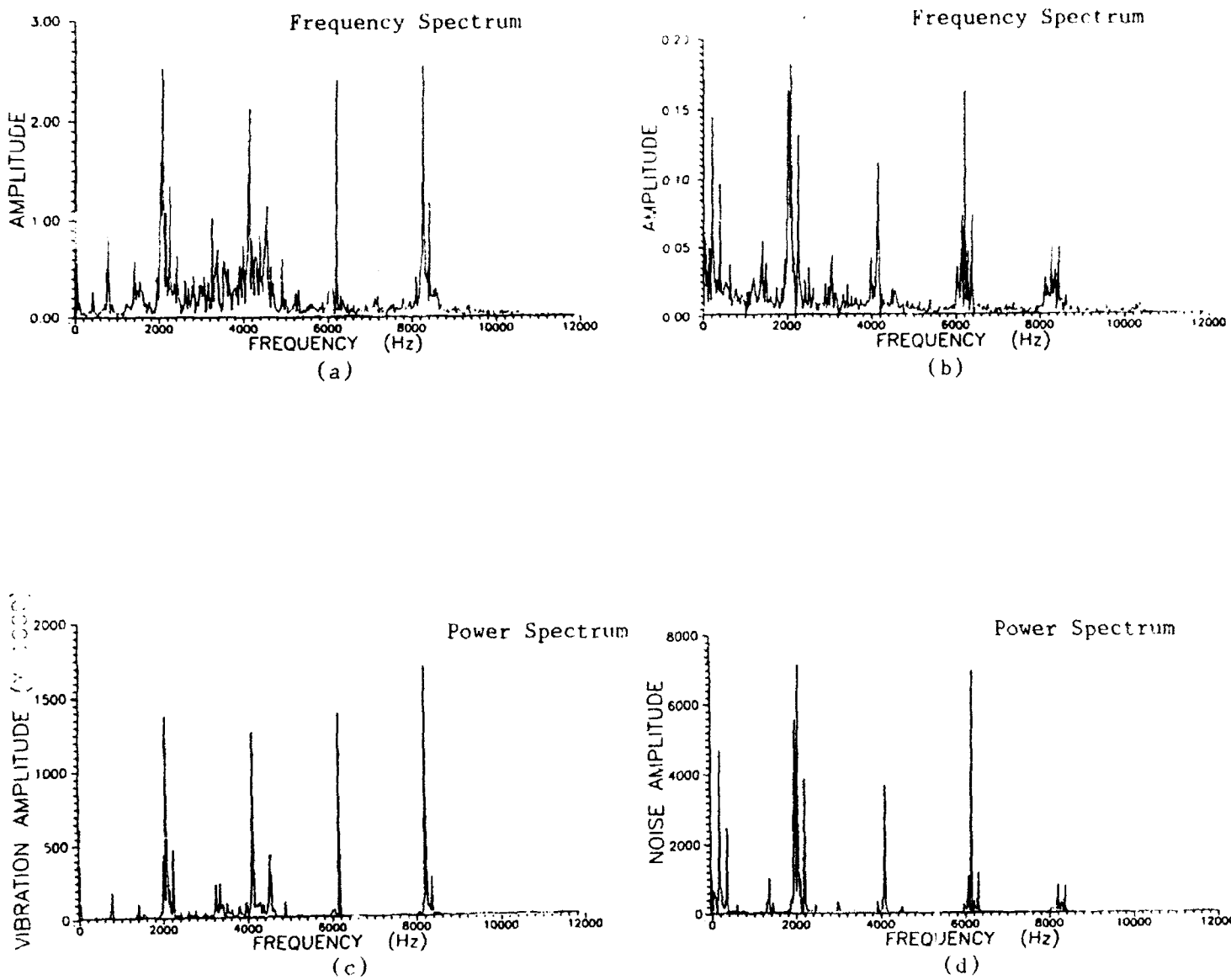


Figure 7.11 Frequency spectrum for (a) vibration, (b) noise from microphone no. 1, and spectrum for (c) vibration, (d) noise from microphone no. 1 at the operating speed of 5,000 rpm.

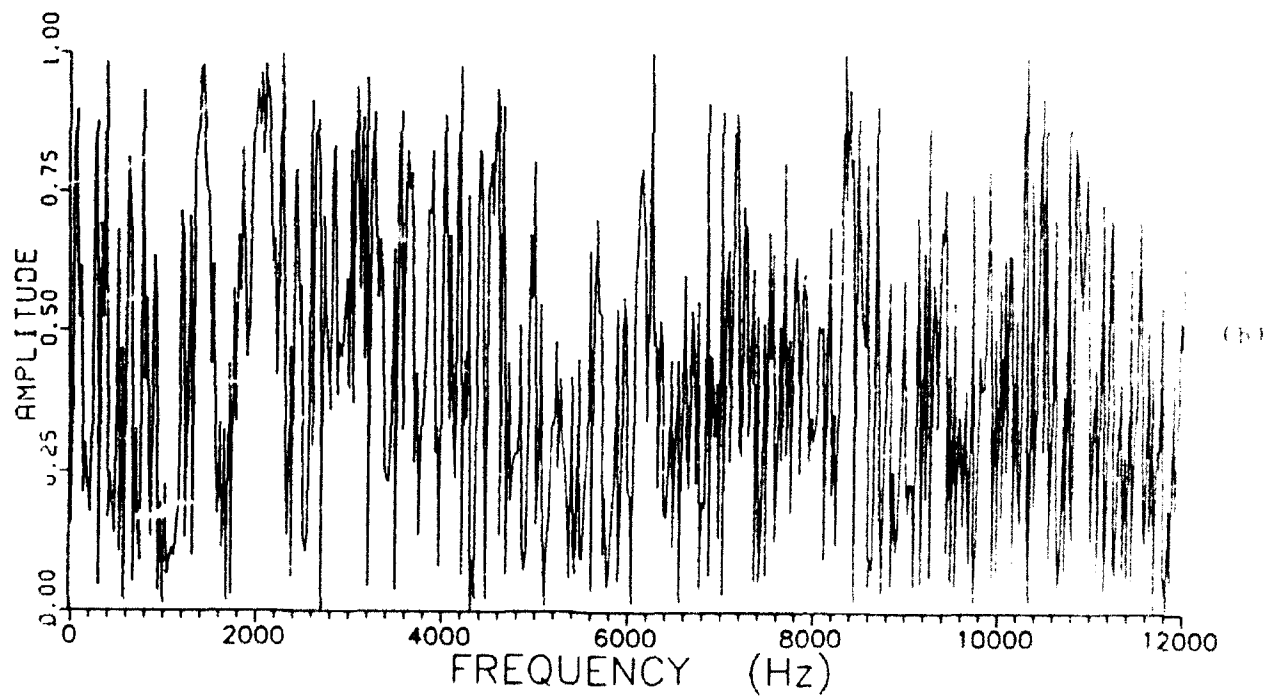
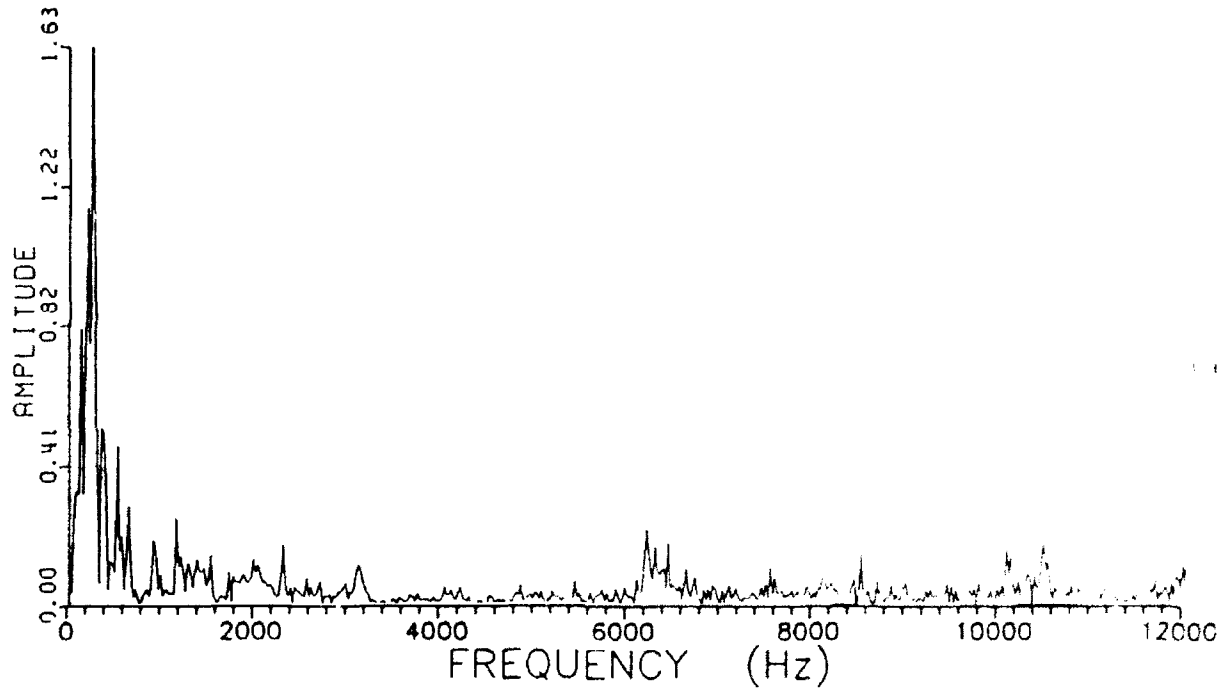


Figure 7.12 (a) Transfer function and (b) coherence function, between noise (microphone no. 1) and vibration at the operating speed of 5,000 rpm

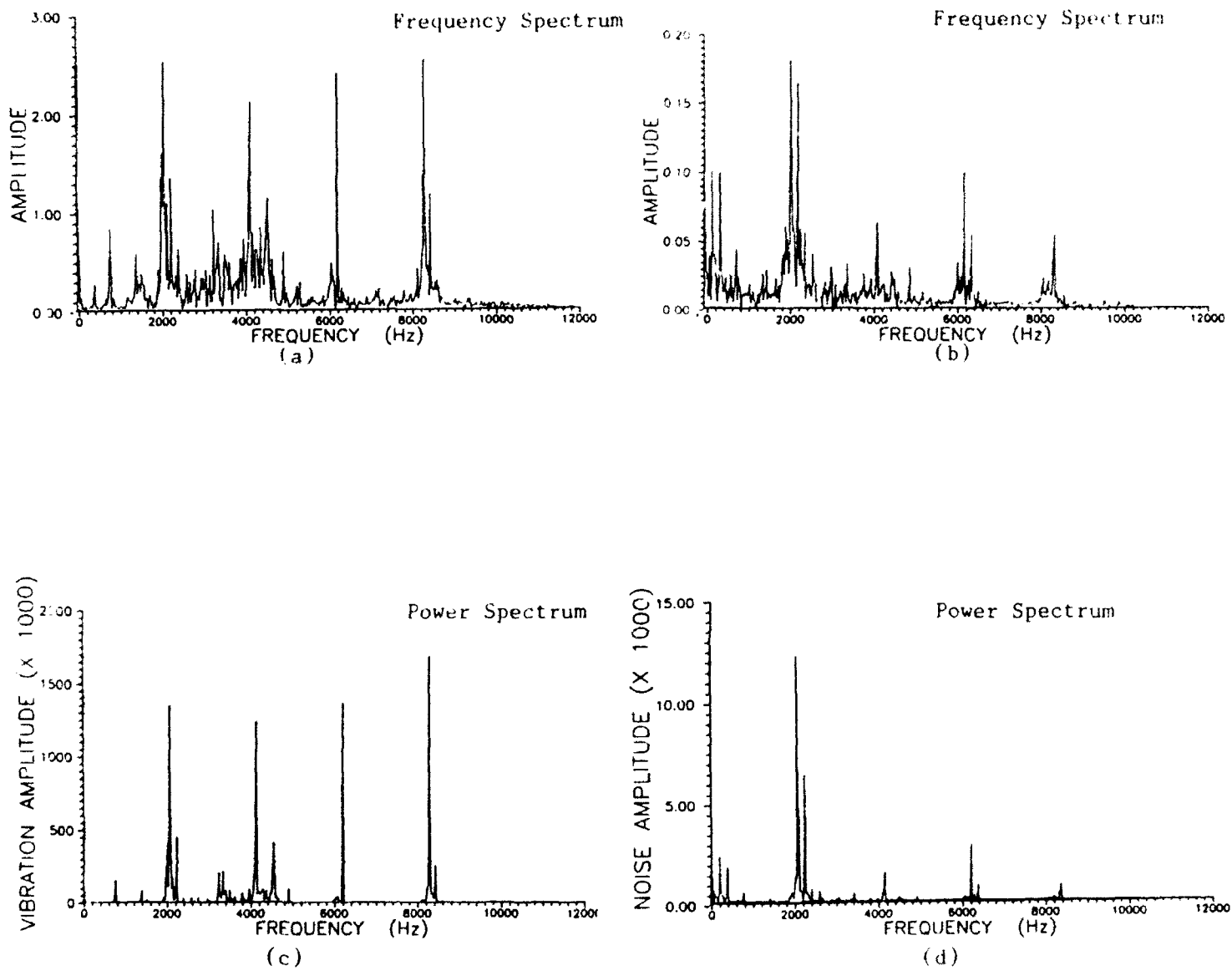


Figure 7.13 Frequency spectrum for (a) vibration, (b) noise from microphone no. 2, and power spectrum for (c) vibration, (d) noise from microphone no. 2, at the operating speed of 5,000 rpm.

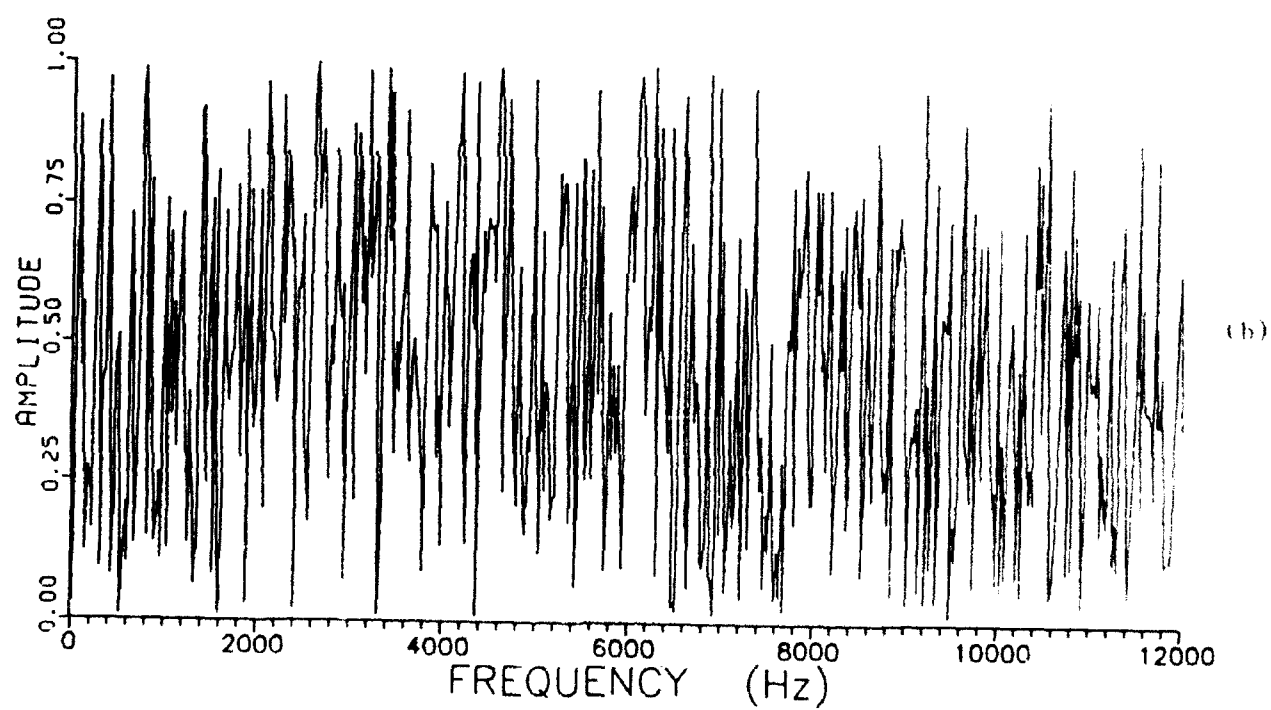
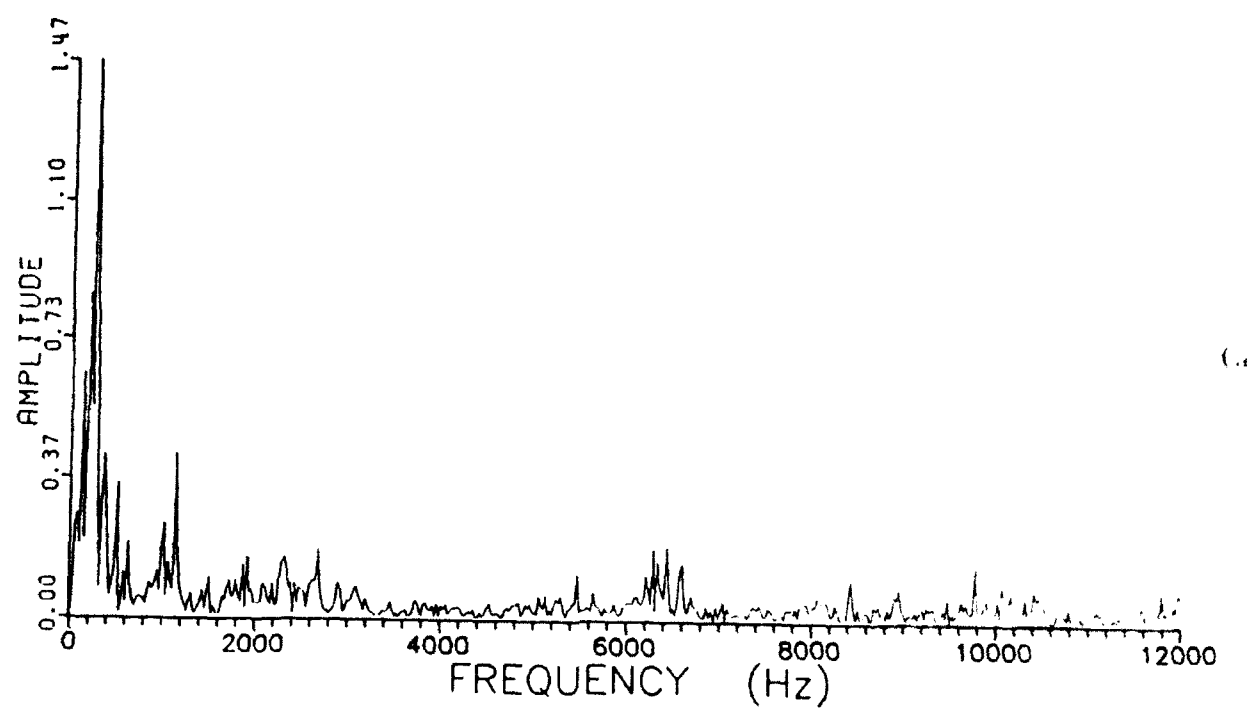


Figure 7.14 (a) Transfer function and (b) coherence function, between noise (microphone no. 2) and vibration at the operating speed of 5,000 rpm

frequency. **The Nonlinear Hypercoherence Function**, developed by NASA Marshall Space Flight Center for the Space Shuttle Noise Test Program, is used for the second phase of this study. The Hypercoherence Function [Jong 1986] will establish a nonlinear relationship between the basic frequency component with its multiple harmonics. Figure 7.15 shows the Hypercoherence functions of the noise signals for the 3000, 4000, and 5000 rpm cases. The magnitudes of the components in the harmonics are the nonlinear relationship of that component with the basic harmonic frequency. These relationships provide a picture of the relative contribution of the higher harmonics with respect to the basic frequency. Note that as the running speed increases, the magnitudes of the higher harmonics also increase. This is very similar to the conclusions drawn from the linear study discussed in the last paragraph. In the next section, this Hypercoherence function will be used on the numerical simulation data to examine the accuracy of the noise prediction.

7.2 Predictions of Noise by Numerical Simulations and Correlation with Experimental Results

In order to predict the noise level of the transmission system during operation, the vibrations of the gear box structure are simulated using the modal synthesis approach discussed in the previous chapters. Figure 7.16B shows the analytically predicted time vibration signal (acceleration) at the top of the casing structure at an operating speed of 3000 rpm while the corresponding experimental results are given in Fig. 7.16A. Note that the amplitudes and general shapes of the two time signals are very similar. The comparison of their frequency contents are given by the frequency spectra in Fig. 7.17. Figure 7.17A shows the frequency components of the measured vibration at the top of the gear box. Note that the major vibration components occur at the mesh frequency of 1250 Hz and at 3-times

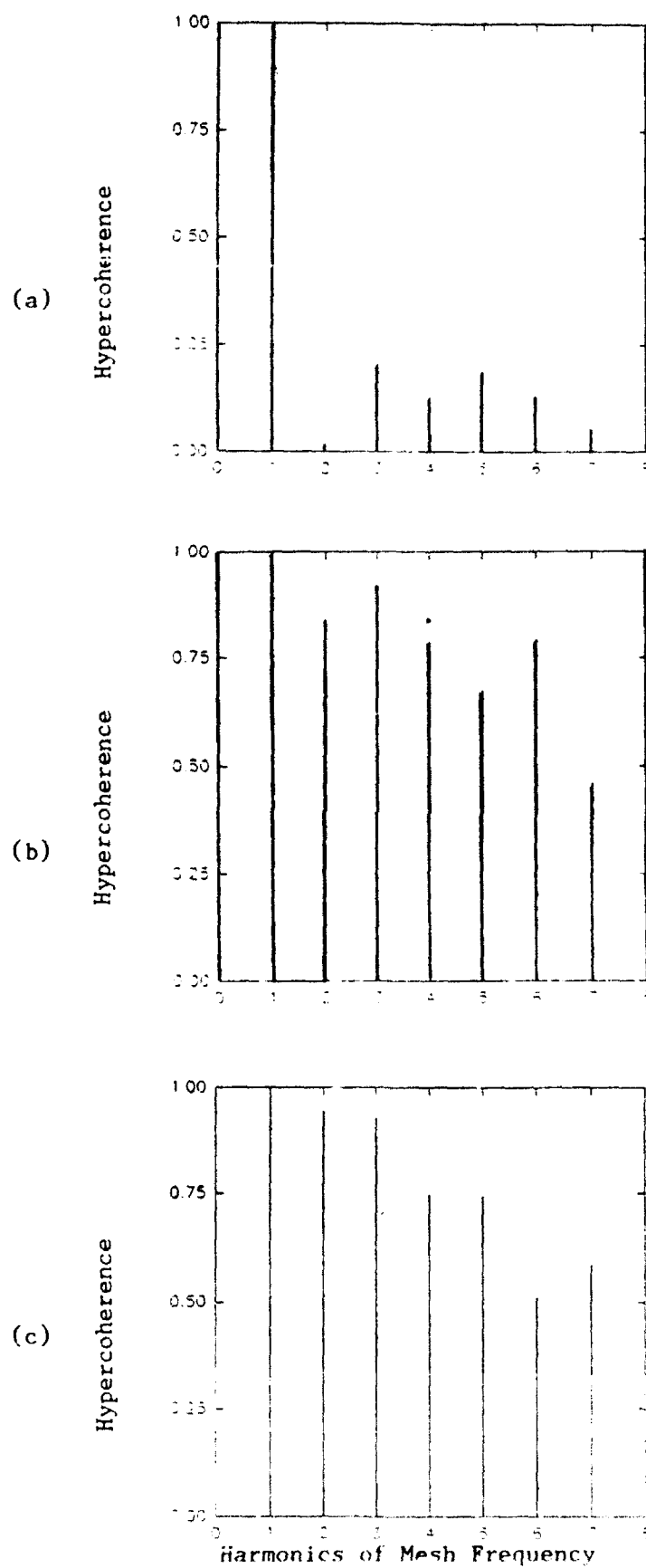


Figure 7.15 Hypercoherence function for the noise signal from microphone no. 1 (a) at 3,000 rpm, (b) at 4,000 rpm, (c) at 5,000 rpm

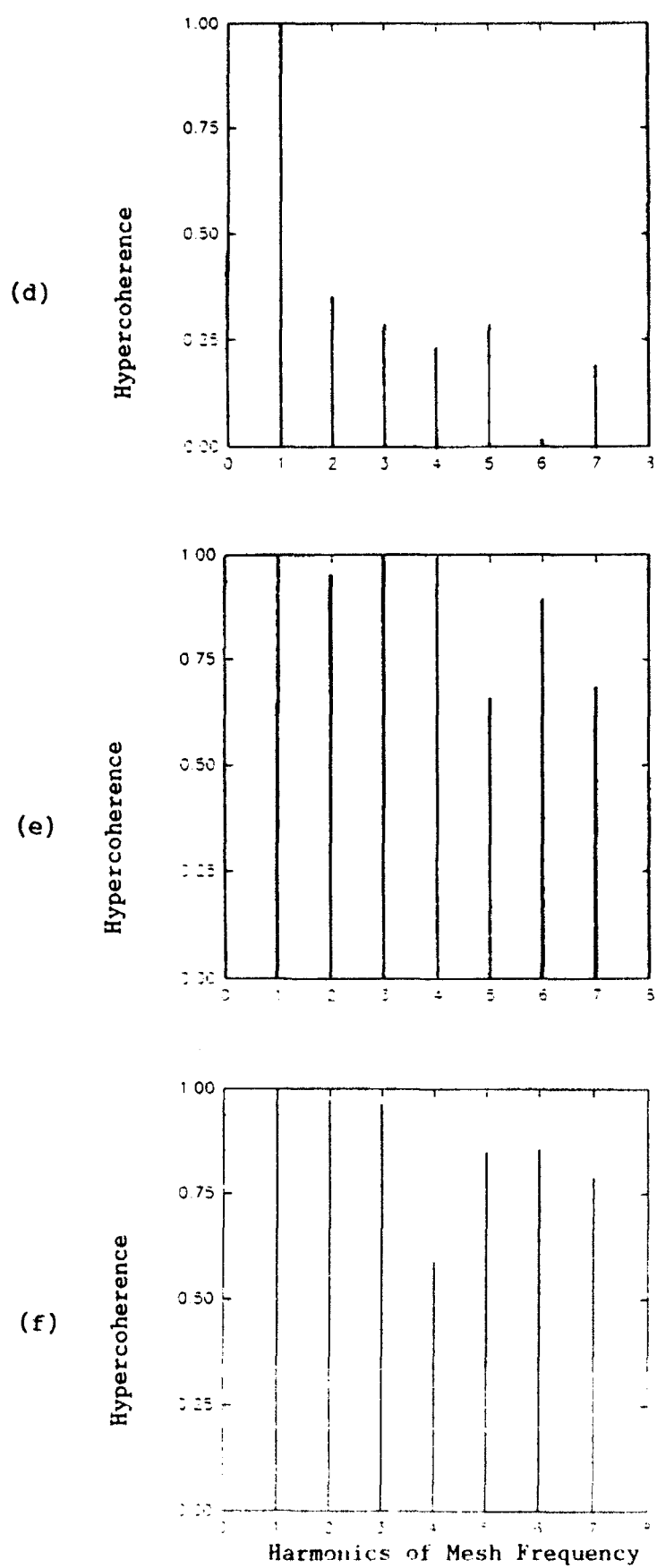


Figure 7.15 Hypercoherence function for the noise signal from microphone no. 2 (d) at 3,000 rpm, (e) at 4,000 rpm, and (f) at 5,000 rpm

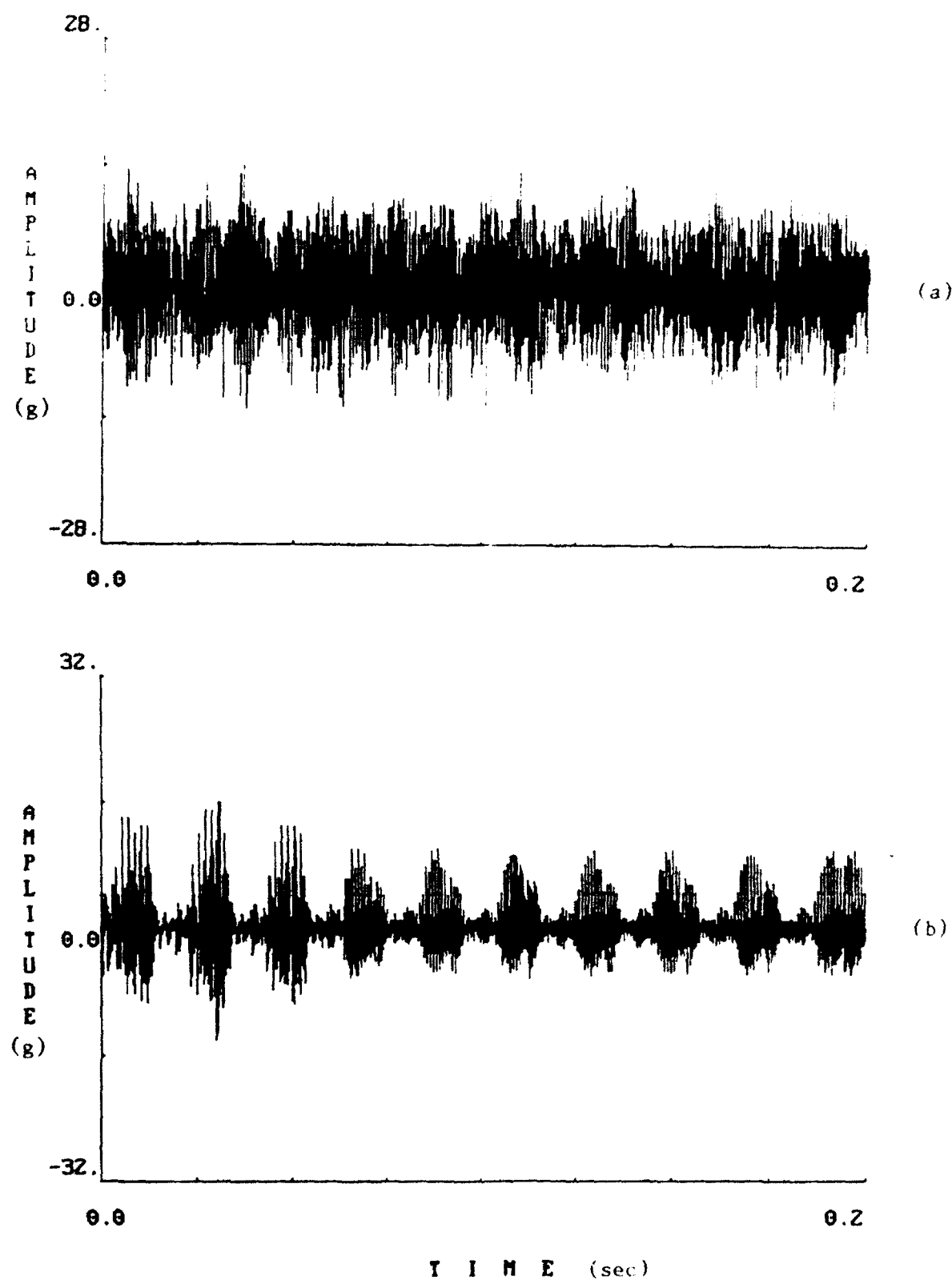


Figure 7.16 Time vibration signal at top of gear box for operating speed of 3,000 rpm from (a) experimental data, and (b) numerical simulations

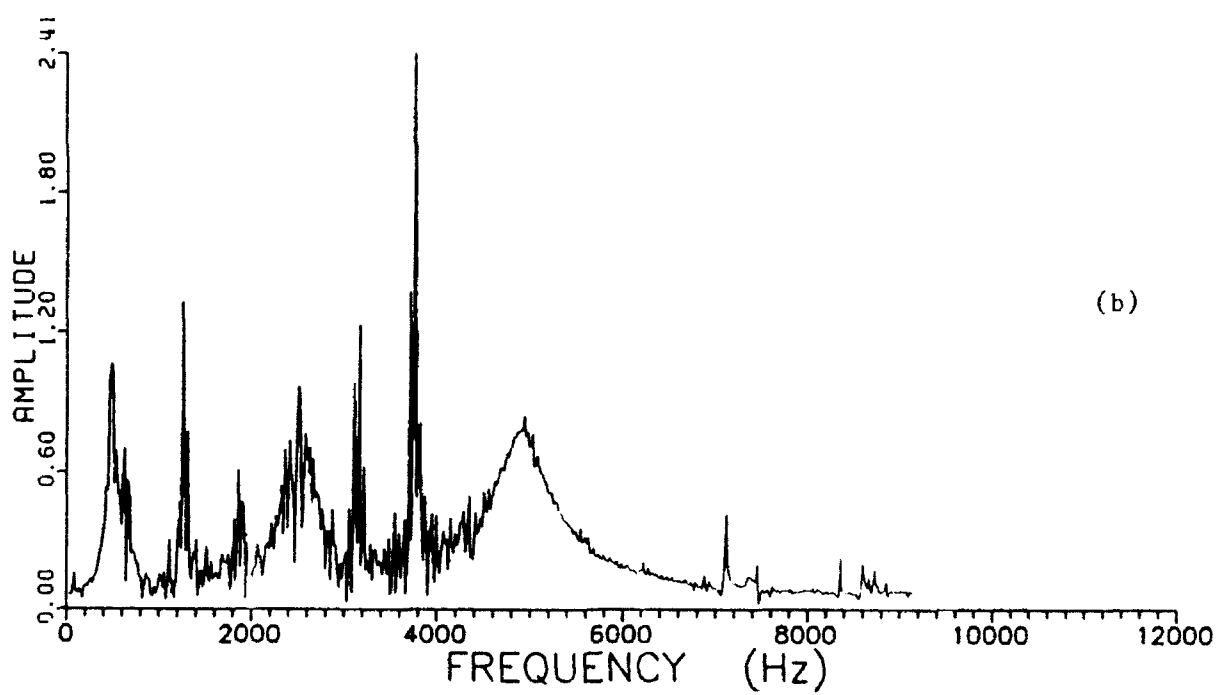
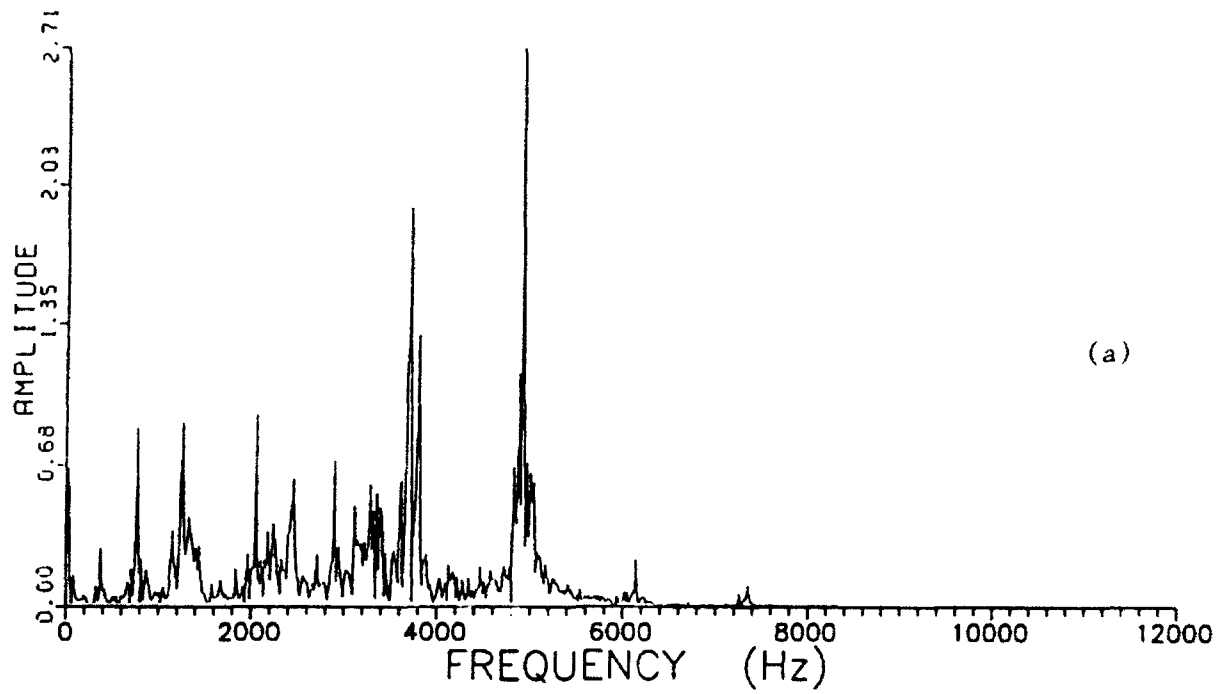


Figure 7.17 Vibration frequency spectra at top of gear box for operating speed of 3,000 rpm from (a) experimental data, and (b) numerical simulations.

(3750 Hz) and 4-times (5000 Hz) the mesh frequency. The very large amplitude in the frequency components at 3750 Hz and 5000 Hz are due to the excitation of the gear box natural frequencies near the 3-times and 4-times multiples of the mesh frequency. The fundamental and the 2-times mesh frequency component are substantially smaller due to the lack of any gear box natural frequencies near 1250 Hz and 2500 Hz. In addition, frequency components of substantial magnitude are also noticed at 700 Hz and 2900 Hz, which are also close to the natural frequencies of the gear box. Figure 7.17B depicts the results from the numerical simulations of the system. The numerical results correspond closely to those from the experimental study with the exception of the 4-times mesh frequency component. The magnitude and the general distribution of the frequency content of the spectrum is very similar to the experimental results.

To develop a predictive algorithm for the noise level in the gear box, the experimental transfer function developed with noise/vibration data is used in this study. The transfer function for Microphone No. 1 (vertical to the plate) is given in Fig. 7.18A and for microphone No. 2 (45 degrees with the plate) is given in Fig. 7.18B. By taking the product of the transfer functions with the vibration frequency spectrum, the frequency spectra for both the microphone cases can be evaluated. Figure 7.19 shows the comparison of the results of the experimental noise, Fig. 7.19A, with the predicted noise, Fig. 7.19B, for the vertical microphone. Although all the major frequency components excited in both cases are very similar, one can see that the predicted noise spectrum, Fig. 7.19B, has a much higher amplitude at mesh frequency and a very small 4-times mesh frequency component as in the vibration spectrum. Comparing the results for the 45-degree microphone, Fig. 7.20, a

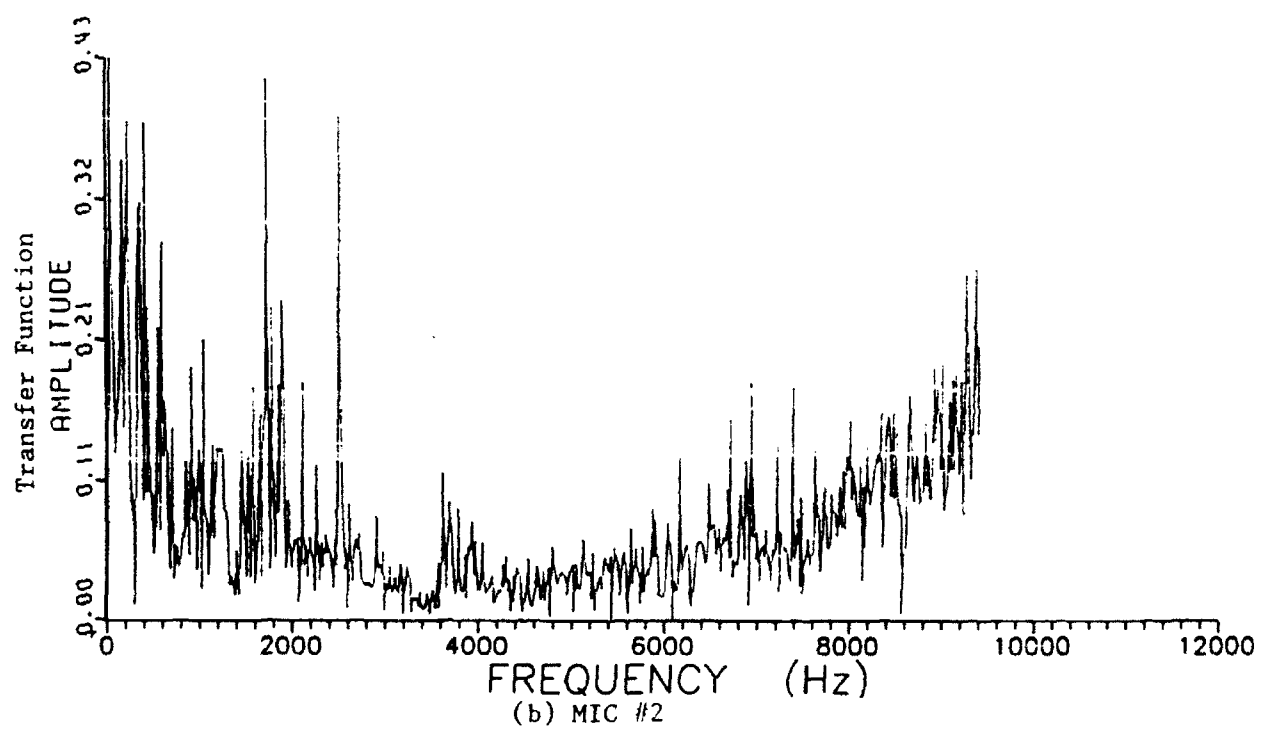
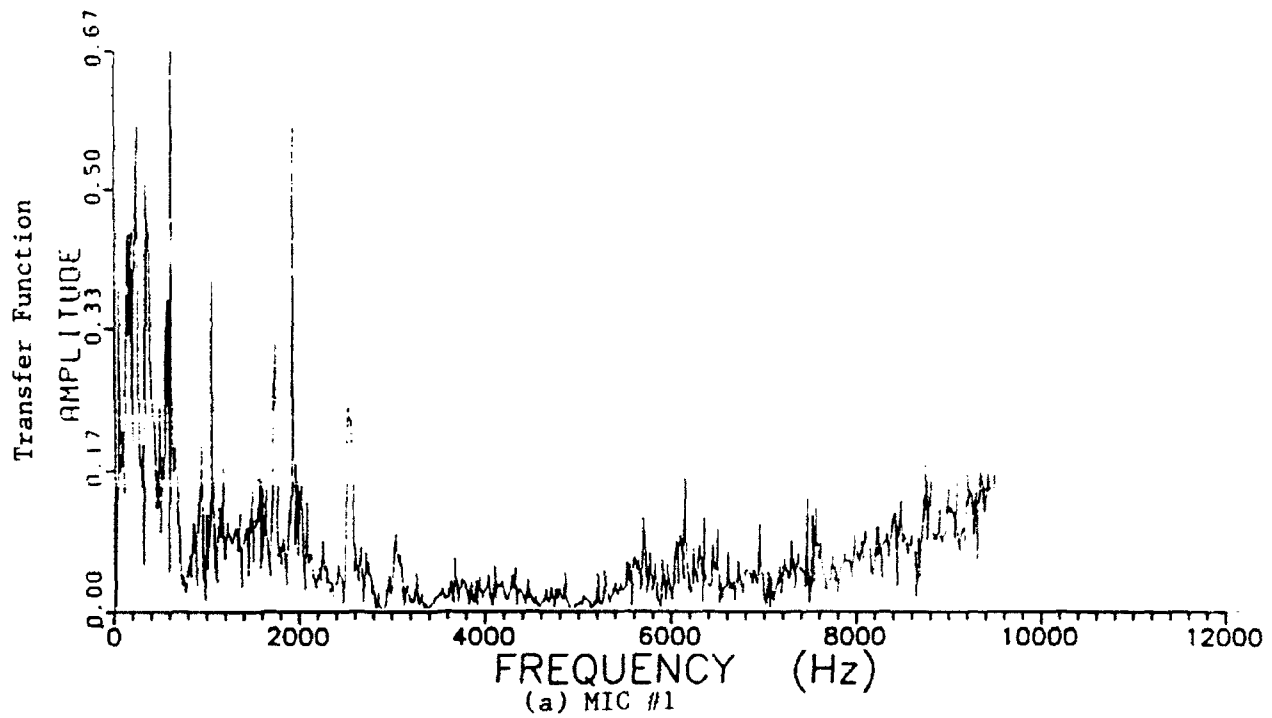


Figure 7.18 Transfer function for noise (a) microphone no. 1, and (b) microphone no. 2, with vibration at operating speed of 3,000 rpm.

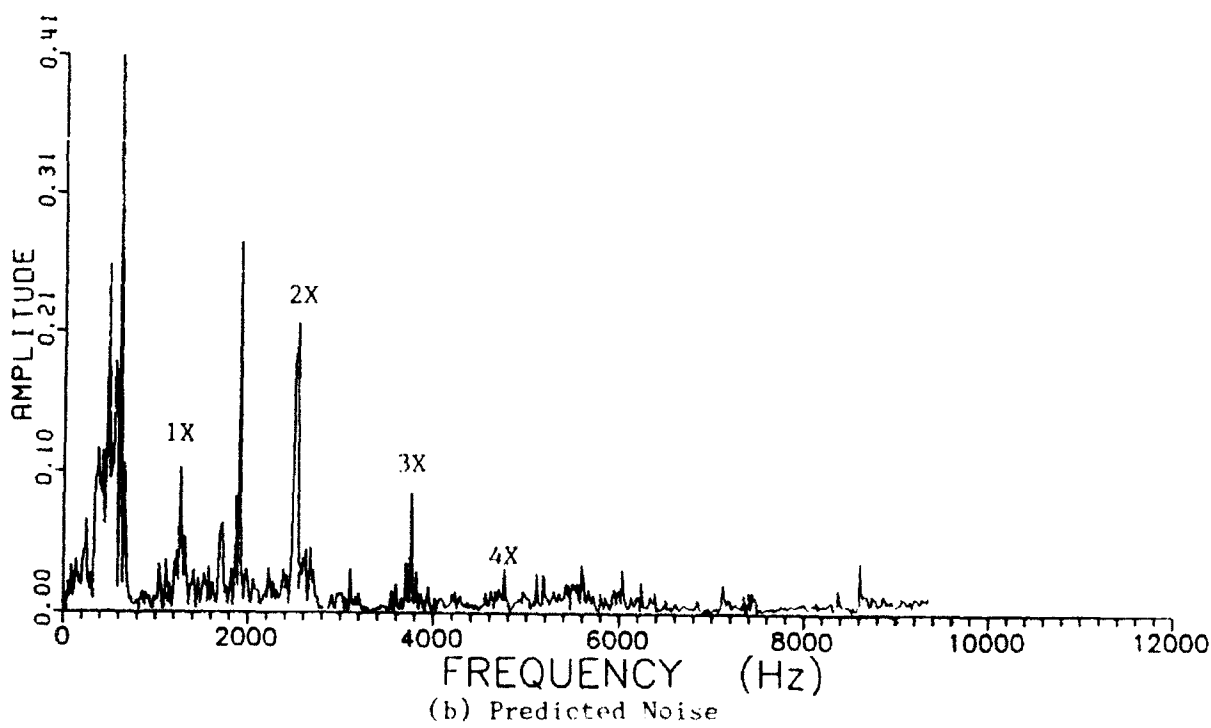
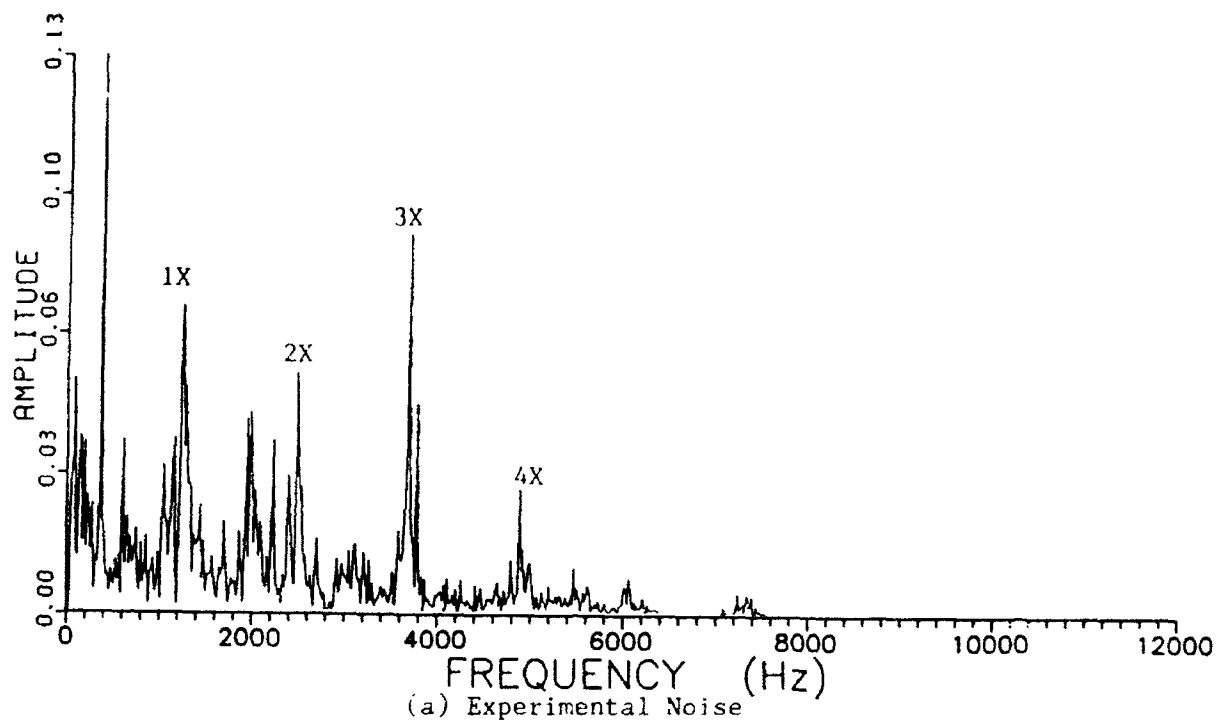


Figure 7.19 Frequency spectra of (a) experimental noise data, and (b) predicted noise results from microphone no. 1 at the operating speed of 3,000 rpm.

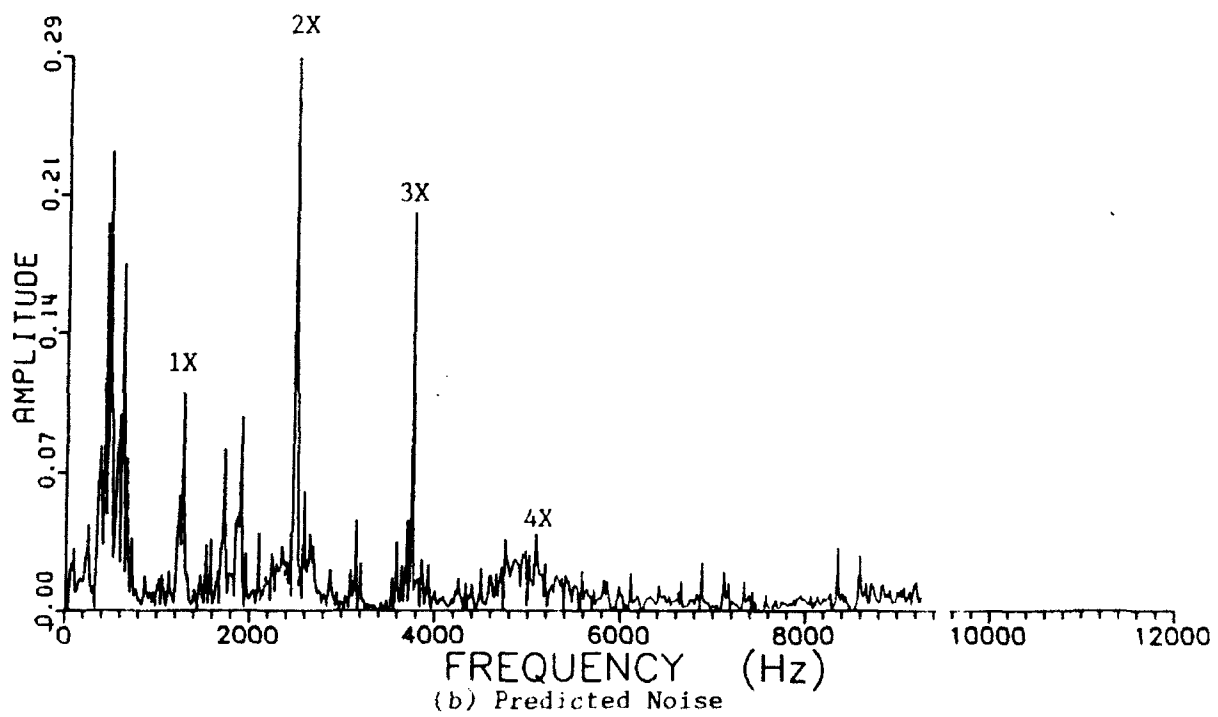
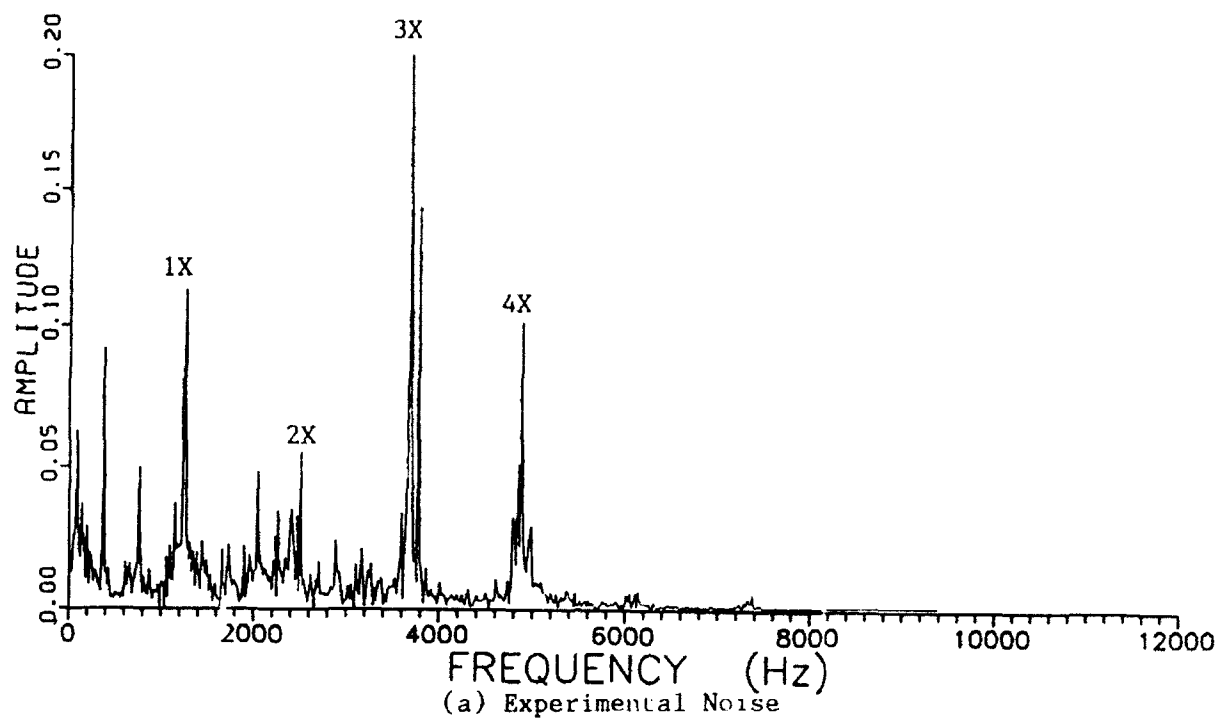
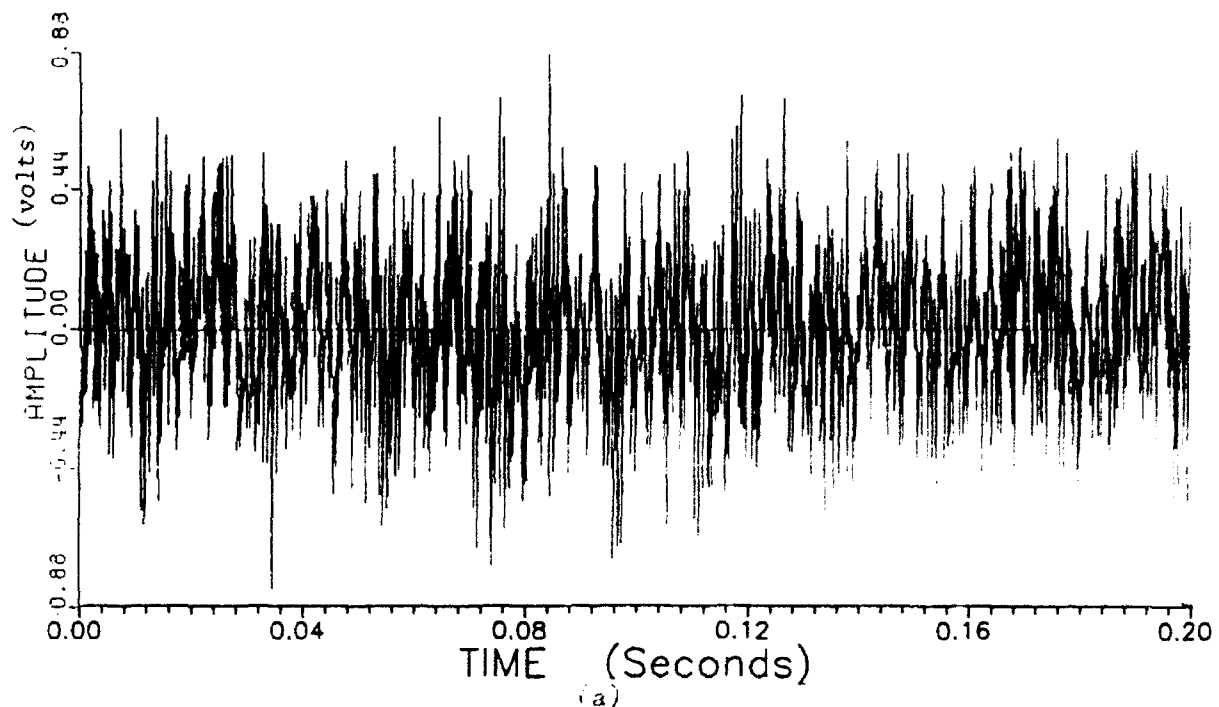


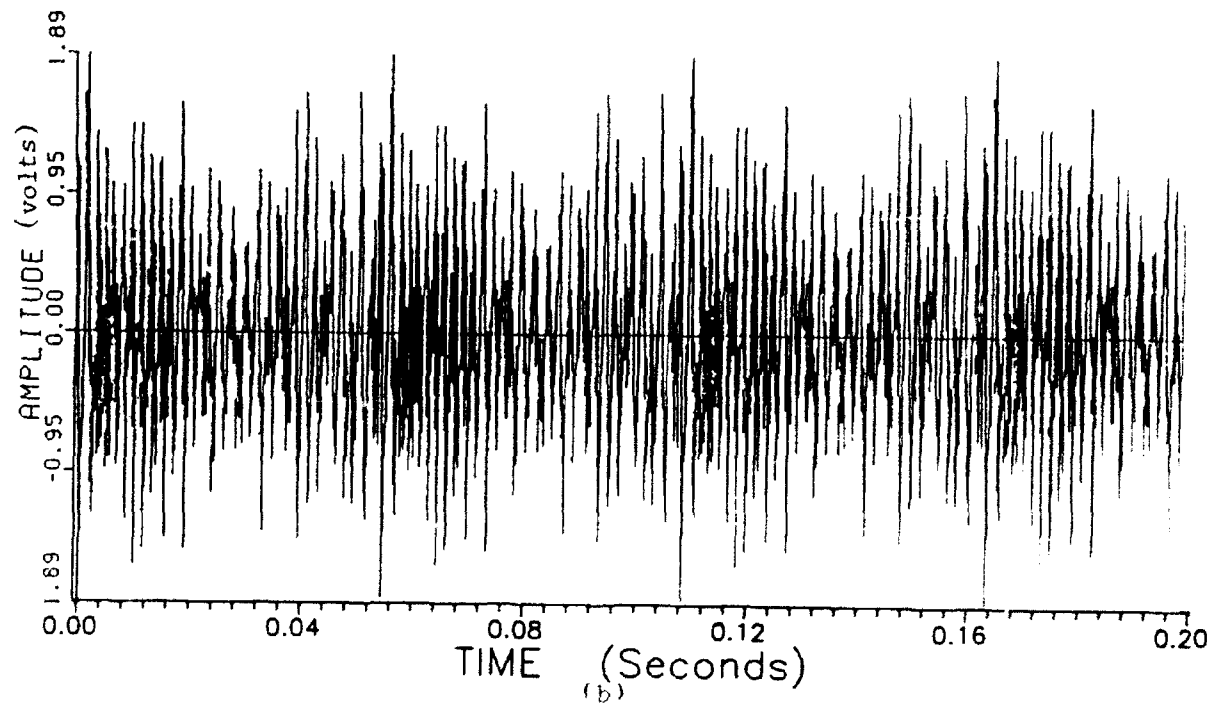
Figure 7.20 Frequency spectra of (a) experimental noise data, and (b) predicted noise results from microphone no. 2 at the operating speed of 3,000 rpm.

similar conclusion can be drawn for the predicted noise (larger amplitudes in most of the frequency components).

Another way of examining the validity of the predicted noise signal is through the nonlinear relationships derived by the Hypercoherence Function. The Hypercoherence function developed by NASA Marshall Space Flight Center is used primarily for the space shuttle noise program to generate nonlinear relationships between the fundamental frequency component and the integer multiples of the fundamental. A time signal for the gear box noise is required for this analysis. Figure 7.21 depicts the time signal for the gear box noise, from experimental study, (Fig. 7.21A), and from numerical simulations (Fig. 7.21B), for microphone No. 1. A set of the experimental and numerical noise data for microphone No. 2 is also given in Fig. 7.22. Figures 7.23 and 7.24 show the comparison of the hypercoherence functions from both experimental and numerical solutions correspondingly for microphone No. 1 and No. 2. For microphone No. 1, both the experimental and numerical results show a very small 2-times component, with a substantial amplitude at 3, 4, and 5 times fundamental frequency. However, a 50% coherence is found in the 3, 4, and 5 times components from numerical predictions, Fig. 7.23B, while only about a 25% coherence is seen from the experimental results, Fig. 7.23A. A similar conclusion can also be drawn from the results of microphone No. 2, Fig. 7.24. The difference in the numerical solution results from the experimental results are possibly due to the limitation of the numerical model in simulating various details and imperfections in the gear box transmission system. A logical explanation of the much higher (nearly double) coherence amplitudes in the numerical study is that only the major frequency-related vibration contributing factors

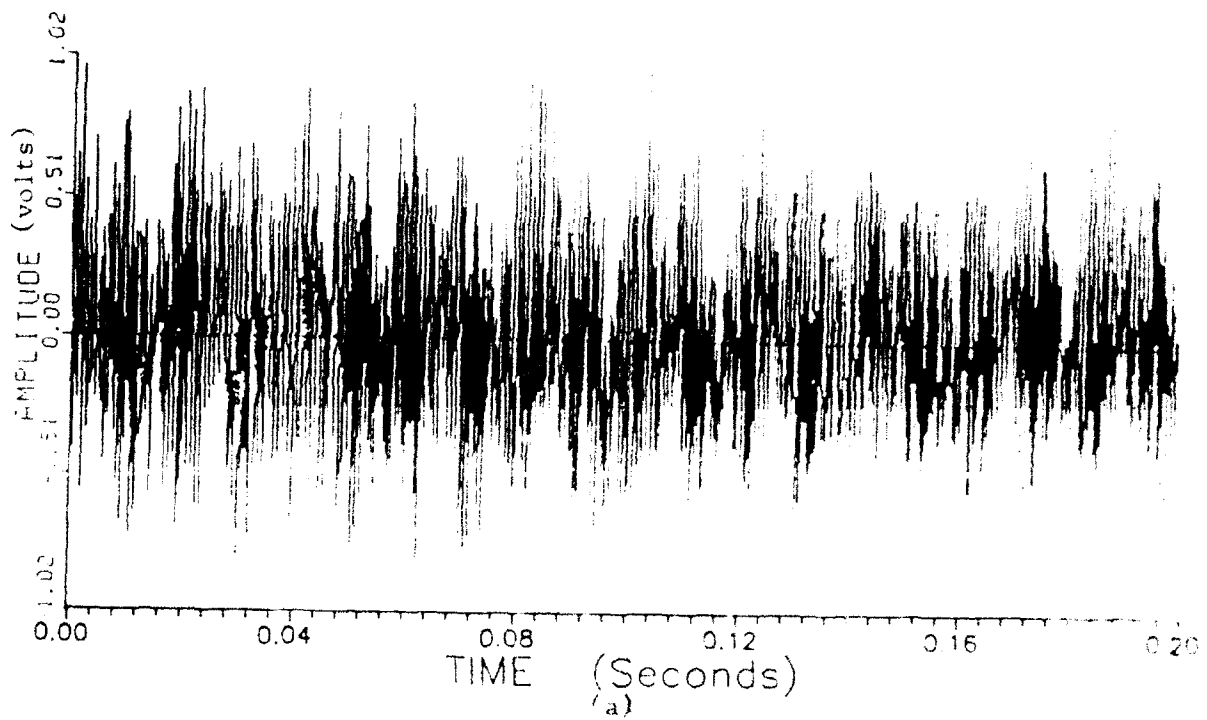


(a)

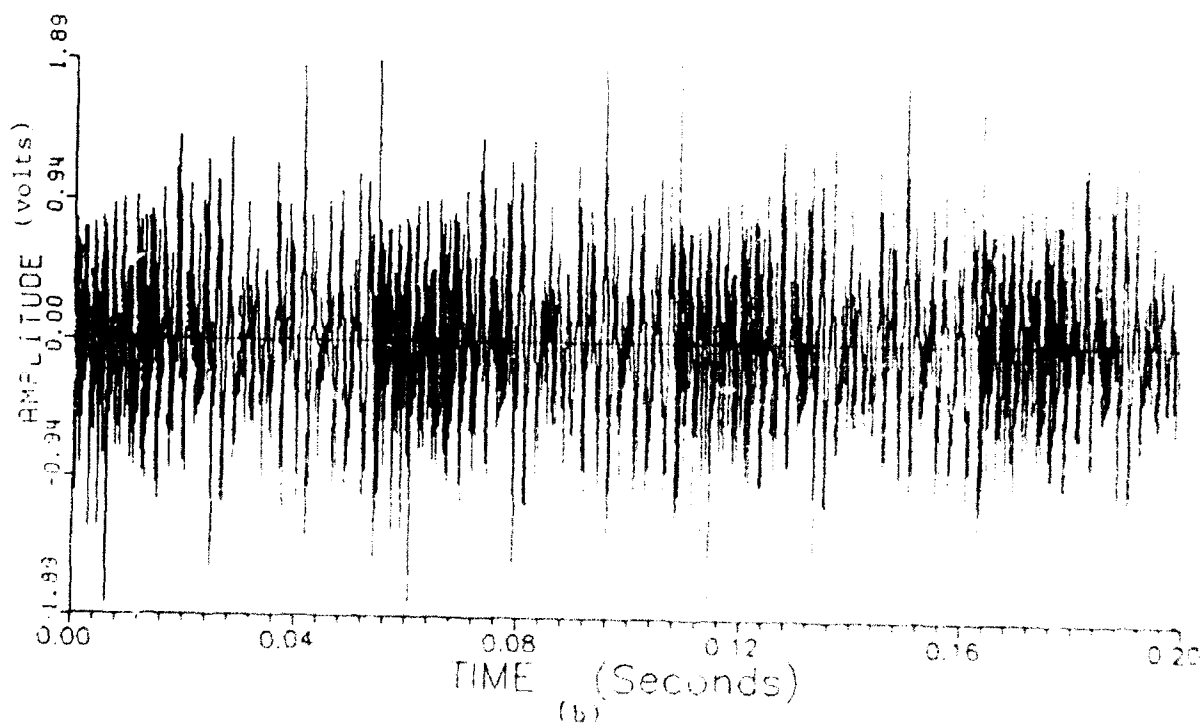


(b)

Figure 7.21 Time noise signal from (a) experimental noise data, and (b) predicted noise results from microphone no. 1 at the operating speed of 3,000 rpm.



(a)



(b)

Figure 7.22 Time noise signal from (a) experimental noise data, and (b) predicted noise results from microphone no. 2 at the operating speed of 3,000 rpm.

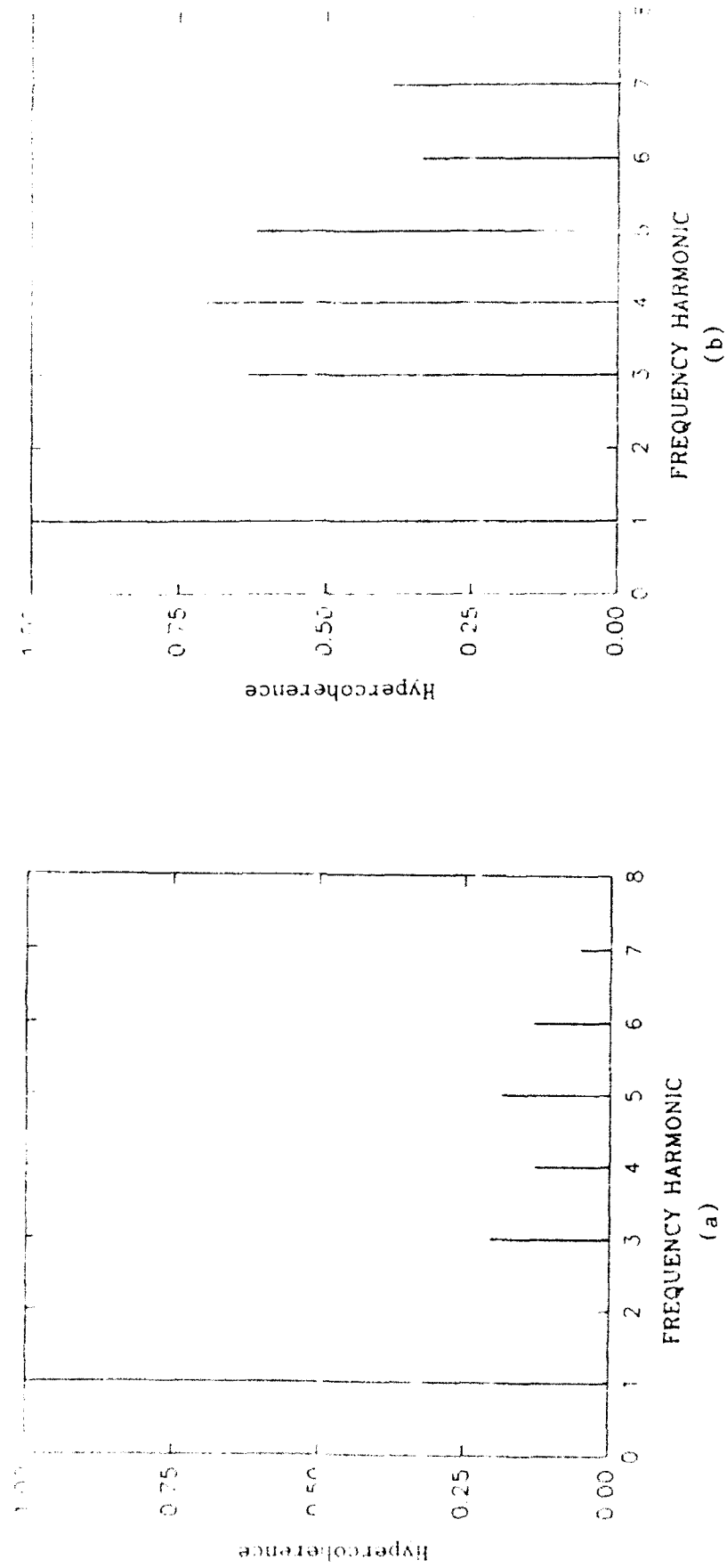


Figure 7.23 Hypercoherence function of the noise signal from (a) experimental data, and (b) from numerical predictions, for microphone no. 1 at the operating speed of 3,000 rpm

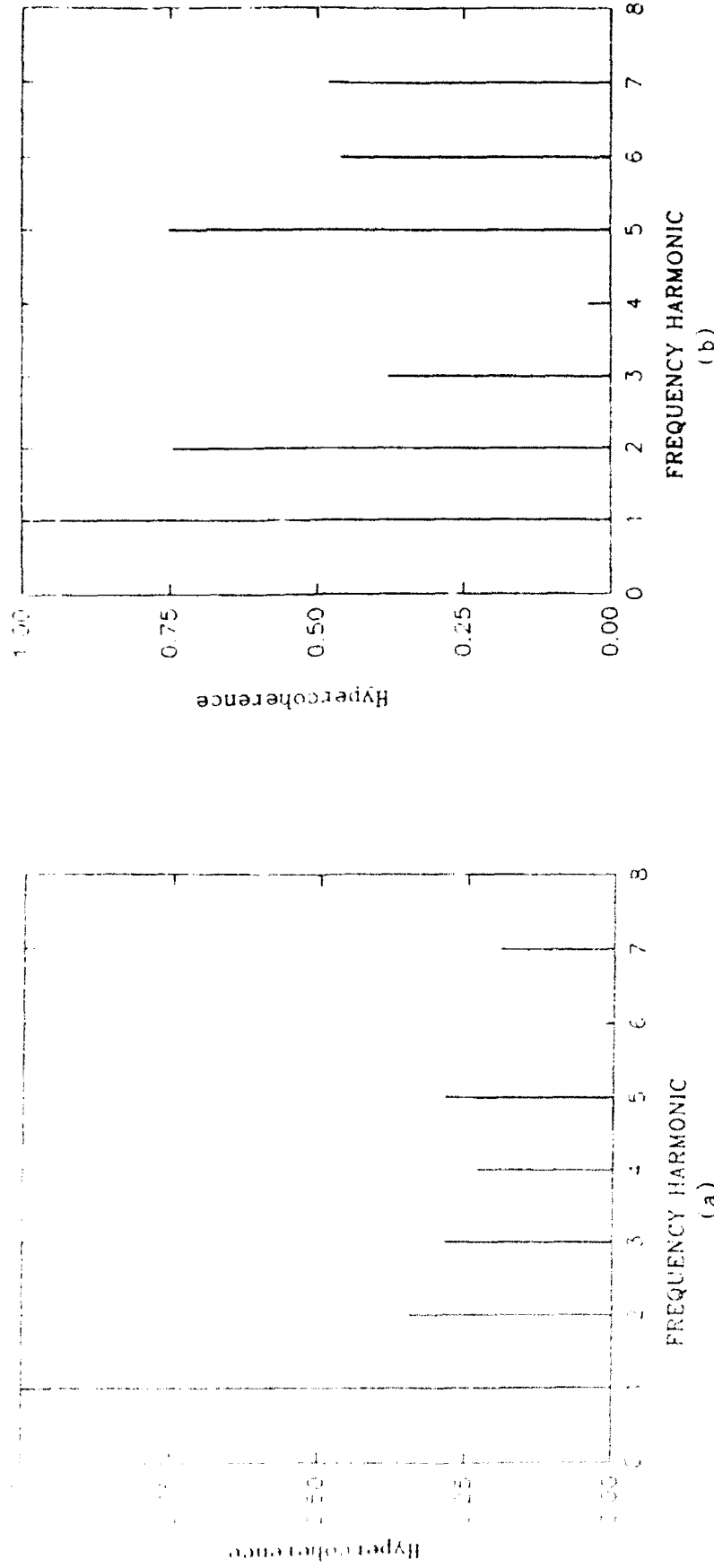


Figure 7.24 Hypercoherence function of the noise signal from (a) experimental data, and (b) from numerical predictions, for microphone no. 2 at the operating speed of 3,000 rpm

are included in the model, which results in a predicted vibration signal consisting mostly of frequency components which are closely related to the fundamental frequency.

8. CONCLUSIONS AND SUMMARY

A methodology has been developed using the modal synthesis technique to simulate the global dynamics of a gear transmission system. Excellent correlation has been obtained using results from the global dynamic model and measured dynamic characteristics from the NASA gear noise test rig. A numerical relationship was also developed from the experimental data to correlate noise and vibrations in the frequency domain. The developed noise\vibration relationships are applied to the vibration simulations to predict the noise of the gear box. Results of the predicted noise are compared to the experimentally measured data linearly using the frequency spectra and nonlinearly using the hypercoherence function.

The major accomplishments/conclusions of this study can be summarized as follows:

1. The dynamics of a gear transmission system coupled with the vibrations of the gear box structure during operation can be simulated accurately using the modal synthesis technique.
2. Gear system dynamic characteristics such as imbalance, shaft residual bow, gear mesh nonlinear stiffness, gear tooth friction, coupled axial and lateral bearing stiffness, and gyroscopic effects are also incorporated into the global dynamic model.
3. Experimental results of both gear vibration and noise are obtained using the NASA gear noise test rig for benchmarking and correlating with the numerical predictions.

4. The accuracy of the rotor and the gear box model can be improved by matching the modal characteristics calculated numerically with those obtained through experimental testing.
5. The choice and the number of vibratory modes selected to simulated the gear box vibration can be selected according to those excited experimentally by the impulse response technique. Such selection not only will reduce the number of modes used, which can significantly improve computational efficiency, it also will provide an accurate simulation of the dynamics of the system.
6. Predicted vibrations at the housing surface using the global dynamic model are in good agreement with measured values.
7. A set of linear relationships are developed between the gear box noise and vibration using transfer functions and both experimental noise and vibration spectra.
8. The developed transfer functions are applied to the numerically simulated gear box vibrations to predict noise generated from the transmission system. Both the frequencies and magnitudes of the predicted noise components are very similar to those obtained from experimental study.
9. An examination of the nonlinear relationships of the noise components with the fundamental frequency (gear mesh frequency) is performed using the hypercoherence function. A comparison of these relationships between the predicted noise and the measured noise is also presented.

9. REFERENCES

1. Akin, L.S. and Townsend, D.P., "Lubricant Jet Flow Phenomena in Spur and Helical Gears with Modified Addendums - for Radially Directed Individual Jets", NASA TM-101460, Technical Report 88-C-034, 1989.
2. August, R. and Kasuba, R., "Torsional Vibrations and Dynamic Loads in a Basic Planetary Gear System", J. of Vibration, Acoustic, Stress, and Reliability in Design, Vol. 108, No. 3, July 1986, pp. 348-353.
3. Boyd, L.S. and Pike, J.A., "Epicyclic Gear Dynamics", AIAA Journal, Vol. 27, No. 5, May 1989, pp. 603-609.
4. Choy, F.K., Townsend, D.P. and Oswald, F.B., "Dynamic Analysis of Multimesh-Gear Helicopter Transmissions", NASA TP2789, 1988.
5. Choy, F.K., Townsend, D.P. and Oswald, F.B., "Experimental and Analytical Evaluation of Dynamic Load and Vibration of a 2240-KW Rotor craft Transmission", J. of The Franklin Institute, Vol. 326, No. 5, 1989, pp. 721-735.
6. Choy, F.K., Tu, Y.K., Savage, M. and Townsend, D.P., "Vibration Signature Analysis of Multistage Gear Transmission", J. of the Franklin Institute, Vol. 328, No. 2/3, 1991, pp. 281-299.
7. Choy, F.K., Ruan, Y.F., Zakrajsek, J.J., Oswald, F.B. and Coy, J.J., "Analytical and Experimental Study of Vibrations in a Gear Transmission", AIAA 27th Joint Propulsion Conference, Sacramento, California, June 24-27, 1991, paper no. AIAA-91-2019.
8. David, J.W., Mitchell, L.D. and Daws, J.W., "Using Transfer Matrices for Parametric System Forced Response", J. of Vibration, Acoustics, Stress and Reliability in Design, Vol. 109, No. 4, October 1987, pp. 355-360.
9. El-Bayoumy, L.E., Akin, L.S., Townsend, D.P. and Choy, F.C., "The Role of Thermal and Lubricant Boundary Layers in the Transient Thermal Analysis of Spur Gears", NASA TM-101435, Technical Report 88-C-032, 1989.
10. Handschuh, R.F. and Litvin, F.L., "A Method for Determining Spiral-Bevel Gear Tooth Geometry for Finite Element Analysis", NASA Technical Paper 3096, AVSCOM Technical Report 91-C-020, 1991.

11. Handschuh, R.F. and Litvin, F.L., "How to Determine Spiral Bevel Gear Tooth Geometry for Finite Element Analysis", NASA TM-105150, Technical Report 91-C-018, 1991.
12. Jong, J. and Coffin, t., "Diagnostic Assessment of Turbomachinery by the Hyper-Coherence Method" NASA Conference Publication 2436, 1986.
13. Kahraman, A., Ozguven, H.N., Houser, D.R. and Zakrajsek, J.J., "Dynamic Analysis of Geared Rotors by Finite Element", NASA TM-102349, AVSCOM-TM-89-C-006, 1990.
14. Kittur, M.G. and Huston, R.L., "Mesh Refinement in Finite Element Analysis by Minimization of the Stiffness Matrix Trace", NASA Contractor Report 185170, Technical Report 89-C-019, 1989.
15. Krantz, T.L., "Gear Tooth Stress Measurements of Two Helicopter Planetary Stages", NASA TM-105651, Technical Report 91-C-038, 1992.
16. Lewicki, D.G. and Coy, J.J., "Vibration Characteristics of the OH-58A Helicopter Main Rotor Transmission", NASA TP-2705, 1987.
17. Lewicki, D.G., Decker, H.J., and Shiinski, J.T., "Full-Scale Transmission Testing to Evaluate Advanced Lubricants", NASA TM-105668, Technical Report 91-C-035, 1992.
18. Lim, T.C., Singh, R. and Zakrajsek, J.J., "Modal Analysis of Gear Housing and Mounts", 7th International Modal Analysis Conference, Vol. 2, Society of Experimental Mechanics, Bethel, CT, 1989, pp. 1072-1078.
19. Lin, H., Houston, R.L. and Coy, J.J., "On Dynamic Loads in Parallel Shaft Transmissions", NASA TM100108, December 1987.
20. Lin, H.H., Townsend, D.P. and Oswald, F.B., "Profile Modification to Minimize Spur Gear Dynamic Loading", NASA TM-89901, 1988.
21. Litvin, F.L., Zhang, Y. and Handschuh, R.F., "Local Synthesis and Tooth Contact Analysis of Face-Milled Spiral Bevel Gears", NASA TM-105182, Technical Report 91-C-039, 1991.
22. Litvin, F.L., Zhang, Y., Kuan, C. and Handschuh, R.F., "Computerized Inspection of Real Surfaces and Minimization of Their Deviations", NASA TM-103798, Technical Report 91-C-008, 1991.

23. Mark, W.D., "Analysis of the Vibratory Excitation Arising From Spiral Bevel Gears", NASA Contractor Report 4081, NAS3-23703, 1987.
24. Mark, W.D., "The Transfer Function Method for Gear System Dynamics Applied to Conventional and Minimum Excitation Gear Design", NASA CR-3626, 1982.
25. Mitchell, Andrew, Oswals, F.B. and Schuller, F.T., "Testing of YUH-61A Helicopter Transmission in NASA Lewis 2240-kW (3000-hp) Facility", NASA Technical Paper 2538, 1986.
26. NASA Conference Publication 2436, "Advanced Earth-to-Orbit Propulsion Technology 1986, Volume I.
27. Oswald, F.B., "Gear Tooth Stress Measurements on the UH-60A Helicopter Transmission", NASA TP-2698, 1987.
28. Oswald, F.B., Seybert, A.F., Wu, T.W., and Atherton, William, "Comparison of Analysis and Experiment for Gearbox Noise", NASA TM-105330, Technical Report 91-C-030, 1992.
29. Oswald, F.B., Zakrajsek, J.J., Townsend, D.P., Atherton, W. and Lin, H.H., "Effect of Operating Conditions on Gearbox Noise", NASA TM-105331, Technical Report 91-C-031, 1992.
30. Ozguven, H.N. and Houser, D.R., "Mathematical Models Used in Gear Dynamics - A Review", J. of Sound and Vibration, Vol. 121, No. 3, March 22, 1988, pp. 383-411.
31. Rebbechi, B., Forrester, David, B. and Oswald, F.B. and Townsend, Dennis P., "A Comparison Between Theoretical Prediction and Experimental Measurement of the Dynamic Behaviour of Spur Gears", NASA TM-105362, Technical Report 91-C-009, 1992.
32. Rebbechi, B., Oswald, F.O. and Townsend, D.P., "Dynamic Measurements of Gear Tooth Friction and Load", NASA TM-103281, 1991.
33. Seybert, Wu, T.W. and Wu, X.F., "Acoustical Analysis of Gear Housing Vibration", NASA TM-103691, TM-90-C-002, 1991.
34. Singh, R. and Lim, T.C., "Vibration Transmission Through Rolling Element Bearings in Geared Rotor Systems" NASA CR 4334, 1990.

35. Townsend, D.P. and Bamberger, E.N., "Surface Fatigue Life of M50NiL and AISI9310 Spur Gears and R C Bars", Proceedings of the 1991 International Conference on Motion and Power Transmissions, Hiroshima, Japan, November 24-26, 1991.
36. Townsend, D.P., Parker, R.J. and Zaretsky, E.V., "Evaluation of CBS 1002 Carburized Steel as a Gear Material", NASA Technical Paper 1390, 1979.
37. Townsend, D.P. and Patel, P.R., "Surface Fatigue Life of CBN and Vitreous Ground Carburized and Hardened AISI 9310 Spur Gears", NASA TM-100960, Technical Report 88-C-019, 1988.
38. Townsend, D.P. and Shimski, J., "Effect of Two Synthetic Lubricants on Life of AISI 9310 Spur Gears", NASA TM-104352, Technical Report 91-C-011, 1991.

APPENDIX A

For the massless beam element shown in Fig. A1-a, the dynamic characteristics of the element can be represented as (16-18):

$$\begin{Bmatrix} Y \\ \phi \\ M \\ V \end{Bmatrix}_i^L = [S_i] \quad \begin{Bmatrix} Y \\ \phi \\ M \\ V \end{Bmatrix}_{i-1}^R \quad A.1$$

where

$$[S_i] = \begin{bmatrix} 1 & L & L^2/2EI & -L^3/6EI \\ 0 & 1 & L/EI & -L^2/2EI \\ 0 & 0 & 1 & -L \\ 0 & 0 & 0 & 1 \end{bmatrix} \quad A.2$$

The subscript i in the matrix equations designates the nodal number of the element and the superscripts L and R designate the left- and right-hand side location at the concentrated mass station. With the inertia model shown in Fig. A1-b the dynamic effects between the mass stations can be expressed in matrix form as

$$\begin{Bmatrix} Y \\ \phi \\ M \\ V \end{Bmatrix}_i^R = [P_i] \quad \begin{Bmatrix} Y \\ \phi \\ M \\ V \end{Bmatrix}_i^L \quad A.3$$

where

$$[P_i] = \begin{bmatrix} 1 & 0 & 0 & 0 \\ 0 & 1 & 0 & 0 \\ 0 & 0 & 1 & 0 \\ K_i - M_i - \omega^2 & 0 & 0 & 1 \end{bmatrix} \quad A.4$$

where K_i is the stiffness of the i^{th} spring.

Using the beam element model developed with the matrix transfer technique, the dynamics of the beam structure can be related from the left end to the right end by multiplying the series of matrices as

$$\begin{Bmatrix} Y \\ \phi \\ M \\ V \end{Bmatrix}_R = \begin{bmatrix} T_{11} & T_{12} & T_{13} & T_{14} \\ T_{21} & T_{22} & T_{23} & T_{24} \\ T_{31} & T_{32} & T_{33} & T_{34} \\ T_{41} & T_{42} & T_{43} & T_{44} \end{bmatrix} \begin{Bmatrix} Y \\ \phi \\ M \\ V \end{Bmatrix}_L \quad A.5$$

where

$$\begin{bmatrix} T_{11} & T_{12} & T_{13} & T_{14} \\ T_{21} & T_{22} & T_{23} & T_{24} \\ T_{31} & T_{32} & T_{33} & T_{34} \\ T_{41} & T_{42} & T_{43} & T_{44} \end{bmatrix} = [P_n] [S_n] [P_{n-1}] [S_{n-1}] \dots [P_1] [S_1] \quad A.6$$

Using a simple support boundary condition such that the displacements and moments at the ends vanish, the overall global matrix can be written as

$$\begin{Bmatrix} 0 \\ \phi \\ 0 \\ V \end{Bmatrix}_R = \begin{bmatrix} T_{11} & T_{12} & T_{13} & T_{14} \\ T_{21} & T_{22} & T_{23} & T_{24} \\ T_{31} & T_{32} & T_{33} & T_{34} \\ T_{41} & T_{42} & T_{43} & T_{44} \end{bmatrix} \begin{Bmatrix} 0 \\ \phi \\ 0 \\ V \end{Bmatrix}_L \quad A.7$$

where

$$[D] = \begin{bmatrix} T_{12} & T_{14} \\ T_{32} & T_{34} \end{bmatrix} = 0 \quad A.8$$

such that the determinant of the matrix will vanish at the natural frequencies of the system.
A marching technique can be used to determine the fundamental frequencies of the system
by searching for the zeros of the determinant at a given range of frequencies.

APPENDIX B
(INPUT INSTRUCTIONS)

1. COM1, COM2, COM3 -- COMMENT CARD
2. NSTA, NKTB, NSK
 - NSTA -- NO. OF TOTAL ROTORS
 - NKTB -- NO. OF CONNECTING GEARS STIFFNESS
 - NSK -- NO. OF SLANTED ROTORS
3. INSK(I), I=1, NSK
LOCATION NO. OF SLANTED ROTOR
4. ANGL(INSK (I), J), J=1, 3; I=1, NSK
ANGLE OF SLANTED ROTOR
5. JST(I), I=i, NSTA
THE LOCATION NO. OF GEAR OF iTH ROTOR
6. ALPH(I,J), I=1, NSTA; J=1, NSTA
ANGLE BETWEEN GEARS
7. RCC(I), I=1, NSTA
RADIUS OF GEARS
8. TOUT(I) , I=1, NSTA
INPUT EXTERNAL TORTIONAL TORQUE OF ROTORS
9. FORCEZ(I), I=1, NSTA
INPUT EXTERNAL AXIAL FORCE OF ROTORS
10. NP1(I), XG1(I), XMAX1(I), PS11(I), I=1, NKTB
NP1 -- NO. OF SPUR'S POINTS OF GEAR
XG1 -- ANGLE BETWEEN THE SPURS OF A PAIR OF GEAR
XMAX1 -- ANGLE DURING TOUCH PERIOD
PS11 -- PHASE ANGLE OF A PAIR OF GEARS
11. XK(K,I), YK(K,I), I=1, NP1(K); K=1, NKTB
XK -- ANGLE OF iTH POINT OF kTH GEAR
YK -- STIFFNESS OF iTH POINT kTH GEAR
12. NTTD(I), I=1, NSTA
NO. OF GEARS FOR EACH ROTOR
13. LLTD(I,J), I=1, NTTD(J); J=1, NSTA
LOCATION NO. OF GEARS
14. TTCC(I,J), I=1, NTTD(J); J=1, NSTA
GEAR DAMPING

15. AB, OMEGA, FAB

AB -- AMPLITUDE IF BASE MOTION
OMEGA -- ROTATION SPEED OF BASE MOTION (RAD/SEC)
FAB -- PHASE ANGLE OF BASE MOTION

16. NMODE

MODES NO. OF ROTORS

17. N, NB, NNLIN, NMB, NF, NU, NS, NBOW, ISTAB, IMODE, ISKU, NCT,
NUFPT

N -- NO. OF MASS STAGE OF ROTOR
NB -- NO. OF REGULAR LINEAR BEARINGS OF ROTOR
NNLIN -- NO. OF NONLINEAR BEARINGS OF ROTOR
NMB -- NO. OF MOMENT RESISTING BEARINGS
NF -- NO. OF EXTERNAL FORCE
NU -- NO. OF UNBALANCE
NS -- NO. OF SKEW DISK
NBOW =1 -- WITH BOW SHAFT
=0 -- NO BOW SHAFT
ISTAB =1 -- NO STABILITY CALCULATION
=0 -- WITH STABILITY CALCULATION
IMODE -- NO. OF DAMPED MODAL SHAPES DESIRED,
IF IMODE = 0, NO MODAL SHAPE CALCULATION
ISKU -- NO. OF SKEW STAGES
NCT -- NO. USED IN MODES CALCULATION
NUFPT -- NO. OF STAHE NEEDED TO PRINTOUT FOR UNBALANCE

18. ISKIP, NSTEP, NSYSLE, NITP, NINT, NPLOT, NORBIT, NTIME, NSPEED,
NINC, NOPT, NT

ISKIP = 1 -- NO CALCULATION
= 0 -- CALCULATE TRANSIENT ORBIT
NSTEP -- NO. OF STEPS OF INTERGRATION PER CYCLE
NCYCLE -- NO. OF CYCLES
NITP -- NO. OF STEPS PER PRINTOUT
NINT = 1 -- NEWWARK BETA METHOD
NPLOT = 1 -- NO PLOT
= 0 -- WITH PLOT
NORBIT -- NO. OF TRANSIENT ORBIT STAGES DESIRED

NTIME -- NO. OF STAGES TO BE PLOTTED IN RESPONSE VS TIME
CURVE

NSPEED = 0

NINC = 0 -- INPUT INITIAL CONDITION
= 1 -- INITIAL CONDITION FROM STEADY STATE ORBIT
(WITH SMALL PERTUBATION)
=2 -- INPUT MODAL INITIAL DATA

NOPT =0

NT -- NO. OF STAGES FOR TRANSIENT PRINTOUT

19. LLBD(J) , J=1, NB
LOCATION NO. OF BEARINGS

20. KXX, KXY, KYX, KYY, KXA, KAX, KAA, KXB, KBX, KBB,
KXZ, KYZ, KZY, KZA, KAZ, KZB, KBZ, KZZ
BEARING STIFFNESS

21 CXX, CXY, CYX, CYY, CXA, CAX, CAA, CXB, CBX, CBB,
CZX, CZY, CZA,
BEARING DAMPING

AND:

X -- DIRECTION OF X
Y -- DIRECTION OF Y
A -- DIRECTION OF X ROTATION
B -- DIRECTION OF Y ROTATION
Z -- DIRECTION OF Z

22. LLNB(J) , NLB(J) , VIS(J) , ANR(J) , ANL(J) , ANC(J) , J=1,NNLIN
LLNB -- LOCATION NO. OF NONLINER BEARINGS
NLB -- BEARING NO. OF NONLINEAR BEATINGS
VIS -- VISCUSITY OF LUBRICATE (LB/IN**2)
ANR -- RADIUS OF BEARING (IN)
ANL -- LENGTH OF BEARINGS (IN)
ANC -- CLEARANCE OF BEARING (IN)

23. LLNMB(J) , J=1,NMB
LOCATION NO. OF MOMENT RESISTING BEARING

24. SLNMB(I,J,K) , CLNMB(I,J,K) , I=1,NMB; J=1,4; K=1,4
NMB SETS, EACH SET 4 CARDS. THESE ARE THE
BEARING STIFFNESS AND DAMPING COEFFICIENTS FOR
MOMENT RESISTING BEARING

25. NGYR -- NO. OF GYROSCOPIC ROTOR
 E -- SECTION YOUNG'S MODULUS
 SPEED1 -- ROTOR'S OPERATING SPEED (RPM)
 SPEED2 -- ROTOR'S INITIAL OPERATING SPEED (RPM)
 ANGACL -- ANGULAR ACCELERATION OF ROTOR
 BETA -- BETA PARAMETER USED FOR NEWMARK BETA METHOD
26. EXTW(J), DX(J), DDXT(J), DDNT(J), RP(J), RT(J), EM6(J),
 RO(J), GGO(J), TK(J), J=1,N
 EXTW -- INPUT EXTERNAL WEIGHT PER ELEMENT OF ROTOR
 DX -- ELEMENT LENGTH OF ROTOR
 DDXT -- EXTERNAL DIAMETER PER ELEMENT OF ROTOR
 DDNT -- INTERNAL DIAMETER PER ELEMENT OF ROTOR
 RP -- POLAR INERTIA MOMENT PER ELEMENT OF ROTOR
 RT -- TRANSVERSE INERTIA MEOMET PER ELEMENT
 OF ROTOR
 EM6 -- YOUNG'S MODULUS PER ELEMENT OF ROTOR
 RO -- DENSITY PER ELEMENT OF ROTOR
 GGO -- SHEAR'S MODULUS PER ELEMENT
 TK -- TORTIONAL CONSTRAINT MOMENT PER ELEMENT
27. LLFF(J), FX(J), FY(J), J=1,NF
 LLFF -- LOCATION NO. OF EXTERNAL FORCE OF ROTOR
 FX -- EXTERNAL FORCE ON X-DIRECTION
 FY -- EXTERNAL FORCE ON Y-DIRECTION
28. LLUF(J), UX(J), UY(J), SUX(J), SUY(J), J=1,NU
 LLUF -- LOCATION NO. OF UNBALANCE OF ROTOR
 UX -- X-DIR UNBALANCE (OZ-IN)
 UY -- Y-DIR UNBALANCE (OZ-IN)
 SUX -- SUDDEN INCREASE UNBALANCE OF X-DIRECTION
 SUY -- SUDDEN INCREASE UNBALANCE OF Y-DIRECTION
29. LLSK(J), FSK(J), PSK(J), J=1,NS
 LLSK -- LOCATION NO. OF SKEW DISK
 FSK -- MAX. SKEW IN RADIANS
 PSK -- ANGLE BETWEEN MAX. SKEW TO THE X AXIS
30. LLUT(J), J=1,NUFPT
 LOCATION NO. FOR PRINTOUT OF UNBALANCE RESPONSE

31. LLNT(J), J=1, NT
LOCATION NO. FOR PRINTOUT OF ROTOR IN TRANSIENT
ANALYSIS

32. NAB, CTIME
SKIP IF NINC IS NOT EQUAL TO 2
NAB -- NO. OF MODES
CTIME -- FINAL TIME OF PRESENT RUN

33. A3(1,J), B3(1,J), A2(1,), B2(1,J), J=1, NAB
SKIP IF NINC NOT EQUAL TO 2
MODAL DISPLACEMENT AND VELOCITY AT FINAL STEP
OF PRESENT RUN

34. BOW(J), PBOW(J), XIDC(J), YIDC(J), VXIDC(J), VYIDC(J), J=1,N
SKIP IF NBOW=0
BOW -- INITIAL BOW
PBOW -- ANGLE OF BOW
XIDC -- INITIAL DISPLACEMENT IN X-DIRECTION
YIDC -- INITIAL DISPLACEMENT IN Y-DIRECTION
VXIDC -- INITIAL VELOCITY IN X - DIRECTION
VYIDC -- INITIAL VELOCITY IN Y- DIRECTION

35. SPI, SPL, DSP
SPI -- INITIAL SPEED FOR CRITICAL SPEED
SPL -- FINAL SPEED FOR CRITICAL SPEED
DSP -- SPEED INCREMENT FOR CRITICAL SPEED

36. SPE1, SPE2, SPE3
SPE1 -- INITIAL SPEED FOR TORTIONAL CRITICAL SPEED
SPE2 -- FINAL SPEED FOR TORTIONAL CRITICAL SPEED
SPE3 -- SPEED INCREMENT FOR TORTIONAL CRITICAL SPEED

37. SPS, SPF, SPN
SPS -- INITIAL SPEED FOR UNBALANCE RESPONSE CAL.
SPF -- FINAL SPEED FOR UNBALANCE RESPONDE CAL.
SPN -- SPEED INCREMENT FOR UNBALANCE RESPONSE CAL.

38. NBMOP
BASE MOTION LOGIC, IF NBMOP = 0, SKIP
1, A(T) = ALPHA * (E**B*T) * COS(W1*T)
2, A(T) = ALPHA * COS(W1*T) * COS(W2*T)

39. ACON1(I), ACON2(I), APH1(I), APH2(I), I=1,NB
SKIP IF NBMOP NOT EQUAL C
EACH VARIABLE FOR ALPHA, B, W1, W2 FOR
 $A(T) = \text{ALPHA} * \cos(W1*T) * \cos(W2*T)$

40. NSRUB, NSEU
SKIP IF NSRUB = 0
NSRUB -- NO. OF RUB STAGES
NSEU -- NO. OF SUDDEN INCREASE UNBALANCE STAGES

41. NFACT, IND, KR, ABSO
SKIP IF NSRUB = 0
NFACT -- STEP FACTOR OF RUB
IND = 0 -- FOR CASING STIFFNESS
=1 -- BLADE EQUATION
=2 -- LINEARIZED STIFFNESS
KR -- DIRECT CASING STIFFNESS
ABSO -- FRICTION COEFFICIENT

42. NRUB(J), CLEAR(J), J=1,NSRUB
SKIP IF NSRUB = 0
NRUB -- LOCATION NO. OF RUB STAGE
CLEAR -- CLEARANCE BETWEEN ROTOR AND CASING

43. ABL1, ABL2, ABL3
THREE TITLE CARDS OFR LABEL IN PLOTS

44. NMBB, NDB, NODEB
NMBB -- MODES NO. OF BOX
NDB -- NO. OF NODES OF BOX
NODEB -- DEGREE OF FREEDOM FOR EACH NODE

45. LBLBT(I,K), I=1, NNB(K), K=1, NSTA
LOCATION NO. OF BEARING ON BOX

46. BKZZ(I,K), I=1, NNB(K), K=1, NSTA
Z-DIRECTION CASING STIFFNESS

47. NPT
NO. OF BOX'S NODES FOR DEFORMATION ANALYSIS

48. NPTNO(I), I=1,NPT
LOCATION NO. OF NODES FOR DEFORMATION ANALYSIS

49. OMEGS(IN), IN=1, NMBB
NATURAL FREQUENCIES OF BOX

50. IA, BX1(IN, ID, IX), IX=1,5; ID=1, NDB; IN=1, NMBB

IA -- NODE NUMBER

BX1 -- MODAL SHAPES OF BOX

AND:

IX = 1 -- MODAL SHAPES IN X-DIRECTION

= 2 -- MODAL SHAPES IN Y-DIRECTION

= 3 -- MODAL SHAPES IN Z-DIRECTION

= 4 -- MODAL SHAPES IN X-ROTATION

= 5 -- MODAL SHAPES IN Y-ROTATION

NOTE: DATA IN CARDS 49 AND 50 CAN BE OBTAINED THROUGH RUNNING
NSTRAN PROGRAM.

APPENDIX C
(COMPUTER PROGRAM LISTING)

```

C ****
C *
C * This program calculates the dynamics of a multi-stage rotor- *
C * bearing-gear system coupling with the vibrations of the gear box *
C * structure. The modal synthesis procedure is used in this program. *
C * Undamped critical speeds and orthonormal modes of the rotor *
C * bearing system is calculated by the matrix transfer method. The *
C * orthonormal modes of the casing(gearbox) structure are evaluated *
C * using a finite approach(NASTRAN) such that output of NASTRAN can *
C * be read directly into the program as data file. Transient and *
C * steady state vibrations of the system will be evaluated by solving *
C * the equations of motion in the modal coordinates. In addition, the *
C * program will handle other dynamic effects such as: *
C *     - multi-stage rotor bearing system *
C *     - mass imbalance, shaft residual bow, and disk skew *
C *     - effects of base motion *
C *     - input of nonlinear gear stiffness *
C *     - 3-dimensional lateral-torsional coupled bearing stiffness *
C *     - coupling casing vibration effects *
C * The output of the program will be given in files that can be read *
C * directly in any IBM compatible PC for plotting of data. The main *
C * files are given as follows: *
C *     - gear.dat    --- gear force *
C *     - box.dat     --- deformation at top of gearbox *
C *     - orbit1.dat   --- first stage orbit at gear station *
C *     - orbit2.dat   --- second stage orbit at gear station *
C *     - x_modal.dat --- modal amplitude in x-dir for each stage *
C *     - y_modal.dat --- modal amplitude in y-dir for each stage *
C *
C * The program is written by: *
C *
C * BY F.K. CHOY & W. QIAN
C *
C * DEPARTMENT OF MECHANICAL ENGINEERING
C *
C * UNIVERSITY OF AKRON, AKRON, OH 44325
C *
C * NOV. 10, 1992
C ****

C ----- THERE ARE THREE PARTS:
C     1. PROGRAM
C     2. SAMPLING DATA
C     3. INPUT DATA INSTRUCTION ( APPENDIX )

C      * * * * *
C PART1. *  PROGRAM  *
C      * * * * *

IMPLICIT REAL(A-H,O-Z)
REAL MFX,MFY,MUY,MUX,KMX,KMY,MBX,MBY,KR
REAL KXX,KXY,KXA,KXB,KXZ
REAL KYX,KYY,KYA,KYB,KYZ
REAL KAX,KAY,KAA,KAB,KAZ
REAL KBX,KBY,KBA,KBB,KBZ
REAL KZX,KZY,KZA,KZB,KZZ
C ----- BEARING STIFFNESS
C     X -- DIRECTION OF X
C     A -- DIRECTION OF X ROTATION
C     Y -- DIRECTION OF Y
C     B -- DIRECTION OF Y ROTATION

```

```

C      Z -- DIRECTION OF Z
CHARACTER COM1(80),COM2(80),COM3(80)
CHARACTER ABL1(80),ABL2(80),ABL3(80)
DIMENSION KXX(30),KXY(30),KXA(30),KXB(30),KXZ(30)
DIMENSION CXX(30),CXY(30),CXA(30),CXB(30),CXZ(30)
DIMENSION KYX(30),KYY(30),KYA(30),KYB(30),KYZ(30)
DIMENSION CYX(30),CYY(30),CYA(30),CYB(30),CYZ(30)
DIMENSION KAX(30),KAY(30),KAA(30),KAB(30),KAZ(30)
DIMENSION CAX(30),CAY(30),CAA(30),CAB(30),CAZ(30)
DIMENSION KBX(30),KBY(30),KBA(30),KBB(30),KBZ(30)
DIMENSION CBX(30),CBY(30),CBA(30),CBB(30),CBZ(30)
DIMENSION KZX(30),KZY(30),KZA(30),KZB(30),KZZ(30)
DIMENSION CZX(30),CZY(30),CZA(30),CZB(30),CZZ(30)

C ----- BEARING STIFFNESS K**
C ----- BEARING DAMPING C**
C           X -- DIRECTION OF X
C           A -- DIRECTION OF X ROTATION
C           Y -- DIRECTION OF Y
C           B -- DIRECTION OF Y ROTATION
C           Z -- DIRECTION OF Z

DIMENSION ENER(100), EY1(100), EY2(100), DPC(100)
DIMENSION DEFL(100), LB(100), SK(100), WA(50)
DIMENSION SW1(100), EI(100)
DIMENSION WMOD(50)
DIMENSION EAN1(100), EAN2(100), EYTH(100), TMX(10,10)
DIMENSION NORUB(100),GAP(100),APH1(10),APH2(10),SNLB(5,8,3)

COMMON /ADD1/ TKXX(10,5),TKXY(10,5),TKXA(10,5),TKXB(10,5),TKXZ(10
1 ,5),TCXX(10,5),TCXY(10,5),TCXA(10,5),TCXB(10,5),TCXZ(10,5)
COMMON /ADD2/ TKYX(10,5),TKYY(10,5),TKYA(10,5),TKYB(10,5),TKYZ(10
1 ,5),TCYX(10,5),TCYY(10,5),TCYA(10,5),TCYB(10,5),TCYZ(10,5)
COMMON /ADD3/ TKAX(10,5),TKAY(10,5),TKAA(10,5),TKAB(10,5),TKAZ(10
1 ,5),TCAX(10,5),TCAY(10,5),TCAA(10,5),TCAB(10,5),TCAZ(10,5)
COMMON /ADD4/ TKBX(10,5),TKBY(10,5),TKBA(10,5),TKBB(10,5),TKBZ(10
1 ,5),TCBX(10,5),TCBY(10,5),TCBA(10,5),TCBB(10,5),TCBZ(10,5)
COMMON /ADD5/ TKZX(10,5),TKZY(10,5),TKZA(10,5),TKZB(10,5),TKZZ(10
1 ,5),TCZX(10,5),TCZY(10,5),TCZA(10,5),TCZB(10,5),TCZZ(10,5)

C ----- BEARING STIFFNESS TK**
C ----- BEARING DAMPING TC**
C           X -- DIRECTION OF X
C           A -- DIRECTION OF X ROTATION
C           Y -- DIRECTION OF Y
C           B -- DIRECTION OF Y ROTATION
C           Z -- DIRECTION OF Z

COMMON /ADD6/ TOC(16),TOD(16),TOE(16)
C           TOC -- BOX'S Z-DIRECTION DEFORMATION
C           TOD -- BOX'S X-ROTATION DEFORMATION
C           TOE -- BOX'S Y-ROTATION DEFORMATION

COMMON /BLK1/ N,NB,NNLIN,NMB,NF,NU,NS,NBOW,ISTAB,IMODE,ISKU,NCT,NU
1 FPT
C           N -- NO. OF MASS STAGE OF ROTOR
C           NB -- NO. OF REGULAR LINEAR BEARINGS OF ROTOR
C           NNLIN -- NO. OF NONLINEAR BEARINGS OF ROTOR
C           NMB -- NO. OF MOMENT RESISTING BEARINGS
C           NF -- NO. OF EXTERNAL FORCE
C           NU -- NO. OF UNBALANCE
C           NS -- NO. OF SKEW DISK
C           NBOW = 1    -- WITH BOW SHAFT

```

```

C      = 0    -- NO SHAFT BOW
C  ISTAB = 1    -- NO STABILITY CALCULATION
C      = 0    -- WITH STABILITY CALCULATION
C  IMODE -- NO OF DAMPED MODAL SHAPES DESIRED
C          IF = 0, NO MODAL SHAPE CALCULATION
C  ISKU -- NO. OF SKEW STAGES
C  NCT -- NO. USED TO CALCULATE MODES OF ROTOR
C  NUFPT -- NO. OF STAGE NEEDED TO PRINTOUT FOR UNBALANCE

COMMON /BLK2/ ISKIP,NSTEP,NCYCLE,NITP,NINT,NPLOT,NORBIT,NTIME,NSPE
1      ED,NINC,NOPT,NT
C  ISKIP = 1    -- NO CALCULATION
C      = 0    -- CALCULATE TRANSIENT ORBIT
C  NSTEP -- NO. OF STEPS OF INTEGRATION PER CYCLE
C  NCYCLE -- NO. OF CYCLES
C  NITP -- NO. OF STEPS PER PRINTOUT
C  NINT = 1    -- NEWWARK BETA METHOD
C  NPLOT = 1    -- NO PLOT
C      = 0    -- WITH PLOT
C  NORBIT -- NO. OF TRANSIENT ORBIT STAGES DESIRED
C  NTIME -- NO. OF STAGES TO BE PLOTTED IN RESPONSE VS TIME CURVE
C  NSPEED = 0
C  NINC = 0    INPUT INITIAL CONDITION
C      = 1    -- INITIAL CONDITION FROM STEADY STATE ORBIT
C          ( WITH SMALL PERTURBATION )
C      = 2    -- INPUT MODAL INITIAL DATA
C  NOPT = 0
C  NT -- NO. OF STAGES FOR TRANSIENT PRINTOUT

COMMON /BLK3/ CRT(10),LLBD(10),LLNB(5),LLNMB(9),LLSK(10),LLNT(10),
1      LLUF(10),LLFF(10),LLUT(10),TCRT(10,5)
C  CRT -- ROTOR LATERAL NATURAL FREQUENCY
C  LLBD -- NO. OF COUPLING BEARING STAGE OF ROTOR
C  LLNB(J) -- STAGE NO. OF JTH NONLINEAR BEARING
C  LLNMB(J) -- STAGE NO. OF THE JTH MOMENT RESISTING BEARING
C  LLSK(J) -- STAGE NO. OF JTH TOTOR SKEW DISK
C  LLNT -- PRINTOUT ROTOR STAGE NO. FOR TRANSIENT ANALYSIS
C  LLUF(J) -- STAGE NO. OF JTH ROTOR UNBALANCE
C  LLFF(J) -- STAGE NO. OF JTH ROTOR EXTERNAL FORCE
C  LLUT -- PRINTOUT STAGE NO. FOR UNBALANCE RESPONSE
C  TCRT -- ROTOR CRETICAL SPEED

COMMON /BLK4/SLNMB(9,4,4),CLNMB(9,4,4)

COMMON /BLK5/ UX(10),UY(10),FX(10),FY(10),FSK(10),PSK(10)
C  UX -- X-DIR UNBALANCE ( OZ-IN )
C  UY -- Y-DIR UNBALANCE ( OZ-IN )
C  FX -- X-DIR EXTERNAL FORCE ( LB )
C  FY -- Y-DIR EXTERNAL FORCE ( LB )
C  FSK -- MAXIMUM STEW OF THE DISK
C  PSK -- ANGLE BETWEN MAXIMUM SKEW & X-AXIS

COMMON /BLK6/ BOW(100),PBOW(100),XIDC(100),YIDC(100),VXIDC(100),VY
1 IDC(100),BXA(100),BYA(100)
C  BOW -- INITIAL BOW OF ROTORS
C  PBOW -- ANGLE OF BOW
C  XIDC -- X-DIR INITIAL DISPLACEMENT
C  YIDC -- Y-DIR INITIAI DISPLACEMENT
C  VXIDC -- X-DIR INITIAL VELOCITY
C  VYIDC -- Y-DIR INITIAL VELOCITY

```

```

COMMON /BLK7/ CMX(10,10),KMX(10,10),EMX(10,10),CMY(10,10),KMY(10,1
10),EMY(10,10)
COMMON /BLK8/ MFX(10),MFY(10),MUX(10),MUY(10),MBX(10),MBY(10)

COMMON /BLK9/ DDPC(10,100),EEYTH(10,100)
C DDPC -- LATERAL MODAL SHAPE OF ROTOR
C EEYTH -- X-DIR TORSIONAL MODAL SHAPE OF ROTOR

COMMON /BLK10/ SPS,SPF,SPN,SPEED1
C SPS -- INITIAL SPEED FOR UNBALANCE CALCULATION ( RPM )
C SPF -- FINAL SPEED FOR UNBALANCE CALCULATION ( RPM )
C SPN -- SPEED INCREMENT FOR UNBALANCE CALCULATION ( RPM )
C SPEED1 -- ROTOR OPERATING SPEED ( RPM )

COMMON /BLK11/ DOX(10,10),DOY(10,10),EOX(10,10),EOY(10,10)
COMMON /BLK15/ RP(100),RT(100)
C RP -- POLAR INERTIA MOMENT OF ROTOR
C RT -- TRANSVERSE INERTIA MOMENT OF ROTOR

COMMON /BLK16/ SPEED2,ANGSP,ANGACL,FSPEED
C SPEED2 -- INITIAL SPEED USED IN TRANSIENT ANALYSIS
C ANGSP -- ANGULAR VELOCITY OF ROTOR
C ANGACL -- ANGULAR ACCELERATION OF ROTOR

COMMON /BLK18/ AKK(10),TAKK(10,5)
C AKK -- AVERAGE BEARING STIFFNESS
C TAKK -- AVERAGE BEARING STIFFNESS

COMMON /BLK19/ DX(100)
C DX(J) -- LENGTH OF JTH ELEMENT OF ROTOR

COMMON /BLK20/ A1(2,10),A2(2,10),A3(2,10),B1(2,10),B2(2,10),B3(2,1
1          0)
C A1,A2,A3,B1,B2,B3 -- USED FOR MATRIX CALCULATION

COMMON /BLK22/ W(100)
C W(J) -- WEIGHT OF JTH ELEMENT OF ROTOR

COMMON /BLK24/ BB(20,21),CC(20)
COMMON /BLK25/ BETA
C BETA -- NEWMARK BETA COEFFICIENT

COMMON /BLK29/ PASP
C PASP -- TRANSIENT ANGLE OF CYCLE

COMMON /BLK40/ BMMFX(10),BMMFY(10),TBMMFX(10,5),TBMMFY(10,5)
COMMON /BLK41/ NBMOP,ACON1(10),ACON2(10),AOMG1(10),AOMG2(10)
C NBMOP = 0 NO CALCULATION
C = 1 A(T)=(E**2*(A(T)*T)*COS(A(T)*T))
C = 2 A(T)=COS(A(T)*T)**2

COMMON /BLK42/ CLEAR(100),NRUB(100),KR,IND,NSRUB,ABSO,NFACT
C CLEAR -- CLEARANCE IN RUB
C NRUB -- LOCATION NO. OF RUB STAGE
C KR -- DIRECT CASING STIFFNESS
C IND = 0 FOR CASING STIFFNESS
C = 1 BLADE EQUATION
C = 2 LINEARIZED STIFFNESS
C NSRUB -- NO. OF RUB STAGES

```

```

C      ABSO -- FRICTION COEFFICIENT
C      NFACT -- STEP FACTOR

C      COMMON /BLK46/ NSEU,SUX(10),SUY(10)
C          NSEU -- NO. OF SUDDEN INCREASE UNBALANCE
C          SUX -- SUDDEN INCREASE UNBALANCE OF X-DIRECTION
C          SUY -- SUDDEN INCREASE UNBALANCE OF Y-DIRECTION

C      COMMON /BLK79/ CTIME
C          CTIME -- FINAL TIME OF RUNNING

C      COMMON /SPEED/ TSPEED(5)
C          TSPEED -- ROTOR OPERATING SPEED

C      COMMON /SHAPE/ NN(5),NNNCT(5),NNB(5)
C          NN -- NO. OF ELEMENTS OF ROTORS
C          NNNCT -- NO. OF MODES OF ROTOR
C          NNB -- NO. OF BEARING OF ROTOR

C      COMMON /OMG/ NNBMOP(5),TACON1(10,5),TACON2(10,5),TAOMG1(10,5),
1          TAOMG2(10,5)
C      COMMON /BLK14/ AAA(42),UUU(42),VVV(42),HHH(42),BBB(42),CCC(42)
C      COMMON /BLK21/ DMX(10,10),DMY(10,10)
C      COMMON /BLK28/ ABL1,ABL2,ABL3
C      COMMON /BLK35/ WMY(10),VIS(5),ANR(5),ANL(5),ANC(5),NLB(5)

C      COMMON /TOU/ TOUT(5),FORCEZ(5)
C          TOUT -- INPUT EXTERNAL TORTIONAL MOMENT ON ROTOR
C          FORCEZ -- INPUT EXTERNAL AXIAL FORCE ON ROTOR

C      COMMON /BLK52/ EXTW(100),DLX(100),DDXT(100),DDNT(100),RO(100),GGO(
1          100)
C          EXTW(J) -- EXTERNAL WEIGHT OF JTH ELEMENT OF ROTOR
C          DLX(J) -- LENGTH OF ELEMENT OF ROTOR
C          DDXT(J) -- EXTERNAL DIAMETER OF ROTOR
C          DDNT(J) -- INTERNAL DIAMETER OF ROTOR
C          RO -- DENSITY OF ROTOR
C          GGO -- SHEAR MODULUS *1.0E-6

C      COMMON /BLK54/ FR(10,5), FFV(10,100,5)
C          FR -- TORTIONAL NATURAL FREQUENCIES OF ROTOR
C          FFV -- TORTIONAL MODAL SHAPES OF ROTOR

C      COMMON /BLK58/ ZF(10,5),ZFV(10,100,5)
C          ZF -- Z-DIR NATURAL FREQUENCIES OF ROTOR
C          ZFV -- Z-DIR MODAL SHAPES OF ROTOR

C      COMMON /BLK56/ SPE1,SPE2,SPE3
C          SPE1 -- INITIAL SPEED FOR TORTIONAL CRITICAL SPEED ANALYSIS
C          SPE2 -- FINAL SPEED FOR TORTIONAL CRITICAL SPEED ANALYSIS
C          SPE3 -- SPEED INCREMENT FOR TORTIONAL CRITICAL SPEED ANALYSIS

C      COMMON /BLK59/ TK(100),EM6(100)
C          TK -- TORTIONAL CONSTRAINT MOMENT OF ROTOR
C          EM6 -- YOUNG'S MODULUS *1.0E-5

C      COMMON /JS/ JST(5)
C          JST(J) -- THE LOCATION NO. OF GEAR OF JTH ROTOR

COMMON /K123/ XK(4,100),YK(4,100)

```

```

C      XK(K,I) -- ANGLE OF ITH POINT OF KTH GEAR
C      YK(K,I) -- STIFFNESS OF ITH POINT OF KTH GEAR

C      COMMON / KK13 / NP1(4),XG1(4),XMAX1(4),PS11(4)
C          NP1 -- NO. OF SPUR'S POINTS OF GEAR
C          XG1 -- ANGLE BETWEEN SPURS OF A PAIR OF GEARS
C          XMAX1 -- ANGLE DURING TOUCH PERIOD
C          PS11 -- THE PHASE ANGLE OF A PAIR OF GEARS

C      COMMON / RDDT / NTTD(5),LLTD(10,5),TTCC(10,5)
C          NTTD -- NO. OF DAMPING STAGE OF ROTOR
C          LLTD -- NO. OF DAMPING STAGE OF ROTOR
C          TTCC -- DAMPING COEFFICIENT OF ROTOR

C      CCOMMON /KTB13 / NKTB,NSK,INSK(5),ANGL(5,3),UANGL(5,9)
C          NKTB -- NO. OF CONNECTING GEARS
C          NSK -- NO. OF SLANTED ROTORS
C          INSK -- THE LOCATION NO. OF SLANTED ROTOR
C          ANGL(I,1) -- ANGLE TO X-AXIS OF SLANTED ROTOR
C          ANGL(I,2) -- ANGLE TO Y-AXIS OF SLANTED ROTOR
C          ANGL(I,3) -- ANGLE TO Z-AXIS OF SLANTED ROTOR

C      COMMON /TMU1/ TMUX(10,5),TMUY(10,5),TEXTW(100,5),TDX(100,5)
C          TMUX -- MODAL UNBALANCE FORCE OF X-DIRECTION
C          TMUY -- MODAL UNBALANCE FORCE OF Y-DIRECTION
C          TEXTW -- INPUT EXTERNAL WEIGHT PER ELEMENT OF ROTOR
C          TDX -- ELEMENT LENGTH OF ROTOR

C      COMMON /TD1/ TDDXT(100,5),TDDNT(100,5),TRP(100,5)
C          TDDXT -- EXTERNAL DIAMETER OF ROTOR
C          TDDNT -- INTERNAL DIAMETER OF ROTOR
C          TRP -- POLAR INERTIA MOMENT OF ROTOR

C      COMMON /TR1/ TRT(100,5),TEM6(100,5),TRO(100,5),TGGO(100,5)
C          TRT -- TRANSVERSE INERTIA MOMENT OF ROTOR
C          TEM6 -- YOUNG'S MODULUS *1.0E-5
C          TRO -- DENSITY OF ROTOR
C          TGGO -- SHEAR MODULUS *1.0E-6

C      COMMON /MF1/ LTLFF(10,5),TSFX(10,5),TSFY(10,5),TMFX(10,5)
C          LTLFF -- ROTOR STAGE NO. OF EXTERNAL FORCE
C          TSFX -- EXTERNAL FORCE OF X-DIRECTION
C          TSYF -- EXTERNAL FORCE OF Y-DIRECTION

C      COMMON /TU1/ LTLUF(10,5),TUX(10,5),TUY(10,5),TSUX(10,5),TSUY(10,5)
C          LTLUF(J) -- STAGE NO. OF JTH ROTOR UNBALANCE
C          TUX -- X-DIR UNBALANCE ( OZ-IN )
C          TUY -- Y-DIR UNBALANCE ( OZ-IN )
C          TSUX -- SUDDEN INCREASE UNBALANCE OF X-DIRECTION
C          TSUY -- SUDDEN INCREASE UNBALANCE OF Y-DIRECTION

C      COMMON /SEU1/ LTLNT(10,5),NTSRUB(5),NTSEU(5),NTFACT(5),ITND(5)
C          LTLNT -- STAGE NO. OF PRINTOUT ROTOR STAGE FOR TRANSIENT ANALYSIS
C          NTSRUB -- NO. OF RUB STAGE
C          NTSEU -- NO. OF SUDDEN INCREASE UNBALANCE STAGES
C          NTFACT -- STEP FACTOR OF RUB
C          ITND = 0 FOR CASING STIFFNESS
C                  = 1 BLADE EQUATION
C                  = 2 LINEARIZED STIFFNESS

```

```

COMMON /AAB1/ KTR(5),TABSO(5),AA1(2,10,5),AA2(2,10,5),AA3(2,10,5)
C   KTR -- DIRECT CASING STIFFNESS
C   TABSO -- FRICTION COEFFICIENT
C   AA1 -- MODAL ACCELERATION OF ROTOR AT X-DIRECTION
C   AA2 -- MODAL VELOCITY OF ROTOR AT X-DIRECTION
C   AA3 -- MODAL DISPLACEMENT OF ROTOR AT X-DIRECTION

COMMON /BBA1/ BB1(2,10,5),BB2(2,10,5),BB3(2,10,5),TA1(2,10,5)
C   BB1 -- MODAL ACCELERATION OF ROTOR AT Y-DIRECTION
C   BB2 -- MODAL VELOCITY OF ROTOR AT Y-DIRECTION
C   BB3 -- MODAL DISPLACEMENT OF ROTOR AT Y-DIRECTION
C   TA1 -- MODAL ACCELERATION OF ROTOR AT TORSIONAL-DIRECTION

COMMON /TKB1/ TA2(2,10,5),TA3(2,10,5),TKB(5,5),ALPH(5,5),RCC(5)
C   TA2 -- MODAL VELOCITY OF ROTOR AT TORSIONAL-DIRECTION
C   TA3 -- MODAL DISPLACEMENT OF ROTOR AT TORSIONAL-DIRECTION
C   TKB -- STIFFNESS BETWEEN GEARS
C   ALPH -- ANGLE BETWEEN GEARS
C   RCC -- RADIUS OF GEAR

COMMON /TMB1/ TMBX(10,5),TMBY(10,5),TWMY(10,5),LTLBD(10,5)
C   LTLBD -- LOCATION NO.OF BEARINGS

COMMON /TCM1/ TCMX(10,10,5),TCMY(10,10,5),TKMX(10,10,5)
COMMON /TDO1/ TDOX(10,10,5),TDOY(10,10,5),TEOX(10,10,5)
COMMON /TD/ TDDPC(10,100,5),TEMX(10,10,5),TEMY(10,10,5)
C   T*MX -- COEFFICIENT OF COMPENSATION TERM IN X-EQUATION
C   T*MY -- COEFFICIENT OF COMPENSATION TERM IN Y-EQUATION
C   TEOX -- COEFFICIENT OF COMPENSATION TERM IN TORSIONAL-EQU.
C   TEOY -- COEFFICIENT OF COMPENSATION TERM IN TORSIONAL-EQU.
C   TDDPC -- LATERAL MODAL SHAPE OF ROTOR

COMMON /TW1/ TDHY(10,10,5),TEYTH(10,100,5),TW(100,5),TWMOD(50,5)
C   TEEYTH -- X-DIR TORSIONAL MODAL SHAPE OF ROTOR

COMMON /LAS/ TTK(100,5),TMFY(10,5),TKMY(10,10,5),TEOY(10,10,5),
1      TDMX(10,10,5)

COMMON /BASE1/ AB,OMEGA,FAB
C   AB -- AMPLITUDE OF BASE MOTION
C   OMEGA -- ROTATION SPEED OF BASE MOTION ( RAD/SEC )
C   FAB -- PHASE ANGLE OF BASE MOTION

COMMON /BOX01/ OMEGS(40),BX1(40,200,6),LBLBT(10,5),NMBB,NODEB
C   OMEGS -- NATURAL FREQUENCY OF BOX
C   BX1 -- MODAL SHAPES OF BOX
C   LBLBT -- NO. OF BEARING LOCATION IN BOX
C   NMBB -- NO. OF MODES OF BOX
C   NODEB -- NO. OF EACH NODE'S DEGREE OF FREEDOM

COMMON /BOX03/ BKZZ(10,5)
C   BKZZ -- Z-DIRECTION STIFFNESS

COMMON /BOX08/ NPT,NPTNO(16)
C   NPT -- NO. OF BOX'S NODES FOR DEFORMATION PLOT
C   NPTNO -- LOCATION NO. OF BOX FOR DEFORMATION PLOT

C   * * * * *
C   ----- * START TO INPUT DATA OF ROTOR-GEAR SYSTEM *
C   * * * * *

```

```

NNPLT=0
READ (5,690) COM1
READ (5,690) COM2
READ (5,690) COM3
C           COM1,COM2,COM3 -- SPECIFICATION OF SAMPLING CASE

WRITE(6,700) COM1,COM2,COM3
WRITE (6,1080)
WRITE (6,700) COM1,COM2,COM3
WRITE (6,710)

READ (5, *) NSTA,NKTB,NSK
C           NSTA -- NO. OF TOTAL ROTORS
C           NKTB -- NO. OF CONNECTING GEARS STIFFNESS
C           NSK -- NO. OF SLANTED ROTORS
WRITE (6, *) NSTA,NKTB,NSK
IF (NSK.EQ.0) GO TO 25

READ (5,*) (INSK(I),I=1,NSK)
C           INSK -- LOCATION NO. OF SLANTED ROTOR
WRITE (6,*) (INSK(I),I=1,NSK)

READ (5,*) ((ANGL(INSK(I),J),J=1,3),I=1,NSK)
C           ANGL -- ANGLE OF SLANTED ROTOR
WRITE (6,*) ((ANGL(INSK(I),J),J=1,3),I=1,NSK)
DO 28 I=1,NSK
DO 28 J=1,4
28 ANGL(INSK(I),J)=ANGL(INSK(I),J)*3.1415926/360.0

25 READ (5,*) (JST(I),I=1,NSTA)
C           JST(J) -- THE LOCATION NO. OF GEAR OF JTH ROTOR
WRITE (6,*) (JST(I),I=1,NSTA)

READ (5,*) ((ALPH(I,J),I=1,NSTA),J=1,NSTA)
C           ALPH -- ANGLE BETWEEN GEARS
WRITE (6,*) ((ALPH(I,J),I=1,NSTA),J=1,NSTA)

READ (5,*) (RCC(I),I=1,NSTA)
C           RCC -- RADIUS OF GEARS
WRITE (6,*) (RCC(I),I=1,NSTA)

READ (5,*) (TOUT(I),I=1,NSTA)
C           TOUT -- INPUT EXTERNAL TORTIONAL TORQUE OF ROTORS
WRITE (6,*) (TOUT(I),I=1,NSTA)

READ (5,*) (FORCEZ(I),I=1,NSTA)
C           FORCEZ -- INPUT EXTERNAL AXIAL FORCE OF ROTORS
WRITE (6,*) (FORCEZ(I),I=1,NSTA)

READ (5,*) (NP1(I),XG1(I),XMAX1(I),PS11(I),I=1,NKTB)
C           NP1 -- NO. OF SPUR'S POINTS OF GEAR
C           XG1 -- ANGLE BETWEEN THE SPURS OF A PAIR OF GEARS
C           XMAX1 -- ANGLE DURING TOUCH PERIOD
C           PS11 -- PHASE ANGLE OF A PAIR OF GEARS
WRITE (6,*) (NP1(I),XG1(I),XMAX1(I),PS11(I),I=1,NKTB)

READ (5,*) ((XK(K,I),YK(K,I),I=1,NP1(K)),K=1,NKTB)
C           XK(K,I) -- ANGLE OF ITH POINT OF KTH GEAR
C           YK(K,I) -- STIFFNESS OF ITH POINT OF KTH GEAR
WRITE (6,*) ((XK(K,I),YK(K,I),I=1,NP1(K)),K=1,NKTB)

```

```

C      READ (5,*)
C      READ (5,*) (NTTD(I),I=1,NSTA)
C      NTTD -- NO. OF GEARS FOR EACH ROTOR
C      WRITE (6,*) (NTTD(I),I=1,NSTA)

C      READ (5,*) ((LLTD(I,J),I=1,NTTD(J)),J=1,NSTA)
C      LLTD -- LOCATION NO. OF GEARS
C      WRITE (6,*) ((LLTD(I,J),I=1,NTTD(J)),J=1,NSTA)

C      READ (5,*) ((TTCC(I,J),I=1,NTTD(J)),J=1,NSTA)
C      TTCC -- GEAR DAMPING
C      WRITE (6,*) ((TTCC(I,J),I=1,NTTD(J)),J=1,NSTA)

C      READ (5,*) AB,OMEGA,FAB
C      AB -- AMPLITUDE OF BASE MOTION
C      OMEGA -- ROTATION SPEED OF BASE MOTION ( RAD/SEC )
C      FAB -- PHASE ANGLE OF BASE MOTION
C      WRITE(6,*) AB,OMEGA,FAB

C      * * * * *
C      ----- * INPUT DATA OF ROTOR PROPERTIES *
C      * * * * * * * * * * * * * * * * * * * * *
C      DO 123 K1=1,NSTA
C      K=5*K1+55
C      READ(5,859) NMODE
C      NMODE -- MODES NO. OF ROTORS
C      WRITE(6,859) NMODE

C      READ(5,720) N,NB,NNLIN,NMB,NF,NU,NS,NBOW,ISTAB,IMODE,ISKU,NUFPT
C      N -- NO. OF MASS STAGE OF ROTOR
C      NB -- NO. OF REGULAR LINEAR BEARINGS OF ROTOR
C      NNLIN -- NO. OF NONLINEAR BEARINGS OF ROTOR
C      NMB -- NO. OF MOMENT RESISTING BEARINGS
C      NF -- NO. OF EXTERNAL FORCE
C      NU -- NO. OF UNBALANCE
C      NS -- NO. OF SKEW DISK
C      NBOW = 1 -- WITH BOW SHAFT
C      = 0 -- NO SHAFT BOW
C      ISTAB = 1 -- NO STABILITY CALCULATION
C      = 0 -- WITH STABILITY CALCULATION
C      IMODE -- NO OF DAMPED MODAL SHAPES DESIRED
C      IF = 0, NO MODAL SHAPE CALCULATION
C      ISKU -- NO. OF SKEW STAGES
C      NCT -- NO. USED IN MODES CALCULATION
C      NUFPT -- NO. OF STAGE NEEDED TO PRINTOUT FOR UNBALANCE
C      WRITE(6,720) N,NB,NNLIN,NMB,NF,NU,NS,NBOW,ISTAB,IMODE,ISKU,NUFPT
C      NN(K1)=N
C      NNB(K1)=NB

C      READ(5,730) ISKIP,NSTEP,NCYCLE,NITP,NINT,NPLOT,NORBIT,NTIME,NSPEE
1D,NINC,NOPT',NT
C      ISKIP = 1 -- NO CALCULATION
C      = 0 -- CALCULATE TRANSIENT ORBIT
C      NSTEP -- NO. OF STEPS OF INTEGRATION PER CYCLE
C      NCYCLE -- NO. OF CYCLES
C      NITP -- NO. OF STEPS PER PRINTOUT
C      NINT = 1 -- NEWWARK BETA METHOD
C      NPLOT = 1 -- NO PLOT
C      = 0 -- WITH PLOT
C      NORBIT -- NO. OF TRANSIENT ORBIT STAGES DESIRED

```

```

C      NTIME -- NO. OF STAGES TO BE PLOTTED IN RESPONSE VS TIME CURVE
C      NSPEED = 0
C      NINC = 0 INPUT INITIAL CONDITION
C          = 1 -- INITIAL CONDITION FROM STEADY STATE ORBIT
C                  ( WITH SMALL PERTURBATION )
C          = 2 -- INPUT MODAL INITIAL DATA
C      NOPT = 0
C      NT -- NO. OF STAGES FOR TRANSIENT PRINTOUT
      WRITE(6,730) ISKIP,NSTEP,NCYCLE,NITP,NINT,NPLOT,NORBIT,NTIME,NSPEE
1D,NINC,NOPT,NT
      IF (NB.EQ.0) GO TO 20

      READ (5,740) (LLBD(J),J=1,NB)
C      LLBD -- LOCATION NO. OF BEARINGS
      WRITE(6,740) (LLBD(J),J=1,NB)

      DO 19 J=1,NB
      READ (5,*) KXX(J),KXA(J),KXY(J),KXB(J),KXZ(J),CXX(J),CXA(J),CXY
1(J),CXB(J),CXZ(J)
      WRITE(6,750) KXX(J),KXA(J),KXY(J),KXB(J),KXZ(J),CXX(J),CXA(J),CXY
1(J),CXB(J),CXZ(J)
      READ (5,*) KAX(J),KAA(J),KAY(J),KAB(J),KAZ(J),CAX(J),CAA(J),CAY
1(J),CAB(J),CAZ(J)
      WRITE(6,750) KAX(J),KAA(J),KAY(J),KAB(J),KAZ(J),CAX(J),CAA(J),CAY
1(J),CAB(J),CAZ(J)
      READ (5,*) KYX(J),KYA(J),KYY(J),KYB(J),KYZ(J),CYX(J),CYA(J),CYY
1(J),CYB(J),CYZ(J)
      WRITE(6,750) KYX(J),KYA(J),KYY(J),KYB(J),KYZ(J),CYX(J),CYA(J),CYY
1(J),CYB(J),CYZ(J)
      READ (5,*) KBX(J),KBA(J),KBY(J),KBB(J),KBZ(J),CBX(J),CBA(J),CBY
1(J),CBB(J),CBZ(J)
      WRITE(6,750) KBX(J),KBA(J),KBY(J),KBB(J),KBZ(J),CBX(J),CBA(J),CBY
1(J),CBB(J),CBZ(J)
      READ (5,*) KZX(J),KZA(J),KZY(J),KZB(J),KZZ(J),CZX(J),CZA(J),CZY
1(J),CZB(J),CZZ(J)
      WRITE(6,750) KZX(J),KZA(J),KZY(J),KZB(J),KZZ(J),CZX(J),CZA(J),CZY
1(J),CZB(J),CZZ(J)
19    CONTINUE
C ----- BEARING STIFFNESS TK**
C ----- BEARING DAMPING TC**
C      X -- DIRECTION OF X
C      A -- DIRECTION OF X ROTATION
C      Y -- DIRECTION OF Y
C      B -- DIRECTION OF Y ROTATION
C      Z -- DIRECTION OF Z

      DO 20 J=1,NB
      LTLBD(J,K1)=LLBD(J)
      TKXX(J,K1)=KXX(J)
      TKXY(J,K1)=KXY(J)
      TKXA(J,K1)=KXA(J)
      TKXB(J,K1)=KXB(J)
      TKXZ(J,K1)=KXZ(J)
      TCXX(J,K1)=CXX(J)
      TCXY(J,K1)=CXY(J)
      TCXA(J,K1)=CXA(J)
      TCXB(J,K1)=CXB(J)
      TCXZ(J,K1)=CXZ(J)
      TKYX(J,K1)=KYX(J)
      TKYY(J,K1)=KYY(J)
      TKYA(J,K1)=KYA(J)

```

```

TKYB(J,K1)=KYB(J)
TKYZ(J,K1)=KYZ(J)
TCYX(J,K1)=CYX(J)
TCYY(J,K1)=CYY(J)
TCYA(J,K1)=CYA(J)
TCYB(J,K1)=CYB(J)
TCYZ(J,K1)=CYZ(J)
TKAX(J,K1)=KAX(J)
TKAY(J,K1)=KAY(J)
TKAA(J,K1)=KAA(J)
TKAB(J,K1)=KAB(J)
TKAZ(J,K1)=KAZ(J)
TCAX(J,K1)=CAX(J)
TCAY(J,K1)=CAY(J)
TCAA(J,K1)=CAA(J)
TCAB(J,K1)=CAB(J)
TCAZ(J,K1)=CAZ(J)
TKBX(J,K1)=KBX(J)
TKBY(J,K1)=KBY(J)
TKBA(J,K1)=KBA(J)
TKBB(J,K1)=KBB(J)
TKBZ(J,K1)=KBZ(J)
TCBX(J,K1)=CBX(J)
TCBY(J,K1)=CBY(J)
TCBA(J,K1)=CBA(J)
TCBB(J,K1)=CBB(J)
TCBZ(J,K1)=CBZ(J)
TKZX(J,K1)=KZX(J)
TKZY(J,K1)=KZY(J)
TKZA(J,K1)=KZA(J)
TKZB(J,K1)=KZB(J)
TKZZ(J,K1)=KZZ(J)
TCZX(J,K1)=CZX(J)
TCZY(J,K1)=CZY(J)
TCZA(J,K1)=CZA(J)
TCZB(J,K1)=CZB(J)
TCZZ(J,K1)=CZZ(J)

```

20 CONTINUE

```

IF (NNLIN.FQ.0) GO TO 30
READ(5,760) (LLNB(J),NLB(J),VIS(J),ANR(J),ANL(J),ANC(J),J=1,NNLIN
1)
C   LLNB -- LOCATION NO. OF NONLINEAR BEARING
C   NLB -- BEARING NO. OF NONLINEAR BEARINGS
C   VIS -- VISCOUSITY OF LUBRICATE ( LB/IN**2 )
C   ANR -- RADIUS OF BEARING ( IN )
C   ANL -- LENGTH OF BEARING ( IN )
C   ANC -- CLEARANCE CF BEARING ( IN )
WRITE(6,760) (LLNB(J),NLB(J),VIS(J),ANR(J),ANL(J),ANC(J),J=1,NNLIN
1)
30 CONTINUE
IF (NMB.EQ.0) GO TO 40

READ (5,770) (LLNMB(J),J=1,NMB)
C   LLNMB -- LOCATION NO. OF MOMENT RESISTING BEARING
WRITE(6,770) (LLNMB(J),J=1,NMB)

DO 35 I=1,NMB
DO 35 J=1,4
READ (5,780) (SLNMB(I,J,K),K=1,4), (CLNMB(I,J,K),K=1,4)

```

```

35   WRITE(6,780) (SLNMB(I,J,K),K=1,4), (CLNMB(I,J,K),K=1,4)
      CONTINUE

40   CONTINUE
      READ (5,*) NGYR,E,SPEED1,SPEED2,ANGACL,BETA
C      NGYR -- NO. OF GYROSCOPIC ROTOR
C      E -- SECTION YOUNG'S MODULUS *1.0E-5
C      SPEED1 -- ROTOR'S OPERATING SPEED ( RPM )
C      SPEED2 -- ROTOR'S INITIAL OPERATING SPEED ( RPM )
C      ANGACL -- ANGULAR ACCELERATION OF ROTOR
C      BETA -- BETA PARAMETER USED FOR NEWMARK BETA METHOD
      WRITE(6,790) NGYR,E,SPEED1,SPEED2,ANGACL,BETA
      TSPEED(K1)=SPEED1

      READ(5,*) (EXTW(J),DX(J),DDXT(J),DDNT(J),RP(J),RT(J),EM6(J),
1           RO(J),GGO(J),TK(J), J=1,N)
1      EXTW -- INPUT EXTERNAL WEIGHT PER ELEMENT OF ROTOR
C      DX -- ELEMENT LENGTH OF ROTOR
C      DDXT -- EXTERNAL DIAMETER PER ELEMENT OF ROTOR
C      DDNT -- INTERNAL DIAMETER PER ELEMENT OF ROTOR
C      RP -- POLAR ENERTIA MOMENT PER ELEMENT OF ROTOR ( LB*IN**2 )
C      RT -- TRANSVERS ENERTIA MOMENT PER ELEMENT OF ROTOR ( LB*IN**2 )
C      EM6 -- YOUNG'S MODULUS PER ELEMENT OF ROTOR *1.E-5
C      RO -- DENSITY PER ELEMENT OF ROTOR
C      GGO -- SHEAR'S MODULUS PER ELEMENT *1.0E-5
C      TK -- TORTIONAL CONSTRAINT MOMENT PER ELEMENT *1.0E-15
      WRITE(6,800) (EXTW(J),DX(J),DDXT(J),DDNT(J),RP(J),RT(J),EM6(J),
1           RO(J),GGO(J),TK(J), J=1,N)
1      DO 33 J=1,N
      TK(J)=1.0D15*TK(J)
      TEXTW(J,K1)=EXTW(J)
      TDX(J,K1)=DX(J)
      TDDXT(J,K1)=DDXT(J)
      TDDNT(J,K1)=DDNT(J)
      TRP(J,K1)=RP(J)
      TRT(J,K1)=RT(J)
      TEM6(J,K1)=EM6(J)
      TRO(J,K1)=RO(J)
      TGGO(J,K1)=GGO(J)
      TTK(J,K1)=TK(J)
33    CONTINUE

      IF (NF.EQ.0) GO TO 50
      READ (5,810) (LLFF(J),FX(J),FY(J),J=1,NF)
C      LLFF -- LOCATION NO. OF EXTERNAL FORCE OF ROTOR
C      FX -- EXTERNAL FORCE ON X-DIRECTION
C      FY -- EXTERNAL FORCE ON Y-DIRECTION
      WRITE(6,810) (LLFF(J),FX(J),FY(J),J=1,NF)
      DO 55 I=1,NF
      LTLFF(I,K1)=LLFF(I)
      TSFX(I,K1)=FX(I)
55    TSFY(I,K1)=FY(I)
50    CONTINUE

      IF (NU.EQ.0) GO TO 60
      READ (5,*) (LLUF(J),UX(J),UY(J),SUX(J),SUU(J),J=1,NU)
C      LLUF -- LOCATION NO. OF UNBALANCE OF ROTOR
C      UX -- X-DIR UNBALANCE ( OZ-IN )
C      UY -- Y-DIR UNBALANCE ( OZ-IN )
C      SUX -- SUDDEN INCREASE UNBALANCE OF X-DIRECTION ( OZ-IN )

```

```

C      SUY -- SUDDEN INCREASE UNBALANCE OF Y-DIRECTION ( OZ-IN )
      WRITE(6,810) (LLUF(J),UX(J),UY(J),SUX(J),SUY(J),J=1,NU)
      DO 60 J=1,NU
      LTLUF(J,K1)=LLUF(J)
      TUX(J,K1)=UX(J)
      TUY(J,K1)=UY(J)
      TSUX(J,K1)=SUX(J)
      TSUY(J,K1)=SUY(J)
60      CONTINUE

      IF (NS.EQ.0) GO TO 70
C ----- SKEW DISK IS NEGLECTED IN THIS PROGRAM
      READ (5,810) (LLSK(J),FSK(J),PSK(J),J=1,NS)
      WRITE(6,810) (LLSK(J),FSK(J),PSK(J),J=1,NS)
70      CONTINUE

      IF (NUFPT.EQ.0) GO TO 80
      READ (5,820) (LLUT(J),J=1,NUFPT)
      WRITE(6,820) (LLUT(J),J=1,NUFPT)
80      CONTINUE

      IF (NT.EQ.0) GO TO 90
      READ (5,820) (LLNT(J),J=1,NT)
C      LLNT -- LOCATION NO. FOR PRINTOUT OF ROTOR IN TRANSIENT ANALYSIS
      WRITE(6,820) (LLNT(J),J=1,NT)
      DO 90 J=1,NT
      LTLNT(J,K1)=LLNT(NT)
90      CONTINUE

      IF(NINC.NE.2)GO TO 94
      READ(5,821)NAB,CTIME
      WRITE(6,821)NAB,CTIME
      DO 92 J=1,NAB
      READ(5,822)A3(1,J),B3(1,J),A2(1,J),B2(1,J)
      WRITE(6,822)A3(1,J),B3(1,J),A2(1,J),B2(1,J)
      AA3(1,J,K)=A3(1,J)
      AA2(1,J,K)=A2(1,J)
      BB3(1,J,K)=B3(1,J)
      BB2(1,J,K)=B2(1,J)
92      CONTINUE
94      CONTINUE

      IF(NBOW.EQ.0) GO TO 95
      READ (5,830) (BOW(J),PBOW(J),XIDC(J),YIDC(J),VXIDC(J),VYIDC(J),J=1
1,N)
      WRITE(6,830) (BOW(J),PBOW(J),XIDC(J),YIDC(J),VXIDC(J),VYIDC(J),J=1
1,N)
95      CONTINUE

      READ (5,*) SPI,SPL,DSP
C      SPI --
      WRITE(6,840) SPI,SPL,DSP

      READ (5,*) SPE1, SPE2,SPE3
C      SPE1 -- INITIAL SPEED FOR TORTIONAL CRITICAL SPEED ANALYSIS
C      SPE2 -- FINAL SPEED FOR TORTIONAL CRITICAL SPEED ANALYSIS
C      SPE3 -- SPEED INCREMENT FOR TORTIONAL CRITICAL SPEED ANALYSIS
C      ( RPM )
      WRITE(6,840) SPE1,SPE2,SPE3

```

```

        IF (ISKU.EQ.1) GO TO 100
        READ (5,*) SPS,SPF,SPN
C          SPS -- INITIAL SPEED FOR UNBALANCE RESPONSE CALCULATION
C          SPF -- FINAL SPEED FOR UNBALANCE RESPONSE CALCULATION
C          SPN -- SPEED INCREMENT FOR UNBALANCE RESPONSE CALCULATION
        WRITE(6,850) SPS,SPF,SPN
100    CONTINUE

        READ(5,851) NBMOP
C          NBMOP = 0 NO CALCULATION
C          = 1 A(T)=(E**(A(T)*T)*COS(A(T)*T))
C          = 2 A(T)=COS(A(T)*T)**2
        WRITE (6,851) NBMOP
        IF (NBMOP.EQ.0) GO TO 103
        READ(5,852) (ACON1(I),I=1,NB)
        WRITE(6,852) (ACON1(I),I=1,NB)
        READ(5,852) (ACON2(I),I=1,NB)
        WRITE(6,852) (ACON2(I),I=1,NB)
        READ(5,853) (APH1(I),I=1,NB)
        WRITE(6,853) (APH1(I),I=1,NB)
        READ(5,853) (APH2(I),I=1,NB)
        WRITE(6,853) (APH2(I),I=1,NB)
        DO 102 J=1,NNB(K1)
        TAOMG1(J,K1)=APH1(J)*3.14159/30.0
        TAOMG2(J,K1)=APH2(J)*3.14159/30.0
        NNBMOP(J)=NBMOP
        TACON1(J,K1)=ACON1(J)
102      TACON2(J,K1)=ACON2(J)

103    CONTINUE
        READ(5,*) NSRUB,NSEU
C          NSRUB -- NO. OF RUB STAGES
C          NSEU -- NO. OF SUDDEN INCREASE UNBALANCE STAGES
        WRITE (6,854) NSRUB,NSEU

        IF(NSRUB.EQ.0) GO TO 106
        READ(5,*) NFACT,IND,KR,ABSO
C          NFACT -- STEP FACTOR OF RUB
C          IND = 0 FOR CASING STIFFNESS
C          = 1 BLADE EQUATION
C          = 2 LINEARIZED STIFFNESS
C          KR -- DIRECT CASING STIFFNESS
C          ABSO -- FRICTION COEFFICIENT
        WRITE (6,855) NFACT,IND,KR,ABSO

        READ(5,*) (NRUB(J),CLEAR(J),J=1,NSRUB)
C          NRUB -- LOCATION NO. OF RUB STAGE
C          CLEAR -- CLEARANCE OF RUB
        WRITE(6,856) (NRUB(J),CLEAR(J),J=1,NSRUB)
        NTSRUB(K1)=NSRUB
        NTSEU(K1)=NSEU
        NTFACT(K1)=NFACT
        ITND(K1)=IND
        KTR(K1)=KR
        TABSO(K1)=ABSO
106    CONTINUE

        READ(5,690) ABL1
        WRITE(6,690) ABL1
        READ (5,690) ABL2

```

```

      WRITE(6,690) ABL2
      READ (5,690) ABL3
      WRITE(6,690) ABL3
C ----- THREE TITLE CARDS FOR LABEL IN PLOTS
      WRITE (6,860) NCYCLE,NSTEP,NINT,NINC,NOPT,SPEED2,ANGACL,BETA
      WRITE (6,870)

C * * * * * * * * * * * * * * * * * * * * * * *
C *   CALCULATE EFFECTIVE ENERTIA MOMENT OF ROTORS  *
C * * * * * * * * * * * * * * * * * * * * * * * *
C
      DO 110 I=1,N
      DLX(I)=DX(I)
      CCRI=RO(I)
      CCEI=EM6(I)
      IF (CCRI.GT.0.001) GOTO 105
      RO(I)=0.283
105    CONTINUE
      ENER(I)=3.14159*(DDXT(I)**4.-DDNT(I)**4.)/64.
      IF (CCEI.GT.0.001) GOTO 107
      EM6(I)=E
107    CONTINUE
      EI(I)=EM6(I)*ENER(I)
      DL=ABS(DX(I))
110    SW1(I)=3.14159*(DDXT(I)**2.-DDNT(I)**2.)*DL*RO(I)/4.0
      W(1)=SW1(1)/2.+EXTW(1)
      WT=W(1)
      ZLT=DX(1)
      DO 120 I=2,N
      W(I)=SW1(I-1)/2.0+SW1(I)/2.0+EXTW(I)
C         W(I) -- TOTAL EFFECTIVE SHAFT WEIGHT
      TW(I,K1)= W(I)
      WT=WT+W(I)
120    ZLT=ZLT+DX(I)
      IF (NGYR) 130,150,130
130    RP(1)=RP(1)+ENER(1)*RO(1)*DX(1)
      RT(1)=RT(1)+SW1(1)*((DDXT(1)**2.0+DDNT(1)**2.0)/16.0+((DX(1)/2.0)*
      1*2.0)/3.0)/2.0
      DO 140 I=2,N
      RP(I)=RP(I)+RO(I)*ENER(I)*DX(I)+ENER(I-1)*DX(I-1)*RO(I-1)
      RT(I)=RT(I)+SW1(I)*((DDXT(I)**2.0+DDNT(I)**2.0)/16.0+((DX(I)/2.0)*
      1*2.0)/3.0)/2.0+SW1(I-1)*((DDXT(I-1)**2.0+DDNT(I-1)**2.0)/16.0+((DX
      2(I-1)/2.0)**2.0)/3.0)/2.0
140    CONTINUE
150    SRP=0.0
      DO 160 I=1,N
160    SRP=SRP+RP(I)
      DO 180 I=1,N
      WRITE (6,880) I,W(I),DX(I),DDXT(I),DDNT(I),ENER(I),RP(I),RT(I),
      1EM6(I),EI(I)
      IF (I-50) 180,170,180
170    WRITE (6,1080)
180    CONTINUE
      WRITE (6,890) WT,ZLT
      WRITE (6,900)
      WRITE (6,910)
      WRITE (6,920) (J,LLBD(J),KXX(J),KXY(J),KYX(J),KYY(J),J=1,NB)
      WRITE (6,930)
      WRITE (6,940)
      WRITE (6,920) (J,LLBD(J),CXX(J),CXY(J),CYX(J),CYY(J),J=1,NB)
      IF (NMB.EQ.0) GO TO 200

```

```

DO 190 I=1,NMB
WRITE (6,950) I,LLNMB(I)
DO 190 J=1,4
WRITE (6,960) (SLNMB(I,J,K),K=1,4),(CLNMB(I,J,K),K=1,4)
190 CONTINUE
200 IF (NNLIN.EQ.0) GO TO 220
WRITE (6,1170)
DO 210 J=1,NNLIN
WRITE (6,1180) J,LLNB(J),NLB(J),VIS(J),ANR(J),ANL(J),ANC(J)
210 CONTINUE
220 IF (NF.EQ.0) GO TO 230
WRITE (6,970)
WRITE (6,980) (LLFF(J),FX(J),FY(J),J=1,NF)
230 IF (NS.EQ.0) GO TO 240
WRITE (6,990)
WRITE (6,1000) (LLSK(J),FSK(J),PSK(J),J=1,NS)
240 IF (NU.EQ.0) GO TO 260
WRITE (6,1010)
WRITE (6,1020)
WRITE (6,1030) (LLUF(J),UX(J),UY(J),J=1,NU)
DO 250 J=1,NU
UX(J)=UX(J)/(16.*386.4)
250 UY(J)=UY(J)/(16.*386.4)
260 CONTINUE
IF (NBOW.EQ.0) GO TO 275
WRITE (6,1040)
DO 270 J=1,N
WRITE (6,1050) J,BOW(J),PBOW(J),XIDC(J),YIDC(J),VXIDC(J),VYIDC(J)
270 CONTINUE
275 CONTINUE
WRITE (6,1060)

C      * * * * * * * * * * * * * * * * * * * * * * *
C ----- *   CALCULATE ROTOR'S LATERAL MODAL SHAPE   *
C      * * * * * * * * * * * * * * * * * * * * * * *
DO 280 I=1,NB
AVK=(KXX(I)+KYY(I))/2.
WRITE (6,1070) I,AVK
280 CONTINUE
WRITE (6,1071) NBMOP
IF(NBMOP.EQ.0) GO TO 283
DO 282 I=1,NB
WRITE (6,1072) I,ACON1(I),ACON2(I),APH1(I),APH2(I)
282 CONTINUE
283 CONTINUE
NC=1
C NC=LOCAL CRITICAL SPEED NO.
WRITE (6,1080)
LN=3
C SPI=INITIAL SPEED,SPL=FINAL SPEED,DSP=SPEED INCREMENT-RPM
SPD=SPI
DETP=0.
MA=0
MB=0
WRITE (6,1080)
WRITE (6,1090) SPI,SPL,DSP
LN=1
WRITE (6,1100)
LN=LN+3
DIN=DSP

```

```

290   I=1
      J=1
      SPSQ=SPD*SPD
C     COMPUTE ANG. VELOCITY
      ANSP=SPD*0.10471976
      ANSP2=ANSP*ANSP
      VP=0.
      ZMP=0.
      EYP=0.
      ETHP=1.0
      M=1
300   I=I+1
      II=I-1
      IF (II-LLBD(J)) 330,310,330
310   AK=(KXX(J)+KYY(J))/2.
      AKK(J)=AK
      TAKK(J,K1)=AKK(J)
      IF (J-NB) 320,340,340
320   J=J+1
      GO TO 340
330   AK=0.
340   VP=VP+(W(I-1)*ANSP2/386.4-AK)*EYP
      ZMP=ZMP-ANSP2*(RT(I-1))*ETHP/386.4
      EY=EYP+DX(I-1)*ETHP+DX(I-1)**2*ZMP/(2.E6*EI(I-1))+DX(I-1)**3*VP/(6
      1.E6*EI(I-1))
      ETH=ETHP+DX(I-1)*ZMP/(1.E6*EI(I-1))+DX(I-1)**2*VP/(2.E6*EI(I-1))
      ZM=ZMP+DX(I-1)*VP
      V=VP
      IF (M.EQ.2) GO TO 350
      EY1(I)=EY
      EAN1(I)=ETH
      IF (I.GT.N) GO TO 360
      ZMP=ZM
      VP=V
      EYP=EY
      ETHP=ETH
      GO TO 300
350   EY2(I)=EY
      EAN2(I)=ETH
      ZMP=ZM
      VP=V
      EYP=EY
      ETHP=ETH
      IF (I.GT.N) GO TO 370
      GO TO 300
360   M=2
      ZM1=ZM
      VR1=V
      J=1
      I=1
      EYP=1.
      ZMP=0.
      ETHP=0.
      VP=0.
      GO TO 300
370   DET=VR1*ZM-V*ZM1
      IF (ABS(DETP).LT.0.0001) GO TO 420
      IF (MA.EQ.1) GO TO 400
      IF (ABS(DET).LT.1.) GO TO 450
      IF (DETP*DET) 380,420,420

```

```

380  DOLD=DETP
390  MA=1
     IF (ABS(DET).LT.1.) GO TO 450
     IF (DIN.LT.1.E-6) GO TO 450
     DIN=DIN/2.
     DETPP=DETP
     DETP=DET
     SPD=SPD-DIN
     GO TO 290
400  IF (ABS(DET).LT.1.) GO TO 450
     IF (DOLD*DET) 390,420,410
410  CONTINUE
     IF (ABS(DET).LT.1.) GO TO 450
     IF (DIN.LT.1.E-6) GO TO 450
     DIN=DIN/2.
     SPD=SPD+DIN
     DETPP=DETP
     DETP=DET
     GO TO 290
420  IF (LN=54) 440,440,430
430  WRITE (6,1080)
     LN=1
440  WRITE (6,1110) SPD,DET
     LN=LN+1
     SPD=SPD+DSP
     DIN=DSP
     IF(NC.GT.NMODE) GO TO 610
     IF (SPD.GT.SPL) GO TO 610
     DETPP=DETP
     DETP=DET
     SSPD=SPD
     GO TO 290
450  MA=0
     WRITE (6,1110) SPD,DET
     LN=LN+1
     IF (LN=50) 470,470,460
460  WRITE (6,1080)
     LN=1
470  WRITE (6,1120) NC
     WRITE (6,1130)
     WRITE (6,1110) SPD,DET
     CRT(NC)=SPD
     TCRT(NC,K1)=CRT(NC)
     NC=NC+1
     LN=LN+3
     EY1(1)=0.
     EY2(1)=1.
     DTX=0.
     I=1
     IF (LN=50) 490,490,480
480  WRITE (6,1080)
     LN=1
490  WRITE (6,1140)
     LN=LN+2
500  DEFL(I)=V*EY1(I)-VR1*EY2(I)
     IF (I.NE.1) GO TO 510
     EYTH(I)=V
     GO TO 520
510  EYTH(I)=EAN1(I)*V-EAN2(I)*VR1
520  DEFA=ABS(DEFL(I))

```

```

DMXA=ABS(DTX)
I=I+1
IF (DEFA-DMXA) 540,540,530
530 DTX=DEFL(I-1)
540 IF (I-N) 550,550,560
550 GO TO 500
560 DO 570 I=1,N
      DPC(I)=DEFL(I)/DTX
      EYTH(I)=EYTH(I)/DTX
      EEYTH(NC-1,I)=EYTH(I)
570 DDPC(NC-1,I)=DPC(I)
      DO 600 I=1,N
      LN=LN+1
      IF (LN-54) 590,590,580
580 WRITE (6,1080)
      LN=1
590 WRITE (6,1150) I,DPC(I),EYTH(I)
      LN=LN+1
600 CONTINUE
      SPD=SSPD+DSP
      DETP=0.
      GO TO 290
610 CONTINUE
      DO 620 IK=1,NB
      KXX(IK)=KXX(IK)-AKK(IK)
620 KYY(IK)=KYY(IK)-AKK(IK)
      NCS=NC-1
      DO 650 II=1,NCS
      WMOD(II)=0.
      DO 630 JJ=1,N
      WMOD(II)=WMOD(II)+RT(JJ)*EEYTH(II,JJ)**2+W(JJ)*DDPC(II,JJ)**2
      WMOD(II)=WMOD(II)/386.4
      TWMOD(II,K1)=WMOD(II)
      DO 640 KI=1,N
      EEYTH(II,KI)=EEYTH(II,KI)/(WMOD(II)**0.5)
      DDPC(II,KI)=DDPC(II,KI)/(WMOD(II)**0.5)
      TEEYTH(II,KI,K1)=EEYTH(II,KI)
640 TDDPC(II,KI,K1)=DDPC(II,KI)
650 CONTINUE
      DO 660 II=1,NCS
      WRITE (6,1190) II,CRT(II),WMOD(II)
      DO 660 JJ=1,N
      WRITE (6,1200) JJ,DDPC(II,JJ),EEYTH(II,JJ)
660 CONTINUE
      WRITE (6,1210)
      DO 680 II=1,NCS
      DO 670 JJ=1,NCS
      TMX(II,JJ)=0.
      DO 670 KI=1,N
      TMX(II,JJ)=TMX(II,JJ)+W(KI)*DDPC(JJ,KI)*DDPC(II,KI)/386.4+RT(KI)*E
      1EYTH(II,KI)*EEYTH(JJ,KI)/386.4
670 CONTINUE
      WRITE (6,1160) (TMX(II,JJ),JJ=1,NCS)
680 CONTINUE
      NCT=NCS
      NNNCT(K1)=NCT

```

```

C * * * * * * * * * * * * * * * * * * * * * * * * * * *
C ----- *   CALCULATE ROTOR'S TORSIONAL MODAL SHAPE   *
C * * * * * * * * * * * * * * * * * * * * * * * * * * * *

```

```

DO 123 I=1,2
1234 CALL TOR(N,NCS,K1,I)
123 CONTINUE

C      * * * * * * * * * * *
C ----- * INPUT BOX'S DATA   *
C      * * * * * * * * * * *
C      READ(5,*) NMBB,NDB,NODEB
C          NMBB -- MODES NO. OF BOX
C          NDB -- NO. OF NODES OF BOX
C          NODEB -- DEGREE OF FREEDOM FOR EACH NODE
C      WRITE(6,*)NMBB,NDB,NODEB
C      WRITE(10,*)NMBB

DO 195 K=1,NSTA
READ (5,*) (LBLBT(I,K),I=1,NNB(K))
C      LBLBT -- LOCATION NO. OF BEARINGS ON BOX
WRITE (6,*) (LBLBT(I,K),I=1,NNB(K))
195 CONTINUE

DO 199 K=1,NSTA
READ (5,*) (BKZZ(I,K),I=1,NNB(K))
C      BKZZ -- Z-DIRECTION CASING STIFFNESS
WRITE (6,*) (BKZZ(I,K),I=1,NNB(K))
199 CONTINUE

READ (5,*) NPT
C      NPT -- NO. OF BOX'NODES FOR DEFORMATION ANALYSIS

READ (5,*) (NPTNO(I),I=1,NPT)
C      NPTNO -- LOCATION NO. OF NODES FOR DEFORMATION ANALYSIS ON BOX

DO 64 IN=1,NMBB
READ (5,1260) OMEGS(IN)
C      OMEGS -- NATURAL FREQUENCIES OF BOX
WRITE(6,1262) OMEGS(IN)

DO 64 ID=1,NDB
READ(5,1265) IA,(BX1(IN,ID,IX),IX=1,5)
READ(5,*) IA,(BX1(IN,ID,IX),IX=1,5)
C      BX1 -- MODAL SHAPES OF BOX
WRITE(6,1265) IA,(BX1(IN,ID,IX),IX=1,5)
64 CONTINUE

N9=NSTEP*NCYCLE
FCYCLE=NCYCLE
C TTIME1=60.0*FCYCLE/SPEED1
TTIME1=60.0/(SPEED1*NSTEP)
FSAMPLE=1.0/TTIME1
WRITE(7,*) NSTA,N9,NNNCT(1),FSAMPLE
WRITE(8,*) NSTA,N9,NNNCT(1),FSAMPLE
WRITE(9,*) NSTA,N9,NNNCT(1),FSAMPLE
WRITE(10,*)NSTA,N9,NNNCT(1),FSAMPLE
WRITE(11,*)NSTA,N9,NNNCT(1),FSAMPLE
WRITE(12,*)NSTA,N9,NNNCT(1),FSAMPLE
WRITE(13,*)NSTA,N9,NNNCT(1),FSAMPLE

C      * * * * * * * * * * *
C ----- * CALCULATE DYNAMIC BEHAVIOR OF THE WHOLE SYSTEM  *

```

```

C ***** CALL TMM (NSTA)

690 FORMAT (80A1)
700 FORMAT (3(80A1,/,))
703 FORMAT (2X,3I6,F10.3,I4,F10.3)
710 FORMAT (/,20X,'MODAL ANALYSIS VERSION 3, OCT. 3,1988')
713 FORMAT ( 20X,'X---DIR. MODAL SHAPE OF ROTOR ')
716 FORMAT ( 20X,'T---DIR. MODAL SHAPE OF ROTOR ')
719 FORMAT ( 20X,'Z---DIR. MODAL SHAPE OF ROTOR ')
720 FORMAT (12I5)
730 FORMAT (12I5)
740 FORMAT (3I5)
750 FORMAT (10G10.3)
760 FORMAT (2I5,4G10.2)
770 FORMAT (9I5)
780 FORMAT (8G10.3)
790 FORMAT (I5,5X,6G10.3)
800 FORMAT (10G8.3)
810 FORMAT (I5,5X,4G10.3)
820 FORMAT (I5)
821 FORMAT(I10,F10.7)
822 FORMAT(4E15.6)
830 FORMAT (6G10.3)
840 FORMAT (3G10.3)
850 FORMAT (3G10.3)
851 FORMAT(I5)
852 FORMAT (8F10.5)
853 FORMAT (8F10.3)
854 FORMAT(2I5)
855 FORMAT(2I5,2F11.1)
856 FORMAT(I5,F10.5)
859 FORMAT(I5)
860 FORMAT (//,10X,'NCYCLE=',I3,5X,'NSTEP=',I3,5X,'NINT=',I3,5X,'NINC=',
1',I3,5X,'NOPT=',I3,/,10X,'SPEED2=',F10.2,5X,'ANGACL(1/SEC)=',F10.3
2,5X,'BETA=',F10.5,/)
870 FORMAT (120H STATION NO.      WEIGHT      LENGTH      SHAFT DIA. SHAFT D
1IA.          I      IP-POLAR MOM. IT-TRANS. MOM. EX10-6 EI
2,/120H          (LP)          (IN.) OUTSIDE      INSIDE   (/
3IN**4)          (LP-IN**2)        (LB-IN**2)
880 FORMAT (I7,F16.3,F12.3,F10.3,F10.3,G11.4,F12.3,F16.3,F11.2,G10.3)
890 FORMAT (16X,7H-----,5X,7H-----/7X,F16.3,F12.3/)
900 FORMAT (/,34X,' LINEAR SUPPORT BEARING STIFFNESS CHARACTERICS')
910 FORMAT (5X,16HBEARING BEARING,12X,3HKXX,16X,3HKXY,16X,3HKYX,16X,3
1HKYY,/5X,6HNUMBER,3X,8HLOCATION,8X,7H(LB/IN),11X,7H(LB/IN),11X,7H(
2LB/IN),11X,7H(LB/IN))
920 FORMAT (5X,I3,8X,I3,9X,F11.1,5X,F11.1,8X,F11.1,8X,F11.1)
930 FORMAT (/,35X,' LINEAR SUPPORT BEARING DAMPING CHARACTERISTICS')
1)
940 FORMAT (5X,16HDAMPING DAMPING,12X,3HCXX,16X,3HCXY,16X,3HCYX,16X,3
1HCYY,/5X,6HNUMBER,3X,8HLOCATION,6X,11H(LB-SEC/IN),10X,11H(LB-SEC/
2IN),10X,11H(LB-SEC/IN),10X,11H(LB-SEC/IN))
950 FORMAT (/,10X,'FULL BEARING NO.',I2,3X,'AT STATION',I3,/)
960 FORMAT (10X,'BEARING STIFFNESS LB/IN',/,4(4(5X,G15.3),/),/,10X,
1BEARING DAMPING LB-SEC/IN',/,4(4(5X,G15.3),/))
970 FORMAT (/,20X,'EXTERNAL FORCES',/,5X,'STATION NO.',10X,'X',15X,'Y
1',/)
980 FORMAT (10X,I3,2(5X,G15.5))
990 FORMAT (/,20X,'SKEWED DISC',/,5X,'STATION NO.',10X,'SKEW(RAD)',5X
1,'PHASE ANGLE DEG.',/)
```

```

1000 FORMAT (10X,I3,2(5X,G15.5))
1010 FORMAT (///,25X,'ROTOR UNBALANCE IN OZ-IN.',/)
1020 FORMAT (5X,'STATION',10X,'X-UNBALANCE',10X,'Y-UNBALANCE',/)
1030 FORMAT (8X,I2,12X,F10.3,11X,F10.3)
1040 FORMAT (///,20X,'SHAFT INITIAL CONDITIONS',///,5X,'STATION NO.',5X,
1' BOW-MILS',5X,'PHASE ANGLE',5X,'X-DISP',10X,'Y-DISP',10X,'X-VEL',
210X,'Y-VEL',/,34X,'(DEGREES)',6X,'(MILS)',10X,'(MILS)',10X,
3'MILS/IN',10X,'MIL/IN',/)
1050 FORMAT (5X,I3,6(5X,F10.2))
1060 FORMAT (/,10X,'AVERAGE BEARING STIFFNESS USED FOR CRITICAL SPEED
1CALCULATIONS')
1070 FORMAT (10X,'BEARING NO.',I2,5X,'STIFFNESS(LB/IN)',F12.2)
1071 FORMAT (10X,'BASE MOTION =',I5)
1072 FORMAT (10X,'BEARING',I5,'CONSTANTS ARE',2(2X,F10.5),2(2X,F10.3))
1080 FORMAT (1H1,/)
1090 FORMAT (/,5X,' INITIAL SPEED=',F10.2,5X,'FINAL SPEED=',F10.2,5X,'
1SPEED INCREMENT=',F10.2,' RPM',/)
1100 FORMAT (/13X,3HRPM,20X,5HDELTA,12X,2HK1,13X,2HK2/)
1110 FORMAT (10X,F8.1,9X,E17.9)
1120 FORMAT (/,10X,'CRITICAL SPEED NO.',I2)
1130 FORMAT (/,10X,14HCRITICAL SPEED,11X,5HDELTA,/)
1140 FORMAT (/,12X,6HSTA NO,10X,14HNET DEFLECTION,10X,5HANGLE)
1150 FORMAT (12X,I5,13X,F9.5,13X,F9.5)
1160 FORMAT (5X,10(F8.2,2X))
1170 FORMAT (/,10X,'NONLINEAR BEARING FORCES',/,5X,'BEARING NO.',4X,'
1STATION NO.',4X,'SEQUENCE ',5X,'VISCOSITY',6X,'RADIUS',9X,'LENGTH
2',9X,'CLEARANCE',/,35X,'NUMBER ',6X,'LB/IN**2',7X,'(IN.)',10X,'(
3IN.)',10X,'(IN.)',/)
1180 FORMAT (10X,I5,10X,I5,10X,I5,5X,E10.4,5X,E10.4,5X,E10.4,5X,E10.4)
1190 FORMAT (1H1,/,10X,'CRITICAL SPED NO.',I5,15X,F10.1,'RPM',/,10X,'
1MODAL MASS=',F10.3,2X,'LB-SEC**2/IN',/,10X,'THE ORTHONORMAL MODE
2SHAPES',/,5X,'STATION',8X,'TRANSLATIONAL',7X,'ROTATIONAL')
1200 FORMAT (9X,I3,10X,F10.5,10X,F10.5)
1210 FORMAT (/,10X,'THE ORTHOGONAL CONDITIONS OF MODES',/)
1262 FORMAT (2X,(1X,E10.3))
1260 FORMAT (18X,E13.6)
1265 FORMAT (1X,I3,5(2X,E13.6))
2109 FORMAT (2X,I5,F13.5)
END

```

SUBROUTINE TMM (NSTA)

```

C ****
C * THIS SUBROUTINE USES MODAL ANALYSIS METHOD TO CALCULATE THE *
C * GENERAL DYNAMIC BEHAVIOR OF SYSTEM AFTER THE MODAL SHAPES OF *
C * BOTH ROTORS & BOX HAVE BEEN OBTAINED. *
C ****
IMPLICIT REAL(A-H,O-Z)
COMPLEX B,C
REAL MFX,MFY,MUX,MUY,KMX,KMY,KR
DIMENSION XDTP(10),XVTP(10),XAC(10,5),XLAC(50,5)
DIMENSION TFX(5,4096),TFY(5,4096),SFX(10),SFY(10)
DIMENSION SFRAD(10),RFST(10,4096),FXF(5),FYF(5),FZF(5)
COMMON /ADD1/ TKXX(10,5),TKXY(10,5),TKXA(10,5),TKXB(10,5),TKXZ(10
1 ,5),TCXX(10,5),TCXY(10,5),TCXA(10,5),TCXB(10,5),TCXZ(10,5)
COMMON /ADD2/ TKYX(10,5),TKYY(10,5),TKYA(10,5),TKYB(10,5),TKYZ(10
1 ,5),TCYY(10,5),TCYA(10,5),TCYB(10,5),TCYZ(10,5)
COMMON /ADD3/ TKAX(10,5),TKAY(10,5),TKAA(10,5),TKAB(10,5),TKAZ(10
1 ,5),TCAX(10,5),TCAY(10,5),TCAA(10,5),TCAB(10,5),TCAZ(10,5)
COMMON /ADD4/ TKBX(10,5),TKBY(10,5),TKBA(10,5),TKBB(10,5),TKBZ(10
1 ,5)

```

```

1      ,5),TCBX(10,5),TCBY(10,5),TCBA(10,5),TCBB(10,5),TCBZ(10,5)
COMMON /ADD5/ TKZX(10,5),TKZY(10,5),TKZA(10,5),TKZB(10,5),TKZZ(10
1      ,5),TCZX(10,5),TCZY(10,5),TCZA(10,5),TCZB(10,5),TCZZ(10,5)
COMMON /ADD6/ TOC(16),TOD(16),TOE(16)
COMMON /TFSA/ ATIME(4100),ANG1(4100),ANG2(4100),ANG3(4100),
1      X1(4100),X2(4100),X3(4100),Y1(4100),Y2(4100),Y3(4100)
COMMON /BLK1/ N,NB,NNLIN,NMB,NF,NU,NS,NBOW,ISTAB,IMODE,ISKU,NNCT,N
1UFPT
COMMON /BLK2/ ISKIP,NSTEP,NCYCLE,NITP,NINT,NPLOT,NORBIT,NTIME,NSPE
1ED,NINC,NOPT,NT
COMMON /BLK3/ CRT(10),LLBD(10),LLNB(5),LLNMB(9),LLSK(10),LLNT(10),
1LLUF(10),LLFF(10),LLUT(10),TCRT(10,5)
COMMON /BLK4/
1      SLNMB(9,4,4),CLNMB(9,4,4)
COMMON /BLK5/ UX(10),UY(10),FX(10),FY(10),FSK(10),PSK(10)
COMMON /BLK6/ BOW(100),PBOW(100),XIDC(100),YIDC(100),VXIDC(100),VY
1IDC(100),BXA(100),BYA(100)
COMMON /BLK7/ CMX(10,10),KMX(10,10),EMX(10,10),CMY(10,10),KMY(10,1
10),EMY(10,10)
COMMON /BLK8/ MFX(10),MFY(10),MUX(10),MUY(10),MBX(10),MBY(10)
COMMON /BLK9/ DDPC(10,100),EEYTH(10,100)
COMMON /BLK10/ SPS,SPF,SPN,SPEED1
COMMON /BLK11/ DOX(10,10),DOY(10,10),EOX(10,10),EOY(10,10)
COMMON /BLK15/ RP(100),RT(100)
COMMON /BLK16/ SPEED2,ANGSP,ANGACL,FSPEED
COMMON /BLK18/ AKK(10),TAKK(10,5)
COMMON /BLK19/ DX(100)
COMMON /BLK20/ A1(2,10),A2(2,10),A3(2,10),B1(2,10),B2(2,10),B3(2,1
10)
COMMON /BLK22/ W(100)
COMMON /BLK24/ B(20,21),C(20)
COMMON /BLK25/ BETA
COMMON /BLK29/ PASP
COMMON /BLK40/ BMMFX(10),BMMFY(10),TBMMFX(10,5),TBMMFY(10,5)
COMMON /BLK41/ NBMOP,ACON1(10),ACON2(10),AOMG1(10),AOMG2(10)
COMMON /BLK42/ CLEAR(100),NRUB(100),KR,IND,NSRUB,ABSO,NFACT
COMMON /BLK43/ RMX(10),RMY(10),TRMX(10,5),TRMY(10,5)
COMMON /BLK46/ NSEU,SUX(10),SUY(10)
COMMON /BLK60/ SFY,SFY
COMMON /BLK61/ TFX,TFY
COMMON /BLK79/ CTIME
COMMON /BLK91/ SFRAD
COMMON /BLK92/ RFST
COMMON /SPEED/ TSPEED(5)
COMMON /JS/ JST(5)
COMMON /SHAPE/ NN(5),NNNCT(5),NNB(5)
COMMON /FOR123/ F12(4100),F13(4100)
COMMON /XYA/ XR1,XR2,XR3,YR1,YR2,YR3,RANG1,RANG2,RANG3
COMMON /OMG/ NNBMOP(5),TACON1(10,5),TACON2(10,5),TAOMG1(10,5),
1      TAOMG2(10,5)
COMMON /FO/ FO(5,5),TBRFX(10,5),TBRFY(10,5)
COMMON /KTB13/ NKTB,NSK,INSK(5),ANGL(5,3),UANGL(5,9)
COMMON /KK13/ NP1(4),XG1(4),XMAX1(4),PS11(4)
COMMON /TMU1/ TMUX(10,5),TMUY(10,5),TEXTW(100,5),TDX(100,5)
COMMON /TD1/ TDDXT(100,5),TDDNT(100,5),TRP(100,5)
COMMON /TR1/ TRT(100,5),TEM6(100,5),TRO(100,5),TGGO(100,5)
COMMON /MF1/ LTLFF(10,5),TSFX(10,5),TSFY(10,5),TMFX(10,5)
COMMON /TU1/ LTLUF(10,5),TUX(10,5),TUY(10,5),TSUX(10,5),TSUY(10,5)
COMMON /SEU1/ LTLNT(10,5),NTSRUB(5),NTSEU(5),NTFACT(5),ITND(5)
COMMON /AAB1/ KTR(5),TABSO(5),AA1(2,10,5),AA2(2,10,5),AA3(2,10,5)

```

```

COMMON /BBA1/ BB1(2,10,5),BB2(2,10,5),BB3(2,10,5),TA1(2,10,5)
COMMON /TKB1/ TA2(2,10,5),TA3(2,10,5),TKB(5,5),ALPH(5,5),RCC(5)
COMMON /TMB1/ TMBX(10,5),TMBY(10,5),TWMY(10,5),LTLBD(10,5)
COMMON /TCM1/ TCMX(10,10,5),TCMY(10,10,5),TKMX(10,10,5)
COMMON /TDO1/ TDOX(10,10,5),TDOY(10,10,5),TEOX(10,10,5)
COMMON /TD/ TDDPC(10,100,5),TEMX(10,10,5),TEMY(10,10,5)
COMMON /TW1/ TDMDY(10,10,5),TEEYTH(10,100,5),TW(100,5),TWMOD(50,5)
COMMON /LAS/ TTK(100,5),TMFY(10,5),TKMY(10,10,5),TEOY(10,10,5),
1      TDMX(10,10,5)
COMMON /BASE1/ AB,OMEGA,FAB
COMMON /BOX01/ OMEGS(40),BX1(40,200,6),LBLBT(10,5),NMBB,NODEB
COMMON /BOX02/OA1(2,40),OA2(2,40),OA3(2,40),OB1(2,40),
1 OB2(2,40),OB3(2,40),TNODE(20),FXFXM(40),FYFYM(20),FZFZM(20)
COMMON /BOX04/OZ1(2,20),OZ2(2,20),OZ3(2,20),AZ1(2,10,5)
1 ,AZ2(2,10,5),AZ3(2,10,5),TBRFZ(10,5),TOA(16),TOB(16),TOZ(16)
COMMON /BOX03/ BKZZ(10,5)
COMMON /BOX08/ NPT,NPTNO(16)
COMMON /BLK58/ ZF(10,5),ZFV(10,100,5)

C      ZF -- Z-DIR NATURAL FREQUENCIES OF ROTOR
C      ZFV -- Z-DIR MODAL SHAPES OF ROTOR

IF (NSK.EQ.0) GO TO 20
DO 10 I=1,NSK
II=INSK(I)
C1=COS(ANGL(II,1))
C2=COS(ANGL(II,2))
C3=COS(ANGL(II,3))
S1=SIN(ANGL(II,1))
S2=SIN(ANGL(II,2))
S3=SIN(ANGL(II,3))
UANGL(II,1)=-C2*C3-C1*S2*S3
UANGL(II,2)=-C2*S3-C1*S2*C3
UANGL(II,3)=S1*S2
UANGL(II,4)=S2*C3+C1*C2*S3
UANGL(II,5)=-S2*S3+C1*C2*C3
UANGL(II,6)=-S1*C2
UANGL(II,7)=S1*S3
UANGL(II,8)=S1*C3
UANGL(II,9)=C1
10  CONTINUE
20  CONTINUE

```

```

C      * * * * * * * * * * * * * * * * * * * * * * * * * * *
C ----- *   CALCULATE THE COEFFICIENT OF COMPENSATION TERM  *
C      * * * * * * * * * * * * * * * * * * * * * * * * * * *
      DO 111 IJK=1,NSTA
111  CALL TMODE1 (IJK)

```

```

IF (ISKIP.EQ.1) GO TO 120
SPEED=TSPEED(1)
NSTEP1=NSTEP+1
STEP=NSTEP
FACT=NFACT
TCYCLE=60./SPEED
TIME=0.0
IINT=1
DO 35 JI=1,NSTA

```

```

DO 35 I=1,NNNCT(JI)
AA3(1,I,JI)=0.0
AA2(1,I,JI)=0.0
35  CONTINUE
DO 39 I=1,NMBB
OA3(1,I)=0.0
OA2(1,I)=0.0
39  CONTINUE
51  CONTINUE
701 FORMAT (3G14.6)
ICOUNT=1
NK=0
NPLUS=0
IF (ABS(ANGACL).LT.0.0001) GO TO 61
NPLUS=9999
61  CONTINUE
DO 19 KI=1,2
DO 19 I=1,NSTA
LB1=LTLBD(1,I)
LB2=LTLBD(2,I)
LB3=LTLBD(3,I)
SPLB=0.0
DO 55 IO=LB1,LB2-1
55  SPLB=SPLB+TDX(IO,I)
SLLE=0.0
LB4=LB1-1
DO 56 I2=1,LB4
56  SLLE=SLLE+TDX(I2,I)
SLGE=0.
DO 57 I3=LB2,LB3-1
57  SLGE=SLGE+TDX(I3,I)
N1=NN(I)
N2=NNNCT(I)
N3=NNB(I)
19   CONTINUE
NJ=NPLUS+1
PASP=0.
ICT=1
ICOM=NFACT
TEAM=TIME
I4=0

```

```

C      * * * * * * * * * * * * * * * * * * * * * * * * * * * * *
C ----- * THE LOOP WHICH CALCULATES DYNAMIC RESPONSE BEGINS *
C      * * * * * * * * * * * * * * * * * * * * * * * * * * * * *
DO 110 I=IINT,NCYCLE
TEEM=TIME
NTCS=NSTEP*NFACT
DO 100 J=1,NTCS
I4=I4+1
DELTAT=TCYCLE/(STEP*FACT)
IF (J.GT.NJ) NK=1

```

```

C      * * * * * * * * * * * * * * * * * * * * * * * * * * * *
C ----- * CALCULATE THE UNBALANCE TERM OF ROTOR EQUATION *
C      * * * * * * * * * * * * * * * * * * * * * * * * * * * *
DO 99 I1=1,NSTA
99  CALL TMODE2 (TIME,DELTAT,TSPEED(I1),NK,I1)

```

```

DO 67 I1=1,NSTA
DO 62 IJK=1,NNCT
TBMMFX(IJK,I1)=0.0
TBMMFY(IJK,I1)=0.0
62    CONTINUE
IF(NNBMOP(I1).EQ.0) GO TO 69
IF(NNBMOP(I1).EQ.2) GO TO 64
DO 63 IJK=1,NNB(I1)
OMGT=TAOMG1(IJK,I1)*TIME
BT=(-1.0)*TACON2(IJK,I1)*TIME
EBT=EXP(BT)
XAC(IJK,I1)=TACON1(IJK,I1)*EBT*COS(OMGT)
63    CONTINUE
GO TO 66
64    CONTINUE
DO 65 IJK=1,NNB(I1)
OMGT1=TAOMG1(IJK,I1)*TIME
OMGT2=TAOMG2(IJK,I1)*TIME
XAC(IJK,I1)=TACON1(IJK,I1)*SIN(OMGT1)*SIN(OMGT2)
65    CONTINUE
66    CONTINUE
STLP=(XAC(2,I1)-XAC(1,I1))/SPLB
XLAC(1,I1)=XAC(1,I1)-STLP*SLLE
DO 67 IJK=2,N
IJJ=IJK-1
XLAC(IJK,I1)=XLAC(IJJ,I1)+TDX(IJJ,I1)*STLP
67    CONTINUE

DO 68 I1=1,NSTA
DO 68 IJK=1,NNCT
DO 68 IJJ=1,N
TBMMFX(IJK,I1)=TBMMFX(IJK,I1)-TW(IJJ,I1)*XLAC(IJJ,I1)*TDDPC
*(IJK,IJJ,I1)/386.4
68    CONTINUE
69    CONTINUE
XXK=360.0*TIME/TCYCLE

C      * * * * * * * * * * * * * * * * * *
C ----- *   CALCULATE THE GEAR STIFFNESS  *
C      * * * * * * * * * * * * * * * * * *
C
DO 27 KK=1,NKTB
NK=KK+1
XXX1=XXK-PS11(KK)
CALL STIFF (KK,NP1(KK),XG1(KK),XMAX1(KK),XXX1,YK12)
TKB(1,NK)=YK12
TKB(NK,1)=YK12
27    CONTINUE

C      * * * * * * * * * * * * * * * * * *
C ----- *   CALCULATE THE BEARING FORCE   *
C      * * * * * * * * * * * * * * * * * *
C
JN=0
DO 999 III=1,NSTA
DO 999 KKK=1,NNNCT(III)
TBRFX(KKK,III)=0.
TBRFY(KKK,III)=0.

```

```

TBRFZ (KKK, III)=0.
999 CONTINUE
DO 998 JJJ=1, NMBB
FXFXM (JJJ)=0.
998 CONTINUE
DO 88 K3=1, NSTA
KJST=JST (K3)
DO 86 J3=1, NNB (K3)
JB=LTLBD (J3, K3)
JBB=LBLBT (J3, K3)
IF (JBB.EQ.0) GO TO 86
JN=JN+1
JNODE (JN)=JBB
XD=0.0
YD=0.0
AD=0.0
BD=0.0
ZD=0.0
XV=0.0
YV=0.0
AV=0.0
BV=0.0
ZV=0.0
DO 84 I3=1, NNNCT (K3)
XD=XD+AA3 (1, I3, K3)*TDDPC (I3, JB, K3)
YD=YD+AA3 (1, I3, K3)*TEEYTH (I3, JB, K3)
AD=AD+BB3 (1, I3, K3)*TDDPC (I3, JB, K3)
BD=BD+BB3 (1, I3, K3)*TEEYTH (I3, JB, K3)
ZD=ZD+AZ3 (1, I3, K3)*ZFV (I3, JB, K3)
XV=XV+AA2 (1, I3, K3)*TDDPC (I3, JB, K3)
YV=YV+AA2 (1, I3, K3)*TEEYTH (I3, JB, K3)
AV=AV+BB2 (1, I3, K3)*TDDPC (I3, JB, K3)
BV=BV+BB2 (1, I3, K3)*TEEYTH (I3, JB, K3)
ZV=ZV+AZ2 (1, I3, K3)*ZFV (I3, JB, K3)
84 CONTINUE
XDB=0.0
YDB=0.0
ADB=0.0
BDB=0.0
ZDB=0.0
XVB=0.0
YVB=0.0
AVB=0.0
BVB=0.0
ZVB=0.0
DO 87 I4=1, NMBB
XDB=XDB+OA2 (1, I4)*BX1 (I4, JBB, 1)
YDB=YDB+OA3 (1, I4)*BX1 (I4, JBB, 4)
ADB=ADB+OA3 (1, I4)*BX1 (I4, JBB, 2)
BDB=BDB+OA3 (1, I4)*BX1 (I4, JBB, 5)
ZDB=ZDB+OA3 (1, I4)*BX1 (I4, JBB, 3)
XVB=XVB+OA2 (1, I4)*BX1 (I4, JBB, 1)
YVB=YVB+OA2 (1, I4)*BX1 (I4, JBB, 4)
AVB=AVB+OA2 (1, I4)*BX1 (I4, JBB, 2)
BVB=BVB+OA2 (1, I4)*BX1 (I4, JBB, 5)
ZVB=ZVB+OA2 (1, I4)*BX1 (I4, JBB, 3)
87 CONTINUE
FD1=TKXX (J3, K3)*(XDB-XD)+TKXA (J3, K3)*(YDB-YD)+TKXY (J3, K3)*(ADB-AD)
& +TKXB (J3, K3)*(BDB-BD)+TKXZ (J3, K3)*(ZDB-ZD)

```

```

FD2=TKAX(J3,K3)*(XDB-XD)+TKAA(J3,K3)*(YDB-YD)+TKAY(J3,K3)*(ADB-AD)
& +TKAB(J3,K3)*(BDB-BD)+TKAZ(J3,K3)*(ZDB-ZD)
FD3=TKYX(J3,K3)*(XDB-XD)+TKYA(J3,K3)*(YDB-YD)+TKYY(J3,K3)*(ADB-AD)
& +TKYB(J3,K3)*(BDB-BD)+TKYZ(J3,K3)*(ZDB-ZD)
FD4=TKBX(J3,K3)*(XDB-XD)+TKBA(J3,K3)*(YDB-YD)+TKBY(J3,K3)*(ADB-AD)
& +TKBB(J3,K3)*(BDB-BD)+TKBZ(J3,K3)*(ZDB-ZD)
FD5=TKZX(J3,K3)*(XDB-XD)+TKZA(J3,K3)*(YDB-YD)+TKZY(J3,K3)*(ADB-AD)
& +TKZB(J3,K3)*(BDB-BD)+TKZZ(J3,K3)*(ZDB-ZD)
FV1=TCXX(J3,K3)*(XVB-XV)+TCXA(J3,K3)*(YVB-YV)+TCXY(J3,K3)*(AVB-AV)
& +TCXB(J3,K3)*(BVB-BV)+TCXZ(J3,K3)*(ZVB-ZV)
FV2=TCAX(J3,K3)*(XVB-XV)+TCAA(J3,K3)*(YVB-YV)+TCAY(J3,K3)*(AVB-AV)
& +TCAB(J3,K3)*(BVB-BV)+TCAZ(J3,K3)*(ZVB-ZV)
FV3=TCYX(J3,K3)*(XVB-XV)+TCYA(J3,K3)*(YVB-YV)+TCYY(J3,K3)*(AVB-AV)
& +TCYB(J3,K3)*(BVB-BV)+TCYZ(J3,K3)*(ZVB-ZV)
FV4=TCBX(J3,K3)*(XVB-XV)+TCBA(J3,K3)*(YVB-YV)+TCBY(J3,K3)*(AVB-AV)
& +TCBB(J3,K3)*(BVB-BV)+TCBZ(J3,K3)*(ZVB-ZV)
FV5=TCZX(J3,K3)*(XVB-XV)+TCZA(J3,K3)*(YVB-YV)+TCZY(J3,K3)*(AVB-AV)
& +TCZB(J3,K3)*(BVB-BV)+TCZZ(J3,K3)*(ZVB-ZV)
DO 82 II3=1,NNNCT(K3)
TBRFX(II3,K3)=TBRFX(II3,K3)+(FD1+FV1)*TDDPC(II3,JB,K3)
& +(FD2+FV2)*TEEYTH(II3,JB,K3)
TBRFY(II3,K3)=TBRFY(II3,K3)+(FD3+FV3)*TDDPC(II3,JB,K3)
& +(FD4+FV4)*TEEYTH(II3,JB,K3)
TBRFZ(II3,K3)=TBRFZ(II3,K3)+(FD5+FV5)*ZFV(II3,JB,K3)
82 CONTINUE
C TBRFX -- MODAL BEARING FORCE OF X-DIRECTION ON ROTOR
C TBRFY -- MODAL BEARING FORCE OF Y-DIRECTION ON ROTOR
C TBRFZ -- MODAL BEARING FORCE OF Z-DIRECTION ON ROTOR

```

```

DO 83 I5=1,NMBB
FXFXM(I5)=FXFXM(I5)-(FD1+FV1)*BX1(I5,JBB,1)
FXFXM(I5)=FXFXM(I5)-(FD2+FV2)*BX1(I5,JBB,4)
FXFXM(I5)=FXFXM(I5)-(FD3+FV3)*BX1(I5,JBB,2)
FXFXM(I5)=FXFXM(I5)-(FD4+FV4)*BX1(I5,JBB,5)
FXFXM(I5)=FXFXM(I5)-(FD5+FV5)*BX1(I5,JBB,3)
83 CONTINUE
C FXFXM -- MODAL BEARING FORCE ON ROTOR

```

```

86 CONTINUE
88 CONTINUE

```

```

C * * * * * * * * * * * * * * * *
C ----- * SOLVE THE MODAL EQUATION OF ROTOR *
C * * * * * * * * * * * * * * * * * *
CALL TACCEL (NSTA)

```

```

NIJ=(I-1)*NSTEP+J
IF(ICOM.NE.NFACT)GO TO 78
IF(NNLIN.NE.0)GO TO 75
DO 74 KK=1,NSTA
DO 74 IJL=1,NB
IB=LTLBD(IJL,KK)
X=0.0
Y=0.0
VX=0.0
VY=0.0
DO 73 IJN=1,NNCT
X=X+AA3(1,IJN,KK)*TDDPC(IJN,IB,KK)

```

```

    VX=VX+AA2(1,IJN,KK)*TDDPC(IJN,IB,KK)
    Y=Y+BB3(1,IJN,KK)*TDDPC(IJN,IB,KK)
73   VY=VY+BB2(1,IJN,KK)*TDDPC(IJN,IB,KK)
    TFX(IJL,ICT)=TCXX(IJL,KK)*VX+ TCXA(IJL,KK)*VY+(TKXX(IJL,KK)+TAKK(I
&JL,KK))*X+TKXA(IJL,KK)*Y
74   CONTINUE
75   IF(NSRUB.EQ.0)GO TO 77
    DO 76 IJL=1,NSRUB
76   RFST(IJL,ICT)=SFRAD(IJL)
77   ICT=ICT+1
    ICOM=0
78   ICOM=ICOM+1
    TIME=TIME+DELTAT

```

```

C      * * * * * * * * * * * * * * * * * * * * * * * * * * * *
C ----- *   SOLVE THE MODAL EQUATION OF BOX & INTEGRATE THE RESULT   *
C      * * * * * * * * * * * * * * * * * * * * * * * * * * * *
C      GO TO (70,80), NINT
C ----- WITH NEWMARK BETA METHOD
70   CALL TBETA (NNCT,DELTAT,NSTA,TIME)
    GO TO 90
C ----- WITH EULER METHOD
80   CALL TINTG (NNCT,DELTAT)
90   CONTINUE

```

```

IF(ICOM.NE.1)GO TO 96
ICOUNT=ICOUNT+1
FI=ICOUNT
ATIME(ICOUNT)=FI*DELTAT*FACT
X1(ICOUNT)=XR1
X2(ICOUNT)=XR2
X3(ICOUNT)=XR3
Y1(ICOUNT)=YR1
Y2(ICOUNT)=YR2
Y3(ICOUNT)=YR3
ANG1(ICOUNT)=RANG1
ANG2(ICOUNT)=RANG2
ANG3(ICOUNT)=RANG3
F12(ICOUNT)=FO(1,2)
F13(ICOUNT)=FO(1,3)
DO 93 JI=1,NSTA
  WRITE (7,707) (AA3(1,II,JI),II=1,NNCT)
93   WRITE (8,708) (BB3(1,II,JI),II=1,NNCT)
  WRITE(10,710) (TOA(JI),JI=1,NPT)
96   CONTINUE
PASP=PASP+DELTAT*SPEED*0.104719
TCYCLE=60./SPEED
100  CONTINUE
110  CONTINUE
120  CONTINUE
901  FORMAT(4E18.6)
902  FORMAT(F10.7)
N9=ICOUNT
707  FORMAT (3G14.6)
708  FORMAT (10X,3G14.6)
709  FORMAT (9G9.2 )
710  FORMAT (8G9.2 )
  WRITE(9,9901)(F12(I),I=1,N9)

```

```

9901 FORMAT(F12.6)
      WRITE(11,9)(X1(I),Y1(I),I=1,N9)
      WRITE(12,9)(X2(I),Y2(I),I=1,N9)
9   FORMAT(2X,2F10.7)
      RETURN
      END

```

```

      SUBROUTINE TMODE1 (I1)
C ****
C * THIS SUBROUTINE CALCULATES THE MODAL COEFFICIENTS WHICH APPEARS *
C * IN THE MODAL EQUATION OF ROTORS
C ****
      IMPLICIT REAL(A-H,O-Z)
      REAL MFX,MFY,MUX,MUY,KMX,KMY
      REAL KXX,KXY,KXA,KXB,KXZ
      REAL KYX,KYY,KYA,KYB,KYZ
      REAL KAX,KAY,KAA,KAB,KAZ
      REAL KBX,KBY,KBA,KBB,KBZ
      REAL KZX,KZY,KZA,KZB,KZZ
      COMMON /ADD1/ TKXX(10,5),TKXY(10,5),TKXA(10,5),TKXB(10,5),TKXZ(10
1           ,5),TCXX(10,5),TCXY(10,5),TCXA(10,5),TCXB(10,5),TCXZ(10,5)
      COMMON /ADD2/ TKYX(10,5),TKYY(10,5),TKYA(10,5),TKYB(10,5),TKYZ(10
1           ,5),TCYX(10,5),TCYY(10,5),TCYA(10,5),TCYB(10,5),TCYZ(10,5)
      COMMON /ADD3/ TKAX(10,5),TKAY(10,5),TKAA(10,5),TKAB(10,5),TKAZ(10
1           ,5),TCAX(10,5),TCAY(10,5),TCAA(10,5),TCAB(10,5),TCAZ(10,5)
      COMMON /ADD4/ TKBX(10,5),TKBY(10,5),TKBA(10,5),TKBB(10,5),TKBZ(10
1           ,5),TCBX(10,5),TCBY(10,5),TCBA(10,5),TCBB(10,5),TCBZ(10,5)
      COMMON /ADD5/ TKZX(10,5),TKZY(10,5),TKZA(10,5),TKZB(10,5),TKZZ(10
1           ,5),TCZX(10,5),TCZY(10,5),TCZA(10,5),TCZB(10,5),TCZZ(10,5)
      COMMON /ADD6/ TOC(16),TOD(16),TOE(16)
      COMMON /BLK1/ N,NB,NNLIN,NMB,NF,NU,NS,NBOW,ISTAB,IMODE,ISKU,NNCT,N
1UFPT
      COMMON /BLK3/ CRT(10),LLBD(10),LLNB(5),LLNMB(9),LLSK(10),LLNT(10),
1LLUF(10),LLFF(10),LLUT(10),TCRT(10,5)
      COMMON /BLK4/
1           SLNMB(9,4,4),CLNMB(9,4,4)
      COMMON /BLK7/ CMX(10,10),KMX(10,10),EMX(10,10),CMY(10,10),KMY(10,1
10),EMY(10,10)
      COMMON /BLK9/ DDPC(10,100),EYTH(10,100)
      COMMON /BLK11/ DOX(10,10),DOY(10,10),EOX(10,10),EOY(10,10)
      COMMON /BLK22/ W(100)
      COMMON /BLK35/ WMY(10),VIS(5),ANR(5),ANL(5),ANC(5),NLB(5)
      COMMON /SHAPE/ NN(5),NNNCT(5),NNB(5)
      COMMON /TDC / TTCD(10,10,5)
      COMMON /BLK54/ FR(10,5),          FFV(10,100,5)
      COMMON /BLK58/ ZF(10,5),ZFV(10,100,5)
      COMMON /RDDT / NTDD(5),LLTD(10,5),TTCC(10,5)
      COMMON /TMU1/ TMUX(10,5),TMUY(10,5),TEXTW(100,5),TDX(100,5)
      COMMON /TD1/ TDDXT(100,5),TDDNT(100,5),TRP(100,5)
      COMMON /TR1/ TRT(100,5),TEM6(100,5),TRO(100,5),TGGO(100,5)
      COMMON /MF1/ LTLFF(10,5),TSFX(10,5),TSFY(10,5),TMFX(10,5)
      COMMON /TU1/ LTLUF(10,5),TUX(10,5),TUW(10,5),TSUX(10,5),TSUY(10,5)
      COMMON /SEU1/ LTLNT(10,5),NTSRUB(5),NTSEU(5),NTFACT(5),ITND(5)
      COMMON /AAB1/ KTR(5),TABSO(5),AA1(2,10,5),AA2(2,10,5),AA3(2,10,5)
      COMMON /BBA1/ BB1(2,10,5),BB2(2,10,5),BB3(2,10,5),TA1(2,10,5)
      COMMON /TKB1/ TA2(2,10,5),TA3(2,10,5),TKB(5,5),ALPH(5,5),RCC(5)
      COMMON /TMB1/ TMBX(10,5),TMBY(10,5),TWMY(10,5),LTLBD(10,5)
      COMMON /TCM1/ TCMX(10,10,5),TCMY(10,10,5),TKMX(10,10,5)
      COMMON /TDO1/ TDOX(10,10,5),TDOY(10,10,5),TEOX(10,10,5)

```

```

COMMON /TD/ TDDPC(10,100,5),TEMX(10,10,5),TEMY(10,10,5)
COMMON /TW1/ TDMDY(10,10,5),TEEYTH(10,100,5),TW(100,5),TWMOD(50,5)
COMMON /LAS/ TTK(100,5),TMFY(10,5),TKMY(10,10,5),TEOY(10,10,5),
1           TDMX(10,10,5)
DO 10 I=1,NNNCT(I1)
DO 10 J=1,NNNCT(I1)
TKMX(I,J,I1)=0.
TKMY(I,J,I1)=0.
TEOY(I,J,I1)=0.
TTCM(I,J,I1)=0.
10      CONTINUE
DO 30 I=1,NNB(I1)
J=LTLBD(I,I1)
DO 20 K=1,NNNCT(I1)
DO 20 L=1,NNNCT(I1)
TKMX(K,L,I1)=TKMX(K,L,I1)+TKXX(I,I1)*TDDPC(K,J,I1)*TDDPC(L,J,I1)
TKMY(K,L,I1)=TKMY(K,L,I1)+TKYY(I,I1)*TDDPC(K,J,I1)*TDDPC(L,J,I1)
TKMX(K,L,I1)=(TKMX(K,L,I1)+TKMY(K,L,I1))/2.
20      TEOY(K,L,I1)=TEOY(K,L,I1)+TKZZ(I,I1)*ZFV(K,J,I1)*ZFV(L,J,I1)
30      CONTINUE
DO 100 I=1,NTTD(I1)
L=LLTD(I,I1)
DO 100 J=1,NNNCT(I1)
DO 100 K=1,NNNCT(I1)
TTCM(J,K,I1)=TTCM(J,K,I1)+TTCC(I,I1)*FFV(J,L,I1)*FFV(K,L,I1)*0.0
100     CONTINUE
RETURN
END

```

```

SUBROUTINE TMODE2 (T,DELTAT,SPEED,NK,I1)
C ****
C * THIS SUBROUTINE CALCULATES THE MODAL UNBALANCE FOR TRANSIENT *
C * RESPONSE ANALYSIS                                              *
C ****
IMPLICIT REAL(A-H,O-Z)
REAL MBX,MBY
REAL MFX,MFY,MUX,MUY,KMX,KMY
REAL KXX,KXY,KXA,KXB,KXZ
REAL KYX,KYY,KYA,KYB,KYZ
REAL KAX,KAY,KAA,KAB,KAZ
REAL KBX,KBY,KBA,KBB,KBZ
REAL KZX,KZY,KZA,KZB,KZZ
COMMON /BLK1/ N,NB,NNLIN,NMB,NF,NU,NS,NBOW,ISTAB,IMODE,ISKU,NNCT,N
1UFPT
COMMON /BLK2/ ISKIP,NSTEP,NCYCLE,NITP,NINT,NPLOT,NORBIT,NTIME,NSPE
1ED,NINC,NOPT,NT
COMMON /BLK3/ CRT(10),LLBD(10),LLNB(5),LLNMB(9),LLSK(10),LLNT(10),
1LLUF(10),LLFF(10),LLUT(10),TCRT(10,5)
COMMON /BLK5/ UX(10),UY(10),FX(10),FY(10),FSK(10),PSK(10)
COMMON /BLK6/ BOW(100),PBOW(100),XIDC(100),YIDC(100),VXIDC(100),VY
1IDC(100),BXA(100),BYA(100)
COMMON /BLK7/ CMX(10,10),KMX(10,10),EMX(10,10),CMY(10,10),KMY(10,1
10),EMY(10,10)
COMMON /BLK8/ MFX(10),MFY(10),MUX(10),MUY(10),MBX(10),MBY(10)
COMMON /BLK9/ DDPC(10,100),EEYTH(10,100)
COMMON /BLK11/ DOX(10,10),DOY(10,10),EOX(10,10),EOY(10,10)
COMMON /BLK15/ RP(100),RT(100)
COMMON /BLK16/ SPEED2,ANGSP,ANGACL,FSPEED
COMMON /BLK18/ AKK(10),TAKK(10,5)

```

```

COMMON /BLK21/ DMX(10,10),DMY(10,10)
COMMON /BLK29/ PASP
COMMON /SPEED/ TSPEED(5)
COMMON /TMU1/ TMUX(10,5),TMUY(10,5),TEXTW(100,5),TDX(100,5)
COMMON /TD1/ TDDXT(100,5),TDDNT(100,5),TRP(100,5)
COMMON /TR1/ TRT(100,5),TEM6(100,5),TRO(100,5),TGGO(100,5)
COMMON /MF1/ LTLFF(10,5),TSFX(10,5),TSFY(10,5),TMFX(10,5)
COMMON /TU1/ LTLUF(10,5),TUX(10,5),TUY(10,5),TSUX(10,5),TSUY(10,5)
COMMON /SEU1/ LTLNT(10,5),NTSRUB(5),NTSEU(5),NTFACT(5),ITND(5)
COMMON /AAB1/ KTR(5),TABSO(5),AA1(2,10,5),AA2(2,10,5),AA3(2,10,5)
COMMON /BBA1/ BB1(2,10,5),BB2(2,10,5),BB3(2,10,5),TA1(2,10,5)
COMMON /TKB1/ TA2(2,10,5),TA3(2,10,5),TKB(5,5),ALPH(5,5),RCC(5)
COMMON /TMB1/ TMBX(10,5),TMBY(10,5),TWMY(10,5),LTLBD(10,5)
COMMON /TCM1/ TCMX(10,10,5),TCMY(10,10,5),TKMX(10,10,5)
COMMON /TDO1/ TDOX(10,10,5),TDOY(10,10,5),TEOX(10,10,5)
COMMON /TD/ TDDPC(10,100,5),TEMX(10,10,5),TEMY(10,10,5)
COMMON /TW1/ TDNY(10,10,5),TEEYTH(10,100,5),TW(100,5),TWMOD(50,5)
COMMON /LAS/ TTK(100,5),TMFY(10,5),TKMY(10,10,5),TEOY(10,10,5),
1      TDMX(10,10,5)

PI=3.14159
ANGSP=TSPEED(I1)*PI/30.
DO 10 I=1,NNCT
TMUX(I,I1)=0.
TUUY(I,I1)=0.
10 CONTINUE
DO 30 I=1,NU
J=LTLUF(I,I1)
PHI=ATAN2(TUY(I,I1),TUX(I,I1))
OMT=ANGSP*T+PHI
C PMT=OMT+3.1415926
IF (NK.EQ.0) OMT=PASP+PHI
TME=(TUX(I,I1)*TUX(I,I1)+TUUY(I,I1)*TUUY(I,I1))**0.5
DO 20 K=1,NNCT
TMUX(K,I1)=TMUX(K,I1)+(ANGACL*SIN(OMT)+ANGSP*ANGSP*COS(OMT))
C 1      *TME*TDDPC(K,J,I1)
C IF(I1.EQ.2) GOTO 654
TMUX(K,I1)=TMUX(K,I1)+(ANGACL*SIN(OMT)+ANGSP*ANGSP*COS(OMT))
C 1      *TME*TDDPC(K,J,I1) +TME*TDDPC(K,J,I1)
C 1 *ANGSP*ANGSP*(I1-1)*(COS(OMT*2.)/4.+COS(OMT*3.)/5.)
TMUY(K,I1)=TMUY(K,I1)+(ANGSP*ANGSP*SIN(OMT))
C 1      *TME*TDDPC(K,J,I1) +TME*TDDPC(K,J,I1)
C 1 *ANGSP*ANGSP*(I1-1)*(SIN(OMT*2.)/4.+SIN(OMT*3.)/5.)
C GO TO 20
C654 TMUX(K,I1)=TMUX(K,I1)+(ANGACL*SIN(PMT)+ANGSP*ANGSP*COS(PMT))
C 1      *TME*TDDPC(K,J,I1) +TME*TDDPC(K,J,I1)
C 1 *ANGSP*ANGSP*(I1-1)*(COS(PMT*2.)/4.+COS(PMT*3.)/5.)
C TMUY(K,I1)=TMUY(K,I1)+(ANGSP*ANGSP*SIN(PMT))
C 1      *TME*TDDPC(K,J,I1) +TME*TDDPC(K,J,I1)
C 1 *ANGSP*ANGSP*(I1-1)*(SIN(PMT*2.)/4.+SIN(PMT*3.)/5.)
C TMUY(K,I1)=TMUY(K,I1)+(ANGSP*ANGSP*SIN(OMT)-ANGACL*COS(OMT))
C 1      *TME*TDDPC(K,J,I1)
20 CONTINUE
30 CONTINUE
RETURN
END

```

SUBROUTINE TACCEL (NSTA)

```

C ****

```

```

C * THIS SUBROUTINE CALCULATES THE MODAL ACCELERATION BY SOLVING *
C * THE MODAL EQUATIONS OF ROTORS *
C ****
C IMPLICIT REAL(A-H,O-Z)
REAL MFY,MFY,MUX,MUY,KMX,KMY,KR
COMMON /ADD1/ TKXX(10,5),TKXY(10,5),TKXA(10,5),TKXB(10,5),TKXZ(10
1 ,5),TCXX(10,5),TCXY(10,5),TCXA(10,5),TCXB(10,5),TCXZ(10,5)
COMMON /ADD2/ TKYX(10,5),TKYY(10,5),TKYA(10,5),TKYB(10,5),TKYZ(10
1 ,5),TCYX(10,5),TCYY(10,5),TCYA(10,5),TCYB(10,5),TCYZ(10,5)
COMMON /ADD3/ TKAX(10,5),TKAY(10,5),TKAA(10,5),TKAB(10,5),TKAZ(10
1 ,5),TCAX(10,5),TCAY(10,5),TCAA(10,5),TCAB(10,5),TCAZ(10,5)
COMMON /ADD4/ TKBX(10,5),TKBY(10,5),TKBA(10,5),TKBB(10,5),TKBZ(10
1 ,5),TCBX(10,5),TCBY(10,5),TCBA(10,5),TCBB(10,5),TCBZ(10,5)
COMMON /ADD5/ TKZX(10,5),TKZY(10,5),TKZA(10,5),TKZB(10,5),TKZZ(10
1 ,5),TCZX(10,5),TCZY(10,5),TCZA(10,5),TCZB(10,5),TCZZ(10,5)
COMMON /ADD6/ TOC(16),TOD(16),TOE(16)
COMMON /BLK1/ N,NB,NNLIN,NMB,NF,NU,NS,NBOW,1STAB,IMODE,ISKU,NNCT,N
1UFPT
COMMON /BLK3/ CRT(10),LLBD(10),LLNB(5),LLNMB(9),LLSK(10),LLNT(10),
1LLUF(10),LLFF(10),LLUT(10),TCRT(10,5)
COMMON /BLK7/ CMX(10,10),KMX(10,10),EMX(10,10),CMY(10,10),KMY(10,1
10),EMY(10,10)
COMMON /BLK8/ MFY(10),MFY(10),MUX(10),MUY(10),MBX(10),MBY(10)
COMMON /BLK9/ DDPC(10,100),EEYTH(10,100)
COMMON /BLK20/ A1(2,10),A2(2,10),A3(2,10),B1(2,10),B2(2,10),B3(2,1
10)
COMMON /BLK21/ DMX(10,10),DMY(10,10)
COMMON /BLK40/ BMMFX(10),BMMFY(10),TBMMFX(10,5),TBMMFY(10,5)
COMMON /BLK42/ CLEAR(100),NRUB(100),KR,IND,NSRUB,ABSO,NFACT
COMMON /BLK43/ RMX(10),RMY(10),TRMX(10,5),TRMY(10,5)
COMMON /BLK54/ FR(10,5), FFV(10,100,5)
COMMON /JS/ JST(5)
COMMON /TOU/ TOUT(5),FORCEZ(5)
COMMON /SHAPE/ NN(5),NNNCT(5),NNB(5)
COMMON /FO/ FO(5,5),TBRFX(10,5),TBRFY(10,5)
COMMON /XYA/ XR1,XR2,XR3,YR1,YR2,YR3,RANG1,RANG2,RANG3
COMMON /TDC/ TTCM(10,10,5)
COMMON /KTB13/ NKTB,NSK,INSK(5),ANGL(5,3),UANGL(5,9)
COMMON /TMU1/ TMUX(10,5),TMUY(10,5),TEXTW(100,5),TDX(100,5)
COMMON /TD1/ TDDXT(100,5),TDDNT(100,5),TRP(100,5)
COMMON /TR1/ TRT(100,5),TEM6(100,5),TRO(100,5),TGGO(100,5)
COMMON /MF1/ LTLFF(10,5),TSFX(10,5),TSFY(10,5),TMFX(10,5)
COMMON /TU1/ LTLUF(10,5),TUX(10,5),TUY(10,5),TSUX(10,5),TSUY(10,5)
COMMON /SEU1/ LTLNT(10,5),NTSRUB(5),NTSEU(5),NTFACT(5),ITND(5)
COMMON /AAB1/ KTR(5),TABSO(5),AA1(2,10,5),AA2(2,10,5),AA3(2,10,5)
COMMON /BBA1/ BB1(2,10,5),BB2(2,10,5),BB3(2,10,5),TA1(2,10,5)
COMMON /TKB1/ TA2(2,10,5),TA3(2,10,5),TKB(5,5),ALPH(5,5),RCC(5)
COMMON /TMB1/ TMBX(10,5),TMBY(10,5),TWMY(10,5),LTLBD(10,5)
COMMON /TCM1/ TCMX(10,10,5),TCMY(10,10,5),TKMX(10,10,5)
COMMON /TDO1/ TDOX(10,10,5),TDOY(10,10,5),TEOX(10,10,5)
COMMON /TD/ TDDPC(10,100,5),TEMX(10,10,5),TEMY(10,10,5)
COMMON /TW1/ TDMDY(10,10,5),TEEYTH(10,100,5),TW(100,5),TWMOD(50,5)
COMMON /LAS/ TTK(100,5),TMFY(10,5),TKMY(10,10,5),TEOY(10,10,5),
1 TDMX(10,10,5)

IF (NNLIN.EQ.0) GO TO 10
CALL BNF
CONTINUE

```

10

C * * * * *

```

C ----- *      CALCULATE ROTOR'S MODAL ACCELERATIONS      *
C * * * * * * * * * * * * * * * * * * * * * * * * * * * * *
DO 30 I1=1,NSTA
DO 30 L=1,NNNCT(I1)
ABC=0.0
BCA=0.0
CAB=0.0
IF (I1.EQ.1) THEN
JT=2
ELSE
JT=23
END IF
TA1(1,L,I1)=FFV(L,JT,I1)*TOUT(I1)-FR(L,I1)**2*TA3(1,L,I1)
AA1(1,L,I1)=TMUX(L,I1)+TBRFX(L,I1)-(TCRT(L,I1)*0.1047195)**2
1   *AA3(1,L,I1)-AA2(1,L,I1)*0.0
BB1(1,L,I1)=TBRFY(L,I1)-(TCRT(L,I1)*0.1047195)**2
1   *BB3(1,L,I1)-BB2(1,L,I1)-TMUY(L,I1)*(I1-2)+TMUY(L,I1)*0.20
DO 34 JK=1,NNNCT(I1)
TA1(1,L,I1)=TA1(1,L,I1)-TTCM(L,JK,I1)*TA2(1,JK,I1)
AA1(1,L,I1)=AA1(1,L,I1)+TKMX(L,JK,I1)*AA3(1,JK,I1)
BB1(1,L,I1)=BB1(1,L,I1)+TKMX(L,JK,I1)*BB3(1,JK,I1)
34 CONTINUE

C * * * * * * * * * * * * * * * * * * * * * *
C ----- *      CALCULATE ROTOR'S GEAR FORCE      *
C * * * * * * * * * * * * * * * * * * * * * *
DO 38 K=1,NSTA
IF (K.EQ.I1) GO TO 38
IF ((I1.GT.1).AND.(K.GT.1))      GO TO 38
AB=0.0
BC=0.0
CD=0.0
DE=0.0
EF=0.0
FG=0.0
VE1=0.0
VE2=0.0
FO(I1,K)=0.0
DO 36 I=1,NNNCT(K)
AB=AB+TA3(1,I,K)*FFV(I,JST(K),K)
BC=BC+TA3(1,I,I1)*FFV(I,JST(I1),I1)
CD=CD+AA3(1,I,K)*TDDPC(I,JST(K),K)
DE=DE+AA3(1,I,I1)*TDDPC(I,JST(I1),I1)
EF=EF+BB3(1,I,K)*TDDPC(I,JST(K),K)
FG=FG+BB3(1,I,I1)*TDDPC(I,JST(I1),I1)
VE1= BB2(1,I,I1)*TDDPC(I,JST(I1),I1)+VE1
VE2= BB2(1,I,K)*TDDPC(I,JST(K),K)+VE2
36 CONTINUE

A=-ABS(RCC(K)*AB+RCC(I1)*BC)
IF(((CD-DE)*SIN(ALPH(I1,K))).GT.0.0) THEN
C=0.0
ELSE
C=(CD-DE)*SIN(ALPH(I1,K))
ENDIF
IF(((EF-FG)*COS(ALPH(I1,K))).GT.0.0) THEN
E=0.0
ELSE
E=(EF-FG)*COS(ALPH(I1,K))
ENDIF

```

```

RUA=(VE2-VE1)/700.

ABCD1=TKB(I1,K)*(A+C+E)*1.50
RUAN=TKB(I1,K)*RUA*0.05
ABCD2=ABCD1*TDDPC(L,JST(I1),I1)
ABCD3=ABCD1*FFV(L,JST(I1),I1)
C ABC=ABC+ABCD2*SIN(ALPH(I1,K))+RUAN
ABC=ABC+RUAN
BCA=BCA+ABCD2*COS(ALPH(I1,K))
CAB=CAB+ABCD3*RCC(I1)
FO(I1,K)=FO(I1,K)+ABCD1
38 CONTINUE
AA1(1,L,I1)=AA1(1,L,I1)+0.2*ABC
BB1(1,L,I1)=BB1(1,L,I1)+(I1-1)*0.05*BCA+0.04*BCA
TA1(1,L,I1)=TA1(1,L,I1)+CAB

C * * * * * * * * * * * * * * *
C ----- * OUTPUT THE ROTOR'S ORBIT *
C * * * * * * * * * * * * * * *
IF(I1.EQ.1) RANG1=BC
IF(I1.EQ.2) RANG2=BC
IF(I1.EQ.3) RANG3=BC
IF(I1.EQ.1) XR1=DE
IF(I1.EQ.2) XR2=DE
IF(I1.EQ.3) XR3=DE
IF(I1.EQ.1) YR1=FG
IF(I1.EQ.2) YR2=FG
IF(I1.EQ.3) YR3=FG
30 CONTINUE
RETURN
END

```

```

SUBROUTINE TINTG (NNCT,DELTAT)
C ****
C * THIS SUBROUTINE INTEGRATES THE MODAL ACCELERATION INTO VELOCITY *
C * AND DISPLACEMENT BY MODIFIED EULER METHOD *
C ****
IMPLICIT REAL(A-H,O-Z)
COMMON /BLK2/ ISKIP,NSTEP,NCYCLE,NITP,NINT,NPLOT,NORBIT,NTIME,NPE
1ED,NINC,NOPT,NT
COMMON /BLK20/ A1(2,10),A2(2,10),A3(2,10),B1(2,10),B2(2,10),B3(2,1
10)

DO 10 I=1,NNCT
A2(2,I)=A2(1,I)+DELTAT*A1(1,I)
B2(2,I)=B2(1,I)+DELTAT*B1(1,I)
A3(2,I)=A3(1,I)+DELTAT*0.50*(A2(1,I)+A2(2,I))
10 B3(2,I)=B3(1,I)+DELTAT*0.50*(B2(1,I)+B2(2,I))
DO 20 I=1,NNCT
A1(1,I)=A1(2,I)
A2(1,I)=A2(2,I)
A3(1,I)=A3(2,I)
B1(1,I)=B1(2,I)
B2(1,I)=B2(2,I)
20 B3(1,I)=B3(2,I)
RETURN
END

```

```

SUBROUTINE TBETA (NNCT, DELTAT, NSTA, TIME)
C **** THIS SUBROUTINE INTEGRATES THE MODAL ACCELERATIONS INTO MODAL *
C * VELOCITY AND DISPLACEMENT BY NEWMARK BETA METHOD *
C ****
      IMPLICIT REAL(A-H,O-Z)
      DIMENSION STORE(21,40)
      COMMON /ADD1/ TKXX(10,5),TKXY(10,5),TKXA(10,5),TKXB(10,5),TKXZ(10
1 ,5),TCXX(10,5),TCXY(10,5),TCXA(10,5),TCXB(10,5),TCXZ(10,5)
      COMMON /ADD2/ TKYX(10,5),TKYY(10,5),TKYA(10,5),TKYB(10,5),TKYZ(10
1 ,5),TCYX(10,5),TCYY(10,5),TCYA(10,5),TCYB(10,5),TCYZ(10,5)
      COMMON /ADD3/ TKAX(10,5),TKAY(10,5),TKAA(10,5),TKAB(10,5),TKAZ(10
1 ,5),TCAX(10,5),TCAY(10,5),TCAA(10,5),TCAB(10,5),TCAZ(10,5)
      COMMON /ADD4/ TKBX(10,5),TKBY(10,5),TKBA(10,5),TKBB(10,5),TKBZ(10
1 ,5),TCBX(10,5),TCBY(10,5),TCBA(10,5),TCBB(10,5),TCBZ(10,5)
      COMMON /ADD5/ TKZX(10,5),TKZY(10,5),TKZA(10,5),TKZB(10,5),TKZZ(10
1 ,5),TCZX(10,5),TCZY(10,5),TCZA(10,5),TCZB(10,5),TCZZ(10,5)
      COMMON /ADD6/ TOC(16),TOD(16),TOE(16)
      COMMON /BLK20/ A1(2,10),A2(2,10),A3(2,10),B1(2,10),B2(2,10),B3(2,1
10)
      COMMON /TMU1/ TMUX(10,5),TMUY(10,5),TEXTW(100,5),TDX(100,5)
      COMMON /TD1/ TDDXT(100,5),TDDNT(100,5),TRP(100,5)
      COMMON /TR1/ TRT(100,5),TEM6(100,5),TRO(100,5),TGGO(100,5)
      COMMON /MF1/ LTLFF(10,5),TSFX(10,5),TSFY(10,5),TMFX(10,5)
      COMMON /TU1/ LTLUF(10,5),TUX(10,5),TUY(10,5),TSUX(10,5),TSUY(10,5)
      COMMON /SEU1/ LTLNT(10,5),NTSRUB(5),NTSEU(5),NTFACT(5),ITND(5)
      COMMON /AAB1/ KTR(5),TABSO(5),AA1(2,10,5),AA2(2,10,5),AA3(2,10,5)
      COMMON /BBA1/ BB1(2,10,5),BB2(2,10,5),BB3(2,10,5),TA1(2,10,5)
      COMMON /TKB1/ TA2(2,10,5),TA3(2,10,5),TKB(5,5),ALPH(5,5),RCC(5)
      COMMON /TMB1/ TMBX(10,5),TMBY(10,5),TWMY(10,5),LTLBD(10,5)
      COMMON /TCM1/ TCMX(10,10,5),TCMY(10,10,5),TKMX(10,10,5)
      COMMON /TDO1/ TDOX(10,10,5),TDOY(10,10,5),TEOX(10,10,5)
      COMMON /TD/ TDDPC(10,100,5),TEMX(10,10,5),TEMY(10,10,5)
      COMMON /TW1/ TDMDY(10,10,5),TEEYTH(10,100,5),TW(100,5),TWMOD(50,5)
      COMMON /JS/ JST(5)
      COMMON /TOU/ TOUT(5),FORCEZ(5)
      COMMON /SPEED/ TSPEED(5)
      COMMON /LAS/ TTK(100,5),TMFY(10,5),TKMY(10,10,5),TEOY(10,10,5),
1 TDMX(10,10,5)
      COMMON /BOX01/ OMEGS(40),BX1(40,200,6),LBLBT(10,5),NMBB,NODEB
      COMMON /BLK58/ ZF(10,5),ZFV(10,100,5)
      COMMON /BOX02/OA1(2,40),OA2(2,40),OA3(2,40),OB1(2,40),
1 OB2(2,40),OB3(2,40),JNODE(20),FXFXM(40),FYFYM(20),FZFZM(20)
      COMMON /BOX04/OZ1(2,20),OZ2(2,20),OZ3(2,20),AZ1(2,10,5)
1 ,AZ2(2,10,5),AZ3(2,10,5),TBRFZ(10,5),TOA(16),TOB(16),TOZ(16)
      COMMON /BOX08/ NPT,NPTNO(16)
      DO 100 I1=1,NSTA

C      * * * * * * * * * * * * * * * *
C ----- *   STORE THE PREVIOUS RESULT *
C      * * * * * * * * * * * * * * * *
      DO 10 I=1,NNCT
      STORE(1,I)=AA1(1,I,I1)
      STORE(2,I)=BB1(1,I,I1)
      STORE(3,I)=AA2(1,I,I1)
      STORE(4,I)=BB2(1,I,I1)
      STORE(5,I)=AA3(1,I,I1)
      STORE(6,I)=BB3(1,I,I1)
      STORE(7,I)=TA1(1,I,I1)
      STORE(8,I)=TA2(1,I,I1)

```

```

      STORE(9,I)=TA3(1,I,I1)
      STORE(16,I)=AZ1(1,I,I1)
      STORE(17,I)=AZ2(1,I,I1)
10     STORE(18,I)=AZ3(1,I,I1)

C      * * * * * * * * * * * * * * * * * * * * * * * *
C ----- * INTEGRATE THE ACC. INTO VEL. & DISP.   *
C      * * * * * * * * * * * * * * * * * * * * * * * *
      DO 20 I=1,NNCT
      AA2(1,I,I1)=STORE(3,I)+DELTAT*STORE(1,I)
      BB2(1,I,I1)=STORE(4,I)+DELTAT*STORE(2,I)
      AA3(1,I,I1)=STORE(5,I)+.5*DELTAT*(STORE(3,I)+AA2(1,I,I1))
      BB3(1,I,I1)=STORE(6,I)+.5*DELTAT*(STORE(4,I)+BB2(1,I,I1))
      TA2(1,I,I1)=STORE(8,I)+DELTAT*STORE(7,I)
      TA3(1,I,I1)=STORE(9,I)+0.5*DELTAT*(STORE(8,I)+TA2(1,I,I1))
      AZ2(1,I,I1)=STORE(17,I)+DELTAT*STORE(16,I)
20     AZ3(1,I,I1)=STORE(18,I)+0.5*DELTAT*(STORE(17,I)+AZ2(1,I,I1))

C      * * * * * * * * * * * * * * * * * * * * * * * *
C ----- * SOLVE THE EQUATION WITH CURRENT MODAL VEL.& DISP.  *
C      * * * * * * * * * * * * * * * * * * * * * * * *
      CALL TACCEL (NSTA)
      DO 25 IJ=1,NNCT
      AZ1(1,IJ,I1)=TBRFZ(IJ,I1)-ZF(IJ,I1)**2*AZ3(1,IJ,I1)
      DO 725 JJI=1,NNCT
      AZ1(1,IJ,I1)=AZ1(1,IJ,I1)+TEOY(IJ,JJI,I1)*AZ3(1,JJI,I1)
725    CONTINUE
25     CONTINUE

C      * * * * * * * * * * * * * * * * * * * * * * * *
C ----- * INTEGRATE THE ACC. OF ROTOR WITH NEWMARK BETA METHOD  *
C      * * * * * * * * * * * * * * * * * * * * * * * *
      DO 30 I=1,NNCT
      AA2(1,I,I1)=STORE(3,I)+.5*DELTAT*(AA1(1,I,I1)+STORE(1,I))
      BB2(1,I,I1)=STORE(4,I)+.5*DELTAT*(BB1(1,I,I1)+STORE(2,I))
      AA3(1,I,I1)=STORE(5,I)+DELTAT*STORE(3,I)+(.5-BETA)*STORE(1,I)
      1      *DELTAT*DELTAT+BETA*DELTAT*DELTAT*AA1(1,I,I1)
      BB3(1,I,I1)=STORE(6,I)+DELTAT*STORE(4,I)+(.5-BETA)*STORE(2,I)
      1      *DELTAT*DELTAT+BETA*DELTAT*DELTAT*BB1(1,I,I1)
      TA2(1,I,I1)=STORE(8,I)+0.5*DELTAT*(TA1(1,I,I1)+STORE(7,I))
      TA3(1,I,I1)=STORE(9,I)+DELTAT*STORE(8,I)+(.5-BETA)*STORE(7,I)
      1      *DELTAT*DELTAT+BETA*DELTAT*DELTAT*TA1(1,I,I1)
      AZ2(1,I,I1)=STORE(17,I)+0.5*DELTAT*(AZ1(1,I,I1)+STORE(16,I))
      AZ3(1,I,I1)=STORE(18,I)+DELTAT*STORE(17,I)+(.5-BETA)*STORE(16,I)
      1      *DELTAT*DELTAT+BETA*DELTAT*DELTAT*AZ1(1,I,I1)
      AA3(2,I,I1)=AA3(1,I,I1)
      BB3(2,I,I1)=BP?(1,I,I1)
      TA3(2,I,I1)=TA3(1,I,I1)
30     AZ3(2,I,I1)=AZ3(1,I,I1)
100    CONTINUE

C      * * * * * * * * * * * * * * * * * * * * * * * *
C ----- * INTEGRATE THE ACC. OF BOX WITH NEWMARK BETA METHOD  *
C      * * * * * * * * * * * * * * * * * * * * * * * *
      DO 12 I =1,NMBB
      STORE(10,I)=OA1(1,I)
      STORE(12,I)=OA2(1,I)
      STORE(14,I)=OA3(1,I)
12     CONTINUE
      DO 14 I=1,NPT

```

```

TOA(I)=0.0
TOB(I)=0.0
14 TOZ(I)=0.0
DO 60 I=1,NMBB
OA2(1,I)=STORE(12,I)+DELTAT*STORE(10,I)
OA3(1,I)=STORE(14,I)+.5*DELTAT*(STORE(12,I)+OA2(1,I))

C      * * * * * * * * * * * * * * * *
C ----- *   SOLVE THE MODAL EQUATION OF BOX   *
C      * * * * * * * * * * * * * * * * * * * *
      IJ=I
OA1(1,IJ)=FXFXM(IJ)-OMEGS(IJ)*OA3(1,IJ)-OA2(1,IJ)
1           *OMEGS(IJ)**0.5*0.09401

OA2(1,I)=STORE(12,I)+.5*DELTAT*(OA1(1,I)+STORE(10,I))
OA3(1,I)=STORE(14,I)+DELTAT*STORE(12,I)+(.5-BETA)*STORE(10,I)
1           *DELTAT*DELTAT+BETA*DELTAT*DELTAT*OA1(1,I)
OA3(2,I)=OA3(1,I)
DO 60 J= 1,NPT
JJ= NPTNO(J)
TOA(J)=TOA(J)+OA1(1,I)*BX1(I,JJ,1)
TOB(J)=TOB(J)+OA1(1,I)*BX1(I,JJ,2)
60 TOZ(J)=TOZ(J)+OA1(1,I)*BX1(I,JJ,3)
RETURN
END

```

SUBROUTINE TINC

```

C ****
C * THIS SUBROUTINE TRANSFORMS THE ROTOR INITIAL CONDITIONS INTO *
C * MODAL INITIAL CONDITIONS OF VELOCITIES AND DISPLACEMENTS   *
C ****
      IMPLICIT REAL(A-H,O-Z)
      DIMENSION XTH(100), YTH(100), VXTH(100), VYTH(100)
      COMMON /BLK1/ N,NB,NNLIN,NMB,NF,NU,NS,NBOW,ISTAB,IMODE,ISKU,NNCT,N
1UFPT
      COMMON /BLK6/ BOW(100),PBOW(100),XIDC(100),YIDC(100),VXIDC(100),VY
1IDC(100),BXA(100),BYA(100)
      COMMON /BLK9/ DDPC(10,100),EYTH(10,100)
      COMMON /BLK15/ RP(100),RT(100)
      COMMON /BLK19/ DX(100)
      COMMON /BLK20/ A1(2,10),A2(2,10),A3(2,10),B1(2,10),B2(2,10),B3(2,1
10)
      COMMON /BLK22/ W(100)

      DO 10 I=1,100
      XIDC(I)=XIDC(I)/1000.
      YIDC(I)=YIDC(I)/1000.
      VXIDC(I)=VXIDC(I)/1000.
      VYIDC(I)=VYIDC(I)/1000.
10    TC=(XIDC(2)-XIDC(1))/DX(1)
      TD=(YIDC(2)-YIDC(1))/DX(1)
      TE=(VXIDC(2)-VXIDC(1))/DX(1)
      TF=(VYIDC(2)-VYIDC(1))/DX(1)
      XTH(1)=ATAN(TC)
      YTH(1)=ATAN(TD)
      VXTH(1)=ATAN(TE)
      VYTH(1)=ATAN(TF)
      TC=(XIDC(N)-XIDC(N-1))/DX(N-1)
      TD=(YIDC(N)-YIDC(N-1))/DX(N-1)

```

```

TE=(VXIDC(N)-VXIDC(N-1))/DX(N-1)
TF=(VYIDC(N)-VYIDC(N-1))/DX(N-1)
YTH(N)=ATAN(TD)
XTH(N)=ATAN(TC)
VXTH(N)=ATAN(TE)
VYTH(N)=ATAN(TF)
N1=N-1
DO 20 I=2,N1
TC=(XIDC(I+1)-XIDC(I-1))/(DX(I-1)+DX(I))
TD=(YIDC(I+1)-YIDC(I-1))/(DX(I-1)+DX(I))
TE=(VXIDC(I+1)-VXIDC(I-1))/(DX(I-1)+DX(I))
TF=(VYIDC(I+1)-VYIDC(I-1))/(DX(I-1)+DX(I))
XTH(I)=ATAN(TC)
YTH(I)=ATAN(TD)
VXTH(I)=ATAN(TE)
VYTH(I)=ATAN(TF)
20 CONTINUE
DO 30 I=1,NNCT
A3(1,I)=0.
B3(1,I)=0.
A2(1,I)=0.
B2(1,I)=0.
DO 30 J=1,N
A3(1,I)=A3(1,I)+(DDPC(I,J)*W(J)*XIDC(J)+EEYTH(I,J)*RT(J)*XTH(J))/3
186.4
B3(1,I)=B3(1,I)+(DDPC(I,J)*W(J)*YIDC(J)+EEYTH(I,J)*RT(J)*YTH(J))/3
186.4
A2(1,I)=A2(1,I)+(DDPC(I,J)*W(J)*VXIDC(J)+EEYTH(I,J)*RT(J)*VXTH(J))
1/386.4
30 B2(1,I)=B2(1,I)+(DDPC(I,J)*W(J)*VYIDC(J)+EEYTH(I,J)*RT(J)*VYTH(J))
1/386.4
RETURN
END

```

SUBROUTINE BNF

```

C ****
C * THIS SUBROUTINE CALCULATES THE NONLINEAR BEARING FORCES FOR EACH *
C * TIME STEP . THE BEARING USED ARE ASSUMED TO BE SHORT JOURNAL *
C * BEARING 180 DEG. CAVITATED FILM OR WITH 360. DEG FLUID FILM. *
C * THIS CAN ALSO BE USED TO APPROXIMATE STRAIGHT SEAL FORCES. *
C ****
IMPLICIT REAL(A-H,O-Z)
REAL LEN
REAL MFX,MFY
REAL KXX,KYY
COMMON /BLK1/ N,NB,NNLIN,NMB,NF,NU,NS,NBOW,ISTAB,IMODE,ISKU,NNCT,N
1UFPT
COMMON /BLK3/ CRT(10),LLBD(10),LLNB(5),LLNMB(9),LLSK(10),LLNT(10),
1LLUF(10),LLFF(10),LLUT(10),TCRT(10,5)
COMMON /BLK4/
1           SLNMB(9,4,4),CLNMB(9,4,4)
COMMON /BLK8/ MFX(10),MFY(10),MUX(10),MUY(10),MBX(10),MBY(10)
COMMON /BLK9/ DDPC(10,100),EEYTH(10,100)
COMMON /BLK16/ SPEED2,ANGSP,ANGACL,FSPEED
COMMON /BLK18/ AKK(10),TAKK(10,5)
COMMON /BLK20/ A1(2,10),A2(2,10),A3(2,10),B1(2,10),B2(2,10),B3(2,1
10)
COMMON /BLK35/ WMY(10),VIS(5),R(5),LEN(5),C(5),NLB(5)
COMMON /BLK60/ SFX(10),SFY(10)
COMMON /ADD1/ TKXX(10,5),TKXY(10,5),TKXA(10,5),TKXB(10,5),TKXZ(10

```

```

1      ,5),TCXX(10,5),TCXY(10,5),TCXA(10,5),TCXB(10,5),TCXZ(10,5)
1 COMMON /ADD2/ TKYX(10,5),TKYY(10,5),TKYA(10,5),TKYB(10,5),TKYZ(10
1      ,5),TCYX(10,5),TCYY(10,5),TCYA(10,5),TCYB(10,5),TCYZ(10,5)
1 COMMON /ADD3/ TKAX(10,5),TKAY(10,5),TKAA(10,5),TKAB(10,5),TKAZ(10
1      ,5),TCAX(10,5),TCAY(10,5),TCAA(10,5),TCAB(10,5),TCAZ(10,5)
1 COMMON /ADD4/ TKBX(10,5),TKBY(10,5),TKBA(10,5),TKBB(10,5),TKBZ(10
1      ,5),TCBX(10,5),TCBY(10,5),TCBA(10,5),TCBB(10,5),TCBZ(10,5)
1 COMMON /ADD5/ TKZX(10,5),TKZY(10,5),TKZA(10,5),TKZB(10,5),TKZZ(10
1      ,5),TCZX(10,5),TCZY(10,5),TCZA(10,5),TCZB(10,5),TCZZ(10,5)

DO 10 I=1,NNCT
MFX(I)=0.
MFY(I)=0.
DO 60 I=1,NNLIN
L=LLNB(I)
X=0.
Y=0.
VX=0.
VY=0.
DO 20 J=1,NNCT
X=X+A3(1,J)*DDPC(J,L)
Y=Y+B3(1,J)*DDPC(J,L)
VX=VX+A2(1,J)*DDPC(J,L)
VY=VY+B2(1,J)*DDPC(J,L)
20 CONTINUE
D=X*X+Y*Y
SD=0.
DEU=0.
SD=SQRT(D)
U=X*VX+Y*VY
DU=C(I)*SD*ANGSP
DEU=U/DU
EU=SD/C(I)
IF (EU.LT.1.0) GOTO 25
EU=0.99
25 CONTINUE
PHIDOT=(X*VY-Y*VX)/(ANGSP*D)
PI=3.14159
TEST=(1.-2.*PHIDOT)
SIGN=1.
SIGN1=1.
IF (TEST.LT.0.) SIGN=-1.
IF (DEU.LT.0.) SIGN1=-1.
CS=EU*ABS(TEST)/SQRT(EU*EU*TEST**2+4.*DEU*DEU)
AS=SQRT((1.+EU)/(1.-EU))
IF (ABS(CS).LT.0.0001) GO TO 30
U=SQRT((1.-CS)/(1.+CS))
GO TO 40
30 U=1.
40 CONTINUE
TI1=SIGN*4.*EU*CS**3/((1.-EU*EU*CS*CS)**2)
C1=(1.-EU*EU)
C2=(3.-5.*AS*AS)
C3=(5.-3.*AS*AS)
TA=ATAN(U*(AS*AS-1.)/(AS*(1.+U*U)))
C4=(1.+2.*EU*EU)
CON=PI*C4/(C1**2.5)
CON2=(C2*U*U+C3*AS*AS)/(U*U+AS*AS)**2+(C2+C3*AS*AS*U*U)/(1.+AS*AS*
1U*U)**2
TI2=CON+SIGN1*(2.*C4*TA/(C1**2.5)-U*CON2/(C1**2))

```

```

CON=2./C1**1.5
TI3=CON*(PI/2.+SIGN1*(TA-AS*U*(U*U-AS*AS)/(U*U+AS*AS)**2-AS*U*(1.-
1AS*AS*U*U)/(1.+AS*AS*U*U)**2))
SOM=VIS(I)*ANGSP*2.*R(I)*LEN(I)**3/(8.*C(I)*C(I))
F1=SOM*(EU*TEST*TI1+2.*DEU*TI2)
F2=SOM*(EU*TEST*TI3+2.*DEU*TI1)
FX=-(F1*X+F2*Y)/SD
FY=(F2*X-F1*Y)/SD
ID=NLB(I)
SFX(I)=FX
SFY(I)=FY
FX=FX+TKXX(ID,1)*X+AKK(ID)*X
FY=FY+TKYY(ID,1)*Y+AKK(ID)*Y
DO 50 K=1,NNCT
50 MFX(K)=MFX(K)+FX*DDPC(K,L)
MFY(K)=MFY(K)+FY*DDPC(K,L)
60 CONTINUE
RETURN
END

```

```

SUBROUTINE TOR(N,NM,NE,NTYPE)
*****  

C * THIS PROGRAM FOR CALCULATE Z-DIRECTION EIGEN PROBLEM *
C *****  

DIMENSION FFR(10),FV(100,10),TV(100,10),AT(5,5),WF(100,100)
COMMON /ADD1/ TKXX(10,5),TKXY(10,5),TKXA(10,5),TKXB(10,5),TKXZ(10
1 ,5),TCXX(10,5),TCXY(10,5),TCXA(10,5),TCXB(10,5),TCXZ(10,5)
COMMON /ADD2/ TKYX(10,5),TKYY(10,5),TKYA(10,5),TKYB(10,5),TKYZ(10
1 ,5),TCYX(10,5),TCYY(10,5),TCYA(10,5),TCYB(10,5),TCYZ(10,5)
COMMON /ADD3/ TKAX(10,5),TKAY(10,5),TKAA(10,5),TKAB(10,5),TKAZ(10
1 ,5),TCAX(10,5),TCAY(10,5),TCAA(10,5),TCAB(10,5),TCAZ(10,5)
COMMON /ADD4/ TKBX(10,5),TKBY(10,5),TKBA(10,5),TKBB(10,5),TKBZ(10
1 ,5),TCBX(10,5),TCBY(10,5),TCBA(10,5),TCBB(10,5),TCBZ(10,5)
COMMON /ADD5/ TKZX(10,5),TKZY(10,5),TKZA(10,5),TKZB(10,5),TKZZ(10
1 ,5),TCZX(10,5),TCZY(10,5),TCZA(10,5),TCZB(10,5),TCZZ(10,5)
COMMON /BLK51/ GJ(100),WJ(100)
COMMON /BLK52/ EXTW(100),DX(100),DDXT(100),DDINT(100),RO(100),GGO
1 (100)
COMMON /BLK54/ FR(10,5),FFV(10,100,5)
COMMON /BLK58/ ZF(10,5),ZFV(10,100,5)
COMMON /BLK56/ SP1,SP2,SP3
COMMON /BLK59/ TK(100),EEO(100)

PI=3.1415926
IF (NTYPE.EQ.1) THEN
DO 10 I=1,N
GGO(I)=GGO(I)*10000000.0
GJ(I)=32.0*DX(I)/(PI*GGO(I)*(DDXT(I)**4-DDINT(I)**4))
WJ(I)=PI*RO(I)*DX(I)*(DDXT(I)**4-DDINT(I)**4)/ 32.0/386.4
* +EXTW(I)/386.4
10 CONTINUE
ELSE
DO 40 I=1,N
TK(I)=0.0
EEO(I)=EEO(I)*1000000.0
GJ(I)= 4.0*DX(I)/(PI*EEO(I)*(DDXT(I)**2-DDINT(I)**2))
WJ(I)=PI*RO(I)*DX(I)*(DDXT(I)**2-DDINT(I)**2)/ 4.0/386.4
* +EXTW(I)/386.4
40 CONTINUE
ENDIF

```

```

MCY=0
ST=20.0
AO1=0.0
200 AO1=AO1+ST
AO2=AO1+ST
CALL CR(N,AO1,B1)
CALL CR(N,AO2,B2)
IF((B1*B2).LE.0.0) GOTO 30
GO TO 200
30 MCY=MCY+1
IF(MCY.GT.NM) GOTO 60
A1=AO1
A2=AO2
100 IF(ABS(A1-A2).LT.0.1) GOTO 50
AA1=A1+0.618*(A2-A1)
CALL CR(N,AA1,BB)
IF ((B1*BB).LE.0.0) THEN
A2=AA1
B2=BB
ELSE
A1=AA1
B1=BB
ENDIF
GOTO 100
50 FR(MCY,NE)=0.5*(A1+A2)
IF (NTYPE.GT.1) ZF(MCY,NE)=FR(MCY,NE)
FFR(MCY)=FR(MCY,NE)/2.0/PI
GOTO 200
60 CONTINUE
N1=N+1
DO 110 MM=1,NM
FV(1,MM)=1.0
TV(1,MM)=-WJ(1)*FR(MM,NE)**2
DO 110 JJ=2,N
TV(JJ,MM)=TV(JJ-1,MM)*(1.0+(TK(JJ)-WJ(JJ)*FR(MM,NE)**2)*GJ(JJ))
* +FV(JJ-1,MM)*(TK(JJ)-WJ(JJ)*FR(MM,NE)**2)
FV(JJ,MM)=TV(JJ-1,MM)*GJ(JJ) +FV(JJ-1,MM)
110 CONTINUE
DO 80 I=1,NM
CO=0.0
DO 70 J=1,N
CO=CO+FV(J,I)**2*WJ(J)
DO 80 K=1,N
FFV(I,K,NE)=FV(K,I)/SQRT(CO)
IF (NTYPE.NE.1) ZFV(I,K,NE)=FFV(I,K,NE)
80 CONTINUE
DO 23 I=1,N
DO 23 J=1,NM
23 WF(I,J)=WJ(I)*FFV(J,I,NE)
DO 27 I=1,NM
DO 27 J=1,NM
AT(I,J)=0.0
DO 27 K=1,N
27 AT(I,J)=AT(I,J)+WF(K,J)*FFV(I,K,NE)
WRITE(6,1105) ((AT(I,J),J=1,NM),I=1,NM)
1105 FORMAT (3(/2X,3F16.8))
IF (NTYPE.EQ.1) THEN
WRITE(6,1101) NE
DO 150 I=1,NM
WRITE(6,1102) I, FR(I,NE) , FFR(I)

```

```

      WRITE(6,1103)
      DO 150 J=1,N
150  WRITE(6,1104) J, FV(J,I), FFV(I,J,NE) , TV(J,I)
      ELSE
      WRITE(6,2101) NE
      DO 250 I=1,NM
      WRITE(6,2102) I, ZF(I,NE)
      WRITE(6,2103)
      DO 250 J=1,N
250  WRITE(6,1104) J, FV(J,I), ZFV(I,J,NE) , TV(J,I)
      ENDIF
1109 FORMAT (2X,I5,2F13.5)
2109 FORMAT (2X,I5,F13.5,2E15.8)
1101 FORMAT('**** TORSION FREQUENCY AND ORTHONOMAL MODE **** NE=',I2)
1102 FORMAT(3X,'I=',I3,30X,'FREQUENCY=',2F10.3)
1103 FORMAT(2X,' J=',14X,'FV(J,I)=',12X,'FFV(J,I)',8X,'TV=')
1104 FORMAT(2X,I3,8X,G14.6,8X,F12.6,6X,G12.5)
2101 FORMAT('** Z-DIRECTION FREQUENCY AND ORTHONOMAL MODE ** NE=',I2)
2102 FORMAT(3X,'I=',I3,30X,'FREQUENCY=',F10.3)
2103 FORMAT(2X,' J=',14X,'ZV(J,I)=',12X,'ZFV(J,I)',8X,'FZ=')
666 RETURN
END

      SUBROUTINE CR(N,OM,A)
C ****
C * THIS IS TO SET BOUNDARY CONDITIONS FOR MATRIX TRANSFORM METHOD *
C ****
      IMPLICIT REAL(A-H,O-Z)
      DIMENSION D(2,2),B(2,2),C(2,2)
      COMMON /BLK51/ GJ(100),WJ(100)
      COMMON /BLK59/ TK(100),E(100)
      C(2,2)=1.0
      B(1,1)=1.0
      B(1,2)=0.0
      B(2,1)=0.0
      B(2,2)=1.0
      DO 20 I=1,N
      C(1,1)=1.0+(TK(I)-WJ(I)*OM**2)*GJ(I)
      C(1,2)=TK(I)-WJ(I)*OM**2
      C(2,1)=1.0*GJ(I)
      D(1,1)=C(1,1)*B(1,1)+C(1,2)*B(2,1)
      D(1,2)=C(1,1)*B(1,2)+C(1,2)*B(2,2)
      D(2,1)=C(2,1)*B(1,1)+C(2,2)*B(2,1)
      D(2,2)=C(2,1)*B(1,2)+C(2,2)*B(2,2)
      B(1,1)=D(1,1)
      B(1,2)=D(1,2)
      B(2,1)=D(2,1)
      B(2,2)=D(2,2)
20    CONTINUE
      IK=2
C FREE-----FIXED
      IF(IK.EQ.1) A=B(2,2)
C FREE-----FREE
      IF(IK.EQ.2) A=B(1,2)
C FIXED-----FIXED
      IF(IK.EQ.3) A=B(2,1)
C FIXED-----FREE
      IF(IK.EQ.4) A=B(1,1)
      RETURN
END

```

```

SUBROUTINE STIFF(KI,NP,XG,XMAX,X1,YK)
C ****
C * THIS SUBROUTINE CALCULATES GEAR STIFFNESS *
C ****
      IMPLICIT REAL(A-H,O-Z)
      COMMON /K123/ X(4,100),Y(4,100)
      3 IF(X1.LT.360.0) GO TO 5
      X1=X1-360.0
      GO TO 3
      5 IF(X1.GE.0.0) GO TO 10
      X1=X1+360.0
      GO TO 5
     10 IF(X1.LE.XMAX) GO TO 20
      X1=X1-XG
      GO TO 10
     20 YK=0.0
      IF(X1.LT.X(KI,1)) GO TO 80
      IF(X1.GT.X(KI,NP)) GO TO 90
      DO 50 I=2,NP
      IF((X1.GE.X(KI,(I-1))).AND.(X1.LT.X(KI,I))) THEN
      YK=((Y(KI,I)-Y(KI,(I-1)))/(X(KI,I)-X(KI,(I-1))))*(X1-X(KI,(I-1)))
      * +Y(KI,(I-1))
      GO TO 60
      ELSE
      CONTINUE
      ENDIF
     50 CONTINUE
     80 YK=Y(KI,1)
      GO TO 60
     90 YK=Y(KI,NP)
     60 CONTINUE
      RETURN
      END

```

APPENDIX D
(SAMPLE DATA INPUT FILE)

GEARBOX VIBRATION TRANSIENT ANALYSIS WITH
 TWO BALL BEARINGS PER ROTORS
 THE MODAL SHAPES ARE CALCULATED FROM NASTRAN

2 1 1

2

0. 0. 0.

12 12

0.0 0.52

3.66 0.0

4.0 4.0

688.5 688.5

217.5 -217.5

25 14.40 23.04 0.0

0.0 938000.

0.960 1138000.

1.920 1338000.

2.880 1538000.

3.840 1538000.

4.800 1538000.

5.760 1338000.

6.720 1138000.

7.680 938000.

8.640 738000.

9.600 598000.

10.56 368000.

11.52 138000.

12.48 368000.

13.440 598000.

14.400 738000.

15.360 938000.

16.320 1118000.

17.280 1338000.

18.240 1538000.

19.200 1538000.

20.160 1538000.

21.120 1330000.

22.080 1138000.

23.040 938000.

1 1

12 12

0.0 0.0

0.0 600. 60.

3

24	2	0	0	0	1	0	0	1	0	1	0	0
0	375	5	40	1	0	1	1	0	1	0	1	1
2	23											

197340.	28.804	-911.3	-34.78	1484.7	8.	0.	0.	0.	0.	0.	0.
---------	--------	--------	--------	--------	----	----	----	----	----	----	----

28.804	78.030	1.7886	0.	171.53	0.	32.	0.	0.	0.	0.
--------	--------	--------	----	--------	----	-----	----	----	----	----

-911.3	1.7886	363370.	33.039	52388.	0.	0.	8.	0.	0.
--------	--------	---------	--------	--------	----	----	----	----	----

-34.78	0.	33.039	48.133	48.032	0.	0.	0.	32.	0.
--------	----	--------	--------	--------	----	----	----	-----	----

1484.7	171.53	52388.	48.032	335220.	0.	0.	0.	0.	16.
--------	--------	--------	--------	---------	----	----	----	----	-----

197340.	28.804	-911.3	-34.78	1484.7	8	0.	0.	0.	0.
---------	--------	--------	--------	--------	---	----	----	----	----

28.804	78.030	1.7886	0.	171.53	0.	32.	0.	0.
--------	--------	--------	----	--------	----	-----	----	----

-911.3	1.7886	363370.	33.039	52388.	0.	0.	8.	0.
--------	--------	---------	--------	--------	----	----	----	----

-34.78	0.	33.039	48.133	48.032	0.	0.	0.	32.
--------	----	--------	--------	--------	----	----	----	-----

1484.7	171.53	52388.	48.032	335220.	0.	0.	0.	0.
--------	--------	--------	--------	---------	----	----	----	----

0	30.	3000.	3000.	0.	.167				
---	-----	-------	-------	----	------	--	--	--	--

0.	0.05	1.2	0.	0.	0.	30.	0.28	1.2	0.0
----	------	-----	----	----	----	-----	------	-----	-----

0.	0.43	1.2	0.	0.	0.	30.	0.28	1.2	0.0
----	------	-----	----	----	----	-----	------	-----	-----

0.	0.43	1.2	0.	0.	0.	30.	0.28	1.2	0.0
----	------	-----	----	----	----	-----	------	-----	-----

0.	0.43	1.2	0.	0.	0.	30.	0.28	1.2	0.0
0.	0.13	1.2	0.	0.	0.	30.	0.28	1.2	0.0
0.	0.43	1.2	0.	0.	0.	30.	0.28	1.2	0.0
0.	0.43	1.2	0.	0.	0.	30.	0.28	1.2	0.0
0.	0.43	1.2	0.	0.	0.	30.	0.28	1.2	0.0
0.	0.43	1.2	0.	0.	0.	30.	0.28	1.2	0.0
0.	0.43	1.2	0.	0.	0.	30.	0.28	1.2	0.0
0.	0.43	1.2	0.	0.	0.	30.	0.28	1.2	0.0
0.	0.43	1.2	0.	0.	0.	30.	0.28	1.2	0.0
0.	0.43	1.2	0.	0.	0.	30.	0.28	1.2	0.0
5.	0.62	1.2	0.	0.	0.	30.	0.28	1.2	0.0
0.	0.53	1.2	0.	0.	0.	30.	0.28	1.2	0.0
0.	0.43	1.2	0.	0.	0.	30.	0.28	1.2	0.0
0.	0.43	1.2	0.	0.	0.	30.	0.28	1.2	0.0
0.	0.43	1.2	0.	0.	0.	30.	0.28	1.2	0.0
0.	0.43	1.2	0.	0.	0.	30.	0.28	1.2	0.0
0.	0.43	1.2	0.	0.	0.	30.	0.28	1.2	0.0
0.	0.43	1.2	0.	0.	0.	30.	0.28	1.2	0.0
0.	0.43	1.2	0.	0.	0.	30.	0.28	1.2	0.0
0.	0.43	1.2	0.	0.	0.	30.	0.28	1.2	0.0
0.	0.43	1.2	0.	0.	0.	30.	0.28	1.2	0.0
0.	0.43	1.2	0.	0.	0.	30.	0.28	1.2	0.0
0.	0.43	1.2	0.	0.	0.	30.	0.28	1.2	0.0
0.	0.43	1.2	0.	0.	0.	30.	0.28	1.2	0.0
0.	0.43	1.2	0.	0.	0.	30.	0.28	1.2	0.0
0.	0.43	1.2	0.	0.	0.	30.	0.28	1.2	0.0
0.	0.43	1.2	0.	0.	0.	30.	0.28	1.2	0.0
0.	0.43	1.2	0.	0.	0.	30.	0.28	1.2	0.0
0.	0.43	1.2	0.	0.	0.	30.	0.28	1.2	0.0
0.	0.43	1.2	0.	0.	0.	30.	0.28	1.2	0.0
0.	0.05	1.2	0.	0.	0.	30.	0.28	1.2	0.0
12		0.00093		0.00093		0.00093		0.00093	
12									
250.	266000.		150.						
0.0	50.		165000.						
0									
1	1								
30	2	10000.		.1					
12		.0001							

GEARBOX VIBRATION TRANSIENT ANALYSIS

TWO BALL BEARINGS PER ROTOR

THE MODAL SHAPES ARE CALCULATED FROM NASTRAN

24	2	0	0	0	1	0	0	1	0	1	1	0
0	375	5	40	1	0	1	1	0	1	0	1	1
2	23											
197340.	28.804	-911.3	-34.78	1484.7	8.	0.	0.	0.	0.	0.	0.	0.
28.804	78.030	1.7886	0.	171.53	0.	32.	0.	0.	0.	0.	0.	0.
-911.3	1.7886	363370.	33.039	52388.	0.	0.	8.	0.	0.	0.	0.	0.
-34.78	0.	33.039	48.133	48.032	0.	0.	0.	0.	32.	0.	0.	0.
1484.7	171.53	52388.	48.032	335220.	0.	0.	0.	0.	0.	0.	16.	0.
197340.	28.804	-911.3	-34.78	1484.7	8.	0.	0.	0.	0.	0.	0.	0.
28.804	78.030	1.7886	0.	171.53	0.	32.	0.	0.	0.	0.	0.	0.
-911.3	1.7886	363370.	33.039	52388.	0.	0.	8.	0.	0.	0.	0.	0.
-34.78	0.	33.039	48.133	48.032	0.	0.	0.	0.	32.	0.	0.	0.
1484.7	171.53	52388.	48.032	335220.	0.	0.	0.	0.	0.	0.	16.	0.
0	30.	3000.	3000.	0.	.167							
0.	0.05	1.2	0.	0.	0.	30.	0.28	1.2	0.0			
0.	0.43	1.2	0.	0.	0.	30.	0.28	1.2	0.0			
0.	0.43	1.2	0.	0.	0.	30.	0.28	1.2	0.0			
0.	0.43	1.2	0.	0.	0.	30.	0.28	1.2	0.0			
0.	0.43	1.2	0.	0.	0.	30.	0.28	1.2	0.0			
0.	0.43	1.2	0.	0.	0.	30.	0.28	1.2	0.0			
0.	0.43	1.2	0.	0.	0.	30.	0.28	1.2	0.0			
0.	0.43	1.2	0.	0.	0.	30.	0.28	1.2	0.0			
0.	0.43	1.2	0.	0.	0.	30.	0.28	1.2	0.0			
0.	0.43	1.2	0.	0.	0.	30.	0.28	1.2	0.0			
0.	0.43	1.2	0.	0.	0.	30.	0.28	1.2	0.0			
5.	0.62	1.2	0.	0.	0.	30.	0.28	1.2	0.0			
0.	0.53	1.2	0.	0.	0.	30.	0.28	1.2	0.0			

0.	0.43	1.2	0.	0.	0.	30.	0.28	1.2	0.0
0.	0.43	1.2	0.	0.	0.	30.	0.28	1.2	0.0
0.	0.43	1.2	0.	0.	0.	30.	0.28	1.2	0.0
0.	0.43	1.2	0.	0.	0.	30.	0.28	1.2	0.0
0.	0.43	1.2	0.	0.	0.	30.	0.28	1.2	0.0
0.	0.43	1.2	0.	0.	0.	30.	0.28	1.2	0.0
0.	0.43	1.2	0.	0.	0.	30.	0.28	1.2	0.0
0.	0.43	1.2	0.	0.	0.	30.	0.28	1.2	0.0
0.	0.43	1.2	0.	0.	0.	30.	0.28	1.2	0.0
0.	0.43	1.2	0.	0.	0.	30.	0.28	1.2	0.0
0.	0.43	1.2	0.	0.	0.	30.	0.28	1.2	0.0
0.	0.43	1.2	0.	0.	0.	30.	0.28	1.2	0.0
0.	0.05	1.2	0.	0.	0.	30.	0.28	1.2	0.0

12 0.00093 0.00093 0.00093 0.00093

12

250. 266000. 150.
0.0 50. 165000.

0

1

30 2 10000. .1

12 .0001

GEARBOX VIBRATION TRANSIENT ANALYSIS

TWO BALL BEARINGS PER ROTOR

THE MODAL SHAPES ARE CALCULATED FROM NASTRAN

5 132 6

115 21

77 19

10000. 10000.

10000. 10000.

1

22

EIGENVALUE = 2.534798E+08 (FREQ = 2.53391E+03 HZ)

1	0.000000e+00	0.000000e+00	0.000000e+00	0.000000e+00	0.000000e+00
2	3.448560E-02	8.036783E-01	-2.037600E-02	6.051830E-01	1.011504E-01
3	-9.057784E-02	1.313704E+00	-9.678650E-02	-2.226727E+00	2.114075E-01
4	8.591101E-03	-1.292542E+00	-5.963318E-02	-8.058454E-01	0.000000e+00
5	6.182482E-01	9.871943E-01	9.928733E-02	0.000000e+00	-1.354058E-02
6	8.015627E-02	7.883143E-01	5.760546E-02	3.560397E-02	-9.211429E-01
7	1.072060E-01	1.440649E+00	-2.722757E+00	9.987959E-01	-1.108560E+00
8	2.268902E-01	1.184208E+00	3.067899E-02	0.000000e+00	-1.718315E-01
9	2.268900E-01	1.184208E+00	-3.067893E-02	0.000000e+00	1.718317E-01
10	3.958876E-01	1.115078E+00	3.924147E-02	0.000000e+00	9.989733E-02
11	5.532086E-02	1.061603E+00	-9.897880E-03	7.403004E-02	-1.024205E-02
12	3.696863E-02	1.848590E+00	-3.545241E+00	1.757919E+00	-9.336358E-02
13	3.711739E-02	-1.924138E+00	-2.060046E-02	-1.086465E-01	0.000000e+00
14	-4.449886E-02	1.833056E+00	-1.566558E-01	-2.526589E+00	1.664701E-01
15	-3.394766E-04	8.591717E-02	-1.033443E-01	4.386343E-01	0.000000e+00
16	1.356463E-02	1.535020E+00	-3.529084E-02	7.012681E-01	0.000000e+00
17	-3.066793E-02	1.179114E+00	7.066858E-02	0.000000e+00	-1.112198E-01
18	5.649020E-02	1.218520E+00	5.441920E-02	3.714950E-01	4.565944E-01
19	8.215582E-02	1.615184E+00	1.918431E+00	1.545835E+00	1.075146E+00
20	3.431828E-02	1.916783E+00	3.703643E+00	1.700075E+00	5.140786E-01
21	-3.431851E-02	1.916783E+00	3.703643E+00	1.700074E+00	-5.140787E-01
22	3.958879E-01	1.115078E+00	-3.924141E-02	0.000000e+00	-9.989762E-02
23	-9.176900E-01	1.313436E+00	5.731493E-03	0.000000e+00	1.565854E-01
24	-3.869911E-01	1.242608E+00	6.925583E-03	0.000000e+00	-1.798946E-01
25	6.182488E-01	9.871943E-01	-9.928727E-02	0.000000e+00	1.354064E-02
26	-3.869914E-01	1.242608E+00	-6.925531E-03	0.000000e+00	1.798949E-01
27	-3.066824E-02	1.179114E+00	-7.066852E-02	0.000000e+00	1.112198E-01
28	-9.176906E-01	1.313436E+00	-5.731449E-03	0.000000e+00	-1.565856E-01
29	5.532086E-02	1.061603E+00	9.897918E-03	-7.402998E-02	1.024207E-02
30	-3.696881E-02	1.848590E+00	-3.545239E+00	1.757919E+00	9.336501E-02

31	3.711740E-02	-1.924138E+00	2.060049E-02	1.086464E-01	0.000000e+00
32	4.449878E-02	1.833056E+00	-1.566558E-01	-2.526589E+00	-1.664702E-01
33	1.356463E-02	1.535020E+00	3.529087E-02	-7.012681E-01	0.000000e+00
34	3.393567E-04	8.591628E-02	-1.033443E-01	4.386334E-01	0.000000e+00
35	-1.356476E-02	1.535018E+00	-3.529084E-02	7.012675E-01	0.000000e+00
36	-1.356477E-02	1.535018E+00	3.529086E-02	-7.012675E-01	0.000000e+00
37	4.079561E-02	1.433638E+00	-1.837622E-02	-8.193132E-01	4.576401E-01
38	5.849652E-02	1.776446E+00	9.177673E-02	-2.362490E+00	-3.333355E-01
39	2.569450E-02	2.044185E+00	-1.037416E+00	-3.966680E+00	-3.544267E-01
40	-1.072062E-01	1.440649E+00	-2.722754E+00	9.987965E-01	1.108560E+00
41	-2.569476E-02	2.044185E+00	-1.037417E+00	-3.966680E+00	3.544254E-01
42	-8.215606E-02	1.615184E+00	1.918431E+00	1.545834E+00	-1.075146E+00
43	-5.849678E-02	1.776445E+00	9.177393E-02	-2.362490E+00	3.333362E-01
44	1.841546E-01	1.508387E+00	-1.028981E-01	9.574949E-01	1.810223E-01
45	3.448561E-02	8.036783E-01	2.037602E-02	-6.051831E-01	-1.011504E-01
46	7.742947E-02	1.393884E+00	-7.515335E-02	4.529952E-02	-1.237930E-02
47	0.000000e+00	0.000000e+00	0.000000e+00	0.000000e+00	0.000000e+00
48	2.098801E-02	1.257155E+00	-2.725329E-02	-1.114506E+00	-1.718097E-01
49	8.015627E-02	7.883143E-01	-5.760538E-02	-3.560395E-02	9.211435E-01
50	2.098801E-02	1.257155E+00	2.725333E-02	1.114506E+00	1.718097E-01
51	5.649020E-02	1.218520E+00	-5.441912E-02	-3.714949E-01	-4.565944E-01
52	7.742947E-02	1.393884E+00	7.515341E-02	-4.529952E-02	1.237932E-02
53	4.079561E-02	1.433638E+00	1.837626E-02	8.193132E-01	-4.576405E-01
54	1.841546E-01	1.508387E+00	1.028982E-01	-9.574949E-01	-1.810223E-01
55	8.591112E-03	-1.292543E+00	5.963321E-02	8.058454E-01	0.000000e+00
56	9.057778E-02	1.313703E+00	-9.678644E-02	-2.226727E+00	-2.114072E-01
57	-3.394727E-04	8.591723E-02	1.033443E-01	-4.386343E-01	0.000000e+00
58	-8.591216E-03	-1.292542E+00	-5.963314E-02	-8.058460E-01	0.000000e+00
59	3.393563E-04	8.591628E-02	1.033443E-01	-4.386334E-01	0.000000e+00
60	-3.711753E-02	-1.924139E+00	-2.060045E-02	-1.086467E-01	0.000000e+00
61	-3.711753E-02	-1.924139E+00	2.060048E-02	1.086466E-01	0.000000e+00
62	-8.591224E-03	-1.292542E+00	5.963318E-02	8.058454E-01	0.000000e+00
63	1.567899E-01	1.891665E+00	-3.028729E-02	2.921868E+00	1.566738E-01
64	0.000000e+00	0.000000e+00	0.000000e+00	0.000000e+00	0.000000e+00
65	6.237902E-02	2.188473E+00	-2.298496E-02	5.778226E+00	8.495444E-02
66	-8.015639E-02	7.883143E-01	5.760550E-02	3.560406E-02	9.211422E-01
67	-6.237932E-02	2.188473E+00	-2.298500E-02	5.778226E+00	-8.495438E-02
68	-5.649043E-02	1.218521E+00	5.441916E-02	3.714946E-01	-4.565946E-01
69	-1.567902E-01	1.891665E+00	-3.028736E-02	2.921870E+00	-1.566737E-01
70	-4.079584E-02	1.433638E+00	-1.837627E-02	-8.193126E-01	-4.576393E-01
71	-1.841549E-01	1.508387E+00	-1.028981E-01	9.574943E-01	-1.810223E-01
72	6.272137E-02	5.116381E+00	-1.614437E-02	-2.255423E+00	0.000000e+00
73	-9.057784E-02	1.313704E+00	9.678656E-02	2.226727E+00	-2.114075E-01
74	1.826673E-02	-4.585258E+00	-4.996870E-03	-5.363324E+00	0.000000e+00
75	1.072060E-01	1.440649E+00	2.722758E+00	-9.987959E-01	1.108560E+00
76	1.826673E-02	-4.585258E+00	4.996918E-03	5.363322E+00	0.000000e+00
77	8.215582E-02	1.615184E+00	-1.918431E+00	-1.545836E+00	-1.075146E+00
78	6.272137E-02	5.116379E+00	1.614441E-02	2.255423E+00	0.000000e+00
79	5.849652E-02	1.776445E+00	-9.177732E-02	2.362490E+00	3.333356E-01
80	1.567899E-01	1.891665E+00	3.028733E-02	-2.921867E+00	-1.566738E-01
81	-4.449886E-02	1.833056E+00	1.566559E-01	2.526589E+00	-1.664701E-01
82	-3.448569E-02	8.036783E-01	-2.037600E-02	6.051829E-01	-1.011503E-01
83	4.449878E-02	1.833056E+00	1.566558E-01	2.526589E+00	1.664703E-01
84	-5.532101E-02	1.061603E+00	-9.897880E-03	7.402998E-02	1.024200E-02
85	9.057778E-02	1.313703E+00	9.678650E-02	2.226727E+00	2.114071E-01
86	-5.532101E-02	1.061603E+00	9.897910E-03	-7.402992E-02	-1.024202E-02
87	-3.448570E-02	8.036783E-01	2.037602E-02	-6.051829E-01	1.011503E-01
88	0.000000e+00	0.000000e+00	0.000000e+00	0.000000e+00	0.000000e+00
89	2.529481E-02	1.006064E+01	-6.337638E-04	-2.354571E+00	0.000000e+00
90	-6.182489E-01	9.871943E-01	9.928733E-02	0.000000e+00	1.354124E-02

91	-2.529510E-02	1.006064E+01	-6.337864E-04	-2.354572E+00	0.000000e+00
92	3.066812E-02	1.179114E+00	7.066858E-02	0.000000e+00	1.112196E-01
93	-6.272167E-02	5.116381E+00	-1.614442E-02	-2.25423E+00	0.000000e+00
94	9.176900E-01	1.313436E+00	5.731463E-03	0.000000e+00	-1.565861E-01
95	-7.742977E-02	1.393885E+00	-7.515341E-02	4.529933E-02	1.237920E-02
96	8.211669E-03	-4.628751E+00	1.786326E-03	-8.116509E+00	0.000000e+00
97	3.696863E-02	1.848590E+00	3.545241E+00	-1.757919E+00	9.336299E-02
98	8.211669E-03	-4.628751E+00	-1.786270E-03	8.116509E+00	0.000000e+00
99	3.431828E-02	1.916783E+00	-3.703643E+00	-1.700075E+00	-5.140788E-01
100	2.529481E-02	1.006064E+01	6.338200E-04	2.354571E+00	0.000000e+00
101	2.569450E-02	2.044184E+00	1.037416E+00	3.966680E+00	3.544270E-01
102	6.237902E-02	2.188473E+00	2.298502E-02	-5.778226E+00	-8.495444E-02
103	-3.696881E-02	1.848590E+00	3.545239E+00	-1.757919E+00	-9.336448E-02
104	-3.958892E-01	1.115078E+00	3.924147E-02	0.000000e+00	-9.989703E-02
105	-1.072062E-01	1.440649E+00	2.722754E+00	-9.987959E-01	-1.108560E+00
106	-3.958895E-01	1.115078E+00	-3.924143E-02	0.000000e+00	9.989735E-01
107	-8.015639E-02	7.883143E-01	-5.760542E-02	-3.560405E-02	-9.211429E-01
108	-6.182494E-01	9.871943E-01	-9.928733E-02	0.000000e+00	-1.354130E-01
109	-8.211952E-03	-4.628753E+00	1.786317E-03	-8.116509E+00	0.000000e+00
110	-2.268897E-01	1.184208E+00	3.067898E-02	0.000000e+00	1.718314E-01
111	-1.826702E-02	-4.585258E+00	-4.996892E-03	-5.363324E+00	0.000000e+00
112	3.869923E-01	1.242608E+00	6.925564E-03	0.000000e+00	1.798941E-01
113	-2.098829E-02	1.257155E+00	-2.725331E-02	-1.114506E+00	1.718097E-01
114	-8.211944E-03	-4.628753E+00	-1.786266E-03	8.116509E+00	0.000000e+00
115	-3.431850E-02	1.916783E+00	-3.703643E+00	-1.700073E+00	5.140789E-01
116	-2.529509E-02	1.006064E+01	6.338370E-04	2.354572E+00	0.000000e+00
117	-2.569475E-02	2.044184E+00	1.037417E+00	3.966680E+00	-3.544257E-01
118	-6.237932E-02	2.188473E+00	2.298505E-02	-5.778226E+00	8.495438E-02
119	-8.215606E-02	1.615184E+00	-1.918431E+00	-1.545834E+00	1.075146E+00
120	-2.268895E-01	1.184208E+00	-3.067894E-02	0.000000e+00	-1.718316E-01
121	-5.649043E-02	1.218520E+00	-5.441912E-02	-3.714946E-01	4.565946E-01
122	3.066837E-02	1.179114E+00	-7.066852E-02	0.000000e+00	-1.112195E-01
123	-1.826701E-02	-4.585258E+00	4.996918E-03	5.363323E+00	0.000000e+00
124	3.869926E-01	1.242608E+00	-6.925538E-03	0.000000e+00	-1.798944E-01
125	-2.098828E-02	1.257155E+00	2.725332E-02	1.114506E+00	-1.718097E-01
126	-6.272161E-02	5.116379E+00	1.614444E-02	2.255423E+00	0.000000e+00
127	-5.849674E-02	1.776445E+00	-9.177446E-02	2.362490E+00	-3.333364E-01
128	-1.567902E-01	1.891665E+00	3.028738E-02	-2.921869E+00	1.566737E-01
129	-4.079584E-02	1.433638E+00	1.837628E-02	8.193126E-01	4.576397E-01
130	9.176906E-01	1.313436E+00	-5.731445E-03	0.000000e+00	1.565862E-01
131	-7.742971E-02	1.393884E+00	7.515341E-02	-4.529933E-02	-1.237923E-02
132	-1.841549E-01	1.508387E+00	1.028982E-01	-9.574943E-01	1.810223E-01
EIGENVALUE = 5.525934E+08 (FREQ = 3.74130E+03 HZ)					
1	0.000000e+00	0.000000e+00	0.000000e+00	0.000000e+00	0.000000e+00
2	-9.017432E-02	3.794850E-01	-1.710561E-02	-3.720020E-01	9.568367E-03
3	2.273129E-02	-3.766249E-02	2.583054E-01	-9.495828E-01	-2.748883E-01
4	-8.189893E-02	-5.354028E+00	1.579300E-01	-6.754655E-01	0.000000e+00
5	3.970646E-01	4.675810E-01	4.292021E-02	0.000000e+00	-6.974553E-01
6	-7.410407E-02	2.617511E-01	3.004587E-02	1.085124E-01	4.095011E-01
7	-4.307524E-02	1.643141E-01	3.107096E+00	-4.490227E-01	3.093104E+00
8	-2.202222E+00	6.436667E-01	1.703527E-02	0.000000e+00	1.850501E+00
9	-2.202222E+00	6.436667E-01	-1.703527E-02	0.000000e+00	-1.850501E+00
10	1.291305E+00	6.182576E-01	1.876486E-02	0.000000e+00	-8.219761E-02
11	-1.110045E-01	6.251503E-01	-8.757446E-03	1.796952E+00	5.086491E-02
12	-1.736602E-02	6.514788E-02	6.862464E+00	-2.427180E+00	1.173689E+00
13	-1.162736E-01	1.550402E+00	5.254602E-02	5.102044E+00	0.000000e+00
14	1.368123E-02	-2.015609E-01	4.928859E-01	-4.920493E-01	-4.003682E-01
15	-3.399730E-02	-8.324932E+00	2.989873E-01	-4.018692E-01	0.000000e+00
16	-4.934616E-02	3.889892E+00	9.955978E-02	8.324385E+00	0.000000e+00
17	1.343695E+00	5.557591E-01	3.739925E-02	0.000000e+00	7.925306E-01

18	-5.877895E-02	4.296376E-01	2.713646E-02	-7.082572E-01	-1.345645E+00
19	-5.334870E-02	3.586955E-01	-2.247919E+00	-1.071558E+00	-1.966455E+00
20	-2.219216E-02	3.074746E-01	-6.960867E+00	-1.900096E+00	-2.339858E+00
21	2.219188E-02	3.074747E-01	-6.960866E+00	-1.900097E+00	2.339859E+00
22	1.291305E+00	6.182576E-01	-1.876486E-02	0.000000e+00	8.219761E-02
23	1.319715E+00	6.236915E-01	4.671562E-02	0.000000e+00	-4.325923E-01
24	5.902687E-01	6.760237E-01	1.957937E-02	0.000000e+00	6.985579E-01
25	3.970646E-01	4.675810E-01	-4.292021E-02	0.000000e+00	6.974553E-01
26	5.902687E-01	6.760237E-01	-1.957937E-02	0.000000e+00	-6.985579E-01
27	1.343695E+00	5.557591E-01	-3.739925E-02	0.000000e+00	-7.925306E-01
28	1.319715E+00	6.236915E-01	-4.671562E-02	0.000000e+00	4.325923E-01
29	-1.110045E-01	6.251503E-01	8.757442E-03	-1.796952E+00	-5.086491E-02
30	1.736566E-02	6.514800E-02	6.862463E+00	-2.427179E+00	-1.173690E+00
31	-1.162736E-01	1.550402E+00	-5.254602E-02	-5.102044E+00	0.000000e+00
32	-1.368161E-02	-2.015607E-01	4.928859E-01	-4.920493E-01	4.003685E-01
33	-4.934616E-02	3.889892E+00	-9.955978E-02	-8.324385E+00	0.000000e+00
34	3.399693E-02	-8.324931E+00	2.989873E-01	-4.018692E-01	0.000000e+00
35	4.934578E-02	3.889892E+00	9.955978E-02	8.324385E+00	0.000000e+00
36	4.934578E-02	3.889892E+00	-9.955978E-02	-8.324385E+00	0.000000e+00
37	-5.116955E-02	5.296052E-01	4.988674E-02	1.224763E+00	-1.500325E-01
38	-4.840098E-02	5.159767E-01	2.774833E+00	2.603818E+00	2.753377E+00
39	-1.936520E-02	5.096145E-01	5.606589E+00	5.781806E+00	6.248997E-01
40	4.307487E-02	1.643143E-01	3.107094E+00	-4.490215E-01	-3.093104E+00
41	1.936511E-02	5.096146E-01	5.606586E+00	5.781805E+00	-6.249012E-01
42	5.334839E-02	3.586957E-01	-2.247916E+00	-1.071558E+00	1.966455E+00
43	4.840085E-02	5.159769E-01	2.774833E+00	2.603817E+00	-2.753375E+00
44	-2.344701E-02	5.683835E-01	1.286226E-01	-1.065287E+00	-1.535243E-01
45	-9.017432E-02	3.794850E-01	1.710561E-02	3.720020E-01	-9.568367E-03
46	-9.843963E-02	6.558044E-01	9.562874E-02	1.053868E+00	-5.399741E-03
47	0.000000e+00	0.000000e+00	0.000000e+00	0.000000e+00	0.000000e+00
48	-1.333230E-01	6.766802E-01	3.525435E-02	-1.501417E+00	2.900030E-01
49	-7.410407E-02	2.617511E-01	-3.004587E-02	-1.085124E-01	-4.095011E-01
50	-1.333230E-01	6.766802E-01	-3.525435E-02	1.501417E+00	-2.900030E-01
51	-5.877895E-02	4.296376E-01	-2.713646E-02	7.082572E-01	1.345645E+00
52	-9.843963E-02	6.558044E-01	-9.562874E-02	-1.053868E+00	5.399741E-03
53	-5.116955E-02	5.296052E-01	-4.988674E-02	-1.224763E+00	1.500325E-01
54	-2.344701E-02	5.683835E-01	-1.286226E-01	1.065287E+00	1.535243E-01
55	-8.189893E-02	-5.354028E+00	-1.579300E-01	6.754655E-01	0.000000e+00
56	-2.273155E-02	-3.766224E-02	2.583053E-01	-9.495828E-01	2.748878E-01
57	-3.399730E-02	-8.324932E+00	-2.989873E-01	4.018692E-01	0.000000e+00
58	8.189863E-02	-5.354026E+00	1.579299E-01	-6.754660E-01	0.000000e+00
59	3.399693E-02	-8.324931E+00	-2.989873E-01	4.018692E-01	0.000000e+00
60	1.162732E-01	1.550401E+00	5.254599E-02	5.102043E+00	0.000000e+00
61	1.162732E-01	1.550401E+00	-5.254599E-02	-5.102043E+00	0.000000e+00
62	8.189863E-02	-5.354026E+00	-1.579299E-01	6.754660E-01	0.000000e+00
63	-1.363751E-02	6.307822E-01	3.573031E-01	-1.876906E+00	-8.814639E-02
64	0.000000e+00	0.000000e+00	0.000000e+00	0.000000e+00	0.000000e+00
65	-3.658583E-03	6.635997E-01	5.784764E-01	-4.014360E+00	-5.691849E-01
66	7.410365E-02	2.617513E-01	3.004592E-02	1.085124E-01	-4.095002E-01
67	3.658720E-03	6.635997E-01	5.784764E-01	-4.014359E+00	5.691849E-01
68	5.877860E-02	4.296378E-01	2.713657E-02	-7.082572E-01	1.345644E+00
69	1.363764E-02	6.307822E-01	3.573030E-01	-1.876906E+00	8.814609E-02
70	5.116946E-02	5.296056E-01	4.988680E-02	1.224762E+00	1.500314E-01
71	2.344714E-02	5.683835E-01	1.286226E-01	-1.065286E+00	1.535244E-01
72	-9.362507E-02	3.002094E+00	2.262314E-01	1.076685E+00	0.000000e+00
73	2.273129E-02	-3.766249E-02	-2.583054E-01	9.495828E-01	2.748883E-01
74	-1.221659E-01	-1.131980E+00	7.748860E-02	-3.664337E+00	0.000000e+00
75	-4.307524E-02	1.643141E-01	-3.107096E+00	4.490227E-01	-3.093104E+00
76	-1.221659E-01	-1.131980E+00	-7.748860E-02	3.664337E+00	0.000000e+00
77	-5.334870E-02	3.586955E-01	2.247919E+00	1.071558E+00	1.966455E+00

78	-9.362507E-02	3.002094E+00	-2.262314E-01	-1.076685E+00	0.000000e+00
79	-4.840098E-02	5.159767E-01	-2.774833E+00	-2.603818E+00	-2.753377E+00
80	-1.363751E-02	6.307822E-01	-3.573031E-01	1.876906E+00	8.814639E-02
81	1.368123E-02	-2.015609E-01	-4.928859E-01	4.920493E-01	4.003682E-01
82	9.017402E-02	3.794852E-01	-1.710561E-02	-3.720016E-01	-9.568159E-03
83	-1.368161E-02	-2.015607E-01	-4.928859E-01	4.920493E-01	-4.003685E-01
84	1.110041E-01	6.251503E-01	-8.757442E-03	1.796951E+00	-5.086538E-02
85	-2.273155E-02	-3.766224E-02	-2.583053E-01	9.495828E-01	-2.748878E-01
86	1.110041E-01	6.251503E-01	8.757442E-03	-1.796951E+00	5.086538E-02
87	9.017402E-02	3.794852E-01	1.710561E-02	3.720016E-01	9.568159E-03
88	0.000000e+00	0.000000e+00	0.000000e+00	0.000000e+00	0.000000e+00
89	-3.936509E-02	3.812664E+00	3.519562E-01	1.776410E+00	0.000000e+00
90	-3.970667E-01	4.675813E-01	4.292027E-02	0.000000e+00	6.974548E-01
91	3.936531E-02	3.812664E+00	3.519562E-01	1.776410E+00	0.000000e+00
92	-1.343696E+00	5.557596E-01	3.739934E-02	0.000000e+00	-7.925306E-01
93	9.362525E-02	3.002092E+00	2.262313E-01	1.076685E+00	0.000000e+00
94	-1.319714E+00	6.236920E-01	4.671568E-02	0.000000e+00	4.325927E-01
95	9.843981E-02	6.558049E-01	9.562874E-02	1.053868E+00	5.399790E-03
96	-5.082608E-02	-1.383284E+00	1.178113E-01	-4.746291E+00	0.000000e+00
97	-1.736602E-02	6.514788E-02	-6.862464E+00	2.427180E+00	-1.173689E+00
98	-5.082608E-02	-1.383284E+00	-1.178113E-01	4.746291E+00	0.000000e+00
99	-2.219216E-02	3.074746E-01	6.960867E+00	1.900096E+00	2.339853E+00
100	-3.936509E-02	3.812664E+00	-3.519562E-01	-1.776410E+00	0.000000e+00
101	-1.936520E-02	5.096145E-01	-5.606589E+00	-5.781806E+00	-6.248997E-01
102	-3.658583E-03	6.635997E-01	-5.784764E-01	4.014360E+00	5.691349E-01
103	1.736566E-02	6.514800E-02	-6.862463E+00	2.427179E+00	1.173690E+00
104	-1.291305E+00	6.182576E-01	1.876487E-02	0.000000e+00	8.219618E-02
105	4.307487E-02	1.643143E-01	-3.107094E+00	4.490215E-01	3.093104E+00
106	-1.291305E+00	6.182576E-01	-1.876487E-02	0.000000e+00	-8.219624E-02
107	7.410365E-02	2.617513E-01	-3.004592E-02	-1.085124E-01	4.095002E-01
108	-3.970667E-01	4.675813E-01	-4.292027E-02	0.000000e+00	-6.974548E-01
109	5.082633E-02	-1.383282E+00	1.178112E-01	-4.746290E+00	0.000000e+00
110	2.202222E+00	6.436672E-01	1.703529E-02	0.000000e+00	-1.850502E+00
111	1.221661E-01	-1.131980E+00	7.748860E-02	-3.664336E+00	0.000000e+00
112	-5.902691E-01	6.760237E-01	1.957938E-02	0.000000e+00	-6.985574E-01
113	1.333232E-01	6.766807E-01	3.525431E-02	-1.501416E+00	-2.900030E-01
114	5.082633E-02	-1.383282E+00	-1.178112E-01	4.746290E+00	0.000000e+00
115	2.219188E-02	3.074747E-01	6.960866E+00	1.900097E+00	-2.339859E+00
116	3.936531E-02	3.812664E+00	-3.519562E-01	-1.776410E+00	0.000000e+00
117	1.936511E-02	5.096146E-01	-5.606586E+00	-5.781805E+00	6.249012E-01
118	3.658720E-03	6.635997E-01	-5.784764E-01	4.014359E+00	-5.691849E-01
119	5.334839E-02	3.586957E-01	2.247916E+00	1.071558E+00	-1.966455E+00
120	2.202222E+00	6.436672E-01	-1.703530E-02	0.000000e+00	1.850502E+00
121	5.877860E-02	4.296378E-01	-2.713657E-02	7.082572E-01	-1.345644E+00
122	-1.343696E+00	5.557596E-01	-3.739934E-02	0.000000e+00	7.925306E-01
123	1.221661E-01	-1.131980E+00	-7.748860E-02	3.664336E+00	0.000000e+00
124	-5.902691E-01	6.760237E-01	-1.957938E-02	0.000000e+00	6.985574E-01
125	1.333232E-01	6.766807E-01	-3.525431E-02	1.501416E+00	2.900030E-01
126	9.362525E-02	3.002092E+00	-2.262313E-01	-1.076685E+00	0.000000e+00
127	4.840085E-02	5.159769E-01	-2.774833E+00	-2.603817E+00	2.753375E+00
128	1.363764E-02	6.307822E-01	-3.573030E-01	1.876906E+00	-8.814609E-02
129	5.116946E-02	5.296056E-01	-4.988680E-02	-1.224762E+00	-1.500314E-01
130	-1.319714E+00	6.236920E-01	-4.671568E-02	0.000000e+00	-4.325927E-01
131	9.843981E-02	6.558049E-01	-9.562874E-02	-1.053868E+00	-5.399790E-03
132	2.344714E-02	5.683835E-01	-1.286226E-01	1.065286E+00	-1.535244E-01

EIGENVALUE = 9.636076E+08 (FREQ = 4.94049E+03 HZ)

1	0.000000e+00	0.000000e+00	0.000000e+00	0.000000e+00	0.000000e+00
2	-2.204335E-01	-9.134558E-01	9.786415E-02	-9.671673E-01	3.471567E-01
3	-1.362807E-01	6.042520E-01	6.709260E-02	6.771230E-01	-6.916553E-01
4	-1.433665E-01	1.525908E+00	5.990286E-02	-7.172636E-01	0.000000e+00

5	-2.749668E+00	-8.418170E-01	-7.844156E-02	0.000000e+00	-9.369984E-01
6	-1.725030E-01	-1.501932E-01	-1.134764E-01	-9.142415E-01	1.307213E+00
7	-1.039136E-01	5.266383E-01	-7.977329E-01	-6.287336E-01	-6.875175E-01
8	-2.717091E+00	-1.237710E+00	-2.057067E-02	0.000000e+00	2.514758E+00
9	-2.717091E+00	-1.237710E+00	2.057068E-02	0.000000e+00	-2.514758E+00
10	2.906806E+00	-1.333014E+00	-2.662497E-02	0.000000e+00	-3.088984E+00
11	-1.129961E-01	-1.517645E+00	5.321137E-02	-1.289827E-01	-7.749307E-01
12	-4.161067E-02	8.480288E-01	8.127363E-01	-4.558187E-01	1.901936E+00
13	-9.085095E-02	-1.261820E+00	1.951224E-02	-1.302364E+00	0.000000e+00
14	-6.269652E-02	7.836103E-01	1.301141E-01	-3.710077E-01	1.041508E+00
15	-5.270659E-02	-1.681621E+00	7.291245E-02	-4.685028E-01	0.000000e+00
16	-3.621293E-02	9.436318E-01	2.187749E-02	1.894675E+00	0.000000e+00
17	2.759181E+00	-7.893918E-01	-5.889059E-02	0.000000e+00	7.627276E-01
18	2.168846E-01	-1.752724E-01	-6.729257E-02	1.637128E+00	-1.066288E+00
19	9.218806E-02	4.955928E-01	8.495526E-01	1.691139E+00	4.570588E-01
20	2.205958E-02	8.776253E-01	-7.371554E-01	3.848539E-02	-1.255874E+00
21	-2.205948E-02	8.776249E-01	-7.371586E-01	3.848138E-02	1.255874E+00
22	2.906806E+00	-1.333014E+00	2.662500E-02	0.000000e+00	3.088984E+00
23	-8.377799E-01	-7.221616E-01	-1.345042E-01	0.000000e+00	1.911979E-01
24	1.216837E+00	-1.249653E+00	-3.938779E-02	0.000000e+00	-6.867892E-01
25	-2.749668E+00	-8.418170E-01	7.844156E-02	0.000000e+00	9.369984E-01
26	1.216837E+00	-1.249653E+00	3.938778E-02	0.000000e+00	6.867891E-01
27	2.759181E+00	-7.893919E-01	5.889060E-02	0.000000e+00	-7.627275E-01
28	-8.377799E-01	-7.221616E-01	1.345042E-01	0.000000e+00	-1.911977E-01
29	-1.129961E-01	-1.517645E+00	-5.321134E-02	1.289827E-01	7.749307E-01
30	4.161183E-02	8.480287E-01	8.127404E-01	-4.558236E-01	-1.901937E+00
31	-9.085095E-02	-1.261820E+00	-1.951218E-02	1.302364E+00	0.000000e+00
32	6.269801E-02	7.836105E-01	1.301142E-01	-3.709958E-01	-1.041507E+00
33	-3.621293E-02	9.436318E-01	-2.187740E-02	-1.894675E+00	0.000000e+00
34	5.270847E-02	-1.681604E+00	7.291251E-02	-4.685031E-01	0.000000e+00
35	3.621491E-02	9.436296E-01	2.187751E-02	1.894667E+00	0.000000e+00
36	3.621491E-02	9.436295E-01	-2.187742E-02	-1.894667E+00	0.000000e+00
37	5.765485E-02	-9.727752E-02	-2.158720E-01	-2.389098E+00	-9.922212E-02
38	1.089216E-01	4.881054E-01	-2.885715E-01	-2.457432E+00	3.233907E-01
39	4.408480E-02	8.937230E-01	3.235229E-01	2.770982E-01	7.550275E-02
40	1.039149E-01	5.266376E-01	-7.977383E-01	-6.287332E-01	6.875185E-01
41	-4.408512E-02	8.937224E-01	3.235171E-01	2.771032E-01	-7.550669E-02
42	-9.218830E-02	4.955921E-01	8.495580E-01	1.691151E+00	-4.570600E-01
43	-1.089219E-01	4.881048E-01	-2.885684E-01	-2.457447E+00	-3.233817E-01
44	3.376811E-01	5.112092E-02	-5.255506E-01	2.675913E+00	7.481520E-01
45	-2.204335E-01	-9.134558E-01	-9.786409E-02	9.671673E-01	-3.471567E-01
46	2.265447E-01	-5.583499E-01	-3.988387E-01	-1.765857E+00	-9.035845E-01
47	0.000000e+00	0.000000e+00	0.000000e+00	0.000000e+00	0.000000e+00
48	4.961613E-01	-1.336038E+00	-1.493480E-01	2.403214E-02	-7.572687E-01
49	-1.725030E-01	-1.501932E-01	1.134764E-01	9.142415E-01	-1.307213E+00
50	4.961613E-01	-1.336038E+00	1.493480E-01	-2.403216E-02	7.572687E-01
51	2.168846E-01	-1.752724E-01	6.729257E-02	-1.637128E+00	1.065288E+00
52	2.265447E-01	-5.583499E-01	3.988387E-01	1.765857E+00	9.035845E-01
53	5.765484E-02	-9.727752E-02	2.158720E-01	2.389098E+00	9.922206E-02
54	3.376811E-01	5.112090E-02	5.255506E-01	-2.675913E+00	-7.481520E-01
55	-1.433665E-01	1.525908E+00	-5.990281E-02	7.172636E-01	0.000000e+00
56	1.362818E-01	6.042512E-01	6.709266E-02	6.771172E-01	6.916546E-01
57	-5.270659E-02	-1.681621E+00	-7.291234E-02	4.685028E-01	0.000000e+00
58	1.433684E-01	1.525901E+00	5.990295E-02	-7.172644E-01	0.000000e+00
59	5.270847E-02	-1.681604E+00	-7.291245E-02	4.685032E-01	0.000000e+00
60	9.085280E-02	-1.261823E+00	1.951225E-02	-1.302364E+00	0.000000e+00
61	9.085280E-02	-1.261823E+00	-1.951218E-02	1.302364E+00	0.000000e+00
62	1.433684E-01	1.525901E+00	-5.990290E-02	7.172645E-01	0.000000e+00
63	3.133246E-01	4.843269E-01	-3.312035E-01	2.101591E+00	-9.552705E-02
64	0.000000e+00	0.000000e+00	0.000000e+00	0.000000e+00	0.000000e+00

65	1.271084E-01	8.988257E-01	-1.583145E-01	-5.593210E-01	8.918363E-02
66	1.725045E-01	-1.501938E-01	-1.134769E-01	-9.142451E-01	-1.307220E+00
67	-1.271092E-01	8.988244E-01	-1.583148E-01	-5.593316E-01	-8.918548E-02
68	-2.168853E-01	-1.752732E-01	-6.729227E-02	1.637136E+00	1.066297E+00
69	-3.133250E-01	4.843268E-01	-3.312039E-01	2.101606E+00	9.553254E-02
70	-5.765487E-02	-9.727788E-02	-2.158716E-01	-2.389109E+00	9.921432E-02
71	-3.376811E-01	5.112093E-02	-5.255505E-01	2.675922E+00	-7.481583E-01
72	1.906072E-01	8.540589E-01	-2.395836E-01	-1.565595E+00	0.000000e+00
73	-1.362807E-01	6.042520E-01	-6.709254E-02	-6.771231E-01	6.916553E-01
74	-2.460053E-01	2.331265E-01	-9.391183E-02	2.182657E-01	0.000000e+00
75	-1.039136E-01	5.266383E-01	7.977328E-01	6.287338E-01	6.875175E-01
76	2.460053E-01	2.331264E-01	9.391183E-02	-2.182657E-01	0.000000e+00
77	9.218806E-02	4.955928E-01	-8.495526E-01	-1.691139E+00	-4.570587E-01
78	1.906072E-01	8.540590E-01	2.395836E-01	1.565595E+00	0.000000e+00
79	1.089216E-01	4.881054E-01	2.885715E-01	2.457432E+00	-3.233907E-01
80	3.133246E-01	4.843269E-01	3.312035E-01	-2.101591E+00	9.552711E-02
81	-6.269652E-02	7.836103E-01	-1.301140E-01	3.710076E-01	-1.041508E+00
82	2.204356E-01	-9.134572E-01	9.786409E-02	-9.671671E-01	-3.471588E-01
83	6.269801E-02	7.836105E-01	-1.301141E-01	3.709956E-01	1.041507E+00
84	1.129975E-01	-1.517646E+00	5.321137E-02	-1.289803E-01	7.749367E-01
85	1.362818E-01	6.042511E-01	-6.709266E-02	-6.771173E-01	-6.916546E-01
86	1.129975E-01	-1.517646E+00	-5.321134E-02	1.289802E-01	-7.749367E-01
87	2.204356E-01	-9.134572E-01	-9.786409E-02	9.671672E-01	3.471587E-01
88	0.000000e+00	0.000000e+00	0.000000e+00	0.000000e+00	0.000000e+00
89	7.068789E-02	-9.310511E-01	-1.136358E-01	-7.224898E-01	0.000000e+00
90	2.749687E+00	-8.418180E-01	-7.844180E-02	0.000000e+00	9.370033E-01
91	-7.068890E-02	-9.310786E-01	-1.136360E-01	-7.224833E-01	0.000000e+00
92	-2.759203E+00	-7.893927E-01	-5.889043E-02	0.000000e+00	-7.627320E-01
93	-1.906080E-01	8.540800E-01	-2.395838E-01	-1.565598E+00	0.000000e+00
94	8.377856E-01	-7.221621E-01	-1.345039E-01	0.000000e+00	-1.911936E-01
95	-2.265449E-01	-5.583495E-01	-3.988387E-01	-1.765857E+00	9.035881E-01
96	7.325935E-02	1.771723E-01	-4.523061E-02	1.542386E+00	0.000000e+00
97	-4.161067E-02	8.480288E-01	-8.127363E-01	4.558188E-01	-1.901936E+00
98	7.325935E-02	1.771721E-01	4.523063E-02	-1.542386E+00	0.000000e+00
99	2.205957E-02	8.776253E-01	7.371554E-01	-3.848554E-02	1.255873E+00
100	7.068789E-02	-9.310509E-01	1.136358E-01	7.224900E-01	0.000000e+00
101	4.408479E-02	8.937230E-01	-3.235229E-01	-2.770980E-01	-7.550281E-02
102	1.271084E-01	8.988257E-01	1.583145E-01	5.593209E-01	-8.918375E-02
103	4.161184E-02	8.480287E-01	-8.127404E-01	4.558237E-01	1.901936E+00
104	-2.906821E+00	-1.333015E+00	-2.662504E-02	0.000000e+00	3.089001E+00
105	1.039149E-01	5.266375E-01	7.977382E-01	6.287333E-01	-6.875185E-01
106	-2.906821E+00	-1.333015E+00	2.662506E-02	0.000000e+00	-3.089001E+00
107	1.725045E-01	-1.501938E-01	1.134769E-01	9.142452E-01	1.307220E+00
108	2.749687E+00	-8.418180E-01	7.844180E-02	0.000000e+00	-9.370034E-01
109	-7.326072E-02	1.771917E-01	-4.523069E-02	1.542413E+00	0.000000e+00
110	2.717109E+00	-1.237711E+00	-2.057060E-02	0.000000e+00	-2.514778E+00
111	-2.460069E-01	2.331120E-01	-9.391201E-02	2.182455E-01	0.000000e+00
112	-1.216844E+00	-1.249654E+00	-3.938764E-02	0.000000e+00	6.867919E-01
113	-4.961632E-01	-1.336039E+00	-1.493480E-01	2.402635E-02	7.572713E-01
114	-7.326072E-02	1.771914E-01	4.523071E-02	-1.542413E+00	0.000000e+00
115	-2.205947E-02	8.776249E-01	7.371586E-01	-3.848153E-02	-1.255874E+00
116	-7.068890E-02	-9.310784E-01	1.136360E-01	7.224836E-01	0.000000e+00
117	-4.408511E-02	8.937223E-01	-3.235172E-01	-2.771031E-01	7.550675E-02
118	-1.271092E-01	8.988244E-01	1.583148E-01	5.593314E-01	8.918560E-02
119	-9.218830E-02	4.955921E-01	-8.495578E-01	-1.691151E+00	4.570599E-01
120	2.717109E+00	-1.237711E+00	2.057061E-02	0.000000e+00	2.514778E+00
121	-2.168853E-01	-1.752732E-01	6.729227E-02	-1.637136E+00	-1.066297E+00
122	-2.759203E+00	-7.893927E-01	5.889044E-02	0.000000e+00	7.627319E-01
123	-2.460069E-01	2.331120E-01	9.391201E-02	-2.182456E-01	0.000000e+00
124	-1.216844E+00	-1.249654E+00	3.938764E-02	0.000000e+00	-6.867918E-01

125	-4.961632E-01	-1.336039E+00	1.493480E-01	-2.402637E-02	-7.572713E-01
126	-1.906080E-01	8.540801E-01	2.395838E-01	1.565598E+00	0.000000e+00
127	-1.089219E-01	4.881047E-01	2.885683E-01	2.457447E+00	3.233817E-01
128	-3.133250E-01	4.843268E-01	3.312039E-01	-2.101606E+00	-9.553266E-02
129	-5.765484E-02	-9.727788E-02	2.158716E-01	2.389109E+00	-9.921426E-02
130	8.377856E-01	-7.221621E-01	1.345039E-01	0.000000e+00	1.911935E-01
131	-2.265449E-01	-5.583495E-01	3.988387E-01	1.765857E+00	-9.035882E-01
132	-3.376811E-01	5.112092E-02	5.255505E-01	-2.675922E+00	7.481583E-01
EIGENVALUE = 1.063199E+09 (FREQ = 5.18952E+03 Hz)					
1	0.000000e+00	0.000000e+00	0.000000e+00	0.000000e+00	0.000000e+00
2	-9.451133E-02	-8.471447E-02	3.096843E-03	-1.275939E+00	1.913482E+00
3	-2.277666E-01	2.889384E-01	-1.542409E+00	3.624273E+00	1.413621E+00
4	-1.018422E-01	2.206059E+00	-1.565207E+00	-3.410224E+00	0.000000e+00
5	3.062222E+00	-7.682985E-02	1.582063E+00	0.000000e+00	5.397369E+00
6	6.724251E-01	-2.813478E-01	1.514244E+00	-2.658940E-01	-6.082453E+00
7	4.080747E-01	4.823969E-02	-3.662162E-01	-1.382513E+00	3.924341E+00
8	-6.382443E+00	1.806549E-02	2.735959E+00	0.000000e+00	-2.699039E+00
9	6.382443E+00	-1.806446E-02	2.735959E+00	0.000000e+00	-2.699040E+00
10	-4.615300E+00	-2.599963E-02	1.629264E+00	0.000000e+00	-1.950772E+00
11	-9.658593E-02	-6.737947E-02	1.341182E-02	6.628470E-01	-1.004295E+00
12	1.357515E-01	1.267214E-01	6.682255E-01	-3.087060E+00	-3.398828E+00
13	-4.790399E-02	-3.077598E+00	-1.591409E+00	1.226150E+00	0.000000e+00
14	-1.153558E-01	4.430590E-01	-2.628884E+00	5.613295E+00	-3.761798E+00
15	-4.326220E-02	2.966340E+00	-2.645970E+00	-5.341032E+00	0.000000e+00
16	-1.499858E-02	-4.455307E+00	-2.652623E+00	1.971824E+00	0.000000e+00
17	4.153708E+00	4.432162E-02	2.726606E+00	0.000000e+00	7.167721E+00
18	8.911163E-01	-2.547168E-02	2.683100E+00	2.176843E+00	-6.874997E+00
19	5.923499E-01	-1.944394E-01	1.434947E-01	1.793740E+00	4.028863E+00
20	2.031730E-01	-3.556420E-01	-4.605522E-01	2.941056E+00	-4.662491E+00
21	-2.031731E-01	-3.556419E-01	-4.605462E-01	2.941056E+00	4.662493E+00
22	4.615300E+00	2.600066E-02	1.629263E+00	0.000000e+00	-1.950772E+00
23	2.795911E+00	2.049360E-01	2.676813E+00	0.000000e+00	5.161032E+00
24	-4.209488E+00	5.668565E-02	2.678936E+00	0.000000e+00	-1.934254E+00
25	-3.062223E+00	7.683051E-02	1.582063E+00	0.000000e+00	5.397369E+00
26	4.209488E+00	-5.668460E-02	2.678936E+00	0.000000e+00	-1.934254E+00
27	-4.153708E+00	-4.432087E-02	2.726606E+00	0.000000e+00	7.167721E+00
28	-2.795911E+00	-2.049353E-01	2.676813E+00	0.000000e+00	5.161032E+00
29	9.658569E-02	6.738049E-02	1.341186E-02	6.628470E-01	-1.004295E+00
30	-1.357517E-01	1.267214E-01	6.682259E-01	-3.087057E+00	3.398826E+00
31	4.790386E-02	3.077598E+00	-1.591409E+00	1.226150E+00	0.000000e+00
32	1.153558E-01	4.430590E-01	-2.628884E+00	5.613295E+00	3.761798E+00
33	1.499853E-02	4.455307E+00	-2.652623E+00	1.971825E+00	0.000000e+00
34	4.326217E-02	2.966342E+00	-2.645970E+00	-5.341031E+00	0.000000e+00
35	1.499856E-02	-4.455307E+00	-2.652623E+00	1.971823E+00	0.000000e+00
36	-1.499851E-02	4.455307E+00	-2.652623E+00	1.971824E+00	0.000000e+00
37	2.380384E-01	4.330818E-01	2.631824E+00	-2.313739E+00	-5.920299E+00
38	1.202772E-01	-3.615993E-01	-1.036809E+00	-2.438682E+00	3.164447E+00
39	3.105013E-02	-7.878942E-01	5.431327E-01	-2.748061E+00	-2.530603E+00
40	-4.080749E-01	4.823974E-02	-3.662177E-01	-1.382515E+00	-3.924339E+00
41	-3.105013E-02	-7.878942E-01	5.431339E-01	-2.748065E+00	2.530602E+00
42	-5.923499E-01	-1.944392E-01	1.434904E-01	1.793739E+00	-4.028865E+00
43	-1.202772E-01	-3.615991E-01	-1.036811E+00	-2.438679E+00	-3.164445E+00
44	-1.231256E+00	6.731454E-01	1.455760E+00	6.244908E-01	-3.520948E+00
45	9.451121E-02	8.471519E-02	3.096922E-03	-1.275940E+00	1.913482E+00
46	-5.769991E-01	2.839333E-01	1.479120E+00	-5.534750E-01	2.154360E+00
47	0.000000e+00	0.000000e+00	0.000000e+00	0.000000e+00	0.000000e+00
48	-2.441611E-01	6.599402E-02	1.488646E+00	-5.853536E-02	-1.142261E+00
49	-6.724251E-01	2.813480E-01	1.514244E+00	-2.658937E-01	-6.082453E+00
50	2.441612E-01	-6.599301E-02	1.488646E+00	-5.853549E-02	-1.142261E+00
51	-8.911163E-01	2.547195E-02	2.683100E+00	2.176843E+00	-6.874997E+00

52	5.769987E-01	-2.839326E-01	1.479120E+00	-5.534750E-01	2.154361E+00
53	-2.380387E-01	-4.330815E-01	2.631824E+00	-2.313739E+00	-5.920299E+00
54	1.231256E+00	-6.731454E-01	1.455760E+00	6.244904E-01	-3.520949E+00
55	1.018422E-01	-2.206059E+00	-1.565207E+00	-3.410224E+00	0.000000e+00
56	2.277665E-01	2.889384E-01	-1.542409E+00	3.624273E+00	-1.413620E+00
57	4.326220E-02	-2.966340E+00	-2.645970E+00	-5.341032E+00	0.000000e+00
58	1.018422E-01	2.206058E+00	-1.565207E+00	-3.410224E+00	0.000000e+00
59	-4.326214E-02	-2.966342E+00	-2.645970E+00	-5.341031E+00	0.000000e+00
60	4.790397E-02	-3.077598E+00	-1.591409E+00	1.226151E+00	0.000000e+00
61	-4.790383E-02	3.077598E+00	-1.591409E+00	1.226151E+00	0.000000e+00
62	-1.018421E-01	-2.206058E+00	-1.565207E+00	-3.410224E+00	0.000000e+00
63	-1.002457E+00	-3.775417E-01	-7.004800E-01	1.312627E+00	1.830906E+00
64	0.000000e+00	0.000000e+00	0.000000e+00	0.000000e+00	0.000000e+00
65	-3.876578E-01	-9.294272E-01	-2.182199E+00	9.483725E-02	-3.7371561+00
66	-6.724251E-01	-2.813478E-01	1.514244E+00	-2.658920E-01	6.0824521+00
67	3.876581E-01	-9.294268E-01	-2.182199E+00	9.483778E-02	3.7371561+00
68	-8.911163E-01	-2.547169E-02	2.683100E+00	2.176842E+00	6.8749981+00
69	1.002457E+00	-3.775414E-01	-7.004787E-01	1.312627E+00	-1.830903E+00
70	-2.380384E-01	4.330818E-01	2.631824E+00	-2.313737E+00	5.920299E+00
71	1.231256E+00	6.731454E-01	1.455761E+00	6.244887E-01	3.520946E+00
72	-4.797553E-01	-7.453079E-01	-6.739606E-01	-8.871293E-02	0.000000e+00
73	2.277667E-01	-2.889388E-01	-1.542409E+00	3.624273E+00	1.413621E+00
74	-1.609535E-01	2.367033E-02	-6.550288E-01	3.305750E-01	0.000000e+00
75	-4.080747E-01	-4.824009E-02	-3.662161E-01	-1.382513E+00	3.924342E+00
76	1.609536E-01	-2.367052E-02	-6.550288E-01	3.305750E-01	0.000000e+00
77	-5.923499E-01	1.944390E-01	1.434943E-01	1.793739E+00	4.028863E-01
78	4.797553E-01	7.453079E-01	-6.739606E-01	-8.871293E-02	0.000000e+00
79	-1.202773E-01	3.615990E-01	-1.036809E+00	-2.438681E+00	3.164448E+00
80	1.002456E+00	3.775414E-01	-7.004800E-01	1.312626E+00	1.830907E+00
81	1.153558E-01	-4.430597E-01	-2.628885E+00	5.613294E+00	-3.761799E+00
82	9.451127E-02	-8.471453E-02	3.096768E-03	-1.275939E+00	-1.913482E+00
83	-1.153558E-01	-4.430598E-01	-2.628884E+00	5.613294E+00	3.761799E+00
84	9.658587E-02	-6.737947E-02	1.341170E-02	6.628466E-01	1.004295E+00
85	-2.277666E-01	-2.889388E-01	-1.542409E+00	3.624272E+00	-1.413621E+00
86	-9.658563E-02	6.738055E-02	1.341174E-02	6.628466E-01	1.0042951+00
87	-9.451115E-02	8.471525E-02	3.096847E-03	-1.275939E+00	-1.9134821+00
88	0.000000e+00	0.000000e+00	0.000000e+00	0.000000e+00	0.000000e+00
89	-1.849937E-01	-1.230235E+00	-2.162570E+00	1.643085E+00	0.000000e+00
90	-3.062223E+00	-7.682991E-02	1.582063E+00	0.000000e+00	-5.397368E+00
91	1.849939E-01	-1.230234E+00	-2.162570E+00	1.643084E+00	0.000000e+00
92	-4.153708E+00	4.432159E-02	2.726606E+00	0.000000e+00	-7.167722E+00
93	4.797553E-01	-7.453071E-01	-6.739597E-01	-8.871388E-02	0.000000e+00
94	-2.795912E+00	2.049360E-01	2.676813E+00	0.000000e+00	-5.161032E+00
95	5.769991E-01	2.839333E-01	1.479120E+00	-5.534754E-01	-2.154359E+00
96	-5.821772E-02	1.723785E+00	-2.134948E+00	-6.396148E-01	0.000000e+00
97	-1.357515E-01	-1.267222E-01	6.682255E-01	-3.087059E+00	-3.398829E+00
98	5.821774E-02	-1.723785E+00	-2.134948E+00	-6.396143E-01	0.000000e+00
99	-2.031730E-01	3.556412E-01	-4.605522E-01	2.941055E+00	-4.662492E+00
100	1.849937E-01	1.230235E+00	-2.162570E+00	1.643084E+00	0.000000e+00
101	-3.105019E-02	7.878933E-01	5.431327E-01	-2.748060E+00	-2.530604E+00
102	3.876576E-01	9.294263E-01	-2.182199E+00	9.483647E-02	-3.737157E+00
103	1.357516E-01	-1.267222E-01	6.682255E-01	-3.087056E+00	3.398827E+00
104	4.615300E+00	-2.599966E-02	1.629263E+00	0.000000e+00	1.950771E+00
105	4.080749E-01	-4.824012E-02	-3.662177E-01	-1.382514E+00	-3.924339E+00
106	-4.615299E+00	2.600069E-02	1.629263E+00	0.000000e+00	1.950771E+00
107	6.724251E-01	2.813480E-01	1.514244E+00	-2.658917E-01	6.082452E+00
108	3.062224E+00	7.683057E-02	1.582063E+00	0.000000e+00	-5.397368E+00
109	5.821777E-02	1.723784E+00	-2.134948E+00	6.396143E-01	0.000000e+00
110	6.382445E+00	1.806548E-02	2.735958E+00	0.000000e+00	2.699040E+00
111	1.609535E-01	2.366930E-02	-6.550274E-01	3.305752E-01	0.000000e+00

112	4.209487E+00	5.668565E-02	2.678936E+00	0.000000e+00	1.934253E+00
113	2.441610E-01	6.599396E-02	1.488646E+00	-5.853504E-02	1.142261E+00
114	-5.821780E-02	-1.723784E+00	-2.134948E+00	-6.396143E-01	0.000000e+00
115	2.031731E-01	3.556411E-01	-4.605462E-01	2.941055E+00	4.662493E+00
116	-1.849939E-01	1.230234E+00	-2.162570E+00	1.643083E+00	0.000000e+00
117	3.105019E-02	7.878933E-01	5.431339E-01	-2.748063E+00	2.530604E+00
118	-3.876580E-01	9.294263E-01	-2.182199E+00	9.483707E-02	3.737157E+00
119	5.923499E-01	1.944389E-01	1.434901E-01	1.793738E+00	-4.028866E+00
120	-6.382445E+00	-1.806445E-02	2.735958E+00	0.000000e+00	2.699041E+00
121	8.911163E-01	2.547196E-02	2.683099E+00	2.176841E+00	6.874999E+00
122	4.153708E+00	-4.432085E-02	2.726606E+00	0.000000e+00	-7.167722E+00
123	-1.609536E-01	-2.366949E-02	-6.550274E-01	3.305752E-01	0.000000e+00
124	-4.209487E+00	-5.668460E-02	2.678936E+00	0.000000e+00	1.934254E+00
125	-2.441611E-01	-6.599301E-02	1.488646E+00	-5.853517E-02	1.142261E+00
126	-4.797553E-01	7.453071E-01	-6.739597E-01	-8.871382E-02	0.000000e+00
127	1.202773E-01	3.615987E-01	-1.036811E+00	-2.438678E+00	-3.164446E+00
128	-1.002456E+00	3.775410E-01	-7.004787E-01	1.312627E+00	-1.830904E+00
129	2.380386E-01	-4.330815E-01	2.631824E+00	-2.313737E+00	5.920299E+00
130	2.795912E+00	-2.049353E-01	2.676812E+00	0.000000e+00	-5.161032E+00
131	-5.769987E-01	-2.839326E-01	1.479120E+00	-5.534754E-01	-2.154360E+00
132	-1.231256E+00	-6.731454E-01	1.455760E+00	6.244887E-01	3.520947E+00
EIGENVALUE = 1.542988E+09 (FREQ = 6.25175E+03 HZ)					
1	0.000000e+00	0.000000e+00	0.000000e+00	0.000000e+00	0.000000e+00
2	4.590805E-01	-3.272731E-01	-1.313581E-01	-3.265678E+00	-7.956802E-01
3	2.040555E-01	7.161067E-01	7.191497E-02	2.607099E+00	-6.243586E+00
4	2.712965E-01	2.856947E+00	1.851650E-01	-5.456234E+00	0.000000e+00
5	2.647571E+00	-2.571492E-01	-5.264793E-01	0.000000e+00	-2.428569E-01
6	4.339200E-01	-4.220100E-02	-3.743654E-01	1.309581E+00	1.092058E+00
7	3.142332E-01	3.312021E-01	9.476547E-01	6.201724E-01	-4.433858E+00
8	-3.654985E+00	-1.464982E-01	-9.227796E-01	0.000000e+00	-1.598598E+00
9	3.654985E+00	1.464982E-01	-9.227796E-01	0.000000e+00	-1.598598E+00
10	7.893673E-01	-1.841950E-01	-5.727791E-01	0.000000e+00	1.933828E+00
11	2.489810E-01	-3.482481E-01	-2.520546E-01	9.744532E-01	-6.296736E-02
12	9.407467E-02	1.614960E-02	-7.354807E-01	8.314003E-01	5.757459E+00
13	1.340160E-01	-8.111287E+00	2.747808E-01	3.877952E+00	0.000000e+00
14	1.276436E-01	-1.707510E-02	6.482824E-01	-2.196457E+00	9.779965E+00
15	8.699143E-02	-1.702477E+00	6.866251E-01	2.725915E+00	0.000000e+00
16	3.863589E-02	4.375741E+00	7.360634E-01	-1.735952E+00	0.000000e+00
17	1.905424E+00	-2.796497E-01	-8.956088E-01	0.000000e+00	3.011215E+00
18	9.190781E-01	-1.870955E-01	-8.362907E-01	-3.131558E+00	-5.172221E-01
19	5.533018E-01	1.538521E-03	1.539549E+00	-1.413861E+00	-8.053227E-01
20	1.738380E-01	-1.338020E-01	-4.395337E-01	-4.497837E-01	3.379663E-01
21	-1.738344E-01	-1.338034E-01	-4.395267E-01	-4.497721E-01	-3.379613E-01
22	-7.893673E-01	1.841950E-01	-5.727791E-01	0.000000e+00	1.933828E+00
23	2.248714E+00	-3.794388E-01	-7.702167E-01	0.000000e+00	2.839219E+00
24	-3.751226E+00	-1.813316E-01	-8.336855E-01	0.000000e+00	-1.620147E+00
25	-2.647571E+00	2.571492E-01	-5.264793E-01	0.000000e+00	-2.428569E-01
26	3.751226E+00	1.813316E-01	-8.336855E-01	0.000000e+00	-1.620147E+00
27	-1.905424E+00	2.796497E-01	-8.956088E-01	0.000000e+00	3.011215E+00
28	-2.248714E+00	3.794388E-01	-7.702167E-01	0.000000e+00	2.839219E+00
29	-2.489810E-01	3.482481E-01	-2.520546E-01	9.744532E-01	-6.296736E-02
30	-9.407103E-02	1.614792E-02	-7.355083E-01	8.314034E-01	-5.757458E+00
31	-1.340160E-01	8.111287E+00	2.747808E-01	3.877952E+00	0.000000e+00
32	-1.276395E-01	-1.707726E-02	6.482837E-01	-2.196479E+00	-9.779966E+00
33	-3.863590E-02	-4.375741E+00	7.360634E-01	-1.735952E+00	0.000000e+00
34	-8.698910E-02	-1.702480E+00	6.866266E-01	2.725936E+00	0.000000e+00
35	-3.863514E-02	4.375768E+00	7.360650E-01	-1.735967E+00	0.000000e+00
36	3.863513E-02	-4.375768E+00	7.360650E-01	-1.735967E+00	0.000000e+00
37	8.172329E-01	-3.306239E-01	-6.634548E-01	3.861403E+00	2.962852E-01
38	5.007378E-01	-2.552581E-01	1.471487E+00	1.536960E+00	-2.500759E+00

39	1.681758E-01	-3.483433E-01	-2.471471E-01	3.589401E-01	3.052584E+00
40	-3.142300E-01	3.311992E-01	9.476887E-01	6.201531E-01	4.433873E+00
41	-1.681724E-01	-3.483449E-01	-2.471702E-01	3.589203E-01	-3.052586E+00
42	-5.532988E-01	1.535898E-03	1.539539E+00	-1.413852E+00	8.052989E-01
43	-5.007344E-01	-2.552607E-01	1.471513E+00	1.536956E+00	2.500772E+00
44	1.389135E-01	-3.968479E-01	-3.026651E-01	-2.210135E+00	4.217731E+00
45	-4.590805E-01	3.272731E-01	-1.313581E-01	-3.265678E+00	-7.956802E-01
46	-3.469369E-01	-5.501581E-01	-3.774725E-01	-3.968828E-01	-3.075078E-01
47	0.000000e+00	0.000000e+00	0.000000e+00	0.000000e+00	0.000000e+00
48	-1.488602E-01	-2.730262E-01	-3.640329E-01	-8.270526E-02	-4.058779E-02
49	-4.339200E-01	4.220100E-02	-3.743654E-01	1.309581E+00	1.092058E+00
50	1.488602E-01	2.730262E-01	-3.640329E-01	-8.270532E-02	-4.058779E-02
51	-9.190781E-01	1.870955E-01	-8.362907E-01	-3.131558E+00	-5.172221E-01
52	3.469369E-01	5.501581E-01	-3.774725E-01	-3.968828E-01	-3.075078E-01
53	-8.172329E-01	3.306239E-01	-6.634548E-01	3.861403E+00	2.962852E-01
54	-1.389135E-01	3.968479E-01	-3.026651E-01	-2.210135E+00	4.217731E+00
55	-2.712966E-01	-2.856947E+00	1.851650E-01	-5.456234E+00	0.000000e+00
56	-2.040533E-01	7.161030E-01	7.191968E-02	2.607108E+00	6.243588E+00
57	-8.699143E-02	1.702477E+00	6.866251E-01	2.725915E+00	0.000000e+00
58	-2.712946E-01	2.856923E+00	1.851691E-01	-5.456229E+00	0.000000e+00
59	8.698910E-02	1.702480E+00	6.866266E-01	2.725936E+00	0.000000e+00
60	-1.340154E-01	-8.111278E+00	2.747845E-01	3.877957E+00	0.000000e+00
61	1.340154E-01	8.111278E+00	2.747845E-01	3.877957E+00	0.000000e+00
62	2.712946E-01	-2.856923E+00	1.851691E-01	-5.456229E+00	0.000000e+00
63	1.771163E-01	-2.916673E-01	9.157900E-03	-2.668100E+00	-6.406188E+00
64	0.000000e+00	0.000000e+00	0.000000e+00	0.000000e+00	0.000000e+00
65	7.165337E-02	-4.530604E-01	2.361302E-01	1.199482E+00	7.835309E+00
66	-4.339179E-01	-4.220150E-02	-3.743649E-01	1.309566E+00	-1.092062E+00
67	-7.165170E-02	-4.530621E-01	2.361264E-01	1.199508E+00	-7.835319E+00
68	-9.190764E-01	-1.870963E-01	-8.362935E-01	-3.131547E+00	5.172588E-01
69	-1.771134E-01	-2.916697E-01	9.153761E-03	-2.668111E+00	6.406200E+00
70	-8.172298E-01	-3.306249E-01	-6.634564E-01	3.861399E+00	-2.962875E-01
71	-1.389098E-01	-3.968488E-01	-3.026676E-01	-2.210135E+00	-4.217740E+00
72	-1.021579E-01	-8.068653E-01	-6.234315E-02	-1.798972E-01	0.000000e+00
73	-2.040556E-01	-7.161067E-01	7.191497E-02	2.607099E+00	-6.243586E+00
74	-6.737101E-02	-1.697833E+00	-1.331440E-01	1.838033E+00	0.000000e+00
75	-3.142332E-01	-3.312021E-01	9.476547E-01	6.201724E-01	-4.433858E+00
76	6.737101E-02	1.697833E+00	-1.331440E-01	1.838033E+00	0.000000e+00
77	-5.533018E-01	-1.538521E-03	1.539549E+00	-1.413861E+00	-8.053227E-01
78	1.021579E-01	8.068653E-01	-6.234315E-02	-1.798971E-01	0.000000e+00
79	-5.007378E-01	2.552581E-01	1.471487E+00	1.536960E+00	-2.500759E+00
80	-1.771163E-01	2.916673E-01	9.157900E-03	-2.668100E+00	-6.406188E+00
81	-1.276436E-01	1.707510E-02	6.482824E-01	-2.196457E+00	9.779965E+00
82	-4.590790E-01	-3.272741E-01	-1.313568E-01	-3.265676E+00	7.956797E-01
83	1.276395E-01	1.707726E-02	6.482837E-01	-2.196479E+00	-9.779966E+00
84	-2.489808E-01	-3.482487E-01	-2.520528E-01	9.744515E-01	6.296998E-02
85	2.040533E-01	-7.161030E-01	7.191968E-02	2.607108E+00	6.243588E+00
86	2.489808E-01	3.482487E-01	-2.520528E-01	9.744515E-01	6.296998E-02
87	4.590790E-01	3.272741E-01	-1.313568E-01	-3.265676E+00	7.956797E-01
88	0.000000e+00	0.000000e+00	0.000000e+00	0.000000e+00	0.000000e+00
89	-1.593731E-02	1.725979E+00	1.806393E-01	-6.609303E-01	0.000000e+00
90	-2.647591E+00	-2.571497E-01	-5.264792E-01	0.000000e+00	2.428544E-01
91	1.593898E-02	1.725978E+00	1.806364E-01	-6.609399E-01	0.000000e+00
92	-1.905444E+00	-2.796503E-01	-8.956113E-01	0.000000e+00	-3.011254E+00
93	1.021596E-01	-8.068604E-01	-6.234740E-02	-1.798891E-01	0.000000e+00
94	-2.248732E+00	-3.794392E-01	-7.702190E-01	0.000000e+00	-2.839220E+00
95	3.469386E-01	-5.501583E-01	-3.774751E-01	-3.968831E-01	3.075162E-01
96	-1.646472E-02	-7.119755E-01	1.152091E-01	-4.596010E-01	0.000000e+00
97	-9.407467E-02	-1.614960E-02	-7.354807E-01	8.314003E-01	5.757459E+00
98	1.646472E-02	7.119756E-01	1.152091E-01	-4.596010E-01	0.000000e+00

99	-1.738380E-01	1.338020E-01	-4.395337E-01	-4.497838E-01	3.379663E-01
100	1.593731E-02	-1.725979E+00	1.806393E-01	-6.609303E-01	0.000000e+00
101	-1.681758E-01	3.483433E-01	-2.471471E-01	3.589401E-01	3.052584E+00
102	-7.165337E-02	4.530604E-01	2.361302E-01	1.199482E+00	7.835309E+00
103	9.407103E-02	-1.614792E-02	-7.355083E-01	8.314034E-01	-5.757458E+00
104	-7.893661E-01	-1.841953E-01	-5.727789E-01	0.000000e+00	-1.933836E+00
105	3.142300E-01	-3.311992E-01	9.476887E-01	6.201531E-01	4.433873E+00
106	7.893661E-01	1.841953E-01	-5.727789E-01	0.000000e+00	-1.933836E+00
107	4.339179E-01	4.220150E-02	-3.743649E-01	1.309566E+00	-1.092062E+00
108	2.647591E+00	2.571497E-01	-5.264792E-01	0.000000e+00	2.428544E-01
109	1.646528E-02	-7.119811E-01	1.152066E-01	-4.595968E-01	0.000000e+00
110	3.655034E+00	-1.464984E-01	-9.227812E-01	0.000000e+00	1.598619E+00
111	6.737131E-02	-1.697830E+00	-1.331480E-01	1.838025E+00	0.000000e+00
112	3.751225E+00	-1.813317E-01	-8.336880E-01	0.000000e+00	1.620139E+00
113	1.488598E-01	-2.730263E-01	-3.640357E-01	-8.270323E-02	4.058736E-02
114	-1.646527E-02	7.119811E-01	1.152066E-01	-4.595968E-01	0.000000e+00
115	1.738344E-01	1.338034E-01	-4.395267E-01	-4.497721E-01	-3.379613E-01
116	-1.593898E-02	-1.725978E+00	1.806364E-01	-6.609399E-01	0.000000e+00
117	1.681724E-01	3.483449E-01	-2.471702E-01	3.589203E-01	-3.052586E+00
118	7.165170E-02	4.530621E-01	2.361264E-01	1.199508E+00	-7.835319E+00
119	5.532988E-01	-1.535898E-03	1.539539E+00	-1.413852E+00	8.052989E-01
120	-3.655034E+00	1.464984E-01	-9.227812E-01	0.000000e+00	1.598619E+00
121	9.190764E-01	1.870963E-01	-8.362935E-01	-3.131547E+00	5.172588E-01
122	1.905444E+00	2.796503E-01	-8.956113E-01	0.000000e+00	-3.011254E+00
123	-6.737131E-02	1.697830E+00	-1.331480E-01	1.838026E+00	0.000000e+00
124	-3.751225E+00	1.813317E-01	-8.336880E-01	0.000000e+00	1.620139E+00
125	-1.488598E-01	2.730263E-01	-3.640357E-01	-8.270317E-02	4.058737E-02
126	-1.021596E-01	8.068604E-01	-6.234740E-02	-1.798891E-01	0.000000e+00
127	5.007344E-01	2.552607E-01	1.471513E+00	1.536956E+00	2.500772E+00
128	1.771134E-01	2.916697E-01	9.153761E-03	-2.668111E+00	6.406200E+00
129	8.172298E-01	3.306249E-01	-6.634564E-01	3.861399E+00	-2.962875E-01
130	2.248732E+00	3.794392E-01	-7.702190E-01	0.000000e+00	-2.839220E+00
131	-3.469386E-01	5.501583E-01	-3.774751E-01	-3.968831E-01	3.075162E-01
132	1.389098E-01	3.968488E-01	-3.026676E-01	-2.210135E+00	-4.217740E+00

REPORT DOCUMENTATION PAGE			Form Approved OMB No. 0704-0188
<p>Public reporting burden for this collection of information is estimated to average 1 hour per response, including the time for reviewing instructions, searching existing data sources, gathering and maintaining the data needed, and completing and reviewing the collection of information. Send comments regarding this burden estimate or any other aspect of this collection of information, including suggestions for reducing this burden, to Washington Headquarters Services, Directorate for Information Operations and Reports, 1215 Jefferson Davis Highway, Suite 1204, Arlington, VA 22202-4302, and to the Office of Management and Budget, Paperwork Reduction Project (0704-0188), Washington, DC 20503.</p>			
1. AGENCY USE ONLY (Leave blank)	2. REPORT DATE	3. REPORT TYPE AND DATES COVERED	
	April 1993	Final Contractor Report	
4. TITLE AND SUBTITLE		5. FUNDING NUMBERS	
Global Dynamic Modeling of a Transmission System		WU-505-62-10 NAG3-900	
6. AUTHOR(S)			
F.K. Choy and W. Qian			
7. PERFORMING ORGANIZATION NAME(S) AND ADDRESS(ES)		8. PERFORMING ORGANIZATION REPORT NUMBER	
University of Akron Department of Mechanical Engineering Akron, Ohio 44325-3903		E-7731	
9. SPONSORING/MONITORING AGENCY NAME(S) AND ADDRESS(ES)		10. SPONSORING/MONITORING AGENCY REPORT NUMBER	
Vehicle Propulsion Directorate U.S. Army Research Laboratory Cleveland, Ohio 44135-3191 and NASA Lewis Research Center Cleveland, Ohio 44135-3191		NASA CR-191117 ARL-CR-11	
11. SUPPLEMENTARY NOTES			
Project Manager, J. Zakrajsek, Propulsion Systems Division, (216) 433-3969.			
12a. DISTRIBUTION/AVAILABILITY STATEMENT		12b. DISTRIBUTION CODE	
Unclassified - Unlimited Subject Category 37			
13. ABSTRACT (Maximum 200 words)			
<p>This report outlines the work performed on global dynamic simulation and noise correlation of gear transmission systems at The University of Akron. The objective of this work is to develop a comprehensive procedure to simulate the dynamics of the gear transmission system coupled with the effects of gear box vibrations. The developed numerical model is benchmarked with results from experimental tests at NASA Lewis Research Center. The modal synthesis approach is used to develop the global transient vibration analysis procedure used in the model. Modal dynamic characteristics of the rotor-gear-bearing system are calculated by the matrix transfer method while those of the gear box are evaluated by the finite element method (NASTRAN). A three-dimensional, axial-lateral coupled bearing model is used to couple the rotor vibrations with the gear box motion. The vibrations between the individual rotor systems are coupled through the nonlinear gear mesh interactions. The global equations of motion are solved in modal coordinates and the transient vibration of the system is evaluated by a variable time-stepping integration scheme. The relationship between housing vibration and resulting noise of the gear transmission system is generated by linear transfer functions using experimental data. A nonlinear relationship of the noise components to the fundamental mesh frequency is developed using the hyperchoherence function. The numerically simulated vibrations and predicted noise of the gear transmission system are compared with the experimental results from the gear noise test rig at NASA Lewis Research Center. Results of the comparison indicate that the global dynamic model developed can accurately simulate the dynamics of a gear transmission system.</p>			
14. SUBJECT TERMS			15. NUMBER OF PAGES
Gearbox; Vibration; Noise			160
			16. PRICE CODE
			A08
17. SECURITY CLASSIFICATION OF REPORT	18. SECURITY CLASSIFICATION OF THIS PAGE	19. SECURITY CLASSIFICATION OF ABSTRACT	20. LIMITATION OF ABSTRACT
Unclassified	Unclassified		